STATISTICAL EVALUATION AND SIMPLIFIED APPROACH FOR ESTIMATING EXCAVATION INDUCED DEFORMATIONS IN SOFT SOILS

YUMUŞAK ZEMİNLERDE KAZI KAYNAKLI DEFORMASYONLARI TAHMİN ETMEK İÇİN İSTATİSTİKSEL DEĞERLENDİRME VE BASİTLEŞTİRİLMİŞ YAKLAŞIM

AHMET ARDA BAHADIR

PROF. DR. BERNA UNUTMAZ
Supervisor

Submitted to
Graduate School of Science and Engineering of Hacettepe University
as a Partial Fulfillment to the Requirements
for be Award of the Degree of Doctor of Philosophy
in Civil Engineering

2022

ABSTRACT

STATISTICAL EVALUATION AND SIMPLIFIED APPROACH FOR ESTIMATING EXCAVATION INDUCED DEFORMATIONS IN SOFT SOILS

Ahmet Arda BAHADIR

Doctor of Philosophy, Department of Civil Engineering

Supervisor: Prof. Dr. Berna UNUTMAZ

May 2022   265 pages

This thesis is about estimating the deformation behavior of supported diaphragm walls and settlements behind the wall due to excavation built on soft ground environments. For this purpose, a finite element model that considers the stiffness of soils at small strain levels was utilized. With this model, numerous generic cases were analyzed. The accuracy of these generic cases and the parameters used were confirmed by a large number of cases, considering the parameters related to soil, wall, and excavation geometry as well as their variations. In this study, based on studies in the literature, the important parameters are selected to be the i) soil strength, stiffness, unit weight, and thickness of the soft soil layer, ii) the depth and width of the excavation, and iii) the stiffness of the support system. Unlike literature studies, the parameters representing the stiffness of the soil at the small strain level were calculated using empirical approaches. In statistical studies, using the multiple regression analyses, a closed-form solution that estimates the ground settlements and wall deflections based on mentioned parameters were proposed as a result of this study. In order to investigate the error level of the model, in addition to the error amount of the obtained regression equation, residuals were determined for the parameters and their ranges, moreover, the importance of each parameter on deformations was investigated. It is seen that the most important parameter affecting the behavior of this supporting system is the depth of the excavation.

The results obtained from statistical approaches were compared with the real cases. It is seen that the proposed equations can predict the wall deformations and settlements in an acceptable range.

Keywords: Supported excavations, finite element method, soft soil, small strain, regression analyses.

ÖZET

YUMUŞAK ZEMİNLERDE KAZI KAYNAKLI DEFORMASYONLARI TAHMİN ETMEK İÇİN İSTATİSTİKSEL DEĞERLENDİRME VE BASİTLEŞTİRİLMİŞ YAKLAŞIM

Ahmet Arda BAHADIR

Doktora, İnşaat Mühendisliği Bölümü

Tez Danışmanı: Prof. Dr. Berna UNUTMAZ

Mayıs 2022, 265 sayfa

Bu tez çalışması yumuşak zeminlerde inşa edilen destekli diyafram duvarların deformasyonlarını ve kazı arkası oturmalarının tahmin edilmesi ile ilgilidir. Bu amaçla, deformasyon tahminleri için, küçük şekil değiştirme seviyelerinde zeminlerin rijitliğini dikkate alan bir sonlu eleman modeli kullanılmıştır. Bu model ile çok sayıda jenerik vaka analiz edilmiştir, vakaların ve kullanılan parametrelerin doğruluğu dünya üzerinde inşa edilmiş çok sayıda vaka ile doğrulanmıştır. Bu çalışmada kullanılan parametreler literatürdeki çalışmalar da dikkate alınarak; i) zeminin mukavemeti, zeminin rijitliği, zemin birim hacim ağırlığı, ii) yumuşak zemin tabakasının kalınlığı, kazı derinliği, kazı genişliği ve iii) destek sisteminin rijitliği olarak seçilmiştir. Literatür çalışmalarından farklı olarak, küçük deformasyon seviyesinde zeminin rijitliğini temsil eden parametreler deneysel yaklaşımlar kullanılarak hesaplanmıştır. İstatistiksel çalışmalarda, çoklu regresyon analizleri kullanılarak, bahsedilen parametrelere dayalı olarak zemin oturmalarını ve duvar sehimlerini tahmin eden kapalı form bir çözüm önerilmiştir. Modelin hata düzeyini araştırmak için, elde edilen regresyon denkleminin hata miktarına ek olarak, parametreler ve aralıkları için hatalar belirlenmiş, ayrıca her bir parametrenin deformasyonlar üzerindeki önemi araştırılmıştır. Çalışmalarda, destekleme sisteminin davranışını etkileyen en önemli parametrenin kazı derinliği olduğu görülmüştür. Modelin

doğruluğunu göstermek için, istatistiksel yaklaşımlardan elde edilen sonuçlar gerçek durumlarla karşılaştırılmıştır.
Çalışma sonucunda, önerilen denklemlerin duvar deformasyonlarını ve oturmaları kabul edilebilir bir aralıkta tahmin edebildiği görülmektedir.

Anahtar Kelimeler: Destekli kazılar, sonlu elemanlar yöntemi, yumuşak zemin, küçük şekil değiştirme, regresyon analizi.

ACKNOWLEDGEMENT

I would like to express my deep gratitude to my advisor Prof. Dr. Berna UNUTMAZ for her guidance and patience during this thesis. In every step, she was very kind and understanding. It was a great chance to study with her.

I owe my sincere thanks to the thesis monitoring committee members, Prof. Dr. Nihat Sinan IŞIK and Assoc. Prof. Dr. Mustafa Kerem KOÇKAR for sparing their valuable time to examine this thesis.

I would also like to thank my head of department at the Ministry of Health, Abdurrahman ATLİ, for his patience, support and kind attitude.

I would like to thank my family for being with me and supporting me throughout my life.

I would also like to express my deepest and special gratitude to my wife Nezire BAHADIR for her great support and encouragement.

Finally, I would like to dedicate this thesis to my dear daughter İpek BAHADIR, who showed great patience throughout the whole process.

TABLE OF CONTENTS

LIST OF TABLES

LIST OF FIGURES

SYMBOLS AND ABBREVIATIONS

Symbols

c'	Effective cohesion
c	Cohesion
c_u	Undrained shear strength
c_c	Compression index
c_s	Swelling index or reloading index
$c_{increment}$	Cohesion increases with depth
D	The length of the embedded wall
d	Wall thickness
e_{init}	Initial void ratio
E	Elastisite(Young) Modülü
EA	Strut stiffness
E_i	Initial modulus
EI	bending stiffness of retaining wall
E_s	Secant modulus of the soil
E_w	Young’s modulus of the wall
E_s/s_u	Normalized stiffness
E_{oed}^{ref}	Tangent stiffness
E_{ur}^{ref}	Loading/unloading stiffness
E_{50}^{ref}	Secant stiffness
E_0	Small strain Young’s modulus
G	Shear stiffness
G_s	Secant shear modulus
G_0^{ref}	Small-strain shear modulus
H_e	Excavation depth
h	Average distance between struts
h_{avg}	Average vertical strut spacing
I_P	Plasticity index
I_w	Moment of inertia of the wall per linear meter

K_0^{nc}	Coefficient of earth pressure at-rest
K	Dimensionless coefficients
K_s	System stiffness
M	Stress-level dependency of the stiffness
N_c	Bearing capacity factor at the bottom of the excavation
P_a:	Atmospheric pressure
q	Deviator stress (shear stress)
ρ	Significance
p'	Average effective stress
p^{ref}	Reference pressure
R	Relative stiffness ratio
R_f	Failure ratio
R_{inter}	Strength reduction factor for interfaces
S	Soft soil thickness
S_{ub}	The undrained shear strength below the bottom of the excavation
S_{uu}	Undrained shear strength above the bottom of the excavation
s_u/σ_v'	Normalized strength
u	Pore pressure
W	Excavation width
ε	Extension or contraction of elastic material
ε_v^p	Plastic volumetric strain
Φ	Strut diameter
ϕ'	Internal friction angle
ϕ_{cv}	Critical state internal friction angle
ϕ_m	Mobilized internal friction angle
ψ	Dilatancy angle
ψ_m	Mobilized dilatation angle
γ	Unit weight of the soil above the bottom of the excavation
γ^p	Shear plastic strain
γ_s	Soft soil unit weight
γ_w	Unit weight of water
γ_{zx}	Shear strain
$\gamma_{0.7}$	Shear strain level

δ_{hm}	Maximum wall deflection
δ_{vm}	Maximum ground surface settlement
β	Standardized Coefficients
$\sigma_{tension}$	Tensile stress
σ'_{v0}	Current vertical effective
σ'_1	Effective vertical stress
$(\sigma_1 - \sigma_3)$	Deviatory stress
$(\sigma_1 - \sigma_3)_{ult}$	Asymptotic value for deviatory stress
v	Specific volume
v_s	Specific volume values based on the stress history of the soil
v_{ur}	Poisson's ratio
λ	Compression index
λ^*	Modified compression index
κ	Swelling index
κ^*	Modified swelling index
δ_{hm}	Maximum Horizontal Wall Displacement
δ_{vm}	Maximum Ground Settlement

Abbreviations

AASHTO	American Association of State Highway and Transportation Officials
AIR	Apparent İnfluence Range
ASTM	American Society for Testing and Materials
BEM	Boundary Element Method
BS8081	British Standard
CLS	Critical State Line
CC	Cam-Clay Model
CIUC	Consolidated Isotopically Undrained Compression Test
CGS	Compaction Grouting System
DMT	Dilatometer test
DDA	Discontinuous Deformation Analysis
DEM	Discrete Element Method
FHWA	Federal Highway Administration
FDM	Finite Difference Method
FEM	Finite Element Method
FOS	Factor of safety against basal heave
HS	Hardening Soil Model
HSS	Hardening Soil Small Strain Model
LE	Linear Elastic Model
MC	Mohr-Coulomb Model
MCC	Modified Cam-Clay Model
NAVFAC	Naval Facilities Engineering Command
PFM	Particle Flow Method
OCR	Over-Consolidated Ratio
USACE	United States Army Corps of Engineers
USC	Undrained Soft Clay Model
VIF	Variance Inflation Factor

1. INTRODUCTION

1.1. The Importance of Deep Excavations

Today, the importance of underground spaces is increasing with increasing urbanization. As a result of this increase, the use of deep excavations has become quite widespread. Especially in city centers, construction sites are costly and excavations cannot be built with slopes. Also, for more space, it is necessary to dig deeper. For the reasons stated above, it is inevitable to construct supported excavations.

Supported deep excavations are frequently used in cities for many different purposes, e.g. parking garages, structures with basements, metro stations, and so on. It is also very important to support these safely. For this purpose, excavation support systems in various forms have been developed. One of the most important of these is the supported diaphragm walls. These walls are often used in environments where there is a structure adjacent to the excavation, soft soil conditions and high groundwater levels.

Although the use of these systems is favorable to obtain the desired spaces in the underground, it can create negative situations for the structures adjacent to the excavation. During the construction of deep excavations, undesirable deformations may occur. Keeping these deformations at a reasonable level is very important in terms of life and property safety.

A lot of work has been done in the estimation of excavation-induced deformations from past to present. However, the importance of the parameters affecting the deformations has not been investigated sufficiently. In this study, the most influential parameters on deformations were determined and it was investigated which parameter was more effective. It is thought that this study will contribute to the literature in estimating the deformation of diaphragm walls built on soft soils.

1.2. Deep Excavations in Soft Soil

Deep braced excavations in soft soil environments are the focus of this research. Due to low strength and great compressibility, normally consolidated soils commonly generate large displacements when paired with high groundwater levels. Soft soils are common in alluvial environments, where fine grained soils such as normally consolidated clay, clayey silt, peat, and fine graded sands were brought in by rivers and oceans. These Deltaic regions are also the world's most densely populated locations.

The findings of this study could be applied in these areas. In particular, settlements at the buildings in the vicinity of deep excavations can be critical. To prevent this type of damage, during the design of the supporting wall, detailed analyses using a suitable soil model with the right parameters before the construction is adequate. This study deals with the response of the soft soils after excavations.

1.3. The Purpose of This Research

The goal of this thesis is to determine how much wall deformation and settlement can occur in supported deep excavations built on soft soils. For the estimation of deformations, a simple regression model was created in this study.

With statistical studies, it was investigated which parameter had a greater effect on the deformation behavior. In addition, error levels according to the values of the parameters affecting the deformations are shown in graphics.

As a result, it is thought that this study would give important ideas to the designers about the amount of deformation and the importance of the selected parameters at the preliminary project stage.

1.4 The Scope of This Study

The research is divided into seven chapters. In the first part of the study, the importance of deep strutted excavations is mentioned, excavations on soft soils are emphasized, and the works carried out are briefly summarized.

In the second part, a general literature study was made about deep excavations, and then the studies used within the scope of the study were evaluated in more detail.

In the third part, the most accepted soil models from past to present were mentioned. Soil models used within the scope of the study were explained in more detail.

In the fourth part of the study, a detailed parameter study was conducted, parameters affecting deformations were investigated and parameter ranges were obtained from comprehensive case studies.

In the fifth part, numerous generic cases analyses have been carried out considering parameters such as excavation geometry, soil stiffness, soil strength, soil unit weight, wall stiffness, and their variations. The data obtained from many cases around the world were compared with the data obtained. With this method, the parameters selected in the first section and their ranges were verified.

In the sixth part of the study, statistical studies were explained in detail and closed-form solutions were proposed for settlement and wall deflection deformation estimations. In addition, the effects of each parameter on these deformations were investigated separately.

In the sixth section of the study, parameter-based analyses were conducted to establish the model's error level. The proposed equations have been validated using the real case history data obtained from the literature.

Finally, the last section presents the summary and conclusions, as well as recommendations and the proposed simplified model. The limitations of the model and future work are also considered in this section. The summary flow chart of the study can be seen in Figure 1.1.

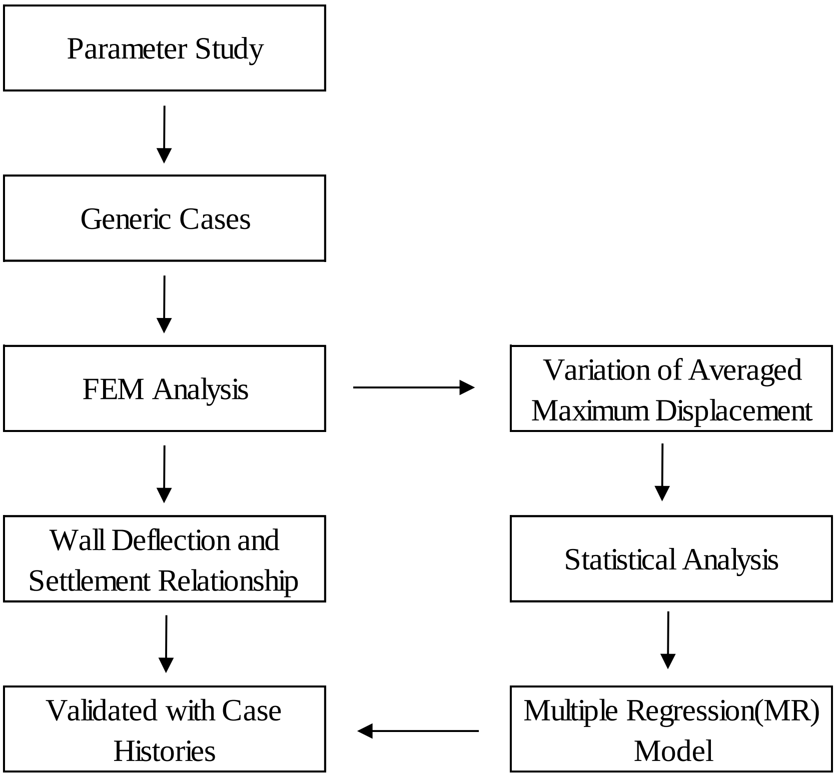

Figure 1.1 Flow Chart of Study.

2. LITERATURE SURVEY

2.1. Introduction

Deflection behavior of braced excavations has been investigated by many researchers around the world for many years (Peck, 1969; Mana & Clough, 1981; O'Rourke 1981; Finno et al., 1989, Finno and Nerby, 1989; Clough and O'Rourke, 1990; Whittle and Hashash, 1993; Ou et al. 2000; Long, 2001).

Although there are many studies on wall deformations for soft soils in the literature, studies on the calculation of settlements are limited (Bryson and Zapata-Medina, 2012). In general, wall deformations due to deep excavations can be estimated with sufficient accuracy (Atkinson, 1993; Hashash and Whittle, 1996), however, the surface settlement estimates are generally far from the observed values. To overcome this situation, some researchers have developed models that consider small strain stiffness (Burland, 1989; Benz et al., 2009; Simpson, 1992; Stallebrass and Taylor, 1997; Kung, 2003). In recent research, it has been shown that the small strain stiffness of soils plays an active role in settlement behavior.

Small-strain stiffness can cause deformations to be overestimated by up to 80%, resulting in a conservative and costly design. (Hsieh et al., 2017). Some of the studies carried out from the past to the present are presented below.

2.2. Previous Studies

Peck (1969) shows that surface settlements depend on the distance to the excavation site in different soil types. Peck proposed three zones of settlement for soil conditions. Excavations in soils with low strength and stiffness cause more wall deflection and ground settlements.

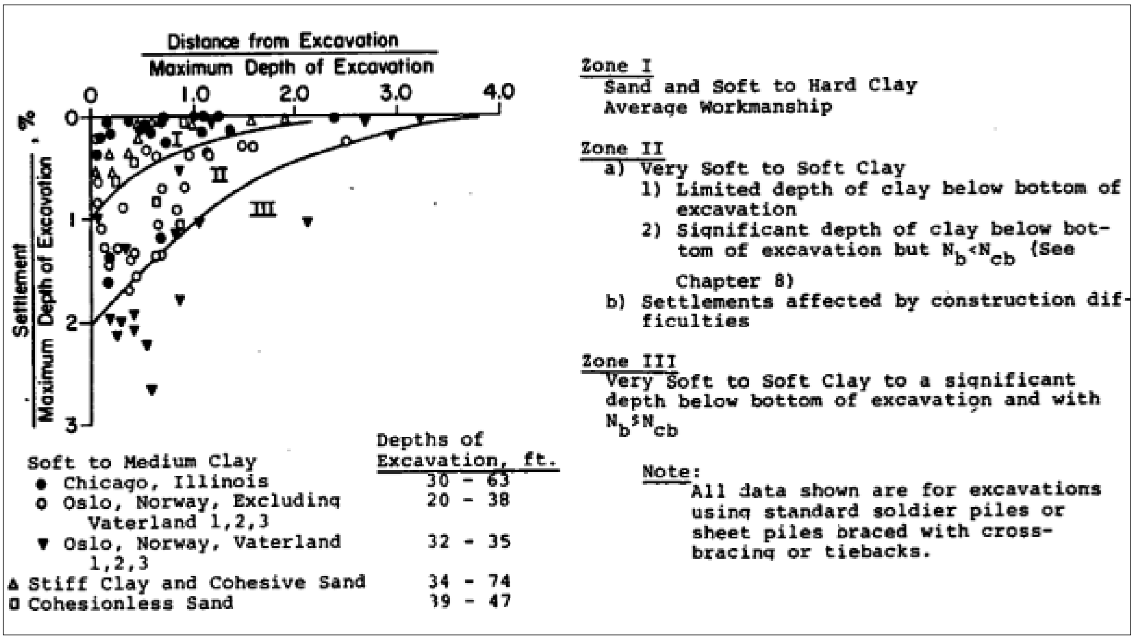

Figure 2.2. Effect of the soil type on the settlements induced by deep excavation (Peck, 1969).

Goldberg et al. (1976) showed the maximum lateral deformations for deep excavations in clays can be estimated using the stability number and the stiffness of the supporting structure

$(\gamma H/c_u)$: The stability number:

where;

γ: Soil unit weight

H: Excavation depth

c_u: Undrained strength

$(E_w I_w/h^4)$: The stiffness of the supporting system

Where;

E_w: Young's modulus of the diaphragm wall

I_w : Inertia of the diaphragm wall per linear meter

h : Distance between struts

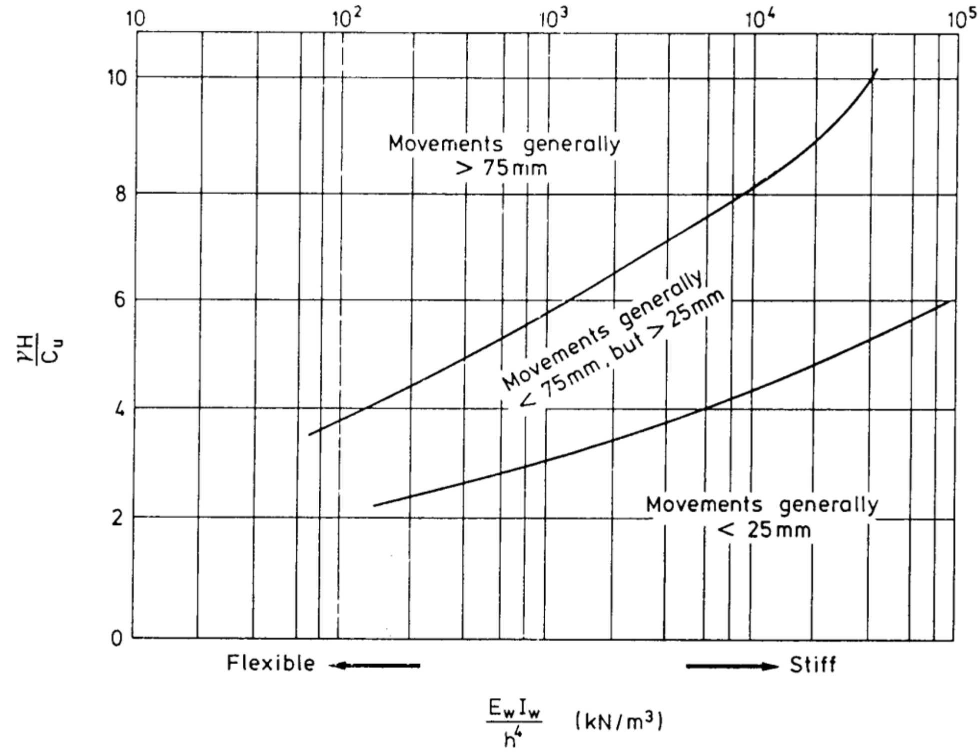

Figure 2.3. Influence of stability number on the wall deformations
(Goldberg et al. 1976).

Mana & Clough (1981) examined range of brace excavation case studies (about 11) and found a relationship between δ_{hm} and the potential for base heave with regards to Terzaghi's factor of safety (1943). Based on case-history data, an empirical chart was created to predict the max. braced wall displacement in normally consolidated clays using a factor of safety number(FoS) against base heave.

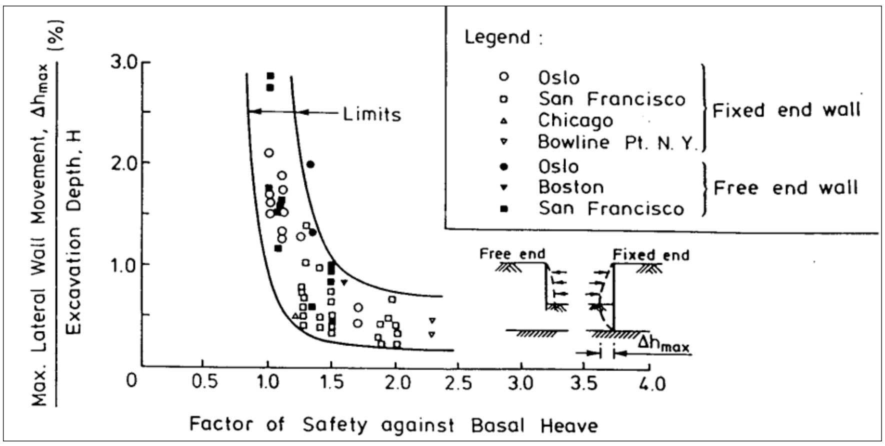

Fig .2.4. Safety factor against base heave (Mana & Clough 1981).

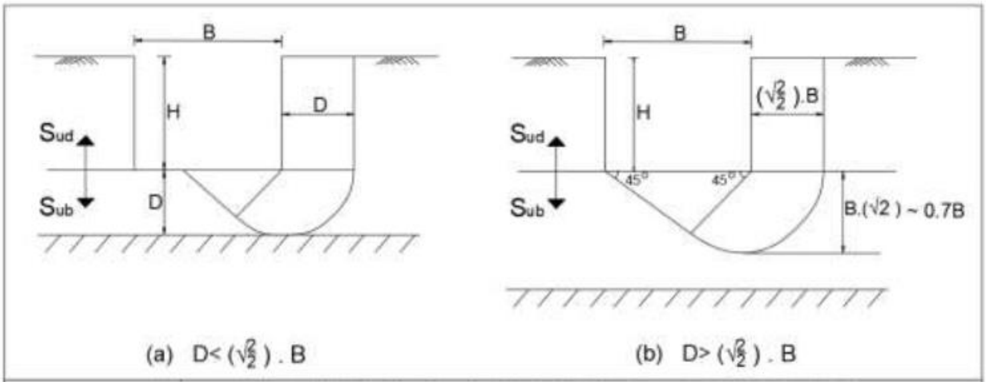

Factor of safety against excavation basal heave		
Terzaghi (1943)	$FS = \frac{1}{H} \cdot \frac{Nc.S_{ub}}{\gamma - S_{ud}/D}$	$FS = \frac{1}{H} \cdot \frac{Nc.S_{ub}}{\gamma(\frac{\sqrt{2}}{2}) - S_{ud}/B}$
Bjerrum ve Eide (1956)	$FS = \frac{1}{H} \cdot \frac{Nc.S_{ub}}{\gamma}$	

Figure .2.5. FoS in terms of base heave on soft soil.

Factor of Safety	Notes	Reference
$FS_{T1} = \frac{5.7c_u B_1}{\gamma H B_1 - c_u H}$	Wide excavations ($B > H$) of rectangular shape	Terzaghi (1943)
$FS_{T2} = \frac{5.14c_u + \sqrt{2}(\frac{H_w}{B}) + 2c_u(\frac{D}{B})}{\gamma H}$	Embedded wall considered; Perfectly smooth footing ($N_c = 5.14$)	Terzaghi (1943)
$FS_{B\&E} = \frac{c_u N_c}{\gamma H + q}$	Narrow excavations ($B < H$)	Bjerrum& Eide (1956)
$FS_{Gh} = \frac{c_u N_h}{\gamma H + q}\mu_t \mu_d \mu_w$	Homogenous and constant c_u; $H/B <$ 0.6	Goh (1994)

Figure 2.6. Conventional methods for the basal heave calculation.

Clough, (1990) suggested system stiffness number to investigate the impact of wall movement on stiffness of braced system. For soft to medium clay, they established a correlation between K_s and maximum lateral wall deflection. This approach has been shown to be useful in soft soil excavation environments.

$$K_S = \frac{E_w I}{\gamma_w h^4}$$

Where:

E_w : Elastic modulus of the braced wall

I: Inertia of the braced wall (I = $t^3/12$)

h: Vertical strut distance

γ_w: Unit weight of water.

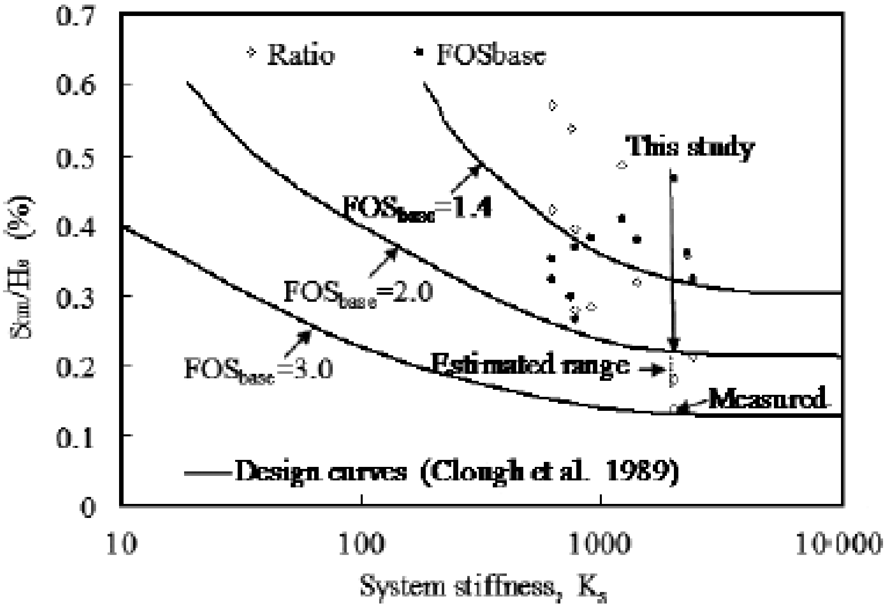

Figure 2.7. Relation between maximum wall deflection and K_s (Clough, et al. 1989).

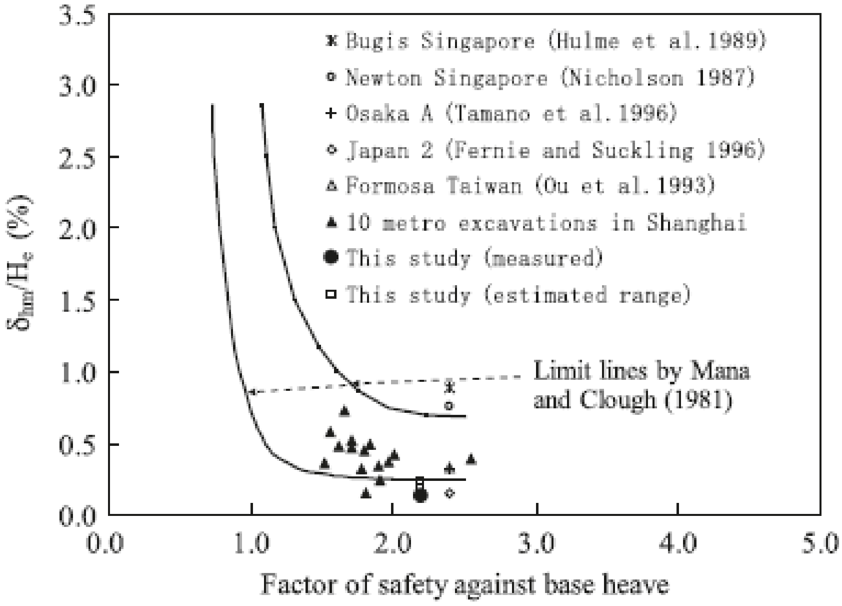

Fig. 2.8. Relationship between max. wall movement- FoS (Clough & O'Rourke 1990)

Clough, (1990) developed the following equation to determine FOS_{base}, which is illustrated in Figure 2.8.

$$FOS_{base} = \frac{N_c S_{ub}}{H[\gamma - (S_{uu}/0{,}7B)]}$$

Where:

N_c: The bearing capacity factor number

S_{ub}: The undrained shear strength below of the excavation

H: The depth of the braced excavation

γ: The unit weight of the soft soil above the bottom of the braced excavation

S_{uu}: The undrained shear strength above the bottom of the braced excavation

B: The effective width of the excavation

Clough and O'Rourke (1990) suggested a semi empirical chart (Figure 2.8) for determining
δ_{hm} for soft clayey soil, which can consider (FoS) and ($EI/\gamma_w h_{avg}^4$). This chart is the most commonly accepted method for simulating the max. wall movement by practicing engineers.

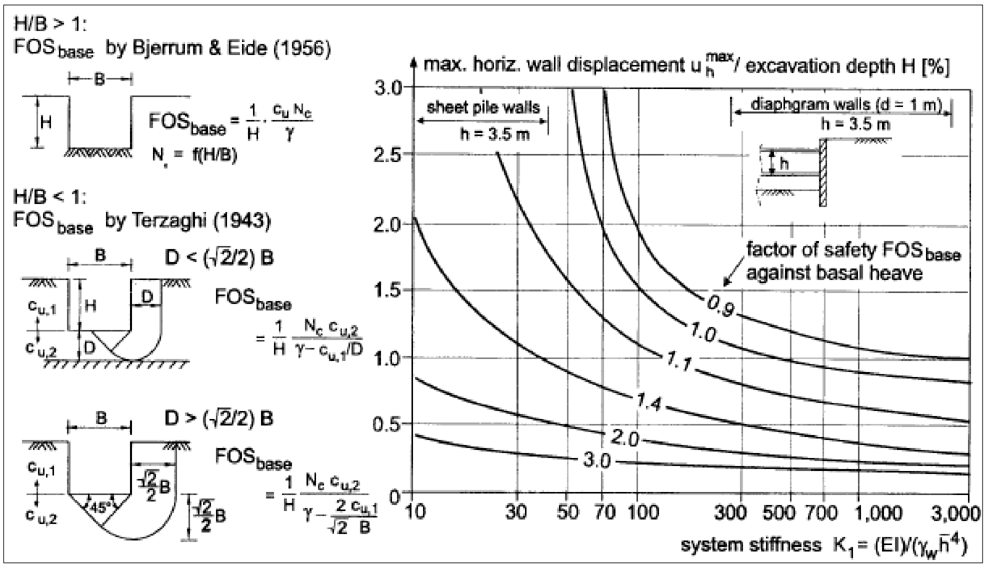

Fig. 2.9. Design charts for max. wall movement for braced cutting systems in soft clayey soils (Clough and O'Rourke 1990).

Clough and O'Rourke (1990) argue that an excavation's maximum surface settlement is often less than 0.5% H_e. They also created settlement envelopes based on soil type for calculating settlement profiles near to excavations. Ground surface settlement shape in the sandy soil and stiff to very hard clayey soils are concave shape, soft to medium clayey soils are trapezoidal shape (Figure 2.9) and Figure 2.10 show that Wall stiffness has important role for soft to medium clay

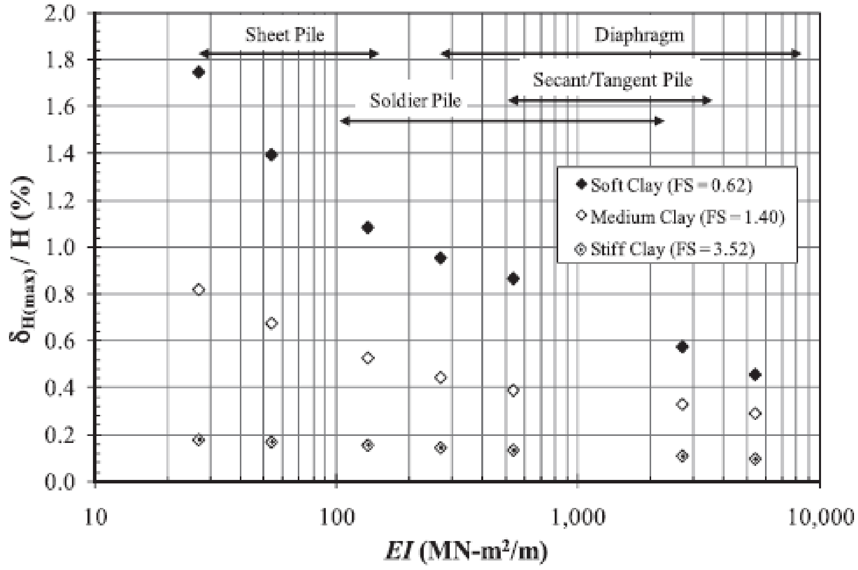

Figure 2.10. The typical ranges of bending stiffness of braced excavations

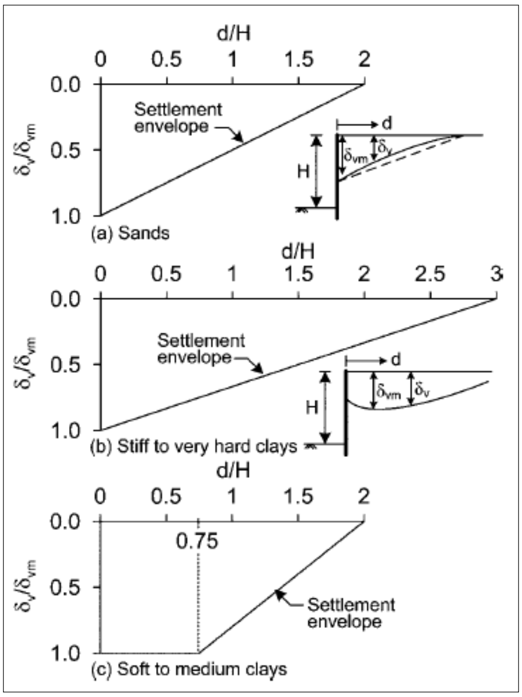

Figure 2.11. Design charts for predicting ground movement

The maximum horizontal wall deflection in stiff over consolidated clays, residual soils, and sandy soils is around 0.2 percent of the braced excavation depth, with a maximum soil settlement behind the braced wall of around 0.15 percent to 0.3 percent of the braced excavation depth. The region of influence extends three times the depth of the excavation.

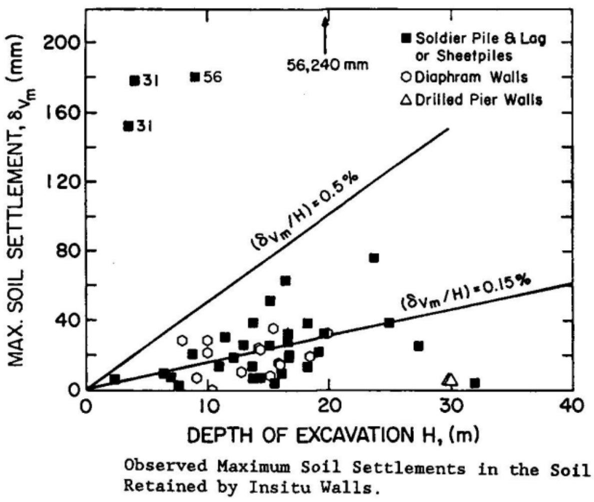

Fig. 2.12. Monitored max. wall movement and surface movements for over consolidated clays (Peck, 1969).

The results reveal a considerable influence of braced wall stiffness and support space on wall displacement in soft clay (Figure 2.12) and typically the same maximum deformations as Peck (1969). The max. surface movement occurs in a region up to 0.75 times the cutting depth from the braced wall, according to the ground surface settlement profile taken from the excavation's border.

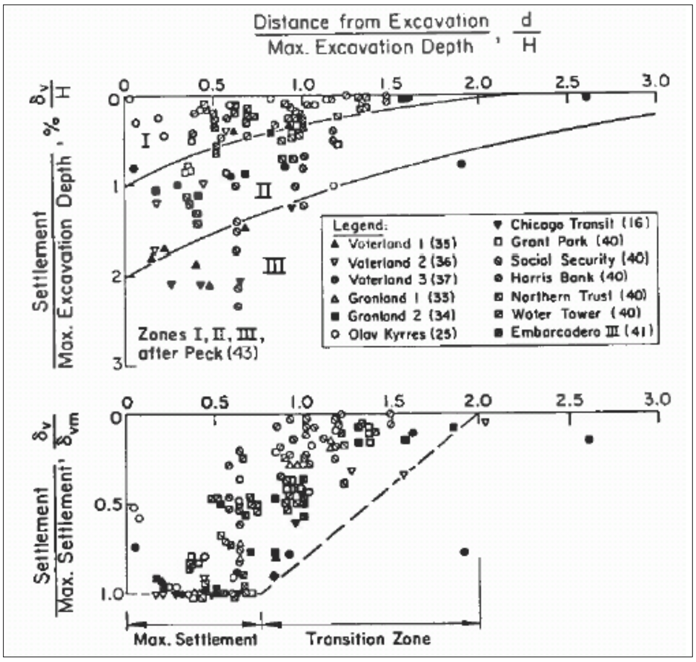

Fig. 2.13. Monitored surface movements next to braced excavations in soft soils (Peck 1969).

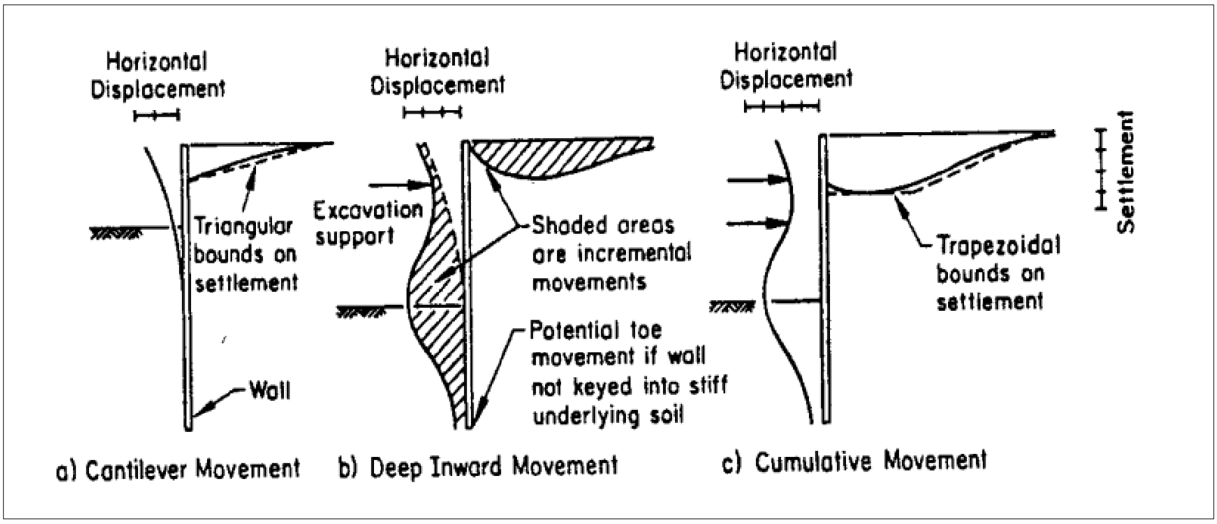

Fig. 2.14. Common displacement characteristics for braced walls.

The position and amount of max. wall deflection, as well as the relation between max. wall deformation and max. ground surface settlement, were investigated by Ou et al. (1993). Apparent Influence Range was suggested by Ou et al. (1993). (AIR)

$$AIR = (H_0 + D)tan(45 - \frac{\varphi}{2})$$

Where;

AIR : Apparent Influence Range

φ : The internal friction angle

H_0 : Depth of the final excavation

D : The embedding wall's total length

To investigate the features of excavation behavior, 10 excavation examples in Taipei were chosen. And an empirical approach is suggested to estimate the ground surface movement.

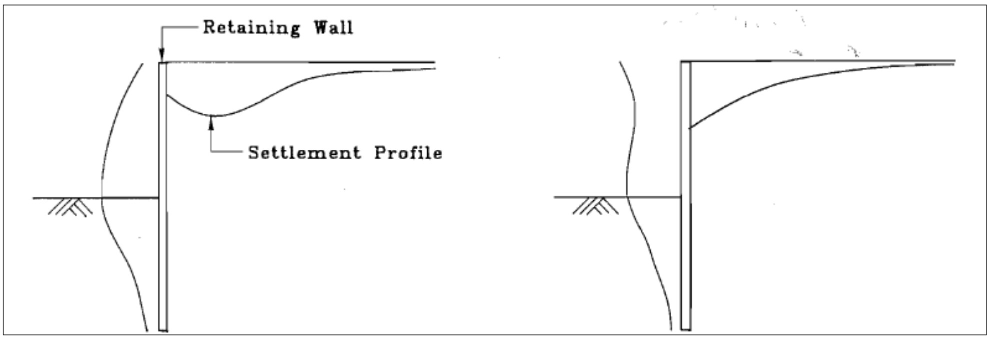

Figure 2.15. Different shapes of settlement (Ou et al. 1993).

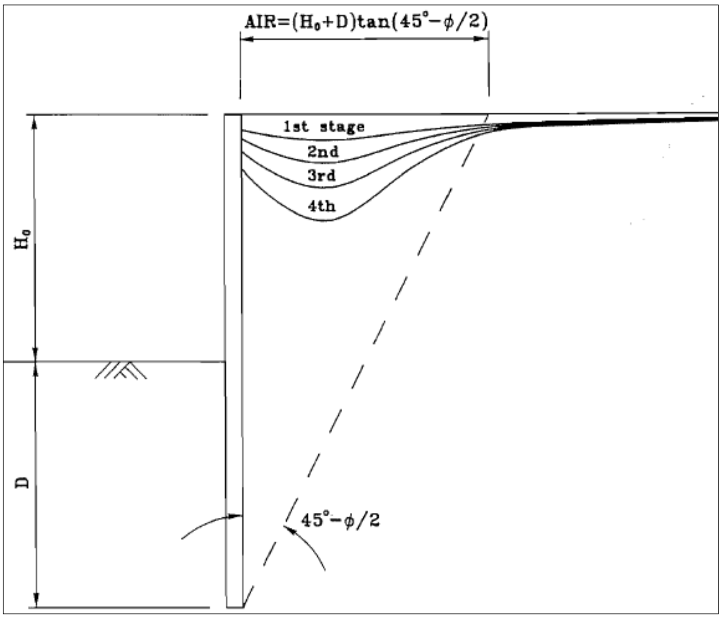

Figure 2.16. Relationship between AIR and length of the braced wall (Ou et al. 1993).

Ou et al. (1993) suggested a trilinear line for estimating surface movement pattern.

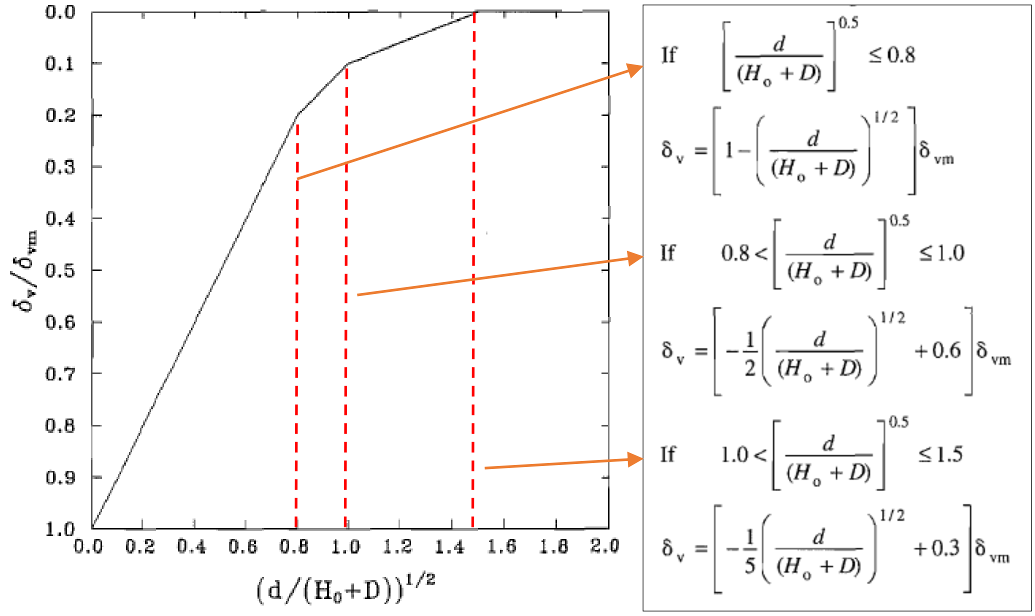

(a) (b)

Figure 2.17. Proposed relationship (a) and equations (b) between settlement and distance from wall (Ou et al. 1993).

As a result, of study;

- Near the excavation surface, the max. wall deflection occurs frequently.
- The max. wall deflection is within the range of $0.002H_0$-$0.005H_0$.
- The max. soil vertical movement is equivalent to the max. wall deformation at its highest limit.
- Generally, the max. vertical movement, δ_{vm} = $0.5\delta_{hm}$-$0.7\delta_{hm}$ for most excavation cases.

Settlement profiles caused by braced excavation were proposed by Hsieh and Ou, (1998). Based on a regression study of surface movement curves with generally cohesive soil conditions seen in the field. In general, the max. settlement, δ_{vm}, is $0.5\delta_{hm}$ to $0.75\delta_{hm}$.

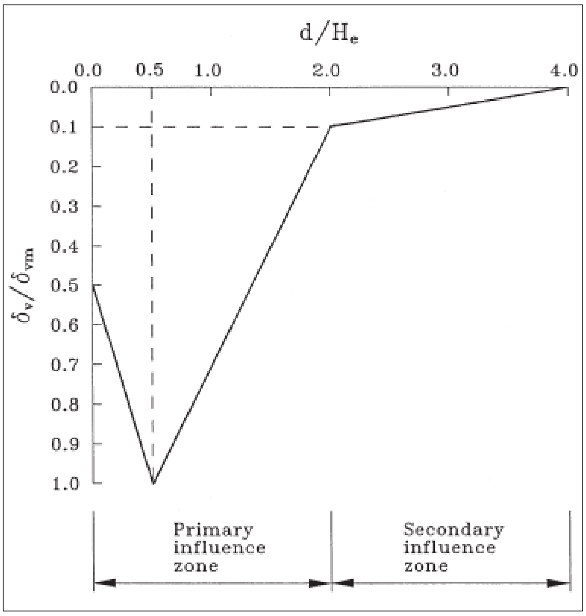

Figure 2. 18. Maximum ground surface settlement (Hsieh and Ou, 1998).

$$\delta_v = \left(-0.636 \sqrt{\frac{d}{H_e}} + 1 \right) \delta_{vm}$$

If $d/H_e \leq 2$;

$$\delta_v = \left(-0.636 \sqrt{\frac{d}{H_e}} + 1 \right) \delta_{vm}$$

If $2 < d/H_e \leq 4$;

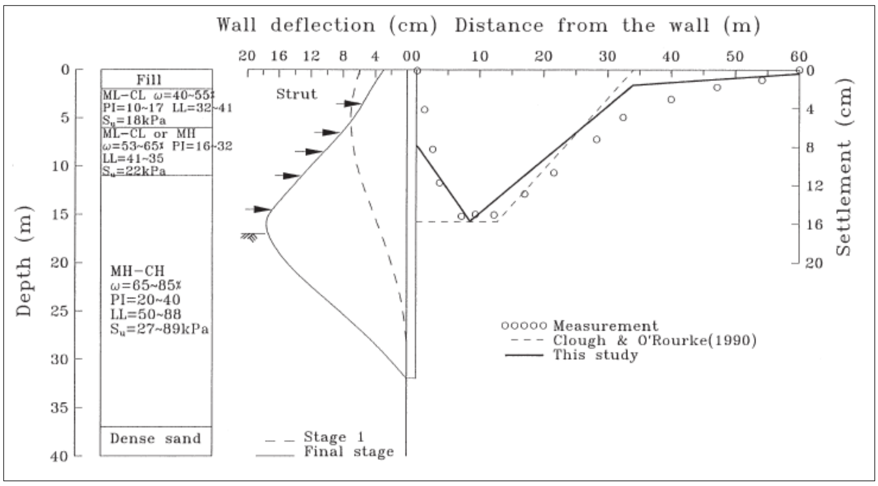

Figure 2. 19. Suggested settlement profile (Hsieh and Ou, 1998).

Long (2001) analyzed 296 case histories and checked Clough, (1990) graph against the study data. He reached the conclusion that if the braced excavation has a factor of safety (FoS) greater than 3, wall stiffness has no effect on deformation.

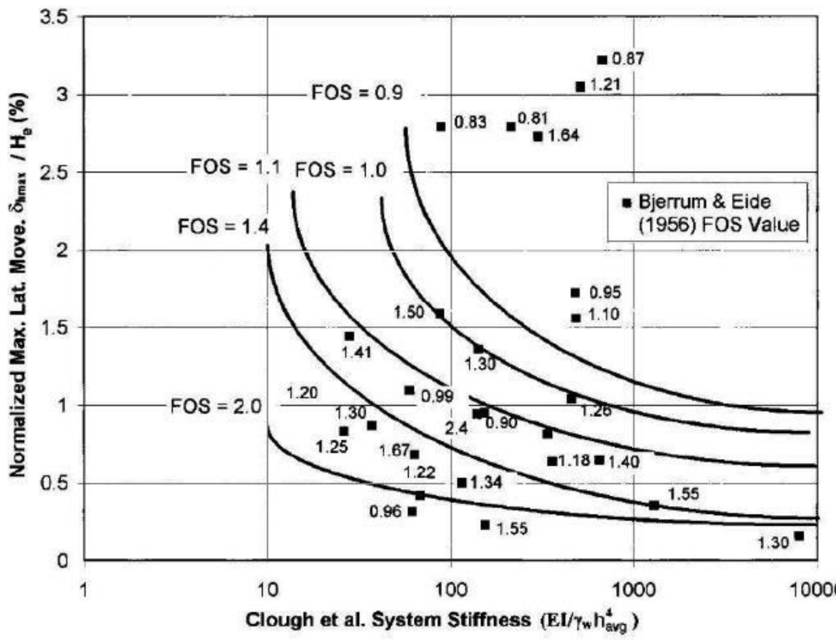

Figure 2. 20. Normalized field measurements of the lateral deformations against Clough & O'Rourke's (1990)

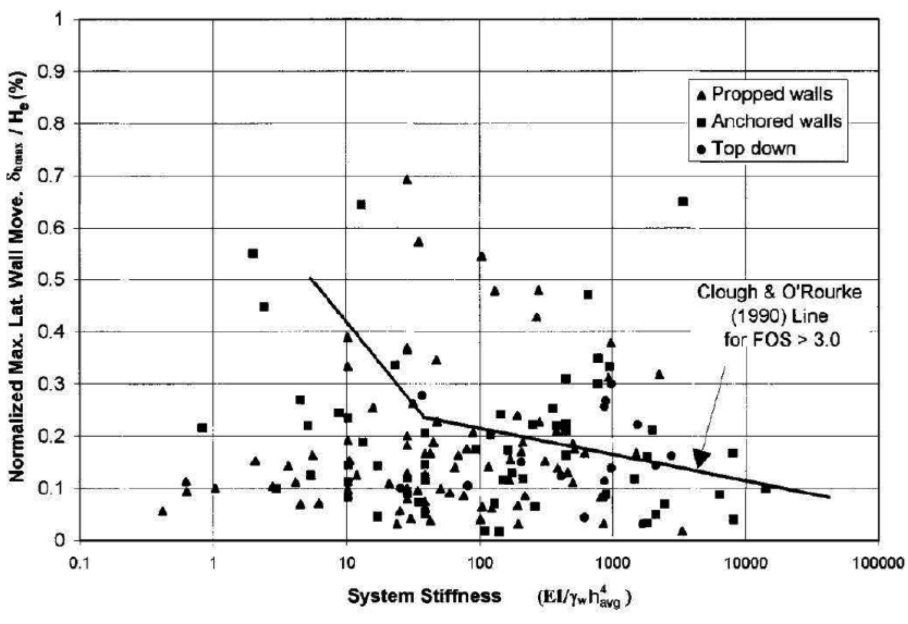

Figure 2.20. Normalized field measurements of the lateral deformations against Clough & O'Rourke's (1990)

The empirical work of retaining wall and surface settlements owing to braced excavations was based on Moormann's (2004) analysis of a comprehensive data base of more than 530 recent worldwide case studies. The gathered information was utilized to examine the primary factors that influence the performance of braced excavations in normally consolidated clays. ($c_u < 75$ kN/m^2).

The main outcomes obtained include the following:

- The max. horizontal wall deflections u_h^{max} quently lie between 0.5%H - 1.0%H, on average at 0.87%H. The max. deflection u_h^{max} is usually measured at a depth of z= 0.5H to 1.0H below ground surface.
- The max. surface settlements at the ground surface behind a braced wall u_v^{max} frequently lie in the range of 0.1% H to 10%H, on average at 1.1%H. The settlement u_v^{max} usually occurs at a distance x of ≤0.5H behind the braced wall, but there are cases in soft soils with up to 2.0H. The quotient u_v^{max}/u_h^{max} mainly between 0.5 and 1.0, but without clear trends.
- The most significant parameters are determined as soil conditions and excavation depth H.
- The retaining wall displacements and surface settlements appear to be mostly unaffected by the retaining system rigidity.

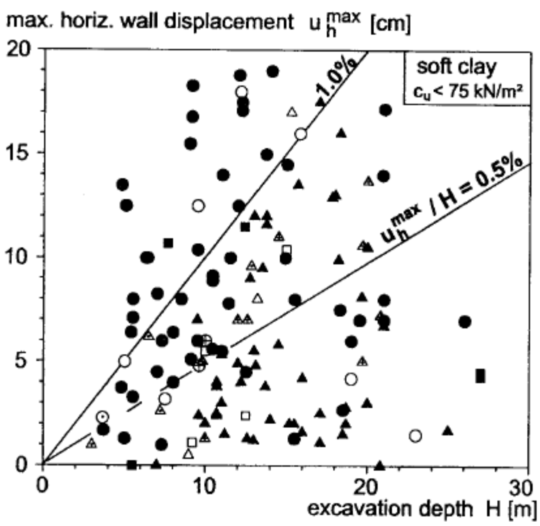

(a)

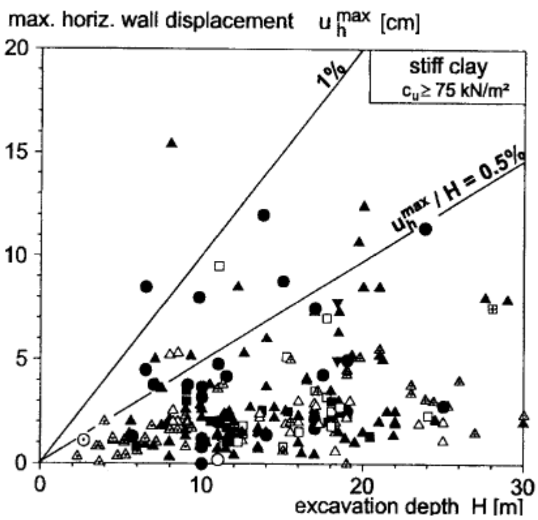

(b)

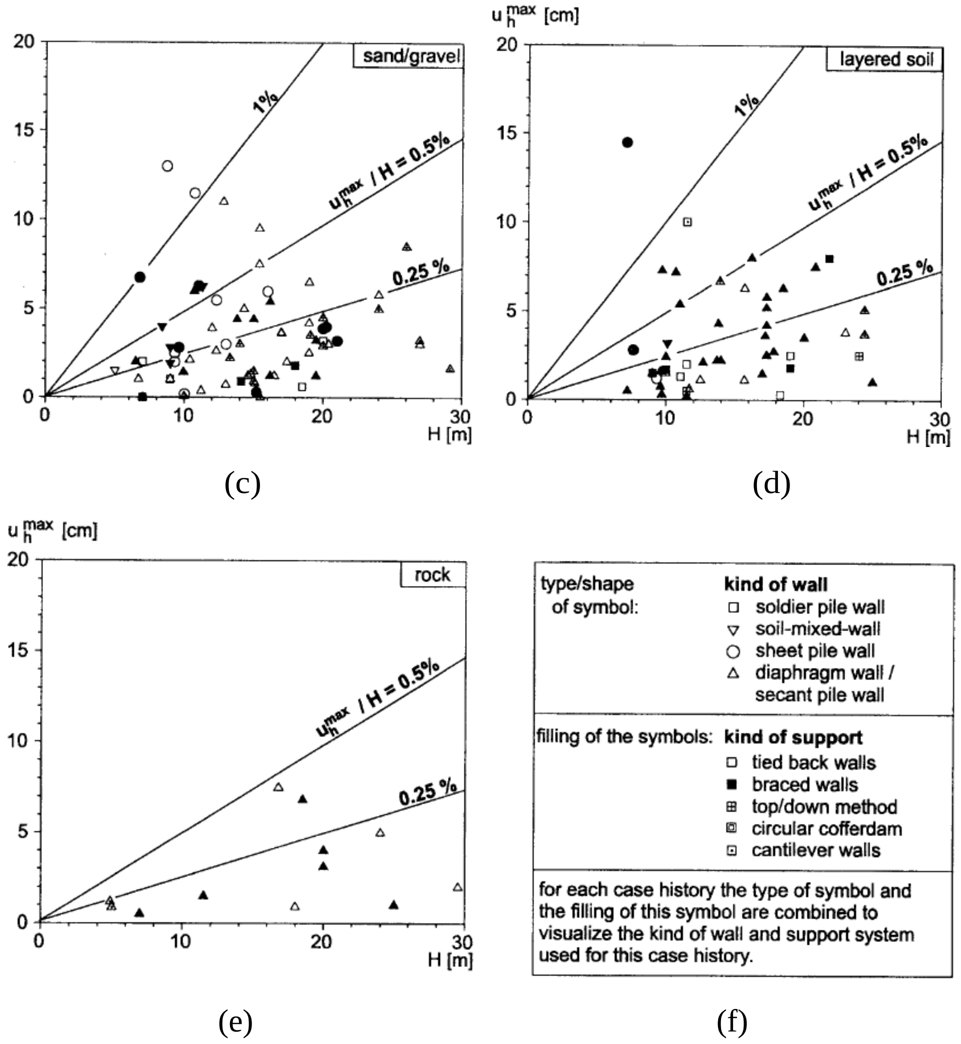

Figure 2. 21. u_h^{max} and .H depending on type of soil, braced wall and support system

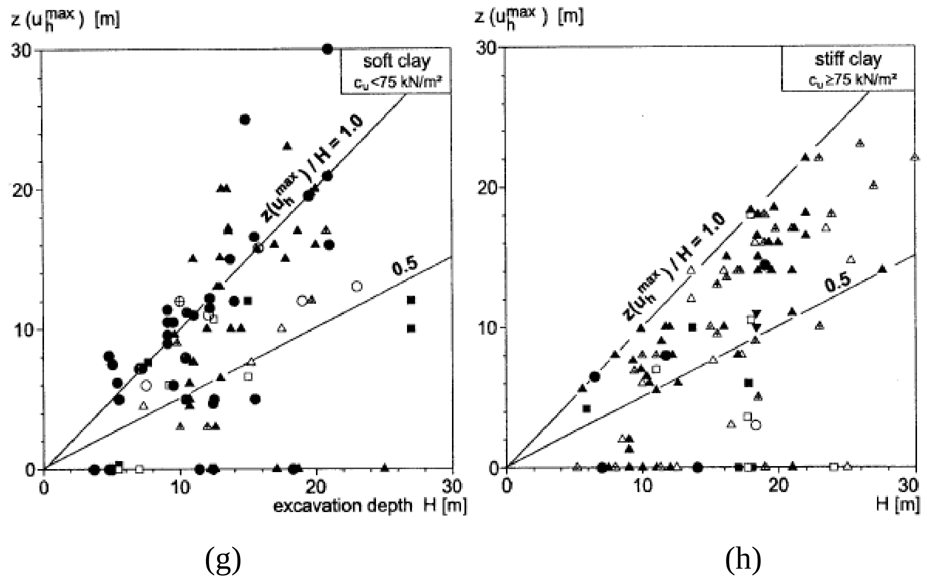

Figure 2.22. Maximum horizontal wall deflection (u_h^{max}) depending on the depth (Moormann, 2004).

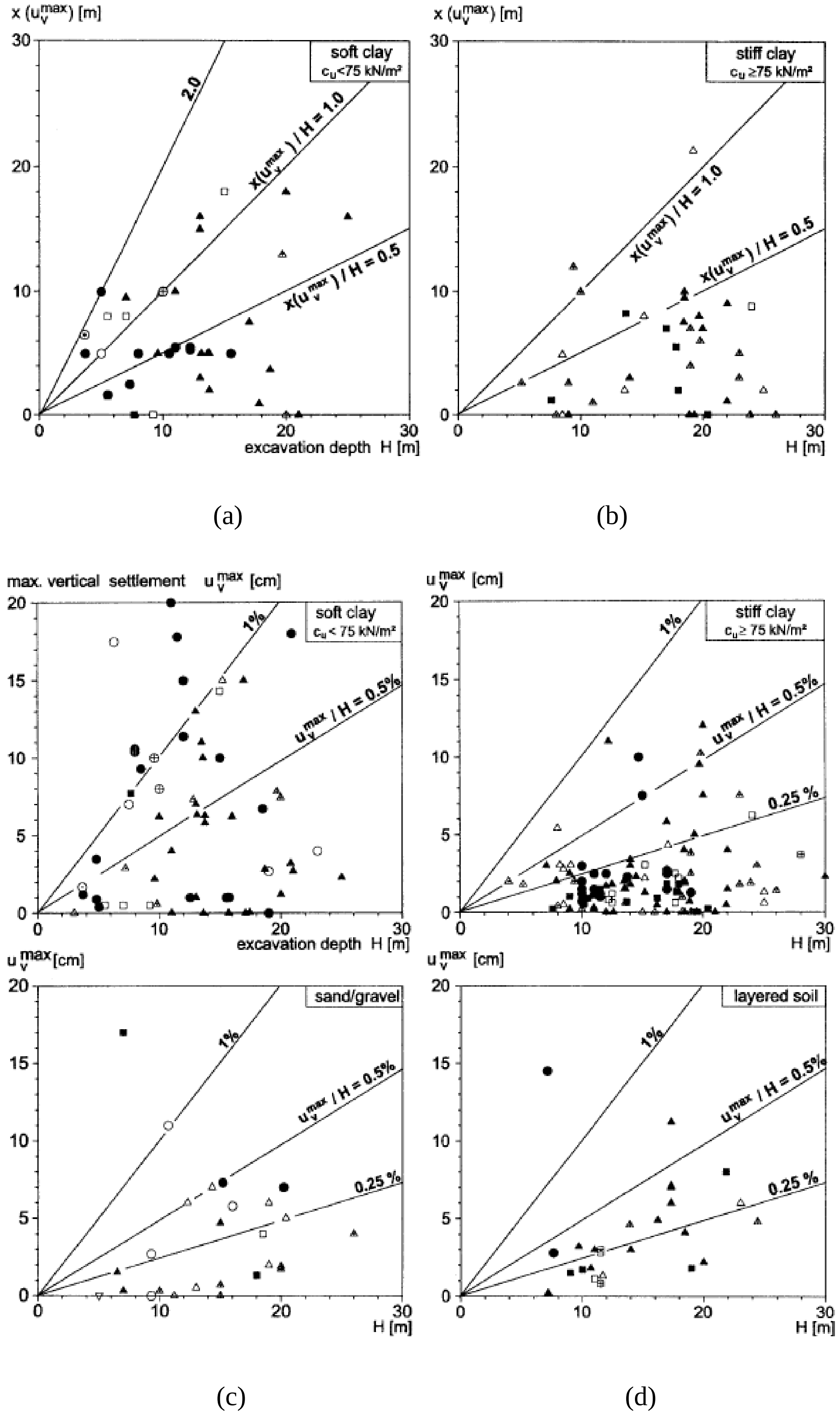

Figure 2. 23. u_v^{max}measured behind retaining wall vs. H depending on type of soil, braced wall and support system.

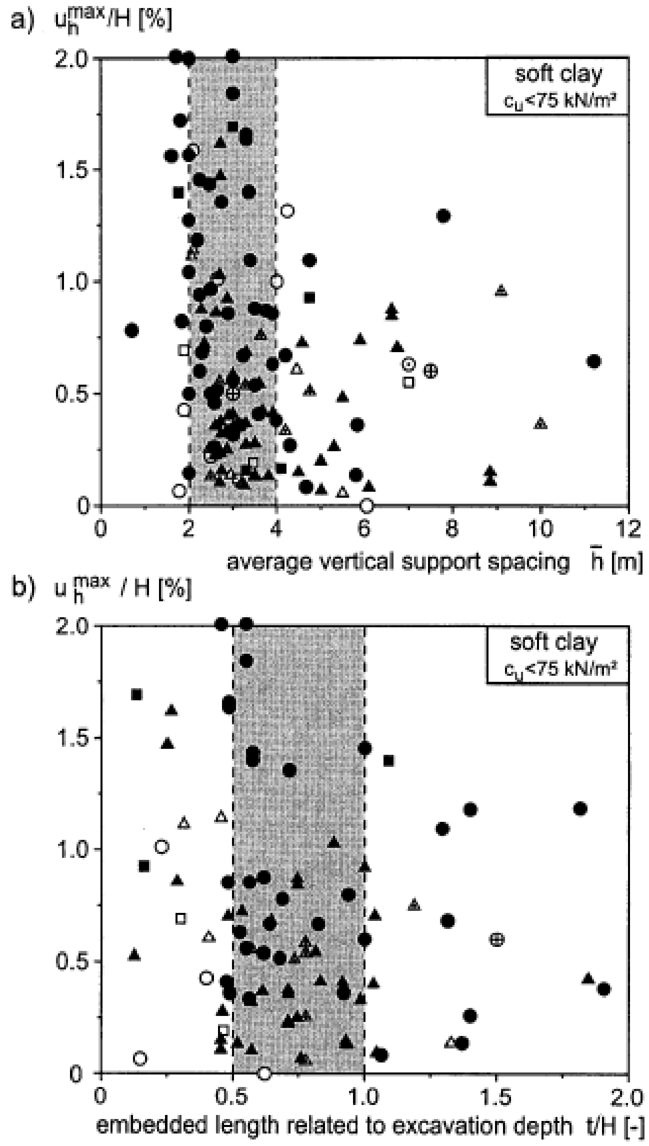

Figure 2. 24. Braced excavations in soft soil: (a) Effect of the average vertical support spacing $\overline{h}$ on the related max. horizontal wall displacement u_h^{max}/H and (b) Influence of embedded length t related to the depth of excavation H (Moormann, 2004).

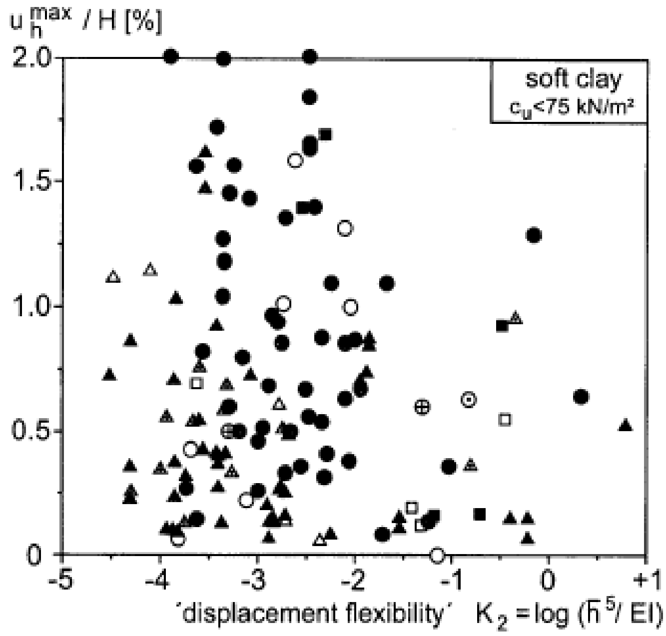

Figure 2. 25. u_h^{max}/H depending on the K_2

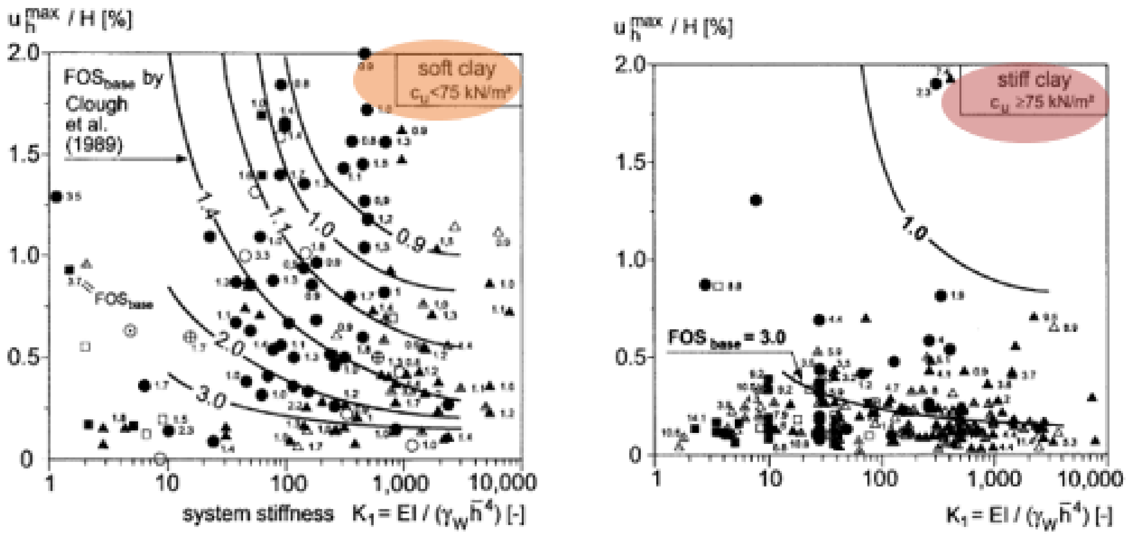

Figure 2. 26. Max. braced wall movement vs. K_1 suggested by Clough, (1990).

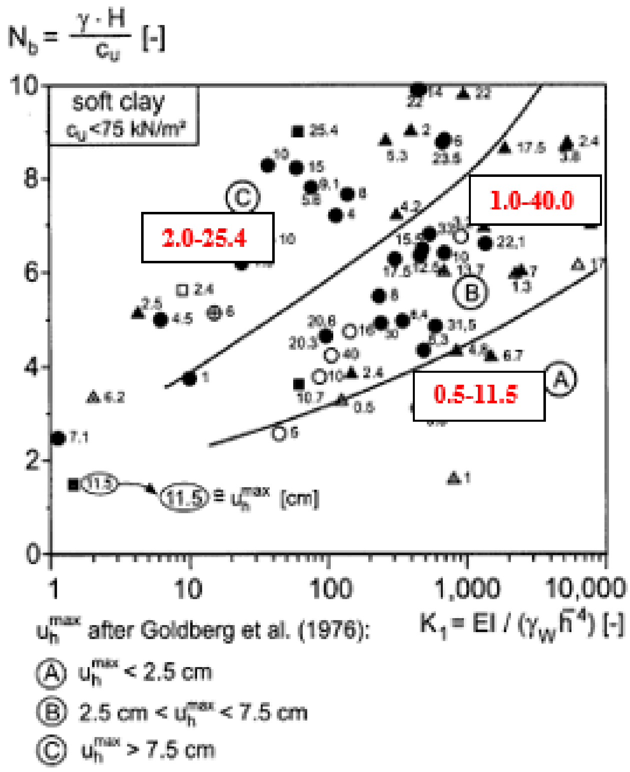

Figure 2. 27. The effect of system stiffness and stability number on soft clay (Goldberg et al. 1976)

Wang et al. (2010) studied 300 case studies of braced wall displacements and ground surface settlements caused by braced excavations in Shanghai soft soils. The maximum lateral displacements of top-down walls, bottom-up walls, diaphragm walls, contiguous pile walls, and compound deep soil mixing walls systems, are 0.27% H, 0.4%H, 1.5%H, 0.55%H, 0.91%H respectively.

The max. surface displacement is 0.42%H on average. The settlement influence region extends from the excavation to a distance of 1.5H to 3.5H. The ratio of max. surface settlement to max. wall deflection typically ranges from 0.4 to 2.0, with an average value of 0.9. The factors that influence the wall's deformation were investigated. It illustrates that with increased system stiffness and the FoS against base heave, there is a small evidence of a trend for reducing wall deflection.

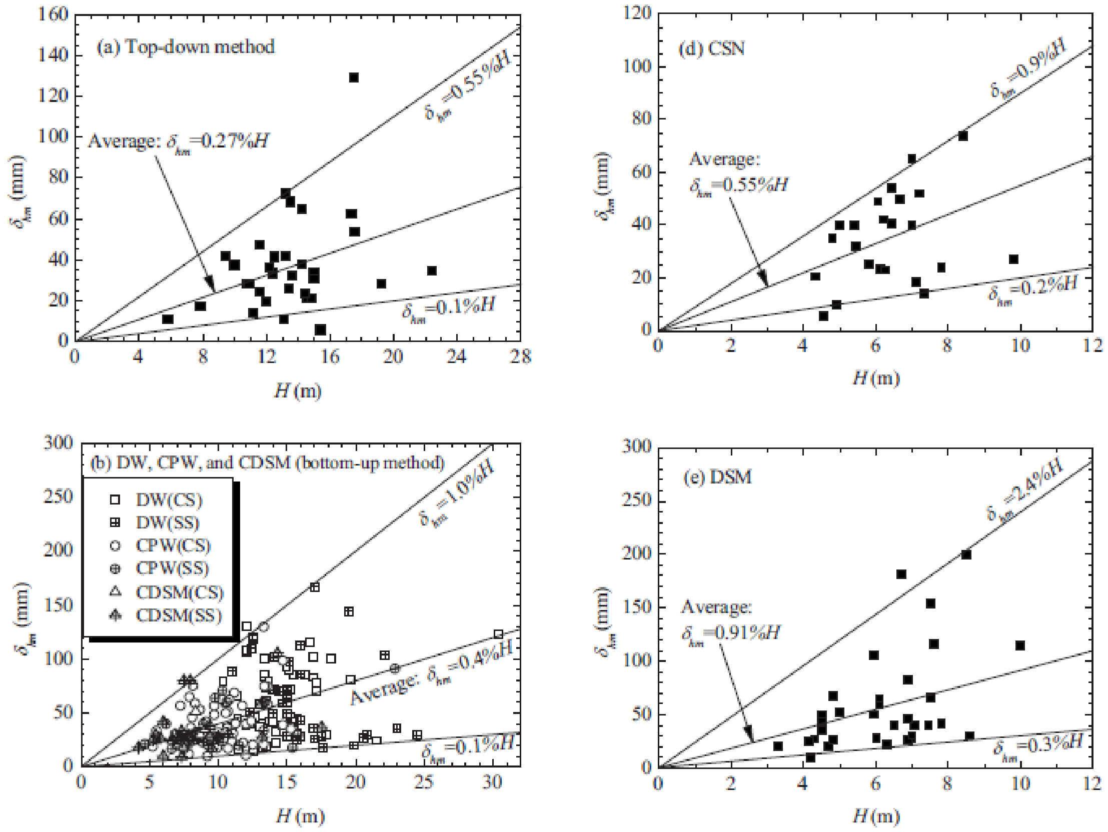

Figure 2. 28. δ_{hm} versus H depending on wall type (Wang et al. 2010).

Bryson and Zapata-Medina, (2012) suggested the relative stiffness ratio .The strength parameters of soil and stiffness parameter of the soil are related to the stiffness of the braced excavation system with this new parameter. Several excavation case histories from around the world were used to assess the suggested methodology's effectiveness. The study revealed that the novel relative stiffness ratio worked effectively in estimating the bending stiffness as well as the actual excavation-induced lateral deformations.

Proposed Stiffness Ratio:

$$R = \frac{E_s}{E} \cdot \frac{S_H S_V H}{I} \cdot \frac{\gamma_s H_e}{s_u}$$

The relative bending resistance

The effects of the soil conditions (Peck 1969) The soil-structure interaction.

Where

R : Relative stiffness ratio

E_s: The soil's Young's modulus

E: The wall's Young's modulus

I: Per unit length of the Wall, the moment of inertia

S_H: Mean horizontal support spacing;

S_V: Mean vertical support spacing

H: Total height of the braced wall;

H_e: Braced Excavation depth

γ_s: Mean unit weight of the soil

s_u: Undrained shear strength of the soil

The data is organized by the (FoS)values. The factor of safety (FoS) is a modified version of Terzaghi's (1943) equation that includes wall embedment effects.

Shear capacity

Shear resistance of the soil mass

Adhesion along the inside faces of the wall assuming a rough surface

$$FS = \frac{s_u N_c + \sqrt{2} s_u (H_e/B) + 2 s_u (D/B)}{\gamma_s H_e}$$

Where:

s_u: Mean undrained shear strength of the soil

N_c: Bearing capacity factor

(Terzaghi (1943) assumed N_c=5.7)

B: Width of the braced excavation

D: Depth of embedment below the braced excavation bottom

γ_s: Unit weight of the soil

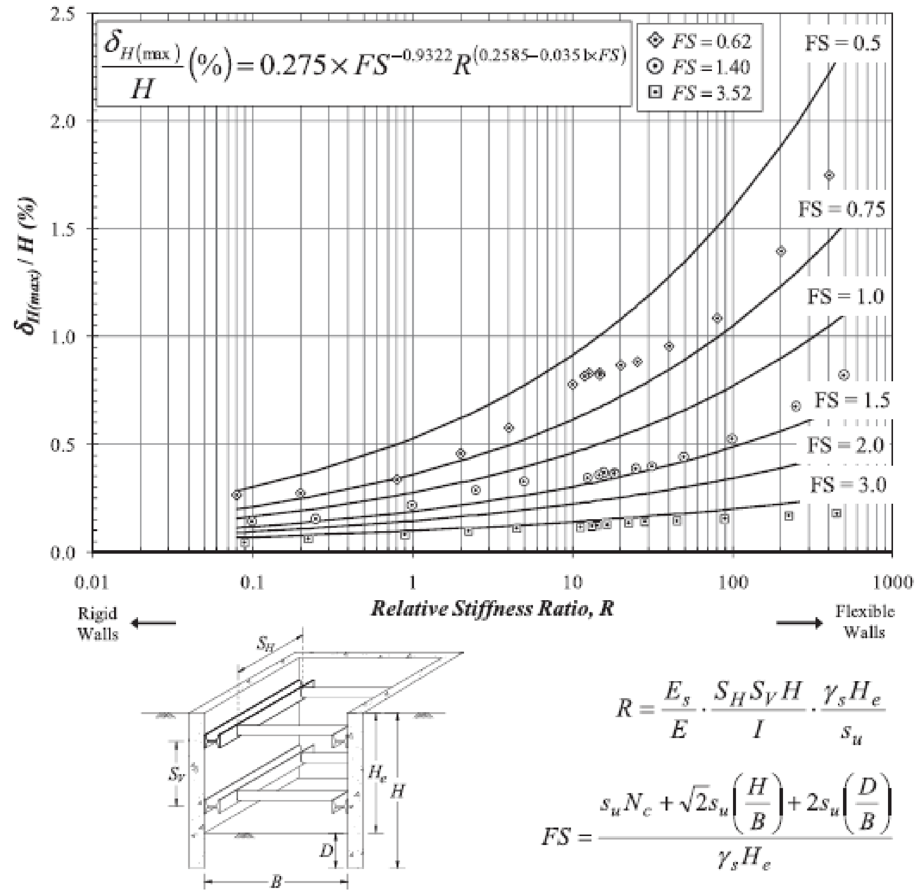

Figure 2. 29. The influence of the stiffness on deformations

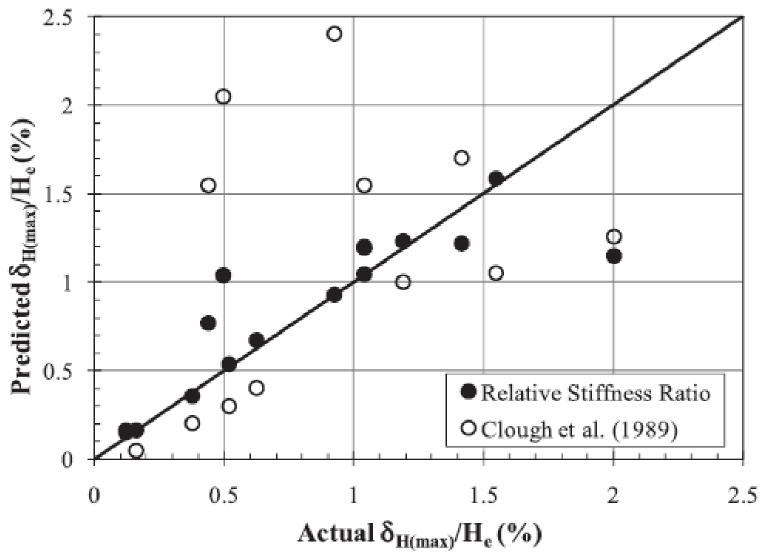

(a)

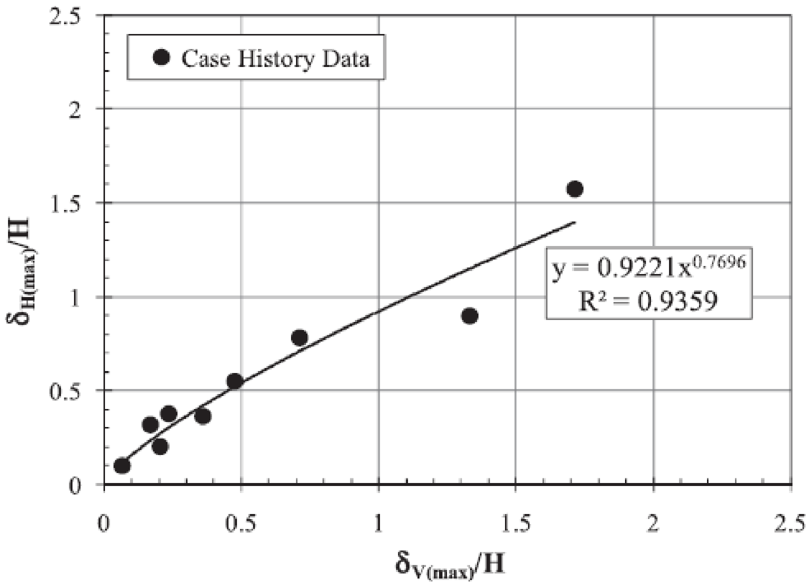

(b)

Figure 2. 30. Estimating for wall deflection (a) and horizontal movements (b).

Lim et al. (2010) investigated the excavation support systems of the Enterprise Center (TNEC) building built on clay soil in Taiwan. In this study, advanced soil such as MCC and HS models were used. As a result of the study, it was investigated which soil model was closer to the real behavior. In addition, it was stated that the MCC model calculated the wall deformations and ground settlements lower than the field measurements. In the HS Model, while the same results were found with the field measurements in the last excavation stage, differences were observed in the other stages. Hardening Soil-Small Strain model predictions were found to be approximately equal to HS Model prediction results. In the MC Model, the deformation estimates for all loading conditions are calculated quite far from field measurements.

Mu and Huang (2015) conducted studies on the effects of deep excavations on the surrounding structures. In this study, they carried out experimental studies on Chicago Clay by using the HS_ss model in PLAXIS, which is a finite element program. Within the scope of the study, empirical methods were developed to estimating the deflection values of the strutted wall in interaction with the ground. The obtained results were compared with other methods in the literature and their accuracy were confirmed.

Goh et al. (2016) analyzed a deep excavation problem in (2D) and three-dimensions (3D) using the HS model in a software that analyzes with the finite element method. Studies were carried out with different ratios of excavation width and excavation length. The results were compared with the semi-empirical tables currently used. The effects of excavation depth and pile embedment depth on the displacement and settlement values of the wall were investigated. As a result of the studies, the wall displacements calculated in three dimensions were calculated lower than the ones obtained from two-dimensional analysis.

Tan et al. (2016), studied the behavior of six currently completed buildings around the excavation of the metro station, whose excavation depths vary between 24.8-25.2 m. Significant displacements have developed in buildings with both shallow and deep foundations in diaphragm walls constructed in slurry trenches 50.2–50.5 m deep. In the station excavation section, a deformation of approximately 10 mm was detected for an excavation of approximately 15.9–17.7 meters. However, as the excavations continued towards the final levels, the buildings with the foundation system of continuous, rigid raft, long pile continuous, short pile raft foundation systems were dramatically displaced up to about 40 mm. No significant deformation occurred in the long-piled raft foundation. In parallel with the settlements mentioned above, significant damage was observed in the buildings. In general, building settlements are mostly affected by the distance between the building and the diaphragm wall as well as by the type of foundation and the weight of the building. Contrary to the literature studies, the building settlements did not develop simultaneously with the development of the ground settlements. Considering the final building settlements; although the settlements in shallow foundations are similar to the ground surface settlements, this similarity remained at a smaller level for short pile foundations.

Çalışan, (2005) studied the advantages and disadvantages of "The Limit Equilibrium Method" used in deep excavation support systems, "The Elastic Foundation Beam Method" in which the support systems and the ground are represented by springs, "The Pseudo Finite Element Method" and "The Finite Element Method", which is the most widely used today. They showed the importance of soil models and parameters used in the finite element method on the applied soil. As a result of the study, it was emphasized that the analyzes made with finite elements should be checked by comparing them with the load distributions in classical methods. In addition, the importance of studies on displacement and load values obtained from similar soils was emphasized.

Demirkoç et al. (2007) evaluated the soil-nail and anchored support systems with classical methods and then analyzed these systems in a program using (FEM). In study, MC and HS Model were used. The behavior of two different support systems under similar ground conditions was compared. As a result, it was observed that the top displacements increased with the increase of the depth in the nail system. For stiff clay and medium stiff clay in anchored systems; it has been observed that the wall moves forward while the displacements increase with depth. On the contrary, the wall moved inward depending on the prestress value on the stiff sand and medium stiff sand. The top displacements of the soil nail system were measured more than the anchored wall. However, the deformations remained within the expected limits in both systems. When the swelling values calculated on the excavation base were examined, the HS model gave better results than the MC model.

Likitlersuang et al. (2013a) conducted research on the small strain stiffness and shear modulus of Bangkok clayey soil by examining the soil data obtained during the deep excavation works in the Bangkok MRT Blu Line metro line. In this study, the HSS Model was used. As a result, it was stated that the Bangkok Clay is uniform throughout the Bangkok region, the shear stiffness values are clearly different between soft and hard clays, and these values tend to increase with depth. As Bangkok Clays are soft clays with slightly over consolidation, the parameter G_{max} was found to be relatively low compared to well documented London Clays. In addition to these studies, it was emphasized that all empirical equations predict G_{max} quite well, however, significant improvements were achieved for the calibration of the constant parameters used in the equations.

Likitlersuang et al. (2013b) conducted studies on deep excavations in underground railway systems in Bangkok. With these studies, the displacements of the diaphragm walls built to support the railway excavation and the settlements of the ground were calculated at the end of each excavation stage and the measurements were compared with the field data. The appropriate soil model was determined by repeating the analyzes with HS, HS_ss, SS (soft soil) models. The study's findings revealed that unless the parameters used in the analysis are appropriately chosen, the numerical methods used in the analyses cannot make accurate predictions.

Hsiung and Sakai (2016) analyzed a deep excavation constructed in an area with thick sand layers in the city of Kaohsiung, Taiwan, using the HS, HS_ss and MC models in the PLAXIS program. As a result of the study, the obtained data and field results were compared. The results show that the HS_ss model gives the best results for wall displacements and settlements, while the MC model gives the worst results. It is stated that this study will help engineers and researchers to perform reliable numerical analysis using soil models.

Lim and Ou (2017) studied the elastic behavior of the soil in loading and unloading conditions with plasticity-based analysis models such as MC, HS and HS_ss in an undrained deep excavation application. The effect of soil models on the elastic behavior was investigated by comparing them with field settlement and displacement measurements. As a result, the HS model showed elastic behavior throughout the excavation area. In addition, with the correct estimation of undrained loading/unloading parameters, elastic-perfect plastic models such as Mohr-Coulomb can also give results suitable for field measurements. The results showed that if an elastic perfect plastic model is used, it is necessary to work with small stress parameters. The use of constant modulus of elasticity overestimated the wall displacements, the creep effect should be included in the analysis, considering the excavation time, to predict wall movements consistently. In addition, studies have shown that using an appropriate soil-wall interface provides a more reasonable prediction on settlements.

2.3. Literature Survey for Model Study

Zhang et al. (2015) carried out studies to investigate the displacements of the support system in an area with soft soils. For this purpose, a study was carried out with the HSss model, which considers the small strain situation in soils. Parameters such as excavation form, soil strength properties, braced wall stiffness were used to examine the bending behavior of the wall. Based on the results of these studies, a Regression model was obtained to estimate the max. wall displacement. The wall displacements calculated by this approach are compared with 21 case studies built on soft ground in countries such as Taiwan, Singapore, US, Shanghai, Japan, and published records. As a result, it was seen that the obtained model was compatible with the case studies.

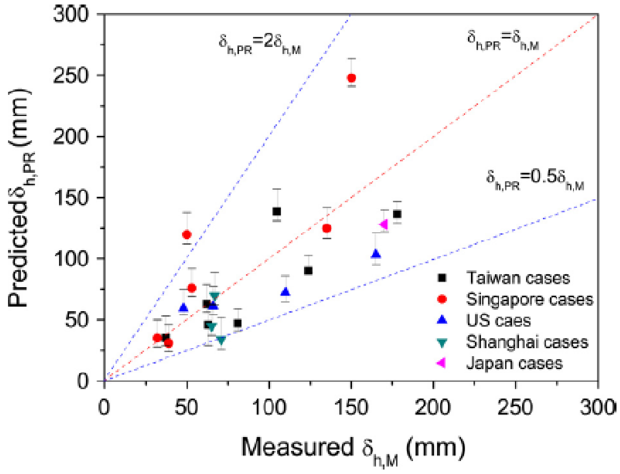

Figure 2. 31. Measured wall deflection versus predicted wall deflection

(Zhang, et al. 2015).

Bryson and Zapata-Medina, (2012) developed a semi-empirical design methodology for determining the stiffness of the braced excavation system. At the suggested design process, a parameter called the relative stiffness was developed. This parameter is based on a complete parametric analysis that included a FEM analysis of a generalized excavation that realistically characterized the excavation geometry, braced excavation system configuration, and excavation operations. Several excavation case histories from around the world were used to verify the suggested methodology's performance. The assessment revealed that the modified relative stiffness value performed well. The red boxes show constructions with diaphragm walls built on soft soils.

Table 2. 1. Excavation case histories.

Soil type	Case ID	Location	Reference	Wall type
Soft	SO1	Excavation in downtown Chicago	Gill and Lucas (1990)	Sheet
	SO2	Peninsula Hotel project in Bangkok	Teparaksa (1993)	Sheet
	SO3	AT&T Corporate Center in Chicago	Baker et al. (1989)	Diaphragm
	SO4	One Market Plaza building in San Francisco	Clough and Denby (1977)	Diaphragm
	SO5	Sheet pile wall field test in Rotterdam	Kort (2002)	Sheet
Medium	M1	Oslo Vaterland 1	NGI (1962a)	Sheet
	M2	Robert H. Lurie Medical Research building in Chicago (west wall)	Finno and Roboski (2005)	Sheet
	M3	Tokyo subway excavation project in Japan	Miyoshi (1977)	Steel-concrete
	M4	HDR-4 project for the Chicago subway	Finno et al. (1989)	Sheet
	M5	Oslo Vaterland 3	NGI (1962b)	Sheet
Stiff	ST1	Smith Tower in Houston, Texas	Ulrich (1989)	Secant
	ST2	New Palace Yard Park project in London	Burland and Hancock (1977)	Diaphragm
	ST3	Far-East Enterprise Center project in Taipei	Hsieh and Ou (1998)	Diaphragm
	ST4	Central Insurance building in Taipei	Ou and Shiau (1998)	Diaphragm
	ST5	National Taiwan University Hospital in Taiwan	Liao and Hsieh (2002)	Diaphragm

Note: Sheet = sheet pile wall; Diaphragm = diaphragm wall; Steel-concrete = steel with concrete lagging wall; and Secant = secant pile wall.

Table 2. 2. Excavation case histories data.

Case ID	H (m)	H_e (m)	B (m)	S_V (m)	S_H (m)	γ_s (kN/m^3)	s_u (kPa)	E_u (kPa)^a	EI (kN-m^2/m)	$\delta_{H(\max)}$ (mm)	$\delta_{V(\max)}$ (mm)
SO1	16.8	7	12.2	2.5	2.5^b	19	22	8,800	55,250	83.27	NA
SO2	18	8	65	2.5	2.5^b	16	23	6,900	50,400	123.65	NA
SO3	18.3	8.5	25	2.75	2.75^b	19	21.5	2,150	951,115	37.39	37
SO4	32	11	11^b	7.6	7.6	16.5	25	5,000	1,857,646	101.60	53.34
SO5	19	8	12.2	7.75	7.2	14	10	9,000	41,370	385.38	NA
M1	14	11	11	2	3.7	19	26	10,400	60,800	220.00	240
M2	17.4	12.8	68	3.6	2.28	18	43	8,600	53,000	63.50	63
M3	32	17	30	2.7	2.7^b	19	42	14,700	1,177,600	176.56	152.42
M4	19.2	12.2	12.2	2.4	3.7	19	27	10,800	161,000	172.64	255.7
M5	16	12	26	2	3.7	19	34	13,600	73,800	125.00	114
ST1	20	12.2	36.6	2.45	2.45^b	20.1	140	16,800	970,313	14.75	NA
ST2	30	18.5	18.5^b	3.08	3.08^b	20	190	190,000	2,500,000	30.00	20
ST3	33	20	70	3.8	3.8	19	76.5	15,300	2,300,000	124.76	77.76
ST4	23	11.8	33.7	3.3	3.3	19.4	105	63,000	468,000	44.53	NA
ST5	27	15.7	140	2.65	1.92	20	77.5	15,500	1,177,600	81.37	NA

Moormann (2004) examined a large database of over 530 foreign case studies on braced excavations in normally consolidated soft soils. The ground movements and wall deformations of the supported excavations were calculated by considering the groundwater condition, the geometry of the excavation area, the type of excavation support system and the excavation method, as well as environmental parameters. Various empirical approaches were developed considering parameters that affect behavior. Support type and excavation method had a significant effect on both wall deformation and shallow settlements. The findings are compared to those of other empirical investigations.

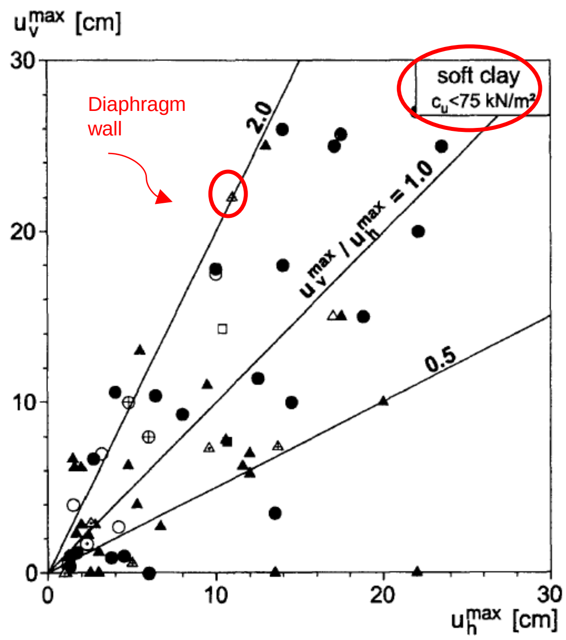

Figure 2. 32. Maximum ground settlement versus maximum lateral displacement of wall (Moormann, 2004).

Long M. (2001) created a database of nearly 300 case histories of wall and ground movements from deep excavations completed worldwide (Table 2.3). Although using a large database brings some disadvantages for this study, general trends were identified. The study showed that the deformations are generally lower than the worldwide accepted approaches suggested by Clough, (1990). Normalized max. deformation values $\delta_{hm}$are commonly between 0.05%H and 0.25%H. Normalized max. settlement values δ_{vm} are usually lower, at values frequently between 0 and 0.20%H. The performance of propped, anchored, and top-down systems is indistinguishable. The evidence suggests that less rigid walls can behave satisfactorily in many situations, and that global design practice is conservative. However, soils with a thick soft soil layer and high base swelling coefficient were well predicted by Clough, (1990). It was observed that deformations are also high in excavations with low basal heave factor. Cantilever walls showed displacements that were generally independent of system stiffness. All cantilever retaining walls built on stiff soil are highly conservative. It's also possible that less stiff walls would suffice in many situations. The red boxes show constructions with diaphragm walls built on soft soils (Table 2.3).

Table 2. 3. Excavation case histories data (Long, M., 2001).

25	Eastbourne 2	Soft clay	?	14	15	Diaphragm	2,500,000	Single prop	13	Yes	15	?	Fernie and Suckling (1996)
26	Pietrafitta, Italy	Soft to firm clay	40 (SPT N)	5.5	20	Sheet	42,000	Multiprop	7.8	No	71	?	Rampello et al. (1992)
27	Chicago	Soft clay	?	13.4	15	Sheet	1,055,000	Multiprop	4.46	?	150	?	Fernie and Suckling (1996)
28	Inland Steel Chicago	Soft clay	?	11	19	Sheet	50,000	Multiprop	2	Yes	55	?	Flaate (1966)
29	Sewage Tr. Tokyo	Soft clay	2.9 × depth (UC)	26	30	Steel pipe pile	8,000,000	Multiprop	4.3	Yes	70	?	Tominaga et al. (1985)
30	Osaka A	Soft clay	?	20.6	25	Diaphragm	2,500,000	Multiprop	3	Yes	78	?	Tamano et al. (1996)
31	Japan 2	Soft clay	?	17.1	20	Steel pipe pile	34,000,000	Multiprop	4.3	?	26	?	Fernie and Suckling (1996)
32	Lake zone, Mexico	Soft clay	25 (various)	15.7	20	Diaphragm	2,500,000	Multiprop	2.62	Yes	135	?	Auvinet and Organista (1998)
33	Shanghi-Jin Mao	Soft/firm clay	N = 1 to 2	19.65	36	Diaphragm	2,500,000	Multiprop	3.93	Yes	81	?	Zhao et al. (1999)
34	Shanghi-Heng Long	Soft/firm clay	N = 1 to 2	18.2	29	Diaphragm	2,500,000	Multiprop	3.64	Yes	99	?	Zhao et al. (1999)
35	Shanghi	Soft/firm clay	N = 1 to 2	17.85	24	Diaphragm	2,500,000	Multiprop	3.57	Yes	129	?	Onishi and Sugawara (1999)
36	River Wall M'Boro	Soft clay	?	9.5	12	Sheet	177,660	Single anch	4.25	Yes	125	?	Baggett and Buttling (1977)
37	Detroit	Soft clay	?	7	10	Sheet	83,400	Single anch	11.2	?	45	?	Fernie and Suckling (1996)
38	TP, Bogota	Soft clay/silt	N = 2 to 4	16	34	Diaphragm	540,000	Multianch	3.75	?	125	1,000	Maldonado (1998)
39	Newton Singapore	Soft clays	18 (vane)	14.5	12	Diaphragm	2,500,000	Top down	3.63	Yes	110	220	Nicholson (1987)
40	Taiwan Chi Ching	Soft clays	N = 2 to 12	13.9	15	Diaphragm	857,500	Top down	2.78	Yes	65	65	Ou et al. (1993)
41	Taiwan Far East	Firm clay	60 (vane) N = 2 to 6	20	24	Diaphragm	857,500	Top down	3.33	Yes	135	67	Ou et al. (1993)
42	Oslo Christiana	Soft clay	?	9.6	23	Sheet	483,600	Top down	3	Yes	48	100	Finstad (1991)

Hsieh and Ou, (1998) proposed an empirical approach for estimating the surface movement profile of support systems constructed in cohesive soils. In general, two types of settlement profiles are mentioned, these are angular and concave types. Several case studies are used to validate the suggested strategy. Other empirical investigations' findings are also offered for comparison. The proposed method offers a better estimate of settlement and angular distortion estimation than previous empirical approaches for concave and angled type surface movement profiles.

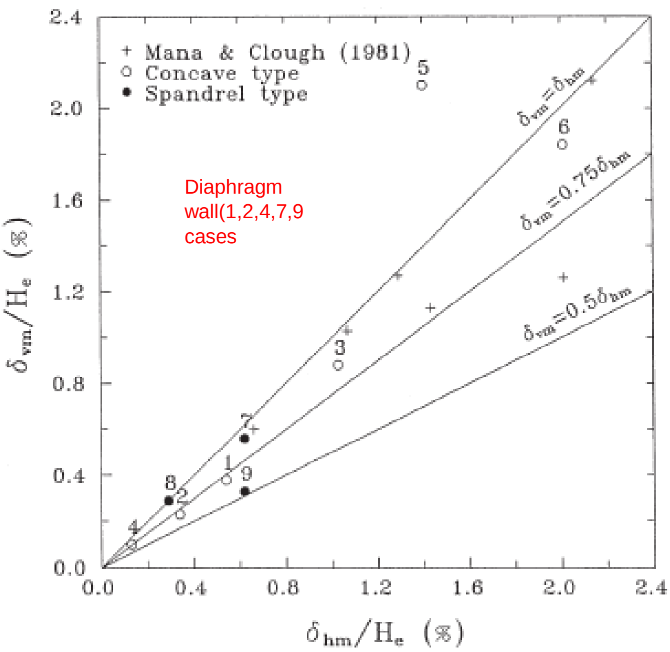

Figure 2. 33. Relation between the wall deformation and settlement (Hsieh and Ou, 1998).

To evaluate the max. wall deflection, max. settlement, and settlement profile due to excavations in soft and medium clays, Kung and Ou (2006) suggested a simplified semi-empirical model. Using a small-strain soil model, a huge amount of simulated data is produced using finite element analysis. The suggested semi-empirical model is based on these data, which include wall deformations and settlements in simulated excavations in normally consolidated soft to medium clays. The suggested model is validated using examples that were not considered in its development. The proposed model is quite well validated in the studied ground conditions.

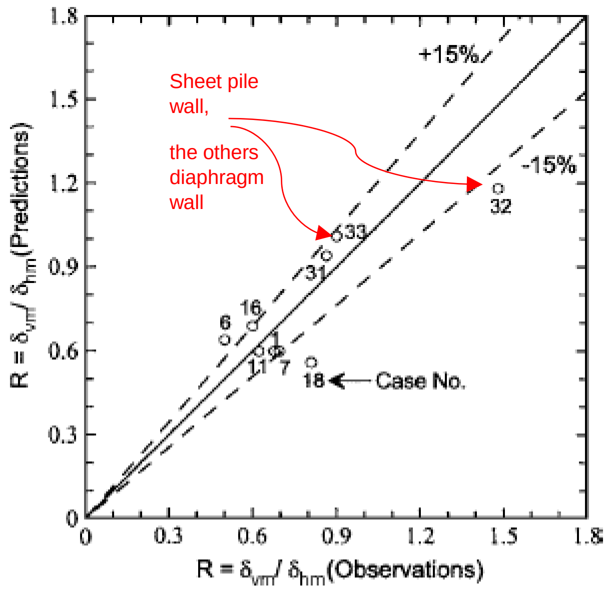

Figure 2. 34. Estimated and observed settlement/wall deformations

(Kung et al., (2007).

Ou et al. (1993) selected ten excavation cases of high-quality structure and ground observation data constructed in Taipei to examine the characteristics of deep excavation behavior. The location and size of the max. wall deformation, the location and size of the maximum surface settlement, and the region affected by the settlement are determined. As a result of this study, an empirical approach is proposed to estimate the surface settlements. The largest lateral wall deflection is frequently located near the surface, between 0.002H and 0.005H. The max. surface movement is equivalent to the max. wall deflection at its highest limit. In most excavation instances, the max. surface movement, δ_{vm} is equal to $0.5\delta_{hm}$-$0.7\delta_{hm}$ (Figure 2.40).

Wall deflection at the first stage of excavation, the max. ground surface settlement normally occurs quite close to the face of the wall (Figure 2.39).

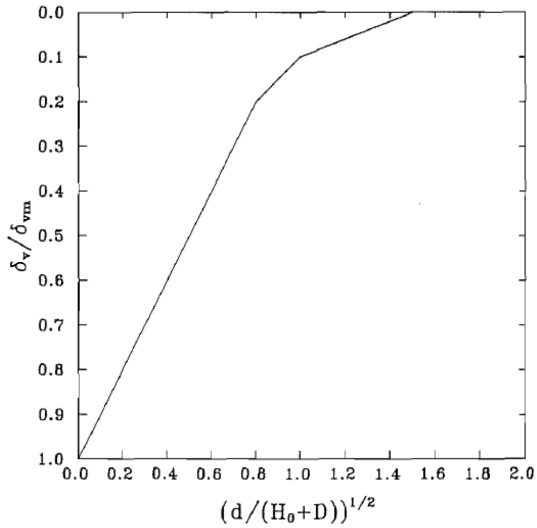

Figure 2. 35. Proposed relationship between settlement and distance (Ou et al., 1993).

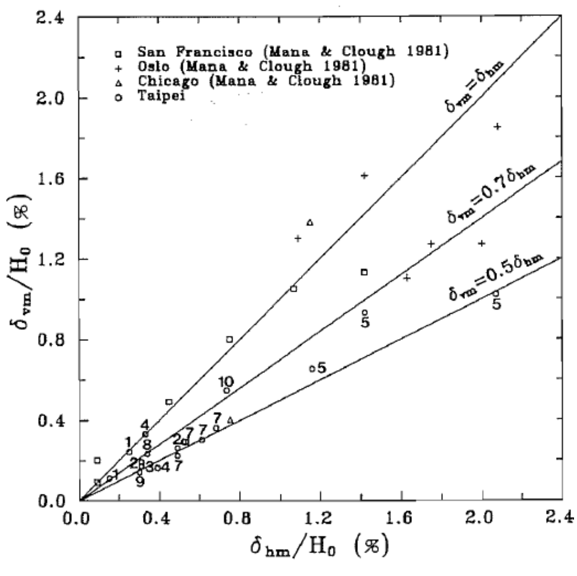

Figure 2. 36. Relation between max. ground settlement and max. wall deflection (Ou et al., 1993).

3. SOIL CONSTITUTIVE MODELS

3.1. An Overview of the Soil Models

The soil behavior is generally predicted according to the Mohr-Coulomb (MC Model) model, which is an elastic perfect plastic model formulated within the framework of the theory of plasticity by adding Coulomb's failure parameters to the linear elastic model (Hook's Law). This model is a general soil model developed in the late 19^{th} century and still in use today. However, the models that calculate with the limit analysis method of this type are insufficient to reflect the real behavior of most soil types, and their usage area is limited. Many reasons such as the stress history of soils, over or normal consolidation in cohesive soils, creep effect, variation of soil stiffness parameters with depth, anisotropy, soil hardening and softening effects under load can be shown as the reasons why the real behavior of soils cannot be predicted successfully with such models. For this reason, models that calculate in the limit analysis type are mostly used for determining the first approach of the problem, pre-dimension and the failure (safety) calculations of the system. Today, although the MC Model is used, a much more sophisticated Hardening soil model (HS Model) is used, which is based on the deformation calculation and considers the above-mentioned behaviors (Figure 3.1).

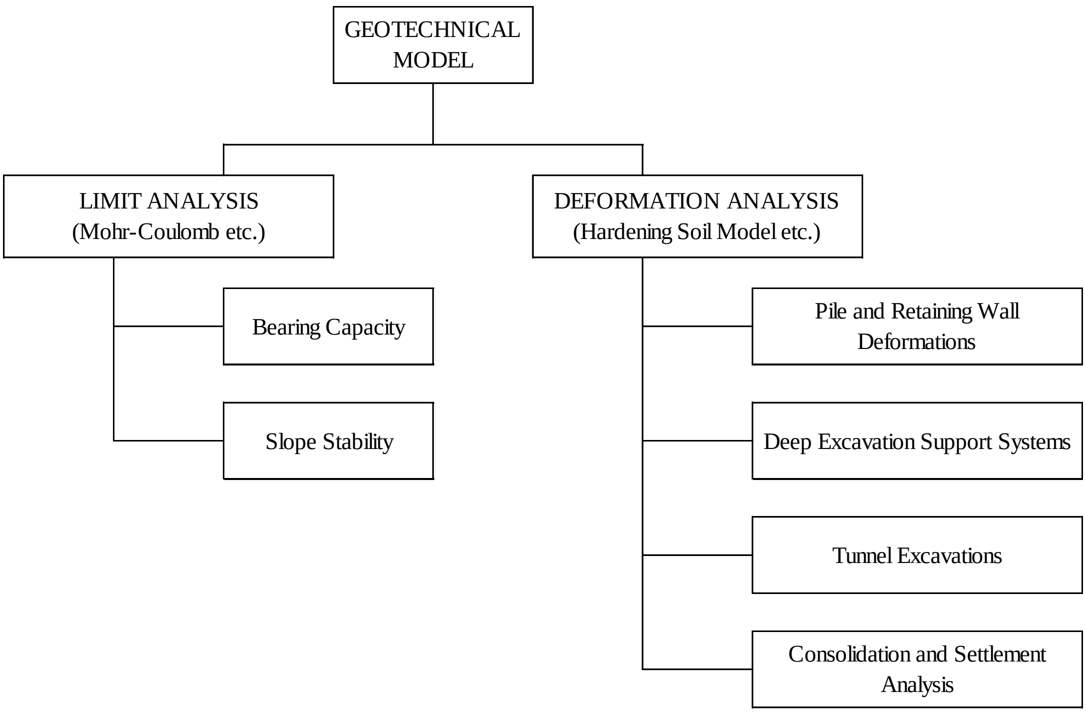

Figure 3. 1. Application areas of soil models.

Models such as Hardening soil cannot be solved or may take too long to solve because they contain very complex mathematical calculations and many parameters. For this reason, the solution of such models is done with the finite element method (FEM), which can only be expressed with partial differential equations. It is also used with software that works with the finite difference method (FDM), which is increasingly used today. Software developed specifically for geotechnical engineering such as PLAXIS, FLAC, DIANA, Z_SOIL, and package programs such as MIDAS, ABAQUS, CRISP, LUSAS, which are used for more general purposes, provide great convenience in solving complex geotechnical problems.

With the development of elastoplastic soil models (Figure 3.2), their use in applications increases and geotechnical problems can be solved more precisely. Thanks to this software, soil profiles with complex structures (surcharge loads, layered status, groundwater level, drainage conditions, etc.) can be created, displacements of deep excavations and surrounding settlements can be modeled close to real behavior.

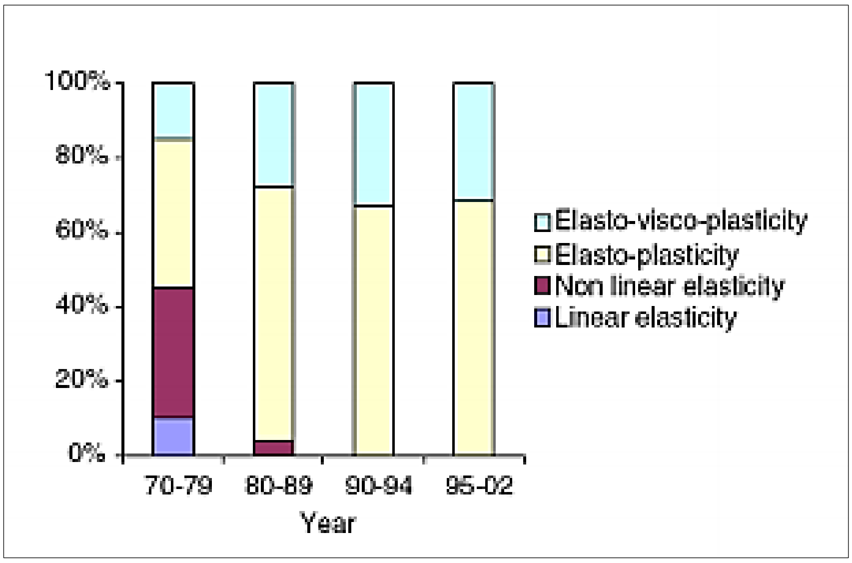

Figure 3. 2. Changes in the use of soil structure models over the years (Mestat, 2004).

3.2. Soil Models

Some of soil constitution models in the material library of PLAXIS finite element software are explained in general terms. Then, HS Model and HS_ss Model used in this thesis are explained in more detail.

3.2.1. Linear Elastic Model(LEM)

This model is based on Hook's Law (1675). This model is the first relationship developed for ideal elastic materials. When an ideal elastic material is stressed, it exhibits unit extension or unit contraction depending on the modulus of elasticity (Önalp and Arel, 2013). The Young's modulus (E) and the position ratio (υ) are the two primary stiffness parameters in this model. The Elastic Model was later used by making certain generalizations for soils. Soils do not behave as a homogeneous, isotropic, and elastic material when loaded with stresses with a sufficient safety number against collapse, but they are considered to have E, G, ν properties in this model. These values are mostly used soil dynamics (Kumbasar and Kip 1999). Since the Linear Elastic Model (LEM) is not used in soil modeling, today this model has been replaced by models based on the theory of plasticity. Although the LE Model is not used as a soil model in deep braced excavations, it is used for modeling the support system elements (piles, anchors, soil nails, geogrids, etc.). Linear elastic model parameters are shown in Equations 3.1, 3.2 and 3.3. The curve drawn for ideal elastic materials is usually as in Figure 3.3.

Extension or contraction of elastic material

$$\varepsilon = \frac{\sigma}{E} \tag{3.1}$$

Shear stiffness

$$G = \frac{E}{2(1+\upsilon)} \tag{3.2}$$

Shear strain

$$\gamma_{zx} = \frac{2(1+\upsilon)}{E}\tau_{zx} \tag{3.3}$$

Linear elastic model(LEM) parameters

Stiffness parameters	Unit
G: Shear stiffness	[kN/m^2]
E: Young modulus	[kN/m^2]
υ : Poisson rotio	[-]
γ_{zx}: Shear strain	[-]

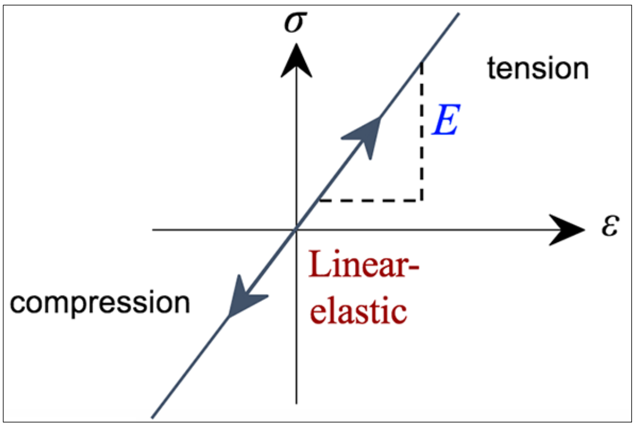

Figure 3. 3. Ideal elastic materials curve.

3.2.2. Modified Duncan-Chang Hyperbolic Model

Kondner (1963) created the hyperbolic soil model, which was then improved and developed by various researchers. This model, later called Duncan and Chang's (1970) Hyperbolic Model, assumes that the stress deformation curves obtained from drainage triaxial pressure tests of both clay and sandy soils are both nonlinear and approximately similar to a hyperbola (Figure 3.4). The parameters of the Duncan hyperbolic model are easy to use because the parameters are easily obtained by triaxial tests. However, the dilatation angle is not defined in this model, no distinction can be made between the loading and unloading stiffness, it does not provide compliance with the ground values, and it is generally suitable for practical models since only one stiffness parameter is defined (Ti, et al., 2009). In this model, ground deformations are gradually increased and analyzed nonlinearly. It is assumed that the stress deformation relationship is linear in each calculated stress region and complies with Hooke's Law.

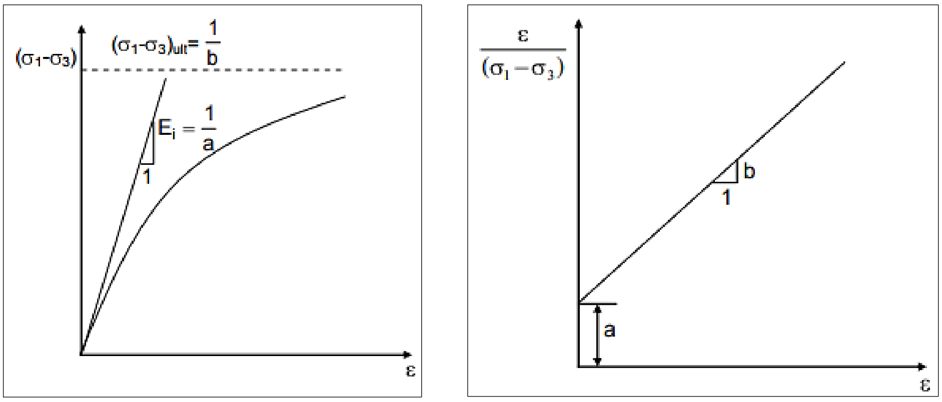

(a) (b)

Figure 3. 4. Hyperbolic real form (a) & converted form (b).

Real form:

$$(\sigma_1 - \sigma_3) = \frac{\varepsilon}{\frac{1}{E_i} + \frac{\varepsilon}{(\sigma_1 - \sigma_3)_{ult}}} \tag{3.4}$$

Converted form:

$$\frac{\varepsilon}{(\sigma_1 - \sigma_3)} = \frac{1}{E_i} + \frac{\varepsilon}{(\sigma_1 - \sigma_3)_{ult}} \tag{3.5}$$

Where;

E_i: Tangent modulus

$(\sigma_1 - \sigma_3)$: Deviatoric stress

$(\sigma_1 - \sigma_3)_{ult}$: Asymptotic value for deviatoric stress

ε: Axial deformation.

Modulus of elasticity under any stress:

$$E_t = \left[1 - \frac{R_f(1 - sin\phi)(\sigma_1 - \sigma_3)}{2c\ cos\phi + 2\sigma_3 sin\phi}\right]^2 KP_a\left(\frac{\sigma_3}{P_a}\right) \tag{3.6}$$

From the Janbu (1985) equation, the initial tangent modulus is:

$$E_i = KP_a\left(\frac{\sigma_3}{P_a}\right)^n \tag{3.7}$$

Where;

P_a: Atmospheric pressure
K : Dimensionless coefficients
R_f: Failure rate
c: Cohesion
ϕ: Shear strength angle

3.2.3. Mohr Coulomb Model(MCM)

MC model was created by adding the linear elastic behavior in Hook's law to Coulomb's behavior at the state of failure. This model was created using the plasticity principle as a framework. and shows elastic perfect plastic behavior. Mohr Coulomb Model assumes that the soil is elastic in the first region of the stress deformation curve and perfect plastic material in the second region. In this model, stress conditions represent the first-order approach of ground behavior since the strain is expressed by the values at the state of failure criteria. For this reason, the Model is suitable for use in preliminary analysis. This model assumes that the stiffness of the soil layers does not change with depth and expresses it using an average stiffness parameter, so the deformation values are unrealistic, but the analyzes are performed relatively quickly.

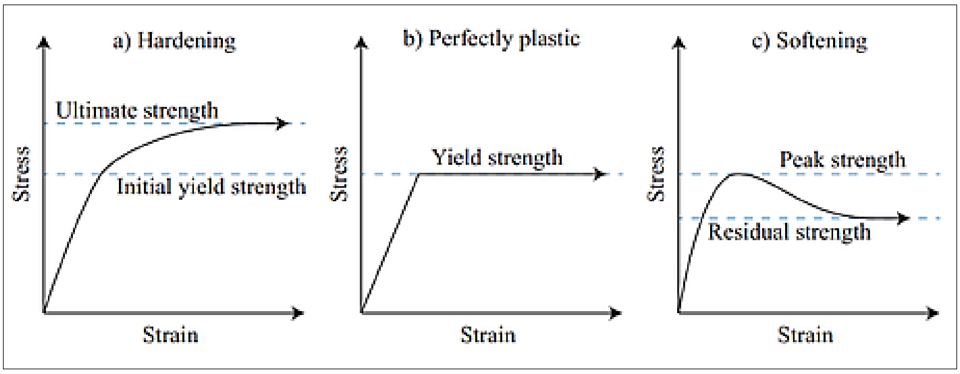

Figure 3. 5. Hardening and softening behavior in soils.

The Mohr Coulomb Model cannot model the properties of soils such as hardening and softening under stress, loose sands that do not contain dilatancy and show a volumetric decrease rather than volumetric increase, and do not make a distinction for loading-unloading conditions (Figure 3.5). Therefore, this model is not recommended for braced excavation problems. It is more appropriate to use in the stability analysis (security analysis) of soil fill dams, fillings, slopes, retaining walls (limit analysis problems) and carrying capacity calculations of foundation (single, surface) projects.

Mohr-Coulomb soil model parameters are summarized below.

Elastic parameters	Unit
E: Stifness modulus	[kN/m^2]
υ: Poisson ratio	[-]
Plastic parameters	
ϕ: Internal friction angle	[°]
c: Cohesion	[kN/m^2]
ψ: Dilatancy angle	[°]

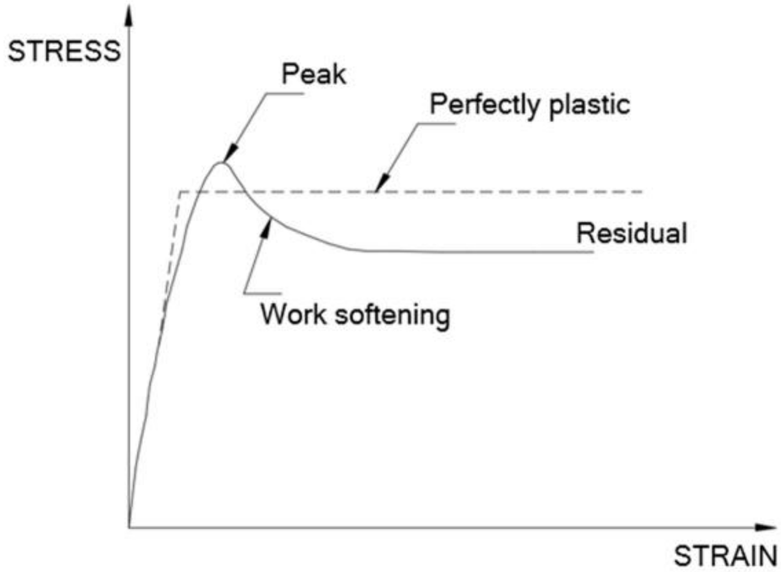

Figure 3. 6. Assumption of Mohr-Coulomb model.

In the MC model, soil behaves as a lineer elastic perfect plastic material on the yield surface(Figure 3.6.). This situation is described by the following six yield functions with respect to the principal stress space. These yield functions are represented by a hexagonal cone in the stress space (Figure 3.7). In addition, six plastic potential functions are defined in this model to simule plastic behavior.

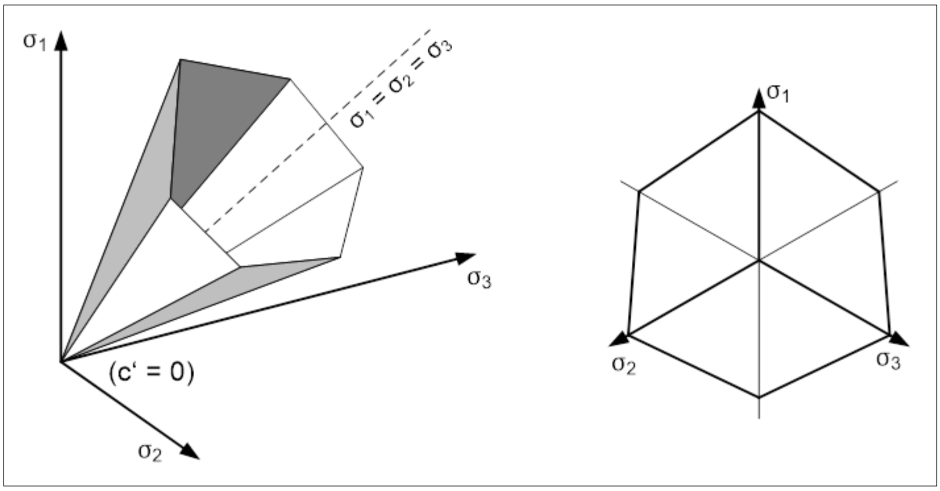

Figure 3. 7. MC model yield surfaces in mean stress space.

Yield functions of the hexagonal cone in the principal stress space:

$$f_{1a} = \frac{1}{2}|\sigma_2' - \sigma_3'| + \frac{1}{2}(\sigma_2' + \sigma_3')sin\phi - c\ cos\phi \leq 0$$

$$f_{1b} = \frac{1}{2}|\sigma_3' - \sigma_2'| + \frac{1}{2}(\sigma_3' + \sigma_2')sin\phi - c\ cos\phi \leq 0$$

$$f_{2a} = \frac{1}{2}|\sigma_3' - \sigma_1'| + \frac{1}{2}(\sigma_3' + \sigma_1')sin\phi - c\ cos\phi \leq 0$$

$$f_{2b} = \frac{1}{2}|\sigma_1' - \sigma_3'| + \frac{1}{2}(\sigma_1' + \sigma_3')sin\phi - c\ cos\phi \leq 0$$

$$f_{3a} = \frac{1}{2}|\sigma_1' - \sigma_2'| + \frac{1}{2}(\sigma_1' + \sigma_2')sin\phi - c\ cos\phi \leq 0$$

$$f_{3b} = \frac{1}{2}|\sigma_2' - \sigma_1'| + \frac{1}{2}(\sigma_2' + \sigma_1')sin\phi - c\ cos\phi \leq 0$$

Plastic potential functions of the hexagonal cone in the principal stress space:

$$g_{1a} = \frac{1}{2}|\sigma_2' - \sigma_3'| + \frac{1}{2}(\sigma_2' + \sigma_3')sin\psi$$

$$g_{1b} = \frac{1}{2}|\sigma_3' - \sigma_2'| + \frac{1}{2}(\sigma_3' + \sigma_2')sin\psi$$

$$g_{2a} = \frac{1}{2}|\sigma_3' - \sigma_1'| + \frac{1}{2}(\sigma_3' + \sigma_1')sin\psi$$

$$g_{2b} = \frac{1}{2}|\sigma_1' - \sigma_3'| + \frac{1}{2}(\sigma_1' + \sigma_3')sin\psi$$

$$g_{3a} = \frac{1}{2}|\sigma_1' - \sigma_2'| + \frac{1}{2}(\sigma_1' + \sigma_2')sin\psi$$

$$g_{3} = \frac{1}{2}|\sigma_2' - \sigma_1'| + \frac{1}{2}(\sigma_2' + \sigma_1')sin\psi$$

In the plastic potential equations above, ψ is the dilation angle and the modeling of dilatancy can be illustrated in Figure 3.8 The direction of plastic deformation is determined by the plastic potential(Figure 3.9).

If ψ=0, no volume change

If ψ<0 there is an increase or decrease in volume

If ψ>0 there is space or increase in volume

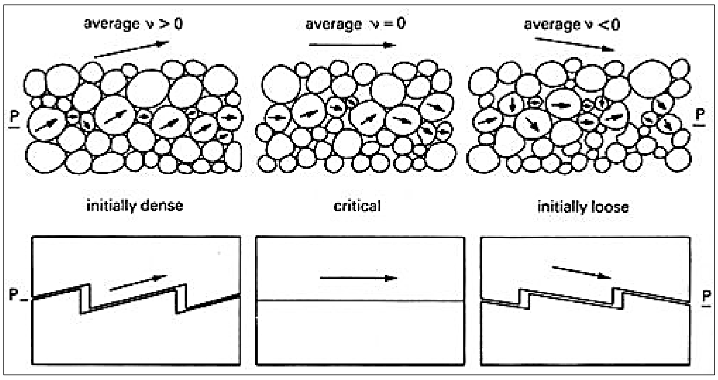

Figure 3. 8. Dilatancy conditions in the ground.

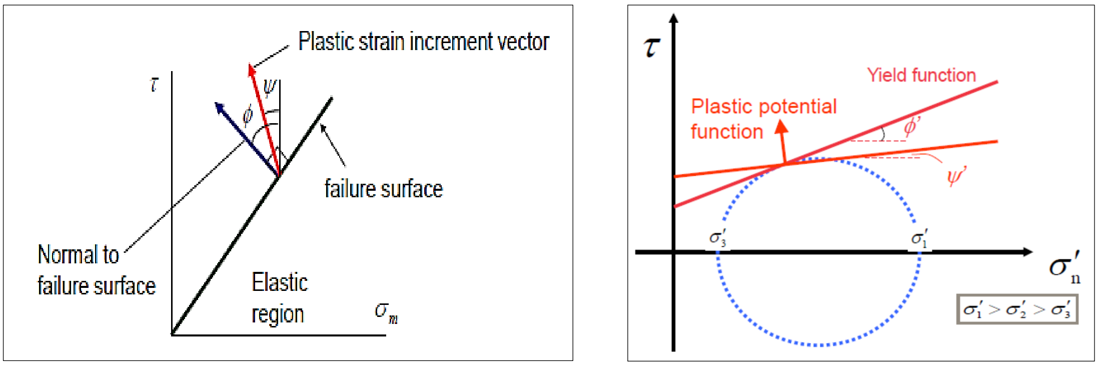

(a) (b)

Figure 3. 9. Plastic deformation according to the dilation angle.

3.2.4. Hardening Soil Model(HSM)

Hardening Soil Model(HS Model) is a sophisticated soil model created within the framework of plasticity theory. This model is Duncan-Chang (1970), a much more advanced version of the hyperbolic model. Unlike Duncan-Chang's hyperbolic model, this model uses plastic theory instead of elastic theory. The plastic deformations calculated according to this theory are calculated according to the multi-surface flow criterion. Hardening Soil Model considers the stress-related stiffness values, which means that all stiffness's increase with increasing pressure. Since HS Model uses three different stiffness parameters unlike the single stiffness parameter used in the hyperbolic model, the loading-unloading conditions of the ground are modeled closer to the actual behavior (Figure 3.10).

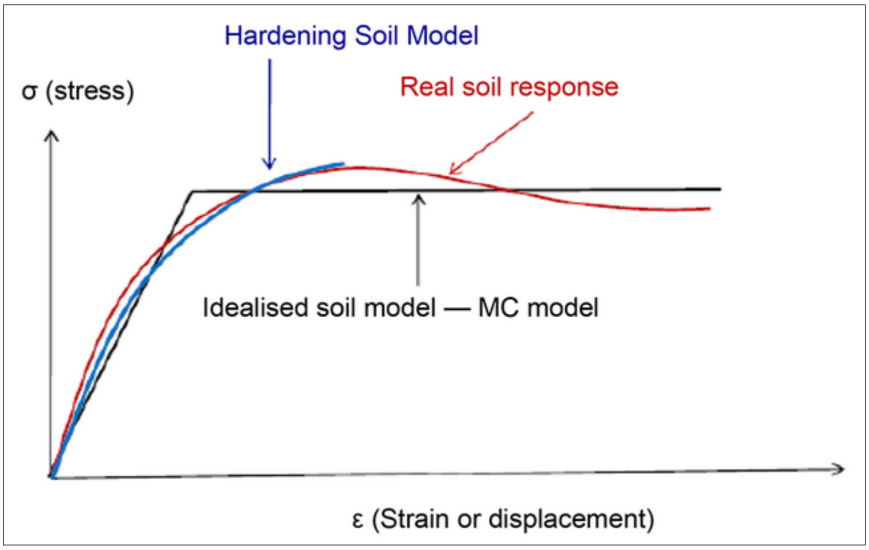

Figure 3. 10. HS, MC and Real soil behavior.

3.2.4.1. Stiffness Parameters

In the HS Model, secant stiffness (E_{50}^{ref}) obtained by drained triaxial tests, tangent stiffness (E_{oed}^{ref}) obtained by drained odometer tests and elastic loading/unloading stiffness (E_{ur}^{ref}) are used. Because of these three different stiffness parameters used, the soil can be modeled more realistically. Hardening soil model stiffness parameters are explained in more detail below.

3.2.4.2. Secant Stiffness (E_{50}^{ref})

The stress-strain behavior at the initial loading is nonlinear. E_{50} is the confining stress dependent stiffness modulus for primary loading E_{50} is used instead of the initial modulus E_i. For small strain because is more difficult to determine experimentally (Schanz et al. 1999).

It is given by the equation 1. Here, the modulus E_{50}^{ref} is the secant stiffness corresponding to the reference stress $\sigma_3^{ref} = p^{ref}$=100 kPa. In triaxial tests, it is calculated from the stress-strain curve. It is the stiffness modulus value corresponding to 50% of the maximum shear strength q_f(Figure 3.11)

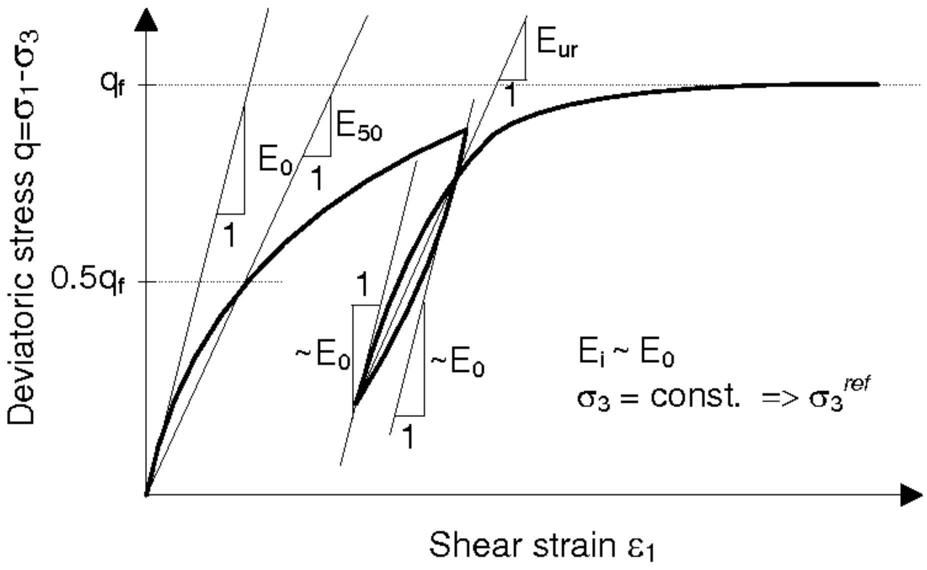

Figure 3. 11. Hyperbolic stress-strain relationship.

$$E_{50}^{ref};\ \ E_{50} = E_{50}^{ref}\left(\frac{c\ cos\phi - \sigma_3' sin\phi}{c\ cos\phi + p^{ref} sin\phi}\right)^m \tag{3.8}$$

Schanz et al. (1999) suggested the following empirical approaches for sands and silts.

For loose sand and silt

$$\frac{E_{50}}{p^{ref}} \approx 150\sqrt{\frac{\sigma_x'}{p^{ref}}} \tag{3.9}$$

For clean and firm sand

$$\frac{E_{50}}{p^{ref}} \approx 500\sqrt{\frac{\sigma_x'}{p^{ref}}} \tag{3.10}$$

3.2.4.3. Unloading/Reloading Stiffness

E_{ur} expresses the stiffness of the soil in the loading and unloading condition in the triaxial compression test, the loading and unloading stress path is elastically modeled in accordance with Hook's Law. E_{ur}^{ref} is the reference Elastic modulus corresponding to the reference stress p^{ref}=100 kPa.

$$E_{ur}^{ref}; E_{ur} = E_{ur}^{ref}\left(\frac{c\ cos\phi - \sigma_3' sin\phi}{c\ cos\phi + p^{ref} sin\phi}\right)^m \tag{3.11}$$

3.2.4.4. Odometer Stiffness

It refers to the tangent modulus corresponding to the pressure p^{ref} in the oedometer test of the soil (Figure 3.12)

$$E_{oed}^{ref}; E_{oed} = E_{oed}^{ref}\left(\frac{c\ cos\phi - \frac{\sigma_3'}{K_0^{NC}} sin\phi}{c\ cos\phi + p^{ref} sin\phi}\right)^m \tag{3.12}$$

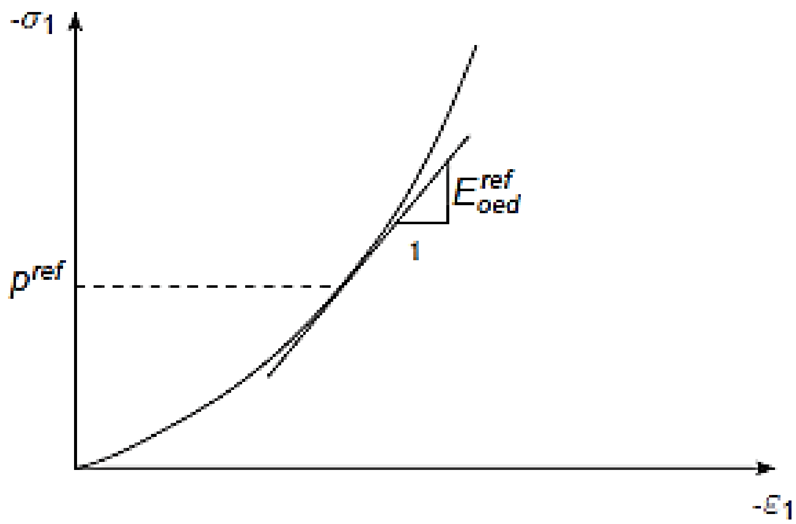

Figure 3. 12. Determination of soil model parameter E_{oed}

Based on the modified compression index λ^* for soft soils; can be calculated with Equations 3.13 and 3.14. Similarly, depending on the modified swelling index κ^*, can be calculated with Equations 3.15 and 3.16. In the following equations, λ and κ are the compression and swelling indices in the Cam-Clay Model.

$$E_{oed}^{ref} = \frac{p^{ref}}{\lambda^*} \quad (3.13)$$

$$\lambda^* = \frac{\lambda}{(1 + e_0)} \quad (3.14)$$

$$E_{oed}^{ref} = \frac{2p^{ref}}{\kappa^*} \quad (3.15)$$

$$\kappa^* = \frac{\kappa}{(1 + e_0)} \quad (3.16)$$

3.2.4.5. Advanced Parameters

In addition to the ones mentioned above, stress-level dependency of the stiffness (m), Reference pressure (p^{ref}), the coefficient of earth pressure at-rest (K_0^{nc}), failure ratio (R_f) and the Poisson's ratio (v_{ur}) are some of the other parameters desired for this model. In the stiffness parameters calculated in the Hardening Soil Model, the exponent value depending on the stress (loading level) "m" is taken as usually 0.5~1 for sand or silts and 1 for soft soils.

Janbu (1985) calculated "m" as 0.5 for Norwegian sand and silt, while Kempfert and Gebreselassie, (2006) calculated it as 0.38 to 0.84 for soft clays. (Soos and Von 2001) calculated it as 0.9 to 1.0 for different soft clays. Reference pressure is taken as p^{ref}=100 kPa and K_0^{nc} is calculated according to $K_0^{nc} = 1 - sin\phi$ (Jaky, 1944).

3.2.4.6. Failure Parameters

Failure in the model is expressed with Mohr-Coulomb parameters as in other advanced models. The parameters for failure are cohesion (c), internal friction angle (ϕ) and dilatancy angle (ψ).

3.2.4.7. Yield Surface, Failure Condition, Hardening Law

For the triaxial test, the two yield functions $f_{12}$and f_{13}defined to Equations. 3.17 and 3.18

$$f_{12} = \frac{q_a}{E_{50}} \frac{(\sigma_1 - \sigma_2)}{q_a - (\sigma_1 - \sigma_2)} - \frac{2(\sigma_1 - \sigma_2)}{E_{ur}} - \gamma^p \quad (3.17)$$

$$f_{13} = \frac{q_a}{E_{50}} \frac{(\sigma_1 - \sigma_3)}{q_a - (\sigma_1 - \sigma_3)} - \frac{2(\sigma_1 - \sigma_3)}{E_{ur}} - \gamma^p \quad (3.18)$$

In these equations, shear plastic strain γ^p can be calculated as follows Equation 3.18.

$$\gamma^p = \varepsilon_1^p - \varepsilon_2^p - \varepsilon_3^p = 2\varepsilon_1^p - \varepsilon_v^p \approx 2\varepsilon_1^p \quad (3.19)$$

In the HS model, shear hardening, which is used for plastic deformations caused by deviatoric loading, can be calculated. However, compression hardening used for strains caused by isotropic or odometer loading is defined. Compression hardening is also referred to as volumetric hardening and this feature is not available in the MC model, it is controlled by the odometer module and preconsolidation pressure is an important factor in defining this feature.

3.2.4.8. Flow Rule and Plastic Potential Functions

In the HS Model, according to the flow rule, the plastic shear strain and the plastic volumetric strain have the following relationship:

$$\varepsilon_v^p = sin\psi_m \gamma^p \quad (3.20)$$

In this equation, ψ_m is the mobilized dilatation angle and is expressed by the following equation.

$$sin\psi_m = \frac{sin\phi_m - sin\phi_{cv}}{1 - sin\phi_m sin\phi_{cv}} \quad (3.21)$$

Also, the mobilized internal friction angle ϕ_m can be expressed by the following approximation.

$$sin\phi_m = \frac{\sigma_1' - \sigma_3'}{\sigma_1' + \sigma_3' - 2c cos\phi} \quad (3.22)$$

In the stress-dilatation angle relationship, dilatation occurs for high stress (ϕ_m<ϕ_{cv}) values, while at low stress (ϕ_m>ϕ_{cv}) values, the soil is subjected to compression. At the moment of collapse, the mobilized friction angle becomes equal to the failure angle (Rowe 1969). In the equations below $c, \phi \ and \ \psi$ are the failure parameters used in the Mohr-Coulomb Model.

$$sin\psi = \frac{sin\phi - sin\phi_{cv}}{1 - sin\phi sin\phi_{cv}} \tag{3.23}$$

$$sin\phi_{cv} = \frac{sin\phi - sin\psi}{1 - sin\phi sin\psi} \tag{3.24}$$

Plastic potential surface functiong_{12}, g_{13} are calculated by the following equations according to the non-associated flow rule due to shear hardening.

$$g_{12} = \frac{(\sigma_1 - \sigma_2)}{2} - \frac{(\sigma_1 + \sigma_2)}{2} sin\psi_m \tag{3.25}$$

$$g_{13} = \frac{(\sigma_1 - \sigma_3)}{2} - \frac{(\sigma_1 + \sigma_3)}{2} sin\psi_m \tag{3.26}$$

As a result, the plastic strain between two yield surfaces can be calculated by the Equation 3.27, according to the rule of Koiter (1960), which is used for multi-surface flow based on the theory of plasticity:

$$\varepsilon^p = \Lambda_{12}\frac{\partial g_{12}}{\partial \sigma} + \Lambda_{13}\frac{\partial g_{13}}{\partial \sigma} = \Lambda_{12}\begin{bmatrix} \frac{1}{2} - \frac{1}{2}sin\psi \\ -\frac{1}{2} - \frac{1}{2}sin\psi \\ 0 \end{bmatrix} + \Lambda_{13}\begin{bmatrix} \frac{1}{2} - \frac{1}{2}sin\psi \\ 0 \\ -\frac{1}{2} - \frac{1}{2}sin\psi \end{bmatrix} \tag{3.27}$$

3.2.4.9. Dilatancy Cut-Off

In addition, an important feature of the HS model compared to the MC model is that the dilatancy equals zero at the moment when the ground becomes critical, that is, when the void ratio reaches e_{max} and the volumetric deformation ends.

In the drained condition, positive dilatancy means that the dilatancy will continue as shear deformation continues. Dilatancy never equals zero in the MC model, which is not a situation in real soils (Figure 3.13).

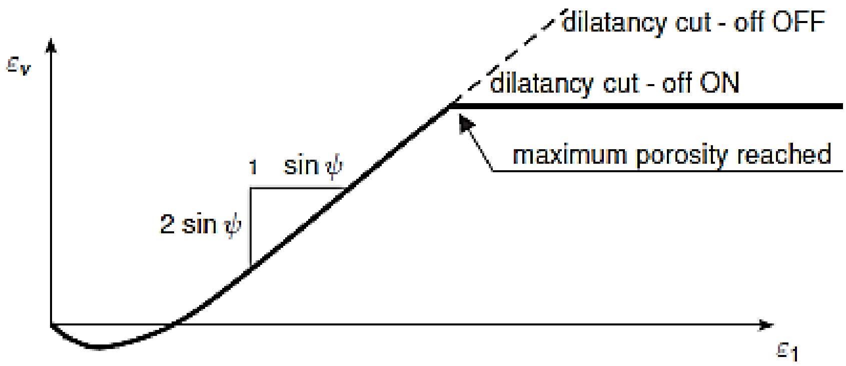

Figure 3. 13. Dilatancy for HSM(PLAXIS Material Models Manuel).

3.2.4.10. Shape of yield surface in the HSM

In contrast to the MC Model, the yield surface (Figure 3. 14) is defined as capped (the dependent flow rule is valid in this region), the triaxial deviator stress-induced shear hardening and the volumetric hardening due to odometer loading can be distinguished. This model is suitable for both cohesive and non-cohesive soils

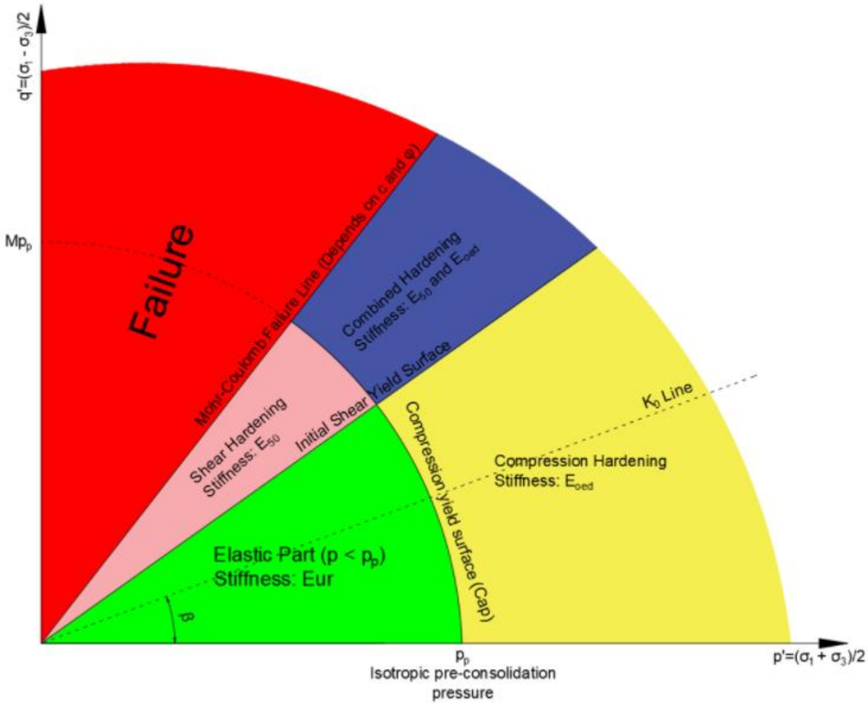

Figure 3. 14. Yield surfaces and regions of stiffness parameters used (https://berkdemir.github.io/)

3.2.4.11. Limits of HS Model

HS Model can be used for overconsolidated soils as it considers the stress history. However, caution should be exercised in modeling the behavior of highly overconsolidated clays. Because the behavior of such soil is very complex and there are many factors that affect behavior (Figure 3. 15) (Schanz et al. 1999)

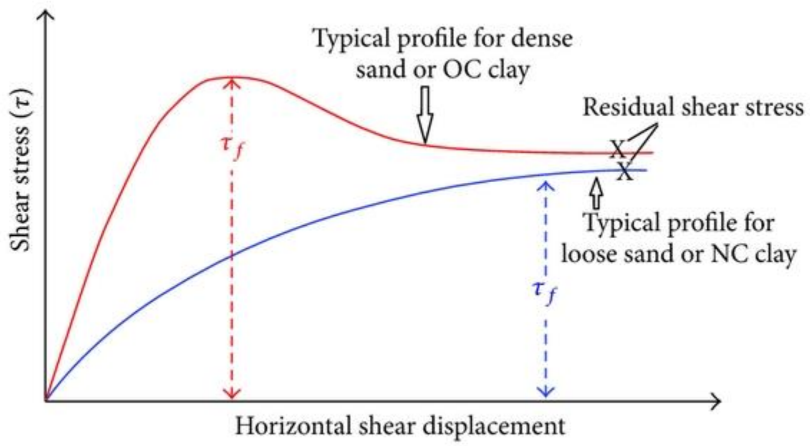

(a)

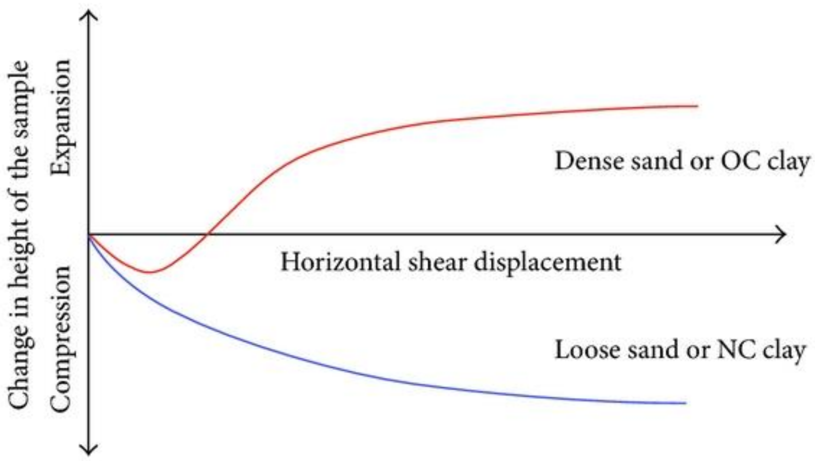

(b)

Figure 3. 15. Over and normal consolidated clay behavior.

Hardening soil parameters are summarized below.

Stiffness parameters	Unit
E_{50}^{ref}: Secant stiffness in standard drained triaxial test	[kN/m^2]
E_{oed}^{ref}: Tangent stiffness for primary odometer loading	[kN/m^2]
E_{ur}^{ref}: Unloading / reloading stiffness	[kN/m2]
m: Power for stress-level dependency of stiffness	[-]
Advanced parameters	
p^{ref}: Reference pressure. ($p^{ref} = 100$ kPa)	[kN/m^2]
K_0^{nc}: Coefficient of normally consolidation	[-]
R_f : Failure ratio	[-]
v_{ur}: Poisson's ratio for unloading-reloading	[-]
p^{ref}: Reference stress	[kN/m^2]
$\sigma_{tension}$: Tensile stress	[kN/m^2]
$c_{increment}$: Cohesion increase with depth	[kN/m^2/m]

Mohr-Coulomb parameters	
c: Cohesion	[kN/m^2]
ϕ: Internal friction angle	[°]
ψ: Dilatancy angle	[°]
Alternative parameters for soil stiffness	
c_c: Compression index	[-]
c_s: Swelling index or reloading index	[-]
e_{init}: Initial void ratio	[-]

3.2.5. Hardening Soil Small Strain Model (HSSM)

HSSM Model considers the increasing stiffness of the soil at the small strain level. All parameters determined for the HS Model are also used in the HSSM (Benz, 2007). The small strain levels of the soils and estimation methods can be seen in Figure 3.16 and Figure 3.17.

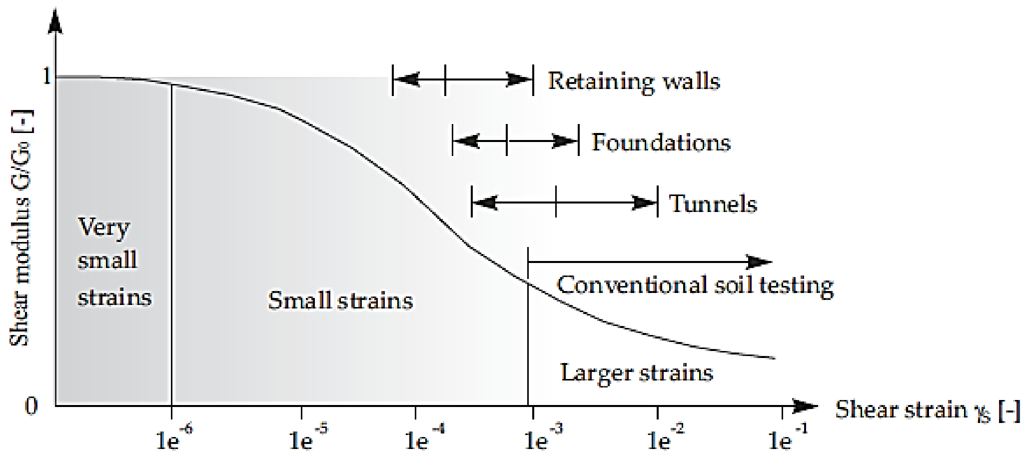

Figure 3. 16. Typical deformation ranges in geotechnical projects

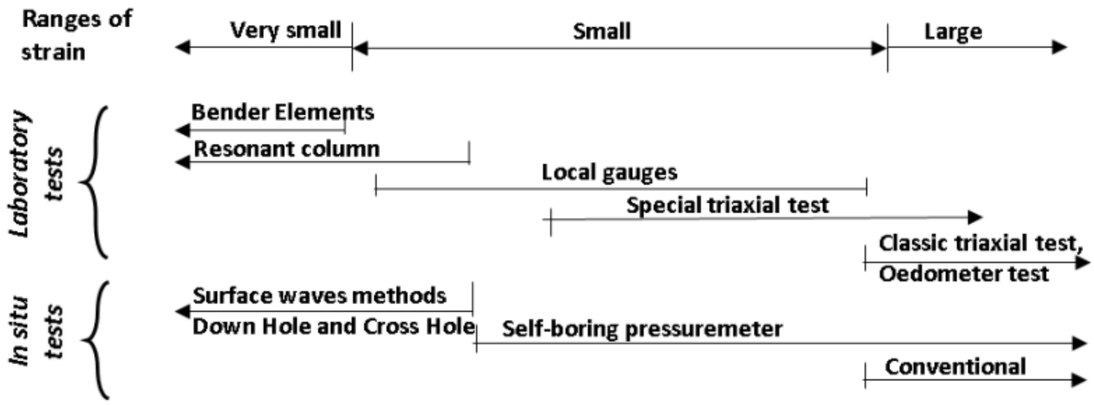

Figure 3. 17. Calculation methods of strain levels

Previous studies show that soil stiffness significantly affect excavation-induced deformations at the small strain level (Brinkgreve et al. 2006; Benz 2007) and models considering the small strain level of the soil can better predict excavation-induced deformations.

Table 3.1. Soil models used for different soil types (Obrzud, 2010).

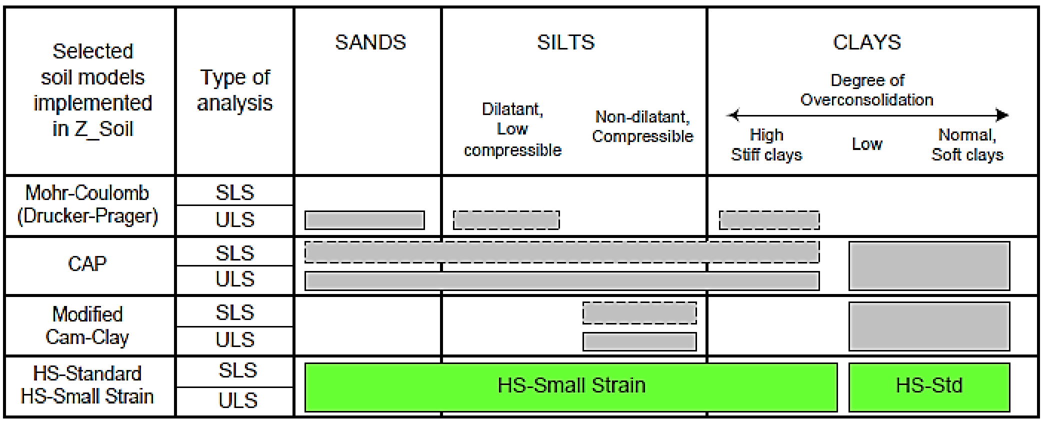

In addition to the parameters used in the HS Model, the HSSM model also considers the increasing stiffness of the soil at the small strain level. Two extra parameters are required to account for small-strain stiffness; these are initial or very small-strain ($\varepsilon < 10^{-6}$) shear modulus G_0^{ref} and the one at the shear strain level $\gamma_{0.7}$, at which the secant shear modulus G_s is reduced to approximately 70% of G_0. HSSM can be applied for almost all soil types (Table 3.1). G_0^{ref} can be calculated according to Equation 3.28.

Summary of Hardening Soil Small Strain Model Parameters

Stiffness parameters (Additional parameters to the HSS model)	Unit
G_0^{ref}: Shear stiffness modulus	[kN/m^2]
$\gamma_{0.7}$: Threshold value of shear strain	[-]

$$G_0 = G_0^{ref}\left(\frac{c\ cos\phi - \sigma_3' sin\phi}{c\ cos\phi + p^{ref} sin\phi}\right)^m \tag{3.28}$$

From laboratory tests, the G_0^{ref}=$(1-4)E_{ur}^{ref}$ approach between shear modulus and elastic loading and unloading stiffness gives suitable estimates for clayey soils (PLAXIS). While the shear modulus G_0 can be calculated precisely in the tests indicated in Figure 3.17. Researchers have conducted numerous studies and obtained a variety of approaches.

Larsson and Mulabdic (1991) also obtained some approximations from the correlations between c_u and the plasticity index (PI) Equations 3.29.

$$G_0 = \left(\frac{280}{I_P} + 250\right) c_u \tag{3.29}$$

The value of $\gamma_{0.7}$ in the HSS Model gives appropriate results in the range of 1.10^{-4}-2.10^{-4} for sands and 5.10^{-5}-1.10^{-4} for clays (Numerics in Geotechnics & Structures, 2010).

Yamashita et al. (2009) calculated these values in the range of 10^{-5}-10^{-3} in their triaxial and cyclic tests on various soils such as sand, clay and soft rock.

Dong et al. (2016) graphically showed the relationships between effective tensile stress σ_1', and small strain shear modulus G_0 for 22 soil types in the literature and 7 soil types in their study(Figure 3.18).

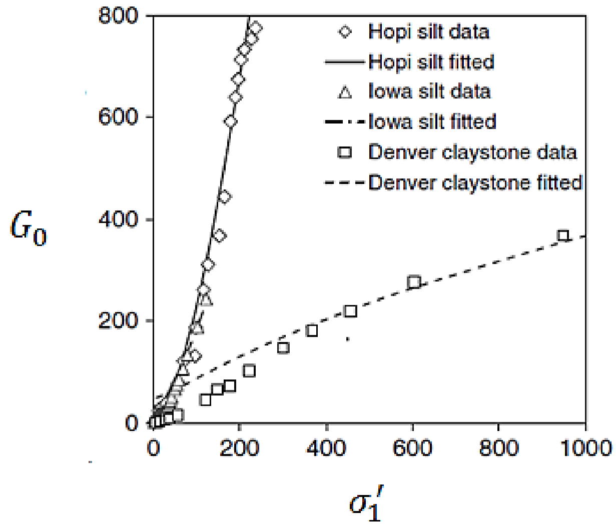

Figure 3. 18. Shear modulus-effective vertical stress relationship for claystone (Dong et al., 2016).

In addition, the shear deformation threshold value was calculated by some researchers by considering the plasticity index and lateral stresses.

Vardanega and Bolton (2013) obtained $G/G_{max} - \gamma$ tables for static and dynamic applications in 67 experiments on 21 clay and silt soils of different plasticity levels and developed various empirical approaches in the light of these data. As seen from the Figure 3.19 and Figure 3.20, it should be noted that the value of the shear modulus decreased by 70% gives different results for static and dynamic applications.

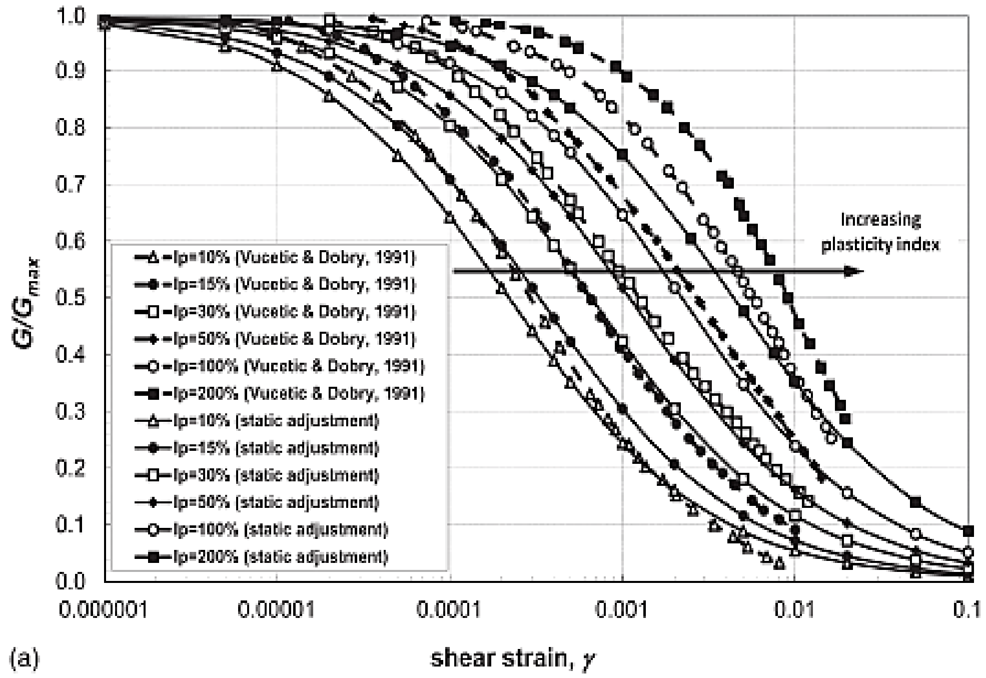

Figure 3. 19. The shear modulus-shear strain relationship for static applications (Vardanega and Bolton 2013).

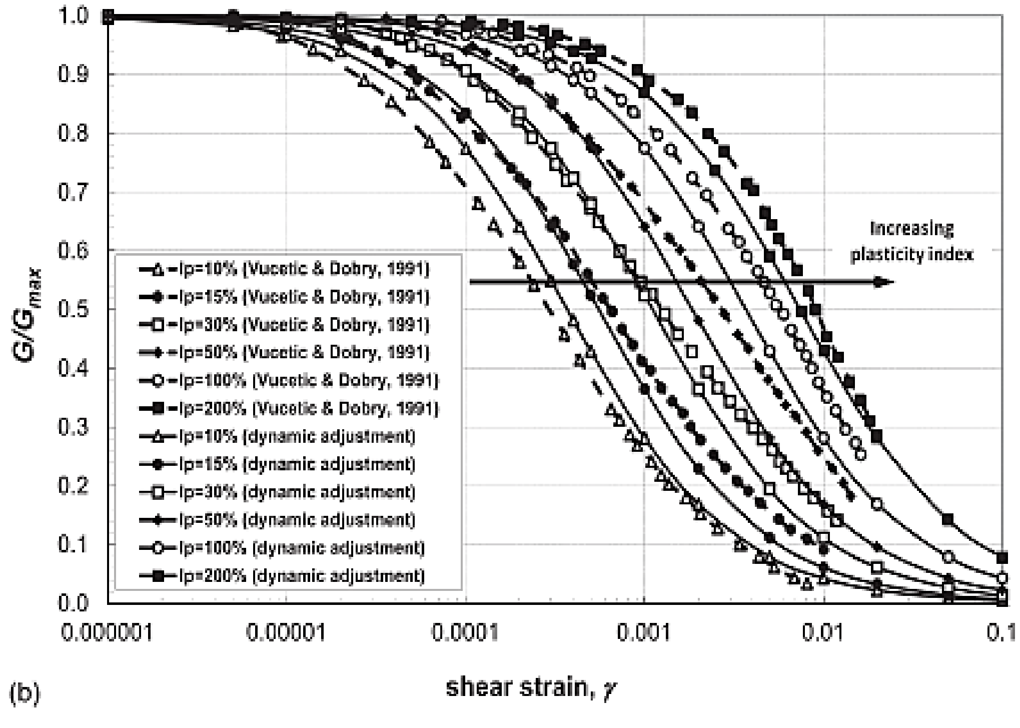

Figure 3. 20. The shear modulus-shear strain relationship for dynamic applications (Vardanega and Bolton 2013).

Solowski (2017) showed empirically $\gamma_{0.7}$ values under plasticity index and lateral stresses from the laboratory studies of Darendeli (2001) on modulus reduction curves (Equations 3.30, 3.31 and 3.32).

$$I_p=0 \qquad \gamma_{0.7} = 0.00015\sqrt{\frac{P'}{P_{ref}}} \tag{3.30}$$

$$I_p=30 \qquad \gamma_{0.7} = 0.00026\sqrt{\frac{P'}{P_{ref}}} \tag{3.31}$$

$$I_p=100 \qquad \gamma_{0.7} = 0.00055\sqrt{\frac{P'}{P_{ref}}} \tag{3.32}$$

Likitlersuang et al. (2013c) determined the relationships between the plasticity index of clay soils and $\gamma_{0.7}$ under different effective stresses. On soils with PI=0 and PI=200; they developed the following empirical relation Equations 3.33. From this relation, the curves in Figure 3.21 can be obtained under different lateral stresses.

$$\sigma'_{m0} = \left(\frac{1+2K_0}{3}\right)\sigma'_{v0} \tag{3.33}$$

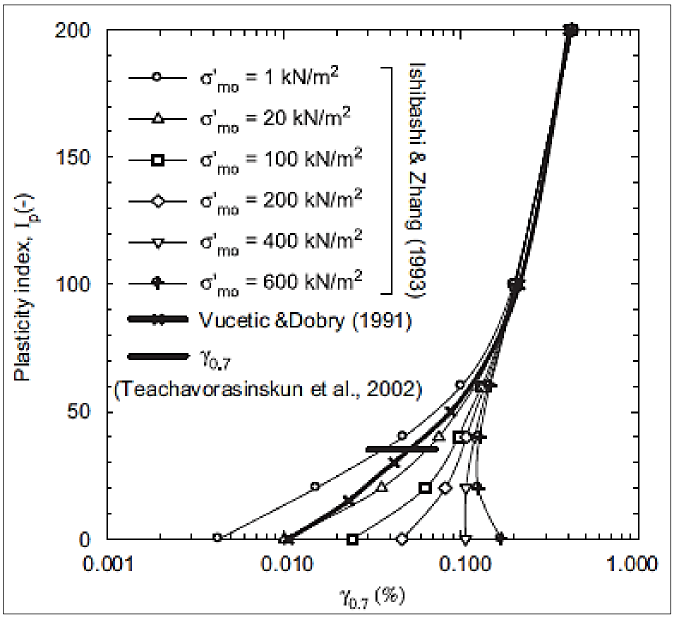

Figure 3. 21. I_p-$\gamma_{0.7}$ curves (Likitlersuang et al. 2013c).

Shear deformation threshold value $\gamma_{0.7}$ can be approximately calculated according to the MC Model failure criterion with the following empirical approximations Equation 3.34 and 3.35 (Hardin & Drnevich, 1972).

$$\gamma_{0.7} \cong \frac{3}{28G_0}[2c'(1 + cos2\phi') - \sigma_1'(1 + K_0)sin2\phi'] \tag{3.34}$$

$$\gamma_{0.7} \cong \frac{3}{9G_0}[2c'(1 + cos2\phi') - \sigma_1'(1 + K_0)sin2\phi'] \tag{3.35}$$

3.2.6. Modified Cam Clay model

It is a model of Cam Clay soil model which is modeled by considering the isotropic yield surface of the prepared or remolded clay soils according to the critical state theory. Critical field theory is the theory based on the assumption that the shear strength of clay soils can be expressed only as a function of effective stress and void ratio regardless of the stress history and drainage condition. The Cam Clay model is based on the elastoplastic behavior of clays. The original cam clay model was first proposed and developed by Roscoe et al. (1963). Later, it was developed by Roscoe and Burland (1968) and named as Modified Cam Clay Model.

Critical state can be expressed following three parameters according to critical state soil mechanics.

p': Average effective stress
q: Deviator stress (shear stress)
v : Specific volume

When the average effective stress, p' and the deviator stress, q are calculated in terms of principal stresses $(\sigma_1', \sigma_2', \sigma_3')$ under general stress conditions: can be calculated with Equations 3.36 and 3.37

$$p' = \frac{1}{3}(\sigma_1' + \sigma_2' + \sigma_3') \tag{3.36}$$

$$q = \frac{1}{\sqrt{2}} + \sqrt{(\sigma_1' - \sigma_2')^2 + (\sigma_2' - \sigma_3')^2 + (\sigma_3' - \sigma_1')^2} \tag{3.37}$$

3.2.6.1. Virgin Consolidation and Swelling Curve

The virgin consolidation and swelling curve is the curve through the virgin consolidation line obtained using the specific volume v and ln p' planes when slowly compressed under isotropic stress ($\sigma_1' = \sigma_2' = \sigma_3' = p'$) and under drained conditions. It is obtained by a series of swelling curves created by the loading and unloading stress (Figure 3.22).

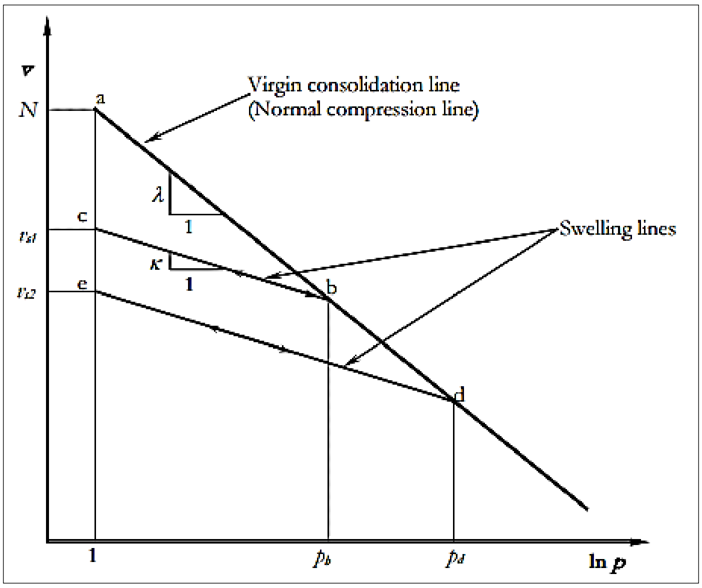

Figure 3. 22. Soil behavior under isotropic loading.

From the virgin compression curve;

$$v = N - \lambda \ln p' \qquad (3.38)$$

Equation form of the swelling line can be expressed as;

$$v = v_s - \kappa \ln p' \qquad (3.39)$$

Equation 3.40 can be used to calculate the elastic volumetric strain ratio for isotropic and axially directional loading.

$$\frac{\partial v^e}{\partial v} = \frac{\kappa}{\lambda} \qquad (3.40)$$

In plastic clays, this ratio varies between 0.2-0.5. However, this relation is valid for a very small stress range in clays (Önalp and Arel, 2013).

As can be seen from the Figure 3.22;

Here;

λ: Slope of the virgin compression curve in the $v - \ln p'$plane (compression index)

κ: Slope of the swelling curve in the $v = N - \lambda \ln p'$ plane (swell index)

N: The specific volume of the virgin compression curve corresponding to p'=1kPa.

v_s: Specific volume values based on the stress history

3.2.6.2. Critical State Concept (CSC)

The concept of critical state refers to the relation between the specific volume of the soil ($v = e_0 + 1$) and the effective stress (σ') in the drained and undrained shear conditions of the clayey soil. In the past, this concept was applied to remolded clay, but today it has been shown to be applicable to natural clays. According to the CSC, there is a characteristic surface in the clay that shows all the stress conditions (Wood, 1990). All effective stress paths reach or closes this surface. When this surface is reached, the soil deforms at constant volume and constant effective stress. This concept applies to two and three-dimensional stress systems. However, different characteristic surfaces occur under different stress systems (Önalp and Arel 2013).

The yield surface equations are as shown below Equation 3.41 and 3.42.

For Cam-Clay Model;

$$q + Mp' \ln\left(\frac{p'}{p'_0}\right) = 0 \tag{3.41}$$

For Modified Cam-Clay Model;

$$\frac{q^2}{p'^2} + M^2\left(1 - \frac{P'_0}{P'}\right) = 0 \qquad (3.42)$$

P'_0 specified in these equations indicates the size of the yield surface. M denotes the slope of the critical state line (CLS) in the $p' - q$ plane. In this plane, the yield surface for the Cam Clay Model is expressed as a logarithmic curve, while the yield surface for the MCC Model is in the form of an elliptic curve, therefore the plastic strain increment vector for the largest value of the mean effective stress is horizontal, and therefore no incremental deviatoric plastic strain takes place for a change in mean effective stress. Figure 3.23.

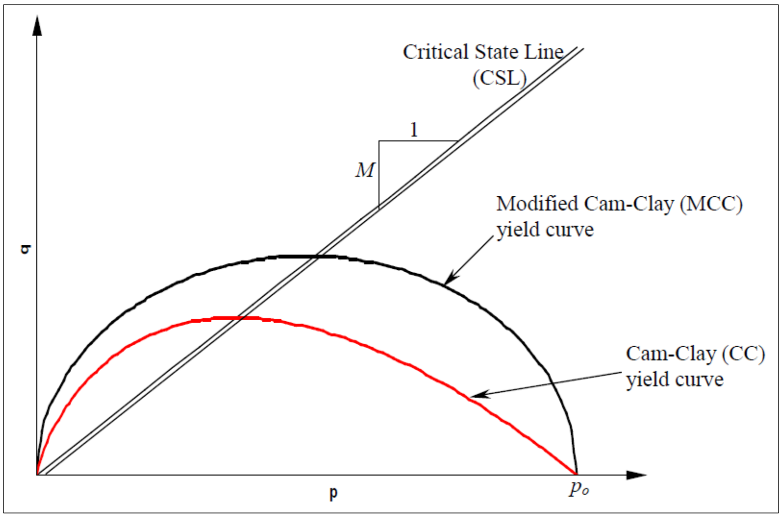

Figure 3. 23. Cam-Clay and Modified Cam-Clay yield surfaces.

3.2.6.3. Modified Cam Clay Model parameters

In Equation 1 below, M is the slope of the CSL in the $p' - q$ plane and can be expressed in terms of its internal friction angle (ϕ') from the Mohr-Coulomb model parameters (Equations 3.42). λ and κ can be calculated from the slopes of the virgin consolidation and loading-unloading curves by means of the $v - \ln p'$ graph obtained from the Odometer experiments. In addition, these parameters can be calculated with compression and swelling indices (Equations 3.43 and 3.44).

$$M = \frac{6 sin\phi'}{3 - sin\phi'} \qquad (3.42)$$

$$\lambda = \frac{C_c}{ln10} \tag{3.43}$$

$$\kappa = \frac{C_s}{ln10} \tag{3.44}$$

3.2.7. Other Models Developed for Soft Soils

In particular, infrastructure projects such as dams, roads, etc. may have to be built on soft soils. In geotechnical engineering, normal consolidated clays, clayey silts and peat soils are accepted as soft soils. In particular, the stress-deformation relationships of soft clays are quite complex and these soils exhibit elasto-viscoplastic behavior under stress over time. In general, soils of this type exhibit anisotropy, bond strength, dissolution between grains, and behavior that develops depending on the time and deformation rate called crypts. This type of soft soil behavior causes significant errors if not included in the calculations. Nowadays, advanced soil models have been developed that take these effects into consideration and it has been found to give very successful results in the calculations (Yıldız et al. 2015).

3.2.7.1. Soft soil model

Soft Soil Model is an improved version of the MCC Model, which was created based on the critical situation theory described in the previous sections. It is used especially in consolidation problems, time and settlement calculations in foundations and fillings. In contrast to the MCC, this model uses the Mohr-Coulomb collapse surface instead of the critical state line (CSL) on the yield surface. Soft Soil Creep model was added to SS model by adding creep effect of clays (stress-deformation relation due to structural viscous properties of clays due to time and deformation rate).

3.2.7.2. S-CLAY1 model

Developed by Dafailas (1987), this model is based on an anisotropic, ellipse-shaped yield surface rather than the isotropic yield surface found in the MCC model. It is mainly developed for normal or less overly consolidated clays. In this model, the increase or decrease of the textural anisotropy due to plastic deformation is calculated according to the rotational hardening rule in the flow curve.

The S-CLAY1S model has been developed by adding parameters that consider the dissolution of the bonding forces between the ground grains.

Leoni et al. (2008), developed the Anisotropic Creep soil Model (ACM), one of the structural equations of the SSL soil model and SCLAY1 model based on anisotropic yield surface.

Karstunen and Yin (2010), modifying the SCLAY1S model, developed an EVP-SCLAY1S (Elasto-Viscoplastic SCLAY1S) soil model that considers anisotropy and structural dissolution in addition to viscous behavior in soils.

Selection of soil model

All the above-mentioned models are used in modeling the behavior of soft soils. However, the use of advanced models such as Hardening Soil is more common in the sector because the parameters are easily obtained from standard laboratory tests and field tests.

When the literature in this study is examined, it is seen that the Hardening Soil model is widely used in infrastructure projects around the world. In this study, the behavior of soils at the small strain level was also investigated.

Due to the above-mentioned situations, the Hardening Soil Small Strain model, which is an improved version of the Hardening Soil model, was used in the analysis.

4. PARAMETER STUDY

Deep excavation works are carried out in soft ground conditions in many countries. In these countries, the ground condition and excavation geometry vary from country to country. In this section, a parameter determination study has been carried out by considering all these different situations. Before starting the numerical analysis, extensive parameter survey was carried out to obtain a large number of generic cases. The parameters to be used in these cases were studied in two groups as soil parameters and geometry parameters.

4.1. Soil Parameters

In this thesis study, since the effect of soft soils on excavation behavior was investigated, a comprehensive study was carried out on this type of soil. The studies in literature (Hashash and Whittle, 1996; Kung et al. 2007; Zhang et al. 2015; Zhang et al. 2020) were used to determine the ranges of soil stiffness, soil strength and soil unit weight. Strength and other parameters of soft soils were selected to be compatible with the literature (D.Roy and Singh, 2009; Vardanega et al. 2012; Varathungarajan et al. 2009; Mesri and Wang 2017; Lemos and Pires 2017; Strahler and Stuedlein 2013; El-Kasaby 1991; Casey et al. 2016; Stroud 1974; Bjerrum 1973; Bowles 1988; Duncan and Buchignani 1976).

4.2. Normalized Strength (s_u/σ'_v)

The undrained strength parameter used in the model was calculated with the SHANSEP approach. For simulating undrained shear strength of specific clay soils, the SHANSEP model (Stress History and Normalized Soil Properties) is utilized (Ladd and Foote, 1974).The estimates of undrained strength ratio, from case studies are plotted against the values of the over consolidation ratio, When Figure 4.1 is examined, the normalized strength for normal and slightly overconsolidated (OCR=1-1,5) soils is between 0.2 and 0.4.

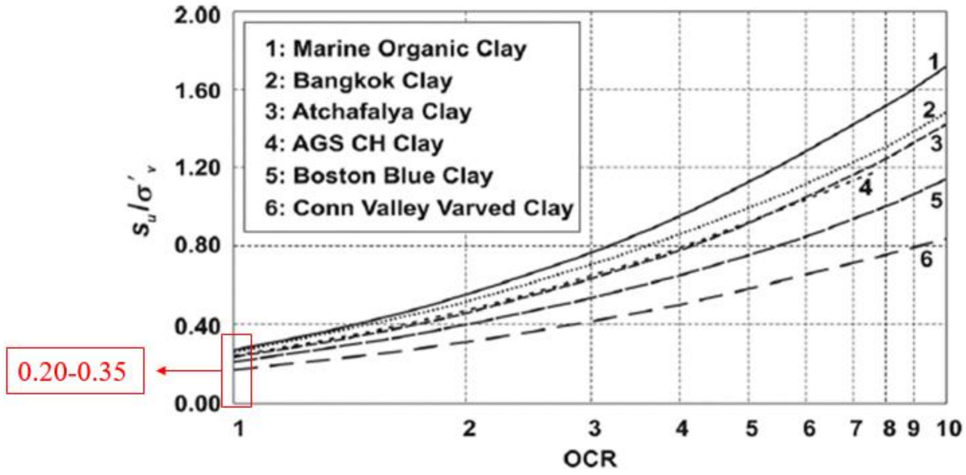

Figure 4. 1. Strength ratio-OCR (Ladd and Foote, 1974).

Mesri and Wang (2017) obtained the following relationship between undrained strength and plasticity index. Figure 4.2 illustrates an empirical correlation based on Bjerrum (1972) data and a large number of in situ vane observations for soft clay and silt layers (e.g., Tavenas and Leroueil 1987).When Figure 4.2 is examined, the normalized strength for soft soils (PI=20-80%) is approximately between 0.2 and 0.35.

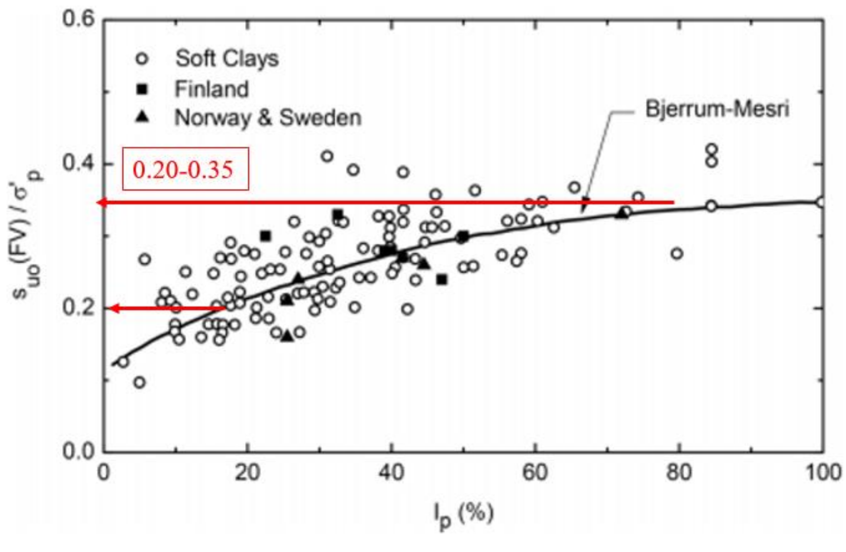

Figure 4. 2. Empirical relationship on $s_u(\text{FV})/\sigma'_p$versus PI. (Mesri and Wang 2017).

On several normally consolidated clays and silts, maximum undrained strength ratios from CK0U (K0-consolidated undrained compression test) triaxial compression and direct simple shear tests are given in Figure 4.3. Undrained strength, with the effect of anisotropy, different values were obtained for three types of tests.

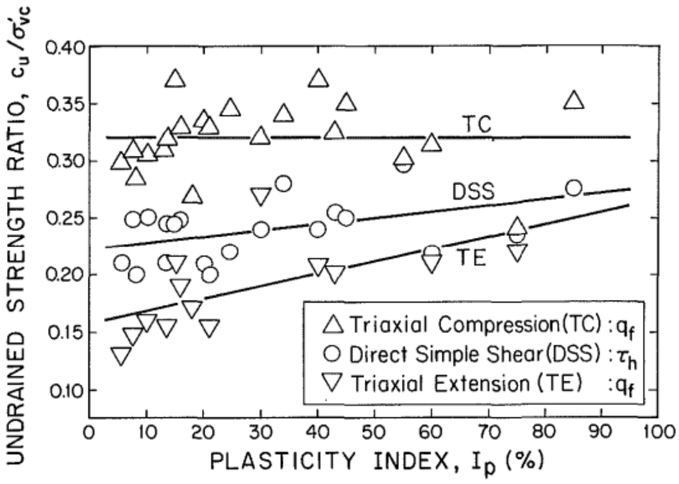

Figure 4. 3. Undrained strength for normally consolidated clays

Figure 4.4 shows data from Ladd and Foott (1974) which illustrates the variation of the undrained shear strength s_u normalized over the current vertical effective σ'_{v0} against the OCR, for some types of clay, in correspondence with their index properties. The data illustrates a similar trend of increasing s_u/σ'_{v0} with *OCR*. Normalized shear strength for normally consolidated clays (OCR=1) varies between 0.18 and 0.30. (Figure 4.4).

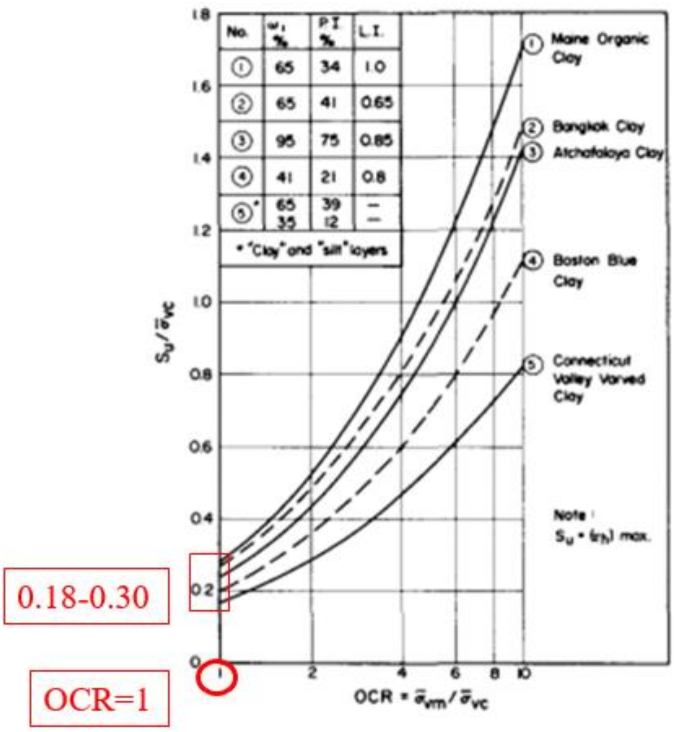

No.	w_l %	PI %	L.I.
①	65	34	1.0
②	65	41	0.65
③	95	75	0.85
④	41	21	0.8
⑤*	65 35	39 12	— —
* "Clay" and "silt" layers			

Figure 4. 4. Variation of s_u/σ'_{v0}versus OCR for five different clays (Ladd & Foot, 1974).

A comparison between the theory and experimental data for Boston blue clay is presented in Figure 4.5. A consolidated isotropic undrained test was conducted by Ladd et al. (1971) for 15 samples. The relationship between shear strength and over consolidated ratio are obtained. Normalized shear strength for normally consolidated clays (OCR=1) varies between 0.25 and 0.35 (Figure 4.5).

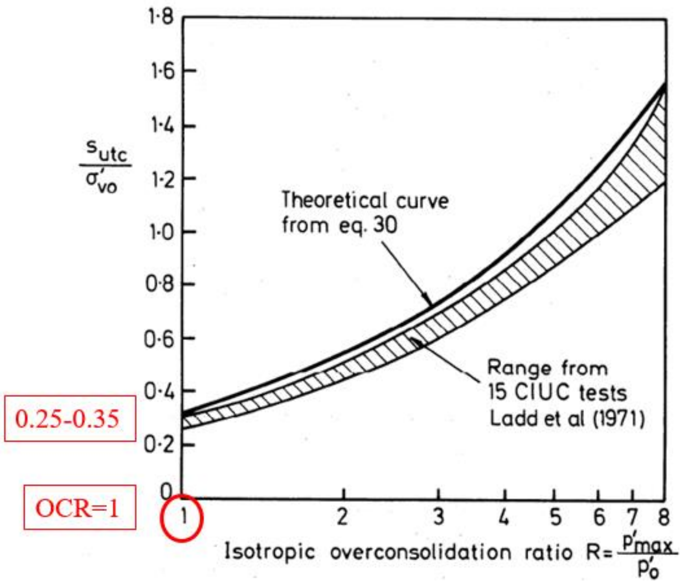

Figure 4. 5. Variation of s_u/σ'_{v0}versus OCR (Ladd et al. 1971).

Ladd and Foote. (1977) determined the undrained strength of different clay groups according to their over consolidation (Table 4.1). In this study, for normally consolidated clay (OCR=1), the undrained strength ratio for OH and CH clays varies between 0.2 and 0.3.

Table 4. 1. Relationship between clay type and overconsolidation (Ladd and Foote, 1977).

Overconsolidation ratio	C_u/σ'_v		
	OH Clays	*CH Clays*	*CL Clays/silts*
1	0.25 to 0.35	0.2 to 0.3	0.15 to 0.20
2	0.45 to 0.55	0.4 to 0.5	0.25 to 0.35
4	0.8 to 0.9	0.7 to 0.8	0.4 to 0.6
8	1.2 to 1.5	0.9 to 1.2	0.7 to 1.0
10	1.5 to 1.7	1.3 to 1.5	0.8 to 1.2

0.2-0.35

Normalized strength can also be determined directly by the DMT field test in Figure 4.6. Marchetti (1980) suggested the following relation between undrained shear strength and horizontal stress for clayey soil. For the DMT test, the normalized strength for normal consolidated clays takes the value 0.22.

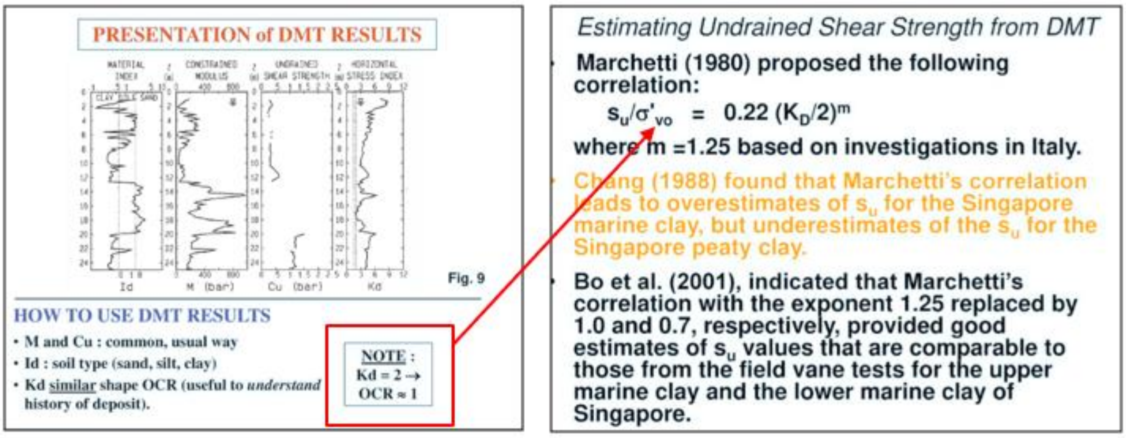

Figure 4. 6. The normalized strength for normal consolidated clays for DMT test.

4.2.1. Internal Friction Angle (ϕ')

In this study, the internal friction angle is derived from the studies carried out by Wroth and Houlsby (1985). According to this approach, the obtained values were used in numerical models. Because of the HS model parameters are derived from consolidated isotropic drained and undrained tests, the internal friction angles in this study were determined by considering the CIUC test mentioned in Figure 4.7 or Equation 4.1. Thus, it is appropriate to use the Wroth and Houlsby approach in this study. In models created with PLAXIS, the internal friction angle was calculated between 18 to 30.

$$(\frac{S_{utc}}{\sigma'_{v0}})_{nc} \cong 0{,}5743\frac{3sin\phi_{tc}}{3-\phi_{tc}} \quad (4.1)$$

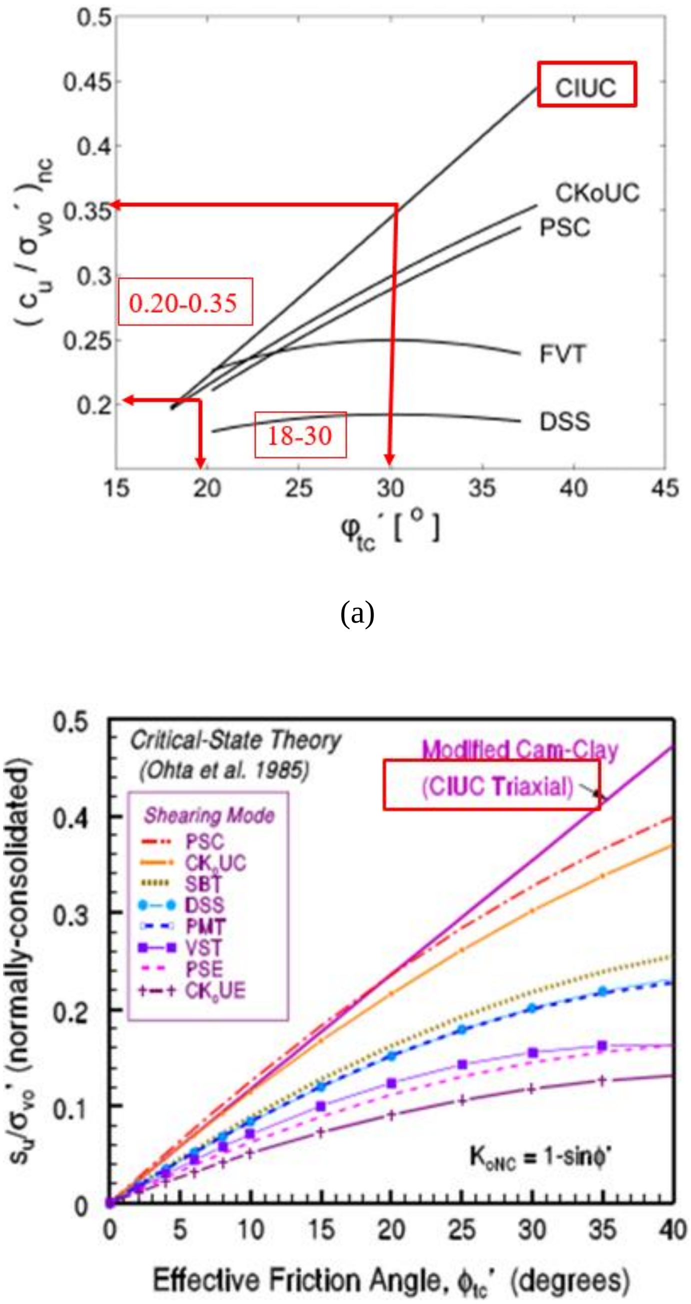

(a)

(b)

Figure 4. 7. Change of undrained strength ratio with effective internal friction angle for normally consolidated clay (a), (b) (Wroth and Houlsby 1985).

Mayne et al. (2001) developed an approach for estimating the undrained strength ratio based on the internal friction angle and over-consolidation condition. According to the study, the undrained strength ratio was approximately 0.22 for most cases (Table 4.2).

Table 4. 2. Obtaining overconsolidated ratios from undrained strength ratio (after Mayne et al., 2001).

C_u/σ'_v	0.2	0.22	0.3	0.4	0.5	0.7	1.0	1.25	1.5	2.0
Friction angle			Over consolidation ratio							
20°	1.5	1.7	2.3	3.1	3.8	5	8	10	11	15
30°	1.0	1.0	1.4	1.9	2.4	3.3	5	6	7	10
40°	1.0	1.0	1.0	1.4	1.7	2.4	3.5	4	5	7

For soft soils (normally consolidated clays and clayey silts), the internal friction angle varies between approximately 18 and 32 degrees in generally accepted studies and codes. The internal friction angle obtained with the empirical approach in the Figure 3.7a confirms the studies in the literature for soft soils (Table 4.3 and Table 4.4).

Table 4. 3. ϕ' values for cohesive soils (AASHTO, T99).

Soil definition	Class	İnternal friction angle(ϕ')
Silty Clay	SM	34
Clayey Sand	SC	30
Silt and Clayey Silt	ML	32
Low plasticity clay	CL	28
Clayey Silt, elastic silt	MH	25
High plasticity clay	CH	19

Table 4. 4. ϕ' values for cohesive soils
(Minnesota Department of Transportation, 2007).

Description	USCS	Soil friction angle (ϕ')	
		Min.	Max.
Silty clay	OL, CL, OH, CH	18	32
Clay	CL, CH, OH, OL	18	28
Peat and other high organic soils	Pt	0	10

4.2.2. Relative Soil Stiffness Ratio (E_s/s_u)

The modulus of elasticity of soil is a measurement of its stiffness. Young's modulus is another name for this property. It is calculated by dividing the tension by the strain within the elastic range of clay soil. The undrained elastic modulus, E_u, will be determined from the undrained triaxial test data, whereas the drained modulus, E_d, will be determined from the drained test data. The elastic modulus of soil can be determined in the laboratory or in-situ studies based on the association with other soil parameters. E_u/c_u values range from 100 for soft clays to 1500 for extremely stiff clays. The unconfined compression strength, which is closer to the back determined range of values, is used to determine the c_u value. The collected data during the unconfined compression strength test is most likely used to calculate soil stiffness. Figure 4.8 illustrates typical test results obtained for a number of cohesive soils. These data were obtained from (DSS) tests and illustrate the range of secant modulus(for undrained test) ratio(E_{us}/s_u) as a function of stress level and (overconsolidation ratio) (OCR). Based on data such as these, Duncan and Buchignani (1976) suggested the broad generalization shown in Figure 4.9.

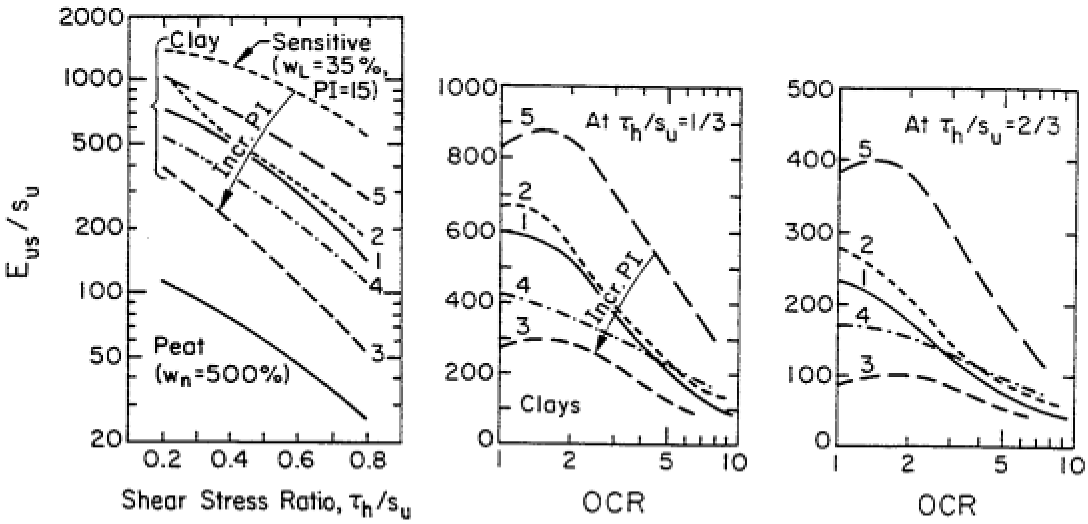

Figure 4. 8. Normalized undrained modulus versus stress level and OCR.

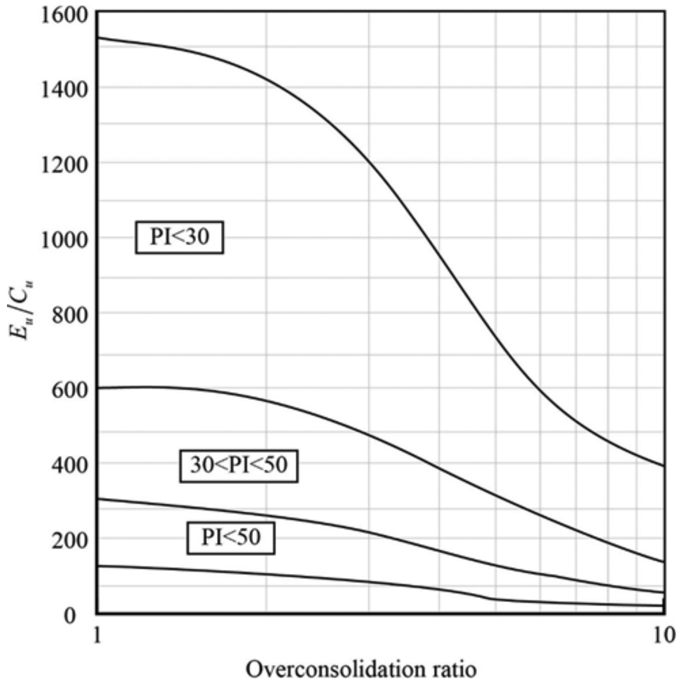

Figure 4. 9. Plate loading tests by Duncan & Buchignani (1976).

Table 4. 5. Range of β for clay.

Plasticity Index	β				
	OCR = 1	OCR = 2	OCR = 3	OCR = 4	OCR = 5
<30	1500–600	1380–500	1200–580	950–380	730–300
30 to 50	600–300	550–270	580–220	380–180	300–150
>50	300–150	270–120	220–100	180–90	150–75

Note: values above are interpolated from Duncan and Buchignani(1976).

The secant modulus (Es) for clays can be given in Equation 4.2;

$$E_s = \beta c_u \quad (4.2)$$

Numerous correlations have been developed between the undrained shear strength and the elastic modulus by different researchers. Some of values determined for soft soils can be seen in the red boxes in Table 4.6 and 4.7.

Table 4. 6. Correlation of modulus of elasticity with undrained shear strength.

Soil type	Relationship	Reference
Clay	E_s=(500 to 1500)c_u	Bjerrum (1972)
Lean organic clays	E_s=(1000 to 1500)c_u	D'Appolonia et al. (1971)
Soft Sensitive clays	E_s=500c_u	NRC of Canada (1975)
Fine to stiff clays	E_s=1000c_u	NRC of Canada (1975)
Very stiff clays	E_s= 1500c_u	NRC of Canada (1975)
Clay Ip>30, or organic	E_s=(100 to 500)c_u	Bowles (1988)
Clay Ip<30, or stiff	E_s=(800 to 1200)c_u	Bowles (1988)
Clay 1<OCR<2	E_s=(500 to 1500)c_u	Bowles (1988)
Clay OCR>2	E_s=(1500 to 2000)c_u	Bowles (1988)

Table 4. 7. Correlation of modulus of elasticity with undrained shear strength.

Equation	Reference	Regions of applicability
$E_{u,i}$=200c_u	Clough & Mana (1976)	San Francisco clay
$E_{u,i}$=(600 to 1200)c_u	Clough & Mana (1976)	San Francisco clay
$E_{u,i}$=280c_u	Ladd & Edgers (1972)	Atchafalya CH clay
$E_{u,i}$=420c_u	Dames & Moore (1975)	AGS CH clay
$E_{u,i}$=600c_u	Ladd & Edgers (1972)	Maine organic CH-OH clay
$E_{u,i}$=6700c_u	Ladd & Edgers (1972)	Bangkok CH clay
$E_{u,i}$=820c_u	Ladd & Edgers (1972)	Boston CL clay
$E_{u,i}$=280c_u	Ladd (1964)	Not known
$E_{u,i}$=(250 to 500)c_u	Bjerrum (1964)	Normally consolidated Norwegian clays
$E_{u,i}$=275c_u	Charles (1964)	Laqunillas normally consolidated clays
$E_{u,i}$=175c_u	Charles (1964)	Kawasaki normally consolidated clays

Note: $c_u/c_{u(max)}$=1/3, $E_{u,i}$=Initial tangent undrained modulus.

Determining the variation range of relative soil stiffness ratio (E_s/s_u) to be used in the study, we need to study the range in which the elastic secant modulus (E_s) changes for soft soils. The undrained modulus of clays is a function essentially of soil plasticity and overconsolidation ratio. The slope of a stress-strain curve generated from an undrained triaxial test can be used to calculate it (Holtz et al. 1981). E_s, on the other hand, is extremely sensitive to sample disruption, resulting in abnormally low amounts observed in laboratory testing (Lambe and Whitman, 1969; Jamiolkowski, 1985). In situ tests can also be used to determine E_s. In this section, secant modulus ranges for soft soils are examined. In the Table 4.8, 4.9 and 4.10 below, experimental studies and field studies have shown that the elastic secant modulus for soft clays varies between approximately 2500 and 20000 kPa (values determined for soft soils can be seen in the red boxes). Thus, the modulus of secant range to be used for numerical analysis is limited between these values.

Table 4. 8. Typical elastic secant moduli of soils.

Soil	E_s (tsf)
Very soft clay	5-50
Soft clay	50-200 (4500-19000 kPa)
Medium clay	200-500
Stiff clay, silty clay	500-1000
Sandy clay	250-2000
Clay shale	1000-2000
Loose sand	100-250
Dense sand	250-1000
Dense sand and gravel	1000-2000
Silty sand	250-2000

Table 4. 9. Elastic parameters of soils (https://structville.com/).

Type of soil	Modulus of elasticity, E_s (MN/m^2)	Poisson's ratio, μ_s	
Loose sand	10–25	0.20–0.40	
Medium dense sand	15–30	0.25–0.40	
Dense sand	35–55	0.30–0.45	
Silty sand	10–20	0.20–0.40	
Sand and gravel	70–170	0.15–0.35	
Soft clay	4–20	→	4000-20000 kPa
Medium clay	20–40	0.20–0.50	
Stiff clay	40–100		

Table 4. 10. Elastic constants of several soils (AASHTO T99).

Soil Type	E_s (tsf)		Poisson's ratio (v)
Clay:			
Soft sensitive clay	25-150	→ 2400-14500 kPa	
Medium stiff to stiff clay	150-500		0.4-0.5
Very stiff clay	500-1000		(undrained)
Loess soils	150-600		0.1-0.3
Silty soils	20-200		0.3-0.35
Fine sand:			
Loose sand	80-120		
Medium dense sans	120-200		0.25
Dense sand	200-300		
Sand:			
Loose	100-300		0.20-0.36
Medium dense	300-500		
Dense	500-800		0.30-0.40
Gravel:			
Loose	300-800		0.20-0.35
Medium dense	800-1000		
Dense	1000-2000		0.30-0.40

The numerical program used in the thesis study makes calculations using drained parameters. Existing studies have generally been performed using undrained parameters as indicated in the tables above.

Stroud, (1974) suggested drained parameters for soft soils based on the plasticity index. In this thesis, considering the approaches developed by Stroud, (1974), the ratio of the drained module to shear strength is limited to between 100 and 300 (Table 4.11).

Table 4. 11. Drained Young's modulus (Stroud, 1974).

Soil plasticity (%)	E'/C_u
10–30	270
20–30	200
30–40	150
40–50	130
50–60	110

4.2.3. Soil Unit Weight(γ_s)

In addition to the stiffness and shear strength of the soil, the effect of the saturated unit weight of the soil on the deformation behavior was also investigated. By considering the values recommended for soft clay in the literature (Table 4.12, 4.13 and 4.14), the soil unit weights of 15, 17 and 19 kN/m^3 were selected (values determined for soft soils can be seen in the red boxes).

Table 4.12. γ_s for cohesive soils based on the SPT number (Bowles 1988).

SPT, N(blows/foot)	γ_{sat} (lb/ft^3)	
0-4	100-120	→ For soft clay 16-19 kN/m^3
4-8	110-130	
8-32	120-140	

Table 4. 13. Unit weights for a variety of soils (Coduto, 2006).

Soil type	Classification	Dry unit weight γ_d (pcf)	Saturated unit weight γ_s (pcf)	
GP, Poorly graded gravel	Sand	110-130	125-140	
GW, Well graded gravel	Sand	110-140	125-150	
GM, Silty gravel	Sand	100-130	125-140	
GC, Clayey gravel	Sand	100-130	125-140	
SP, Poorly graded sand	Sand	95-125	120-135	
SW, Well graded sand	Sand	95-135	120-145	
SM, Silty sand	Sand	80-135	110-140	
SC, Clayey sand	Clay	85-130	110-135	
ML, Low plasticity silt	Clay	75-110	80-130	
MH, High plasticity silt	Clay	75-110	75-130	
CL, Low plasticity clay	Clay	80-110	75-130	12-21 kN/m^3
CH, High plasticity clay	Clay	80-110	70-125	

Table 4.14. The correlation between N_{spt} with unit weight of cohesive soil, γ_{sat} (Terzaghi and Peck, 1967).

Standard Penetration Resistance, N-SPT	Consistency	Unconfined Compression Strength, q_u (tons/ft^2)	γ_{sat} (kN/m^3)
0.0 - 2 .0	Very Soft	<0.25	16 - 19
2.0 - 5.0	Soft	0.25 - 0.5	16 - 19
5.0 - 10.0	Medium Stiff	0.50 - 1.00	17 - 20
10.0 - 20.0	Stiff	1.00 - 2.00	19 - 22
20.0 - 30.0	Very Stiff	2.00 - 4.00	19 - 22
>30	Hard	> 4.00	19 - 22

4.3. Model Geometry and Support System Parameters

Model geometry parameters such as excavation width, soft soil thickness(S), excavation depth (H_e), and the wall thickness (d) parameter of the structural element were obtained by examining many cases. Within this scope, a comprehensive case study was conducted to investigate parameter ranges used in the analysis studies. For this purpose, 70 "diaphragm wall" cases on "soft soils" were examined (Table 4.11).

(Zapata-Medina 2007; Long 2001; Wang et al. 2005, 2010; Zhang et al. 2015; Ou et al. 1993; Bryson and Zapata-Medina 2012; Likitlersuang et al. 2013a; Moormann 2004; Kung et al. 2009; Bhatkar et al. 2017; Hsieh and Ou 1998; Ying et al. 2020; Ding et al. 2018). When the case studies shown in Table 4.11 are examined, it is seen that the excavation depth is 15m on average, the diaphragm wall depth is 26m on average, the wall stiffness is on average 5.73, the soft soil thickness is on average 23m, and the excavation width is 52m on average. Considering the intervals and averages indicated in Table 4.15, the excavation depth, 11, 14, 17 and 20 m was chosen, the soft soil thickness was selected as 23, 28 and 33 m, the excavation width was chosen as 20, 40 and 60m, and the wall thickness was selected as 60, 80 and 120cm

Table 4. 15. Case Study.

Case Number	Case Name	δ_{vm}(mm)	δ_{hm}(mm)	H_e(m)	H_w(m)	s_u/σ_v' or c_u	E_s/s_u	$ln(K_s)$	S(m)	W(m)	γ_s (kN/m^3)
1	Taiwan Formasa (Ou et al. 1993)	42	60	18.5	31	0.34	200	7.30	27	35	19
2	Pudian Road (Zhang et al. 2015)	64	71	17	27	0.3	190	6.12	15.5	20.4	18
3	Yishan Road (Wang et al. 2005)	22.15	38.75	15.5	28	40-60	300	6.5	18	20	16-19
4	TNEC Taipei (Zapata-Medina 2007)	78	106.4	19.7	35	0.3	300	7.15	20	40	18.9
5	Bangkok MRT Project (Likitlersuang et al. 2013a)	24	36	20	25	20-60	250	7.63	13	23	16-20
6	China Airline (Ou et al. 1993)	25	25	9.6	16.75	45	NA	2.46	22	62	NA
7	Taiwan Power (Zhang et al. 2015)	56	80	16.2	22	0.3	150	6.65	13.5	60	19
8	Queng Ming (Ou et al. 1993)	35	70	10.7	17	45	NA	6.097	20	51.6	NA
9	New Cathay Life (Ou et al. 1993)	37	68	21	33	50	NA	6.56	24	42.5	NA
10	State Street (Finno et al, 2002)	27.5	32	12.2	18.3	20	NA	6.05	14	22	19
11	Shanghai Metro (Hu et al., 2003)	7	15.39	11.5	21	22	NA	6.96	18	28.5	18
12	MUNI Metro Project US (Koutsoftas et al., 2000)	30.2	48.1	13	41	0.22	250	7.3	34	16	16.5
13	South Xid Road (Zapata-Medina 2007)	23.7	47.4	20.6	38	20-50	300	6.96	15	22.8	18

14	Howrah Railway Station, India (Bhatkar et al. 2017)	58	42	30	35	NA	NA	NA	28	20.5	19
15	Tai Kai (Kung et al. 2007)	39	48.5	12.6	22	0.31	300	6.09	12.6*	54.1	NA
16	MRT-2 (Kung et al. 2007)	30	60.5	16.8	30	0.31	300	6.53	16.8*	19	NA
17	MRT-4 (Kung et al. 2007)	24.5	41	16.2	33	0.31	300	7.25	16.2*	20	NA
18	Norway Subway (Kung et al. 2007)	15.5	17.2	17	NA	0.23	100	5.2	17*	30	NA
19	HDR-4 (Finno and Nerby 1989)	19.5	23	12.2	16	0.22	100	4.7	12.2*	12.2	NA
20	Tokyo Subway (Miyoshi 1977)	8.5	17	11	32	0.22	100	5.20	11*	11	NA
21	AT&T Corporate Center in Chicago US (Bryson and Zapata-Medina 2012)	37	37.39	8.5	18.3	21.5	100	6.77	8.5*	25	19
22	One Market Plaza US (Zapata-Medina 2007)	53.34	101.6	11	32	25	200	3.50	11*	11	16.5
23	Far East (Ou et al. 1993)	80	124	20	33	0.31	325	6.44	24	70	19
24	Taiwan Chi Ching (Long 2001)	65	65	13.9	15	N=2-15	NA	6.73	13.9*	NA	17-20
25	China Subway Station Area A (Ding et al. 2018)	41	31.5	26.3	38.48	30-65	100-120	6.95	20	21	18-19
26	China Subway Station Area B (Ding et al. 2018)	41	24	24.5	38.48	30-65	100-120	6.95	20	24	18-19
27	Shanghai Cases(2 cases) (Wang et al. 2010)	15	18	9-17	NA	25-72	NA	NA	NA	NA	16-20
28		13	35								

29	Shanghai Cases(12 cases) (Wang et al. 2010)	15	28	9-17	NA	25-72	NA	NA	NA	NA	16-20
30		45	50								
31		35	45								
32		35	50								
33		69	40								
34		65	52								
35		30	70								
36		110	73								
37		112	90								
38		100	98								
39		70	103								
40		60	100								
41		123	124								
42	Moormann Cases(12 cases) (Moormann 2014)	21	15	9-21	NA	Cu<75	NA	NA	NA	NA	NA
43		22	20								
44		20	21								
45		22	23								
46		12	24								
47		23	62								
48		39	55								
49		61	50								
50		60	18								
51		61	55								
52		65	120								
53		110	95								

54	Moormann Cases(3 cases) (Moormann 2014)	115	58	9-21	NA	$c_u<75$	NA	NA	NA	NA	NA
55		75	105								
56		71	64								
57	Pio-Go Hsieh and Chung-Yu Ou Case-1(1998)	75	104	19.7	35	0.32	NA	NA	20	41	NA
58	Pio-Go Hsieh and Chung-Yu Ou Case-2(1998)	40.5	59	18.45	31	0.3	NA	NA	25	35	NA
59	Pio-Go Hsieh and Chung-Yu Ou Case-3(1998)	18.5	28	17	32	22	NA	NA	35	30	NA
60	Pio-Go Hsieh and Chung-Yu Ou Case-4(1998)	110	122	18.5	30	100-200	NA	NA	30	50	NA
61	Hangzhou China(10 cases) (Ying et al. 2020)	64	112.7	10.2	13	25-40	NA	6	NA	162	16.8-18
62		55	88	11.1	22			4.78		135	
63		37	69.4	10.3	18			4.2		60	
64		39.6	85	9.6	14.5			4.01		60	
65		20	77.3	9.7	13.5			4.78		100	
66		68	102.4	9.5	20.2			4.3		180	
67		15	35	9.6	19.5			4.3		30	
68		89	122	14.9	27			4.78		120	
69		85	172	12.9	23.5			4.7		160	
70		37	58.1	13.2	24.2			6.55		58	

Note: NA=not available.

* Assumed values= S was assumed equal to H_e

4.4. Parameter Study Summary

In this section, a preliminary study was carried out to determine the parameters and ranges to be used in generic cases. These parameters are modified for use in the soil model in later chapters. As a result of the above study, the following summary Table 4.16 was obtained.

Table 4. 16. Ranges of parameters used in this study.

Parameter Name	Abbreviation	Values	Unit
Normalized strength	s_u/σ'_v	0.20-0.25-0.30-0.35	(-)
Normalized stiffness	E_s/s_u	100-200-300	(-)
Soft soil unit weight	γ_s	15-17-19	(kN/m^3)
Soft soil thickness	S	23-28-33	(m)
Excavation width	W	20-40-60	(m)
Excavation depth	H_e	11-14-17-20	(m)
System stiffness	$ln(K_s)$	6.097-7.313-8.176	(-)

5. NUMERICAL ANALYSIS

With the rapid developments in software and computing in recent years, studies on numerical analysis have been increasing. In this way, studies with numerical analysis become indispensable in geotechnical studies. In this thesis, PLAXIS program, which is accepted in the world and accepted in the academy and the industry was used, this program calculates according to the finite element method (FEM). The PLAXIS program began to be developed for geotechnical engineering applications at the University of Delft in the late 1970s. Although it was initially used to analyze applications on sandy soils, many features were added to the later versions and took its current form (H.J.Burd, Beyond 2000 computational Geotechnics).

5.1. Model Study

In the previous section, extensive studies carried out to determine soft soil and model geometry and support system parameters were explained in detail. In this section, generic models were generated with various soil, support and excavation types and were solved using finite element methodology. The software PLAXIS-2D has been adopted for analyses. For estimates of maximum wall deflection and surface settlements, the HSS model was chosen.

5.2. Generic Cases

To determine the interaction of soil and wall, 972 generic cases, with 3888 total deformation pairs were conducted. A generic case is shown in Figure 5.1. As the excavation depth ranges between 11 to 20 m, each depth is considered to be a different case, thus resulting in a value of 3888.

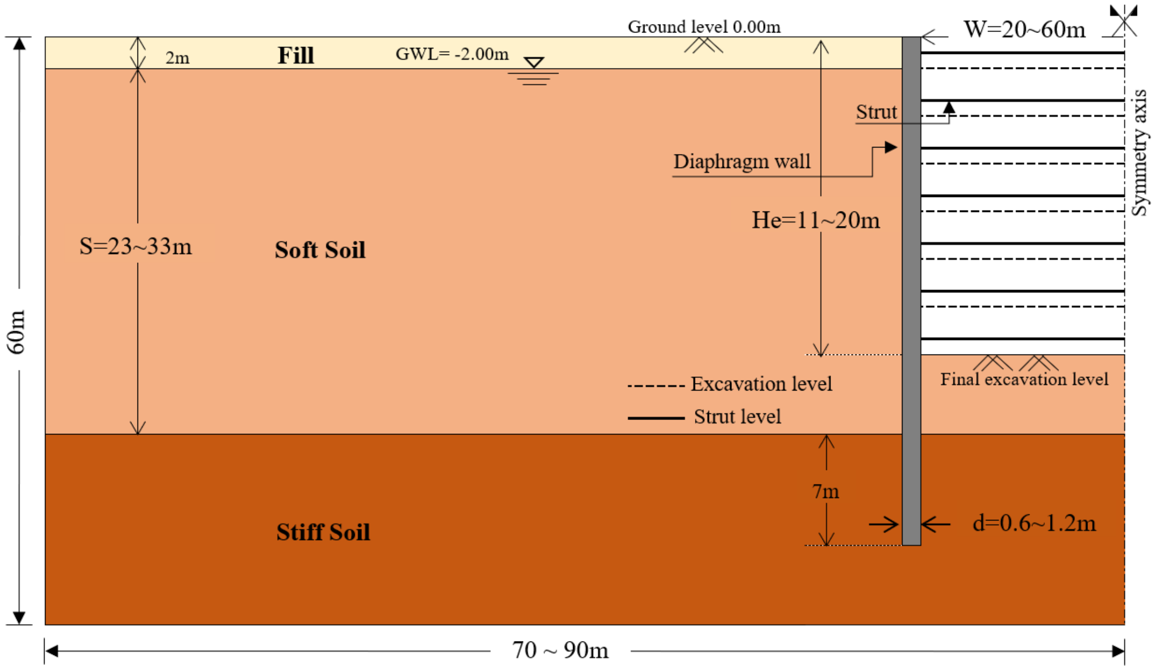

Figure 5. 1. Typical cross-sectional geometry model for FEM analysis (not to scale).

Figure 5.1 illustrates that the excavation is performed in soft clay, and the support system is embedded in stiffer soil. In the previous section, parameters and their ranges were calculated. The obtained strength and stiffness parameters were modified for the HSS model. The effect of wall stiffness was investigated by changing the thickness of the walls(d). EA is the strut (lateral support) stiffness per meter, Φ is strut diameter. The parameters of the braced wall and strut are shown in Table 5.1.

5.2.1. Determining System Stiffness(Ks)

In the model, instead of the bending stiffness (EI) used for the diaphragm wall, the approach suggested by Clough, (1990) is used (Equation 5.1). In this approach, "system stiffness" is obtained by including the effect of strut spacing on the wall strength. In the study, system stiffness was used on a logarithmic scale. Other structural element information used in the study is presented in Table 5.1.

$$K_s = EI/\gamma_w h_{avg}^4 \tag{5.1}$$

Where;

EI: The bending stiffness of retaining wall
h_{avg}: Average vertical strut spacing (h_{avg} =3m is taken in this study)
γ_w: The unit weight of water

Table 5. 1. Ranges of retaining wall-related parameters used in this study.

Parameter	Range of Diaphragm Wall	Strut	Unit
$ln(K_s), \Phi$	6.097-7.313-8.176	0.6	(m)
EA	1.20×10^7 - 1.80×10^7 - 2.40×10^7	3.80×10^7	(kN/m)
EI	3.60×10^5 - 1.21×10^6 - 2.88×10^6	-	(kN/m^2/m)
h_{avg}	-	3	(m)

5.2.2. Determining the Parameters for the HSS Model

5.2.2.1. Determining E_{50}^{ref}, E_{oed}^{ref} and E_{ur}^{ref}

To obtain the HSS model parameters of soft clay; E_{50}^{ref} ranges were determined by writing the normalized shear strength and normalized stiffness values in terms of each other (Zhang et al. 2015). The necessary transformations can be made with the help of the following equations. Other stiffness parameters are calculated as $E_{50}^{ref} = E_{oed}^{ref} = E_{ur}^{ref}/3$.

$$s_u/\sigma_v'=\alpha$$

$$E_s/s_u=\beta$$

$$K_0 = 1 - sin\varphi = \frac{\sigma_h'}{\sigma_v'}$$

From here E_{50}^{ref} can be expressed as:

$$E_{50}^{ref} = \frac{E_{50}}{\left(\frac{\sigma_h'}{p^{ref}}\right)^m} = \frac{\alpha c_u}{\left(\frac{K_0 \times c_u}{\beta \times p^{ref}}\right)} = \frac{\alpha\beta p^{ref}}{K_0}$$

Where:

K_0: Coefficient of earth pressure at rest

p^{ref}: Reference pressure (=100 kPa)

5.2.2.2. Determining G_0^{ref} and $\gamma_{0.7}$

The HSS model has two extra parameters in addition to the HS model parameters; these are initial small-strain ($\varepsilon < 10^{-6}$) shear modulus G_0^{ref} and the one at the shear strain level $\gamma_{0.7}$, at which the secant shear modulus G_s is reduced to approximately 70% of G_0. G_0^{ref} was obtained by first determining the E_0/E_{ur} ratio based on the chart by Alpan (1970) (Figure 5.2). Where E_0 is the small strain Elastic modulus G_0 can be calculated according to the elastic theory shown in Equation 5.2 (Wichtmann and Triantafylidis, 2009).

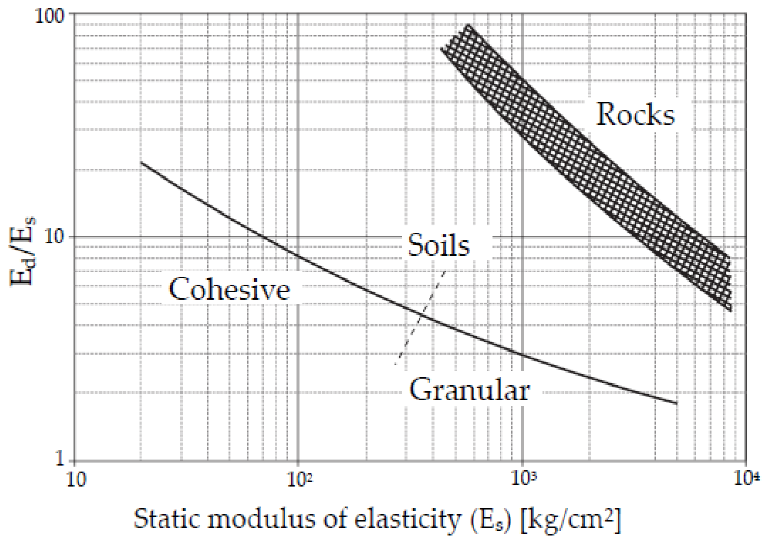

Figure 5. 2. Relationship between dynamic modulus (Ed = E0) and static modulus (Es ≈ Eur) Alpan (1970).

$$G_0 = E_0 \frac{1}{2(1+ v_{ur})} \tag{5.2}$$

$\gamma_{0.7}$ can be calculated approximately with Equation 5.3 (Hardin and Drnevich, 1972). Here, c' is the cohesion, ϕ' is the internal friction angle, and σ_1' is the effective vertical stress.

$$\gamma_{0.7} \approx \frac{1}{9G_0}[2c'(1 + cos2\phi') + \sigma_1'(1 + K_0)sin2\phi'] \tag{5.3}$$

For clayey soil, G_0^{ref}=$(1-4)E_{ur}^{ref}$ and $\gamma_{0.7}$=1.10^{-4}- 4.10^{-4} are appropriate estimations used generally in previous studies (PLAXIS 2020). Small strain parameters for all models were computed using Equations 5.2 and 5.3 in this study.

5.2.2.3. Determining ϕ'

ϕ'can be obtained by empirical relationships associated with the normalized shear strength (for consolidated isotropically undrained compression test, CIUC). In this study, empirical relationship proposed by Wroth and Houlsby (1985) is presented in Figure 5.3 and Equation 5.4. Optimized parameter ranges for the HSS model used in this study are shown in Table 5.2.

$$(\frac{S_{utc}}{\sigma_{v0}'})_{NC} \cong 0{,}5743\frac{3sin\phi_{tc}}{3-\phi_{tc}} \tag{5.4}$$

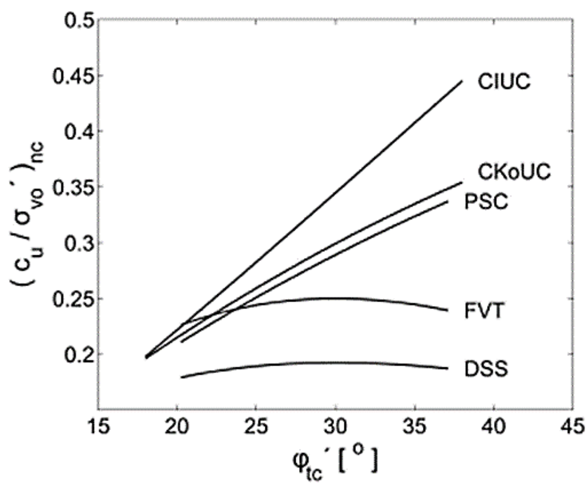

Figure 5. 3. Change of undrained strength ratio with internal friction angle for normally consolidated clay (Wroth and Houlsby 1985).

5.2.2.4. Determining the Other HSSM Parameters

The HSSM model, like other advanced models, uses Mohr-Coulomb model parameters to simulate the failure condition.

Here, effective cohesion was taken as c'=0 for normal consolidated clay, dilatancy angle was calculated as $\psi = \phi' - 30°$.

For all soil layers, poison's ratio is taken as v_{ur} =0.2, reference pressure is p^{ref}=100 kPa and the coefficient of earth pressure at-rest is calculated using $K_0 = 1 - sin\phi$.

The power for stress-level dependency of the stiffness is $m = 1$, Failure ratio is $R_f = 0.9$ and the strength reduction factor for interfaces is taken as R_{inter} =0.65.

As a result, soft clay parameters prepared for generic cases are showed in Table 5.2.

Table 5. 2. Soft clay parameters used in this study.

s_u/σ'_v (-)	E_s/s_u (-)	E_{50}^{ref} (kPa)	E_{oed}^{ref} (kPa)	E_{ur}^{ref} (kPa)	G_0^{ref} (kPa)	$\gamma_{0.7}$ (-)	ϕ' (°)	K_0 (-)	E_0/E_{ur} (-)
	100	2895	2895	8685	30759	3.59E-4			8.5
0.20	200	5789	5789	17367	43418	2.54E-4	18	0.691	6
	300	8685	8685	26055	54281	2.03E-4			5
	100	4000	4000	12000	35000	3.58E-4			7
0.25	200	8000	8000	24000	50000	2.51E-4	22	0.625	5
	300	12000	12000	36000	67500	1,86E-4			4.5
	100	5400	5400	16200	40500	3,40E-4			6
0.30	200	10800	10800	32400	60750	2.27E-4	26.4	0.555	4.5
	300	16200	16200	48600	75938	1,48E-4			3.75
	100	7000	7000	21000	52500	2,75E-4			6
0.35	200	14000	14000	42000	73500	1.96E-4	30	0.5	4.2
	300	21000	21000	63000	99750	1.45E-4			3.8

5.2.3. Determining the Stiff Clay and Fill Layers Parameters

The properties of the fill/sand soil and the hard soil/stiff clay layer were determined by considering the studies in the literature. These parameters are the same in all models. HS model is selected for these layers and shown in Table 5.3.

Table 5. 3. Firm clay and fill layers parameters (HS).

Layer name	Stiff Clay Undrained	Fill Drained	Unit
E_{50}^{ref}	1.00E+05	1.50E+04	(kPa)
E_{oed}^{ref}	1.00E+05	1.50E+04	(kPa)
E_{ur}^{ref}	3.00E+05	4.50E+04	(kPa)
ϕ'	26	30	(°)
K_0	0.562	0.5	(-)
c'_{ref}	25	1	(kPa)
v'_{ur}	0.2	0.2	(-)
p^{ref}	100	100	(kPa)
R_f	0.9	0.9	(-)
$\gamma_{unsat}/\gamma_{sat}$	20/20	16/20	(kN/m^3)
R_{inter}	0.65	0.65	(-)
m	1	1	(-)

5.2.4. Excavation Geometry

In the generic models analyzed, the thickness of the soft soil varies between 23m to 33m, excavation width is 20m to 60m, and excavation depth is 11m to 20m (Figure 5.4), similarly, 27 "Model groups" were created by including all parameters and ranges. Other model geometries used in generic cases are given in the appendices.

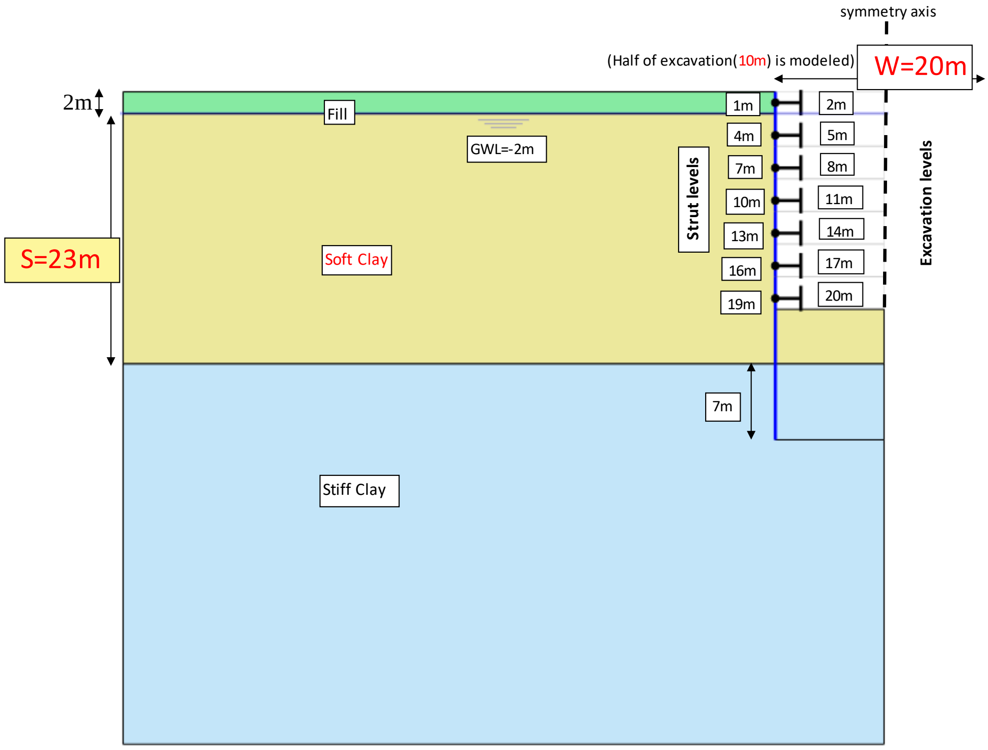

Figure 5. 4. Model Geometry

5.2.5. Support System

Due to the presence of adjacent structures in city centers, strut is generally used instead of anchorage. In this study, the Strutted diaphragm wall system was used and the system stiffness was chosen 6 to 8. Diaphragm wall and strut parameters are shown in the Table 5. 4. For all generic cases these parameters are presented in the appendices.

Table 5. 4 Structure parameters

Diaphragm Wall (E=2.0E+7)			Strut	
			EA	3.80E+06
d	EA	EI	$L_{spacing}$	5m
0.6	1.2E+07	3.60E+05	h_{avg}	3m
0.9	1.8E+07	1.215E+06		
1.2	2.4E+07	2.88E+06		

5.2.6. Fill/Sand Layer

Natural soils are usually in layers. Soft soil environments usually have a top layer of sand or a fill layer. For the continuity of the model, 2-meter fill layer on the top is included in the calculations.

These ranges were obtained by considering their applicability in real life, going through about 70 real cases. The fill/sand parameters used in the analyzes are given in the Table 5.5. Parameters used in all generic models are given in the appendices.

Table 5. 5 Fill/Sand parameters

Default Soil Parameters		
Stiff Clay		Fill
HS		HS
Undrained(A)		Drained
E_{50}^{ref}	1.00E+05	1.50E+04
E_{oed}^{ref}	1.00E+05	1.50E+04
E_{ur}^{ref}	3.00E+05	4.50E+04
ϕ'	26	30
K_0	0.562	0.5
c'_{ref}	25	1
v'_{ur}	0.2	0.2
p_{ref}	100	100
R_f	0.9	0.9
$\gamma_{unsat/sat}$	20/20	16/20
R_{inter}	0.65	0.65
m	1	1

5.2.7. Soil Parameters

The unit weight was taken as 15 to 19 kN/m^3 (Bowles, 1988) consistent with the literature, shear strength and stiffness parameters for soft soils have been obtained from empirical studies on soft soils (Stroud, 1974; Bjerrum, 1972; Duncan and Buchignani, 1976). The parameters for the stiff clay and fill/sand layer are taken the same for each model.

5.2.8. Wall Penetration Depth

It is known that wall penetration depth is an important parameter for deformations in environments where all layers are soft soils. Zhang et al. (2015) showed that penetration of 3 to 5 m into the hard stratum gave similar results in deformation values.

Similarly, Moorman (2014) and Wang et al. (2010) showed that the effect of penetration depth on deformations is minimal in cases built on soft soils. Therefore, to minimize the effect of penetration depth on deformations, this value was accepted as 7m and not included as a parameter in the closed-form solution.

5.2.9. Analysis Type

Generic cases were studied in 2D and the analyses are based on a plane strain excavation with a bracing wall system. Only half of the cross-section was examined due to symmetry. Considering the short-term behavior of the soil, undrained analysis was carried out.

5.2.10. Traffic/Surcharge Load

Although it is known that the loads around the excavation have an effect on the wall deformations; in the case studies examined, no information was given about the load situation in the excavation area. So, no traffic or surcharge loading has been incorporated into the system.

5.2.11. Staged Construction

15-noded triangular elements were used to model the soil. The structural elements(strut and wall) were considered to be linear elastic, the wall is represented by 5-noded beam elements and the 7 levels of struts were placed at depths of 1 m, 4 m, 7 m, 10 m, 13 m, 16 m, and 19 m below the original ground surface and they were represented by 3-noded bar elements. Excavation steps were taken as 3 m, i.e. the first excavation elevation was 2m, and the next ones were 5m, 8m, 11m, 14m, 17m, and 20m in consequence. All stages of excavation and numerical studies are shown in Table 5.4.

Table 5. 6. Construction procedure.

Phase	Construction stages
Phase 1	K_0 Procedure
Phase 2	Install the diaphragm wall
Phase 3	Reset displacement to zero, excavate to 2 m below ground surface
Phase 4	Install strut systems at 1 m below ground surface
Phase 5	Excavate to 5 m below ground surface
Phase 6	Install strut systems at 4 m below ground surface
Phase 7	Excavate to 8 m below ground surface
Phase 8	Install strut systems at 7 m below ground surface
Phase 9	Excavate to 11 m below ground surface
Phase 10	Install strut systems at 10 m below ground surface
Phase 11	Excavate to 14 m below ground surface
Phase 12	Install strut systems at 13 m below ground surface
Phase 13	Excavate to 17 m below ground surface
Phase 14	Install strut systems at 16 m below ground surface
Phase 15	Excavate to 20 m below ground surface
Phase 16	Install strut systems at 19 m below ground surface

5.2.12. Model Boundaries

The nodes along the mesh's side boundaries were restricted from moving horizontally (only vertical movement was permitted), but the nodes along the mesh's bottom boundary were restricted from moving both horizontally and vertically (totally fixed). Model boundaries are determined as 60x70m, 60x80m, and 60x90m considering the excavation width, excavation depth, and other relevant parameters. These measures were chosen to minimize the effect of the analysis results (Brinkgreve et al. 2007).

5.2.13. Structural Elements and Interface

Diaphragm wall (Plates) and Strut (Anchors) structural elements are used. An interface is defined around the diaphragm wall to simulate the interaction between the diaphragm wall and the soil (interface). Soil and structural parameters are assigned to the soil layers and structural elements in the idealized soil profile for each model.

5.2.14. Groundwater (GWL) Level

Groundwater (GWL) is defined as 2m below the ground surface. Since all layers in the soil are considered horizontal, the K_0 procedure is defined for the initial stresses.

5.2.15. Mesh Study

The software is based on the finite element method(FEM) where the area is divided into finite number of elements (mesh). The soil elements are analyzed with “fine” mesh to make the analyzes more sensitive.

5.2.16. Calculation

After the above-mentioned stages, structural elements and excavations were defined in “staged construction” and the system was analyzed “plastically” in 16 phases. As a result of these analyses, total displacements for back-excavation settlements and wall deformations were obtained at different excavation depths: a total of 3888 deformations of pairs.

The Table below shows the settlement and wall deformation results of generic cases 1 to 36. All deformations obtained from all generic models are given in the appendices.

Table 5. 7. Deformation results for generic models

H=11m	d=0.6	d=0.9	d=1.2	E_{50}/c_u	H=11m	d=0.6	d=0.9	d=1.2
δ_{vm}(mm)	115	66	48	100	δ_{hm}(mm)	147	80	57
	107	58	41	200		127	72	50
	96	54	37	300		120	68	47
H=14m	d=0.6	d=0.9	d=1.2	E_{50}/c_u	H=14m	d=0.6	d=0.9	d=1.2
δ_{vm}(mm)	157	90	62	100	δ_{hm}(mm)	201	108	74
	145	79	56	200		179	99	68
	136	75	52	300		170	95	65
H=17m	d=0.6	d=0.9	d=1.2	E_{50}/c_u	H=17m	d=0.6	d=0.9	d=1.2
δ_{vm}(mm)	201	112	76	100	δ_{hm}(mm)	250	132	89
	185	100	69	200		221	124	83
	174	96	65	300		212	119	79
H=20m	d=0.6	d=0.9	d=1.2	E_{50}/c_u	H=20m	d=0.6	d=0.9	d=1.2
δ_{vm}(mm)	235	126	85	100	δ_{hm}(mm)	285	149	99
	218	114	78	200		252	140	93
	206	112	75	300		242	134	90

Figure 5.4 illustrates the findings of the investigations. Almost all points are within the 50% - 10% range of the δ_{hm}=δ_{vm} line (predicted wall deflections are equal to the settlement values).

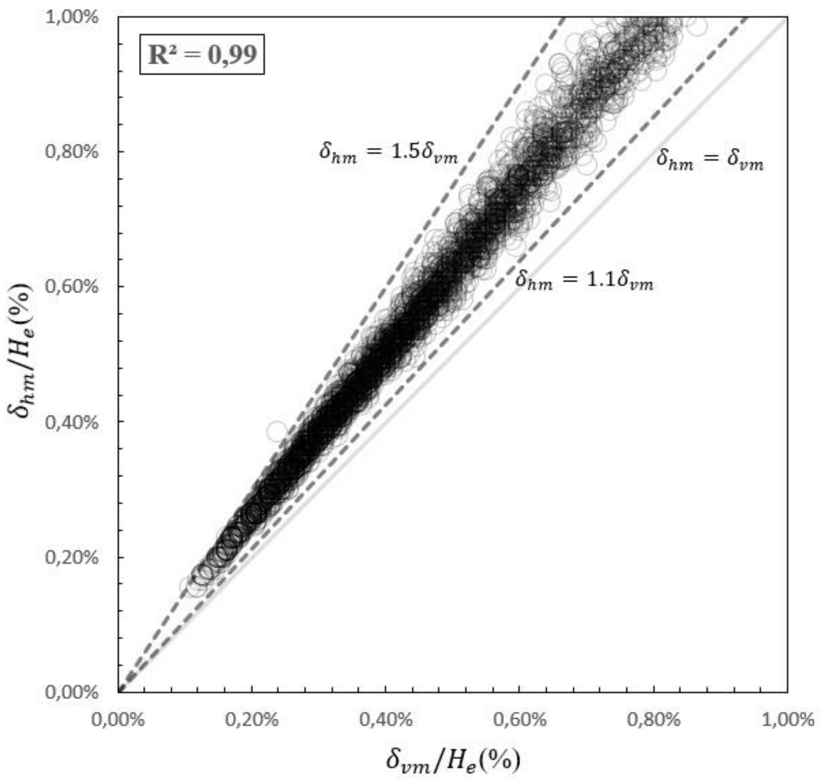

Figure 5. 5. Relationship between settlement and wall deflection.

5.3. Verification Data

To assess the accuracy of the parameters and ranges employed in the analysis studies, a detailed case study was performed.

For this purpose, a comprehensive literature survey has been conducted, and 54 “diaphragm wall” cases on “soft soils” were examined (Zapata-Medina 2007; Long 2001; Wang et al. 2005, 2010; Zhang et al. 2015; Ou et al. 1993; Bryson and Zapata-Medina 2012; Likitlersuang et al. 2013a; Moormann 2004; Kung et al. 2007; Bhatkar et al. 2017; Hsieh and Ou 1998; Ying et al. 2020; Ding et al. 2018).

As can be seen in Fig.5, about 30% of the settlement and wall deformation pairs fall in the range obtained from this study. If we extend the limits ±30%, almost all cases fall in this area as can be seen in Figure 5.5.

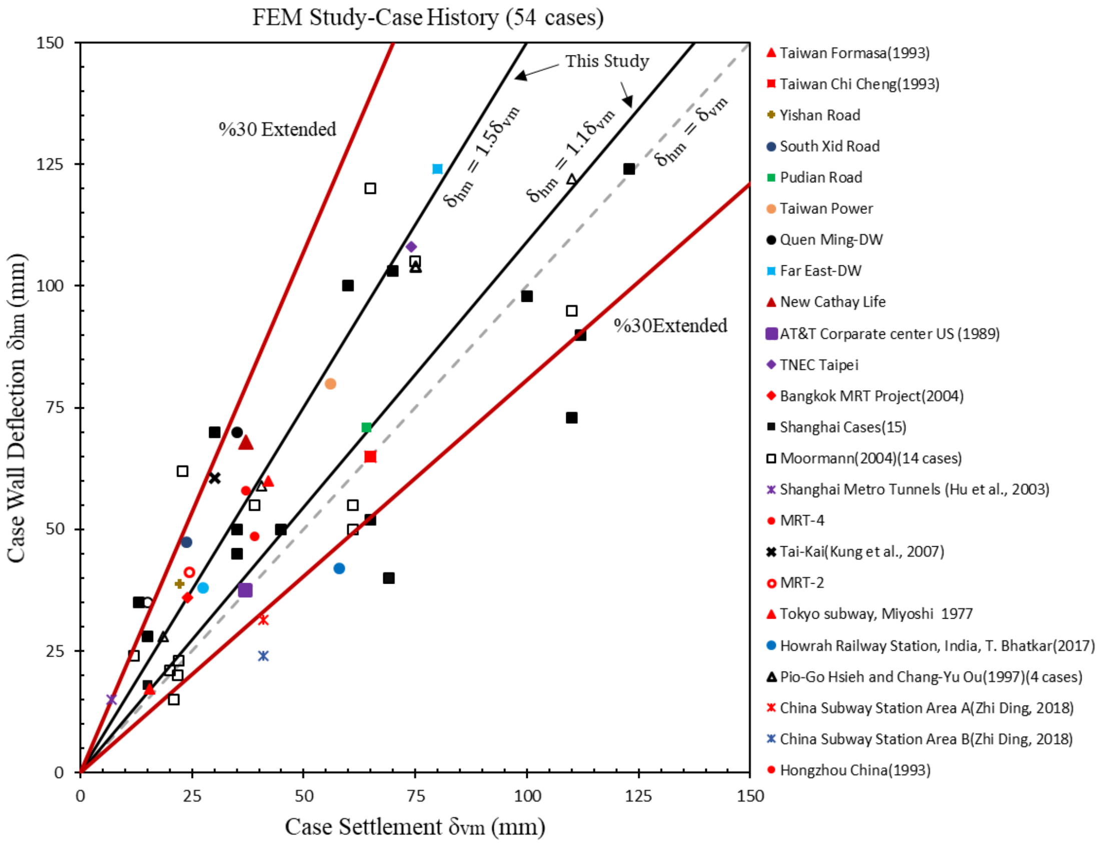

Figure 5. 6. Performance of selected parameters and ranges in terms of case studies.

6. STATISTICAL ANALYSIS

Data analysis is carried out today using field research and various statistical methods in almost all academic studies. Statistical studies are frequently used in social sciences, market research, engineering, health research, and academic research. As in other engineering disciplines, statistics are widely used for geotechnical engineering. Due to soils' very complex and heterogeneous structure, it is not possible to know the physical and strength parameters exactly. Furthermore, geomaterials are naturally complex and varied at all scales, from microstructure to regional scale. However, in geotechnical design and characterization, the significance of explicitly modeling and measuring the variability of geotechnical parameters (i.e. quantifying, processing, and reporting the related uncertainty) is becoming increasingly recognized. The precise modeling of uncertainty in geotechnical engineering allows for more complete and accurate information about the level of risk associated with design. (Uzielli, 2008).

6.1. IBM SPSS Statistics

SPSS is a statistical analysis program that was initially launched in 1968. Although SPSS was first used in the field of social sciences, it has become a very popular software in the fields of engineering and science over time. Statistical studies in this thesis were prepared by using the SPSS v.21 package program.

6.2. Determining Averaged Deformations

To study the effect of the parameters on wall deformations and settlements, different sets of analyses were performed for each parameter. In the sets, one of the parameters is kept constant and the others take values within the ranges mentioned in Table 4.16. Then the average of the deformations and settlements are taken corresponding to the constant parameters. By this method, the effect of that constant parameter can be obtained and the form of that parameter in the regression equation is determined (Zhang et al. 2020). The curves obtained as a result of different sets of analyses are presented in Figure 6.1.

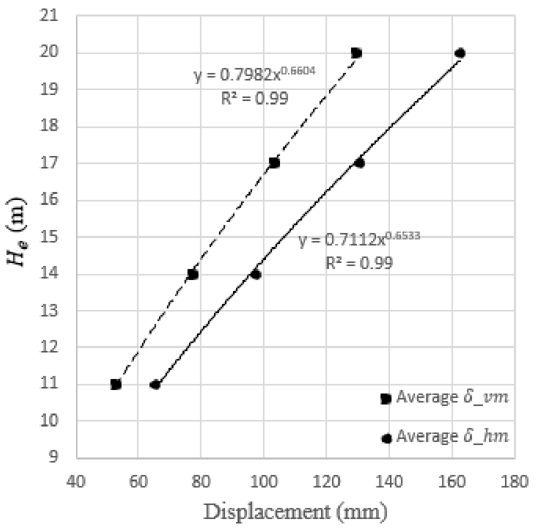

H_e (m)
Displacement (mm)
y = 0.7982x^0.6604
R² = 0.99
y = 0.7112x^0.6533
R² = 0.99
Average δ_vm
Average δ_hm

(a)

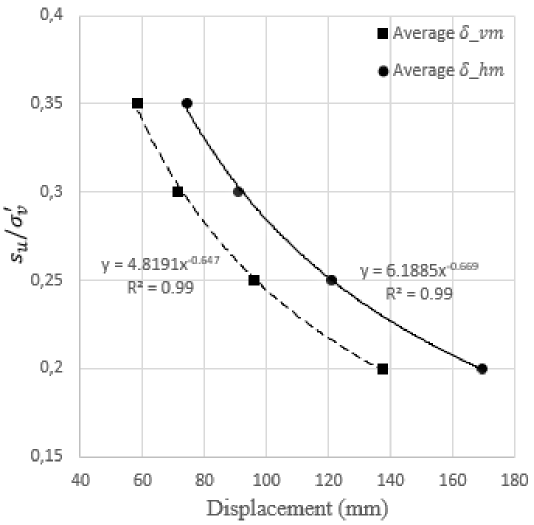

s_u/σ_v'
Displacement (mm)
Average δ_vm
Average δ_hm
y = 4.8191x^-0.647
R² = 0.99
y = 6.1885x^-0.669
R² = 0.99

(b)

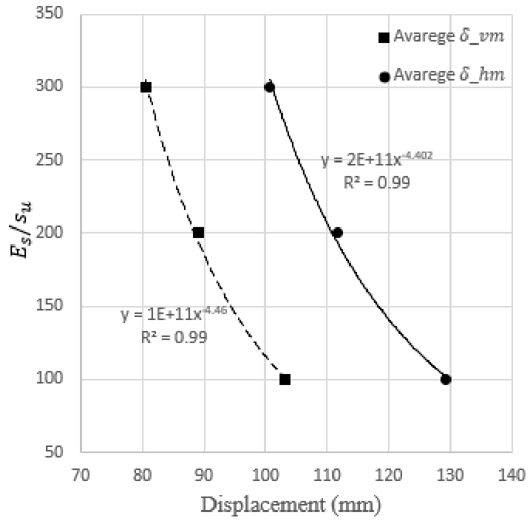

E_s/s_u
Displacement (mm)
Avarege δ_vm
Avarege δ_hm
y = 2E+11x^-4.402
R² = 0.99
y = 1E+11x^-4.46
R² = 0.99

(c)

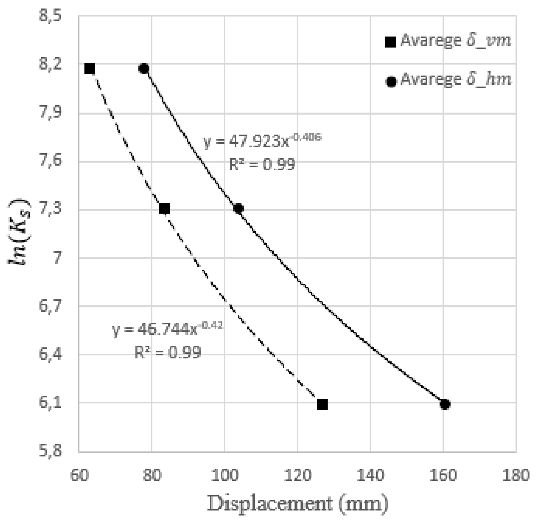

$ln(K_s)$
Displacement (mm)
Avarege δ_vm
Avarege δ_hm
y = 47.923x^-0.406
R² = 0.99
y = 46.744x^-0.42
R² = 0.99

(d)

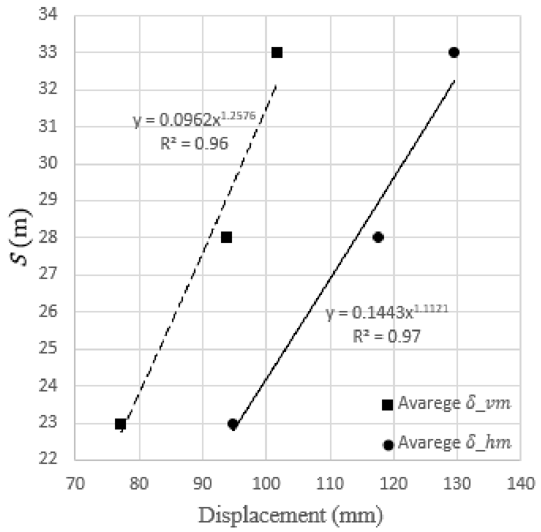

S (m)
Displacement (mm)
y = 0.0962x^1.2576
R² = 0.96
y = 0.1443x^1.1121
R² = 0.97
Avarege δ_vm
Avarege δ_hm

(e)

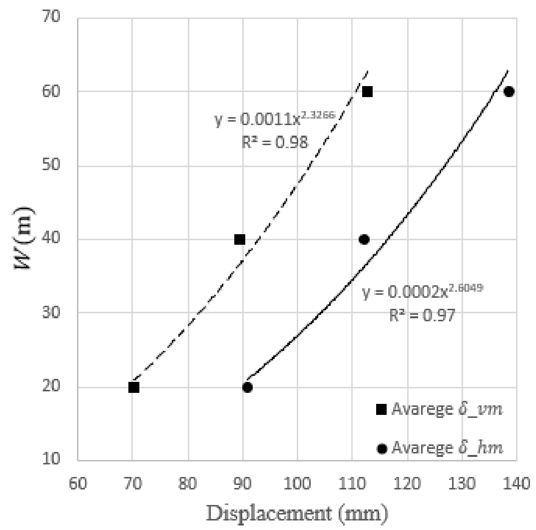

W (m)
Displacement (mm)
y = 0.0011x^2.3266
R² = 0.98
y = 0.0002x^2.6049
R² = 0.97
Avarege δ_vm
Avarege δ_hm

(f)

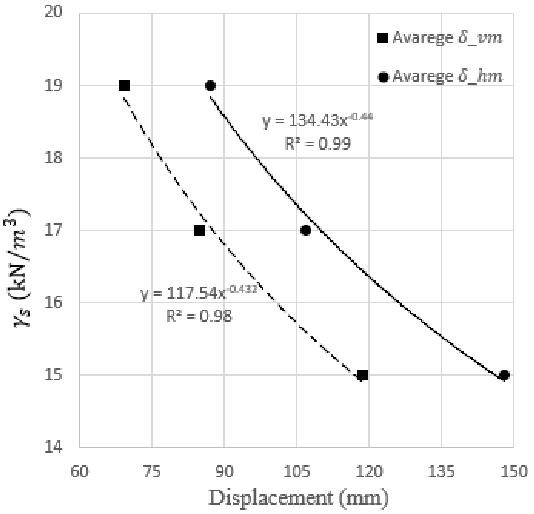

(g)

Figure 6. 1. Variation of averaged maximum excavation deformation with (a) excavation depth, (b) normalized strength, (c) normalized stiffness, (d) system stiffness, (e) soft soil thickness, (f) excavation width, (g) soft soil unit weight.

When the graphs are examined, the exponential function gives the best fit for the results. The logarithms of both axes are taken to obtain a linear relationship in the estimation of the deformations. While these modified deformation pairs are determined as the dependent variable, data containing parameter ranges were determined as independent variables.

6.3. Multiple regression equation(MR)

The obtained data were analyzed using the IBM-SPSS software, which is a well-known statistical program. As a result of this study, regression Equations 6.1 and 6.2 were obtained. The coefficients in these equations are shown in Table 6.1.

$$log\delta_{vm} = \alpha_0 + \alpha_1 logH_e + \alpha_2 log\, s_u/\sigma_v' + \alpha_3 log\, E_s/s_u + \alpha_4\, log(ln(K_s)) + \alpha_5 logS + \alpha_6 logW + \alpha_7 log\gamma_s \quad (6.1)$$

$$log\delta_{hm} = \beta_0 + \beta_1 logH_e + \beta_2 log\, s_u/\sigma_v' + \beta_3 log\, E_s/s_u + \beta_4\, log(ln(K_s)) + \beta_5 logS + \beta_6 logW + \beta_7 log\gamma_s \quad (6.2)$$

Table 6. 1. Coefficients of regression equations.

Coefficients of Settlement	Value	Coefficients of Wall Deflection	Value
α_0	2.780	β_0	2.817
α_1	1.398	β_1	1.406
α_2	-1.286	β_2	-1.236
α_3	-0.277	β_3	-0.256
α_4	-1.875	β_4	-1.943
α_5	0.353	β_5	0.432
α_6	0.459	β_6	0.416
α_7	-1.877	β_7	-1.840

6.4. Statistical Results

Statistical results used to estimate the accuracy of the model are shown in Table 6.2. According to this table,

6.4.1. Significance (ρ)

We use the p (Probability) value to decide whether the relationship or difference we found in hypothesis testing is statistically significant. The p value we obtained in statistical analyzes is used not only to determine whether the relationship or difference is significant, but also to determine the level of this relationship or difference. In research articles, statistical significance is commonly referred to as the p-value (short for "probability value") or simply as p. (https://www.spss-tutorials.com/). If the P-value found in a test result is less than 0.05, it means that there is a significant difference between the parameters. In this study, since Significance (ρ) is less than 0.05, there is a statistically significant difference and the relationship between the parameters.

6.4.2. Beta (Standardized Coefficients)

Beta (Standardized Coefficients) indicates the importance of the independent variable (regardless of the sign), the variable with the highest Beta is the most important independent variable. When Figure 6.2 is examined, the relative effect of each input variable on displacement is represented by standardized beta coefficients. Green bars indicate positive effects on displacement, and red bars indicate negative effects, if the beta coefficient is positive, the result will increase by the beta coefficient value for every 1-unit increase in the input variable. If the beta coefficient is negative, the result will decrease by the beta coefficient value for every 1-unit increase in the input variable.

6.4.3. Variance Inflation Factor (VIF)

Variance Inflation Factor (VIF) measures the severity of multicollinearity in regression analysis. Regression Analysis is a set of statistical methods used to estimate the relationships between a dependent variable and one or more independent variables. It can be used to evaluate the strength of the relationship between variables and to model the future relationship between them. It is a statistical concept that indicates the increase in the variance of a regression coefficient as a result of linearity. (https://www.statology.org/). In this study, since VIF (Collinearity diagnostics) was <5 (10 in some sources), there is no linear relationship between independent variables, so all parameters should be included in the model (Montgomery, et al. 2012).

Table 6. 2. Statistical results.

Parameter	Significance (ρ)	Beta		VIF
	Settlement/Wall Deflection	Settlement	Wall Deflection	Settlement/Wall Deflection
H_e	0.00	0.656	0.672	1.013
s_u/σ'_v	0.00	-0.531	-0.519	1.072
E_s/s_u	0.00	-0.260	-0.245	1.006
$ln(K_s)$	0.00	-0.448	-0.472	1.072
S	0.00	0.109	0.136	1.015
W	0.00	0.435	0.401	1.015
γ_s	0.00	-0.372	-0.371	1.031

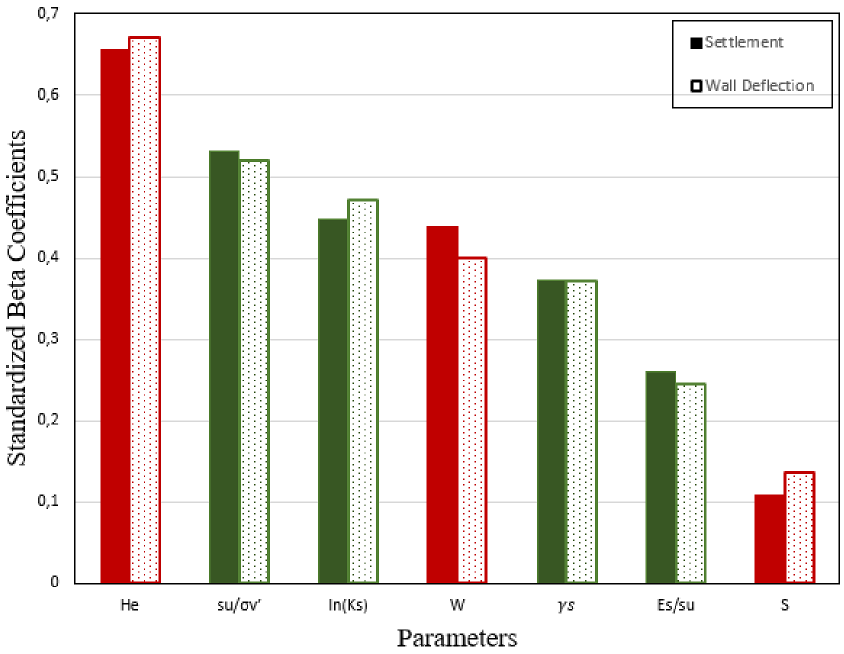

Figure 6. 2. Parameters' relative effects.

The settlement and deformation estimates obtained by Equation 6.1 and 6.2 were compared with the data obtained with finite elements, and the graphs in Figure 6.3 were obtained.

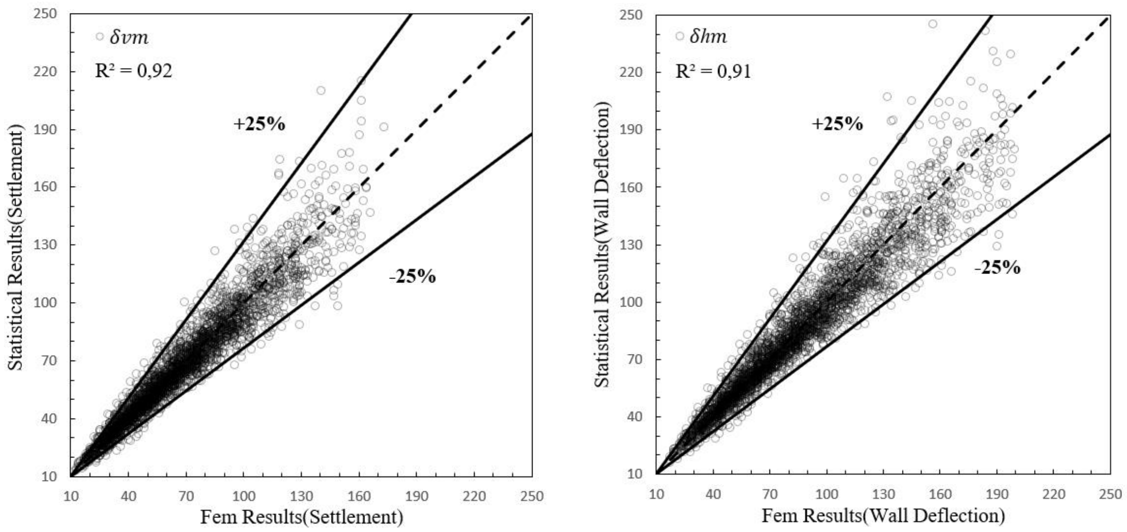

(a) (b)

Figure 6. 3. Predicted deformation versus calculated deformation.

6.5. Sensitivity of the Model

The sensitivity of the selected model is defined as the ratio of results obtained from FEM analysis to the ones estimated from statistical analysis. The closer this ratio unity, the more accurate the model is. The standard deviation closer to "0" indicates the precision of the model. When the histograms in Figure 6.4 are examined, it is seen that the proposed model has an approximately normal distribution. The mean and standard deviation values were calculated as 1.01 and 0.1 for settlement and wall deformation, respectively. The findings suggest that the proposed model's accuracy and precision are sufficient.

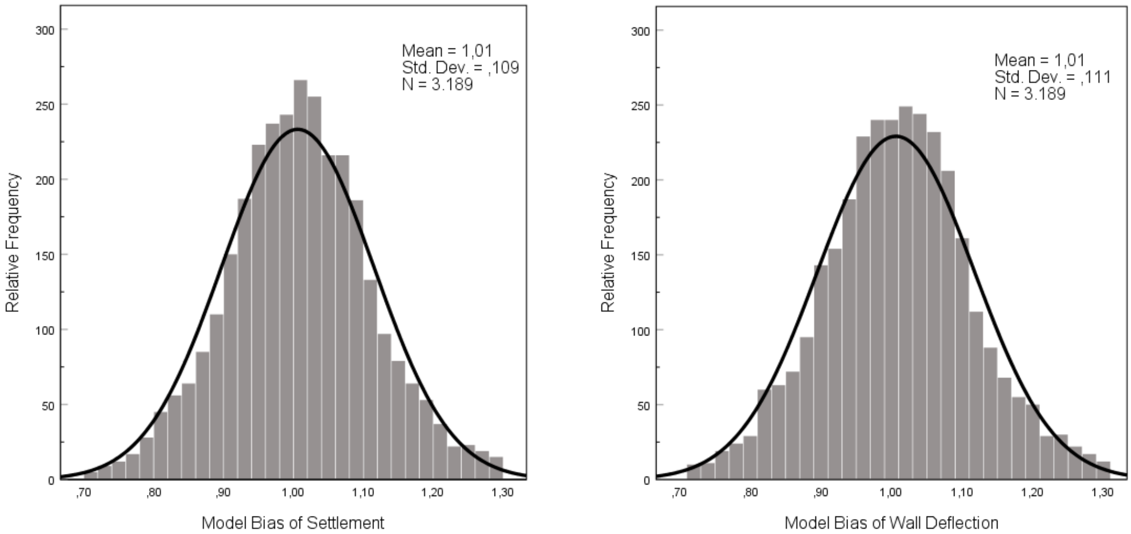

(a) (b)

Figure 6. 4. Model histograms for the suggested model.

6.6. Checking the Model Residuals

Histogram, P-P and scatter plot graph methods were used to check residuals for settlement and wall deflection. Standardized estimates and residuals are derived from Equations 6.3 and 6.4.

$$S_p = \frac{U_p - P_m}{P_S} \tag{6.3}$$

$$S_r = \frac{U_r - R_m}{R_S} \tag{6.4}$$

Where;

Sp: Standardized predicted value
Up: Unstandardized predicted value
Pm: Predicted mean
Ps: Predicted standard deviation
Sr: Standardized residual value
Ur: Unstandardized residual value
Rm: Residual mean
Rs: Residual standard deviation

6.6.1. Histogram Method

The histograms of the standardized residuals for both models are shown in Figure 6.5. The expected value (mean) of the normality curve drawn on the histogram of the residuals in the models was found to be 0, and the standard deviation was 0.99. For confidence interval, 95% of the values in the normal distribution are between ±2 standard deviations from the mean. Since the values found are in this range, it can be said that the residual terms for “Settlement” and "Wall deflection" are normally distributed.

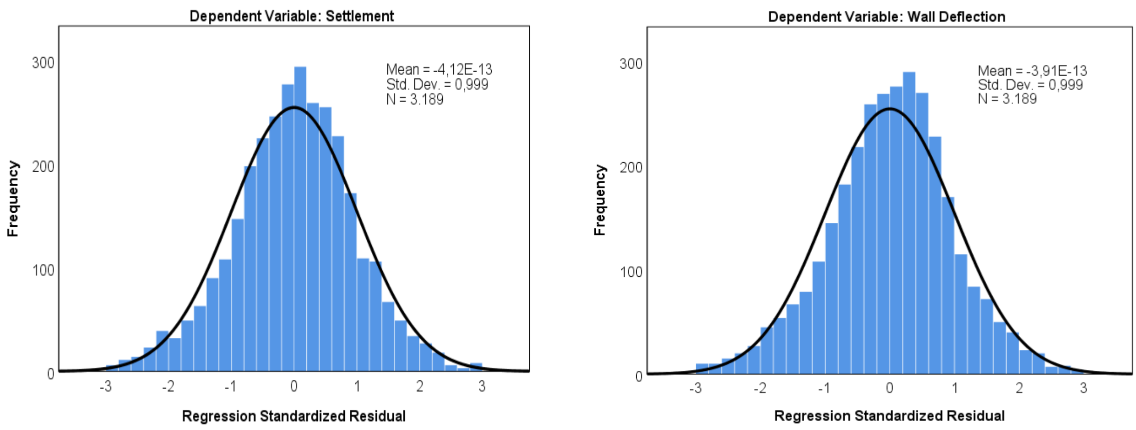

(a) (b)

Figure 6. 5. Histograms of standardized residual for the proposed model.

6.6.2. Scatter Plot Graph Methods

To control bias, the standardized estimate values drawn against standardized residual values were used. If the residual term values are randomly distributed under the zero axis, then there is unbiased assumption. It is seen in Figure 6.6; the residual terms are randomly distributed around the zero axis for both models. Therefore, the assumption of unbiased can be accepted (Montgomery, et al. 2012).

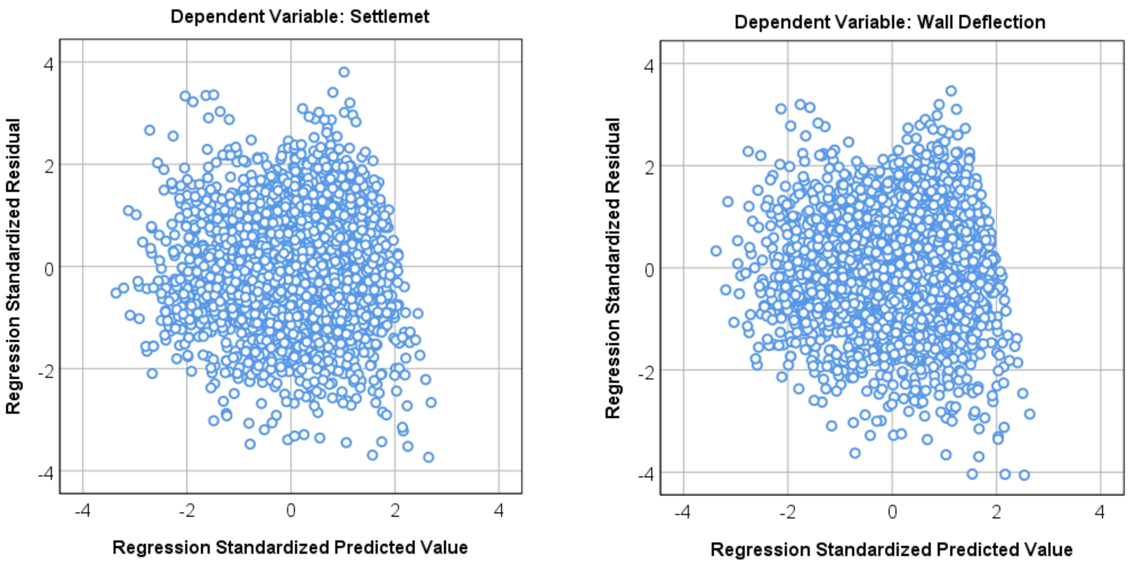

(a) (b)

Figure 6. 6. Bias control

6.6.3. P-P Plots

The assumption that the residues are normally distributed was also checked with another graphical method, the P-P (additive probability) plot. Here, for the acceptance of normality, the residual terms must be distributed around the diagonal line. When Figure 6.7 is examined, it is seen that the residuals are gathered around this line for both models.

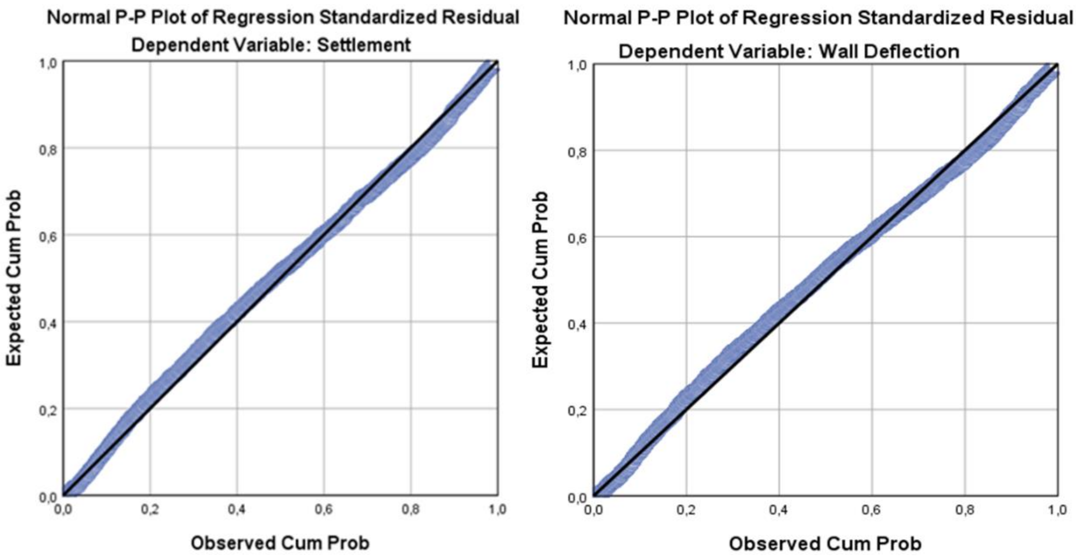

(a) (b)

Figure 6. 7. P-P plots.

6.7. Checking the Parameter Residuals

To demonstrate the validity of the model, parameter-based residual studies were carried out. For this purpose, Parameter-Residual graphs were drawn in Figure 6.7 as well as relative errors (Equation 6.6). "Residual" is the subtraction of deformations predicted by the regression model from deformations simulated by FEM (Equation 6.5).

$$R = \delta^{FEM} - \delta^{MR} \quad (6.5)$$

$$R_e = \frac{\delta^{MR} - \delta^{FEM}}{\delta^{FEM}} \times 100 \quad (6.6)$$

Where;

R: Residual

δ^{FEM}: Deformations simulated by FEM

δ^{MR} : Deformations predicted by multiple regression model (MR)

Re: Relative error

6.7.1. Drawing Error Graphs

When Figure 6.8 is examined wall deflection and settlement residuals are superimposed on the same graphs to see the mean error. The boundaries of the resulting errors are approximately indicated by the error boundary (the blue ring is settlement residual; the yellow ring is wall deformation residual and the red line is error boundary). Positive values indicate that the model is overestimating, negative values indicate that it is underestimating. For example, for this model, regardless of other parameters, an excavation with an excavation depth of 11-14m would have a maximum error of 25mm and a relative error of 10%. The errors obtained are confirmed by the case studies in Table 6.3 (in Figure 6.8, the “Settlement error” shows subtraction of the predicted settlements from observed case settlements, while the “Wall deflection error” shows subtraction of the predicted case wall deflections from the observed wall deformations).

$$E_{set} = \delta_{set.}^{CASE} - \delta_{set.}^{MR} \tag{6.7}$$

$$E_{set} = \delta_{wall}^{CASE} - \delta_{wall}^{MR} \tag{6.8}$$

Where;

Eset : Error for settlement deformations

Ewall : Error for wall deflections

$\delta_{set.}^{CASE}$: Observed case settlements

$\delta_{set.}^{MR}$: Predicted settlements by multiple regression model (MR)

δ_{wall}^{CASE} : Observed case wall deflection

δ_{wall}^{MR} : Predicted wall deflection by multiple regression model (MR)

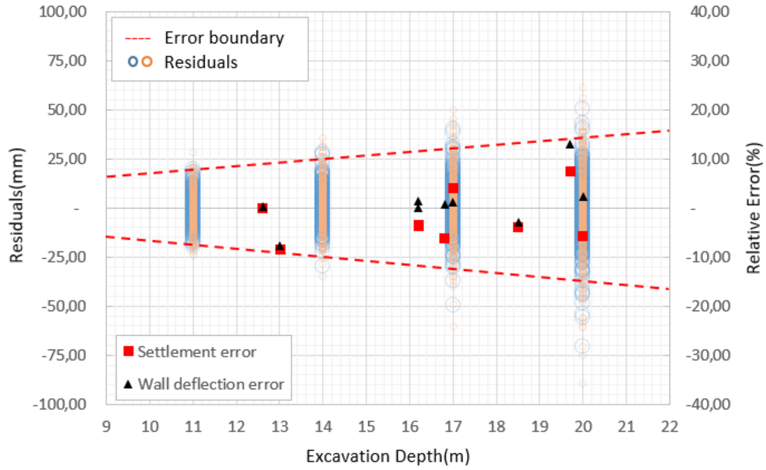
Error boundary
Residuals
Settlement error
Wall deflection error
Residuals(mm)
Relative Error(%)
Excavation Depth(m)
100,00
75,00
50,00
25,00
-
-25,00
-50,00
-75,00
-100,00
40,00
30,00
20,00
10,00
-10,00
-20,00
-30,00
-40,00
9 10 11 12 13 14 15 16 17 18 19 20 21 22

(a)

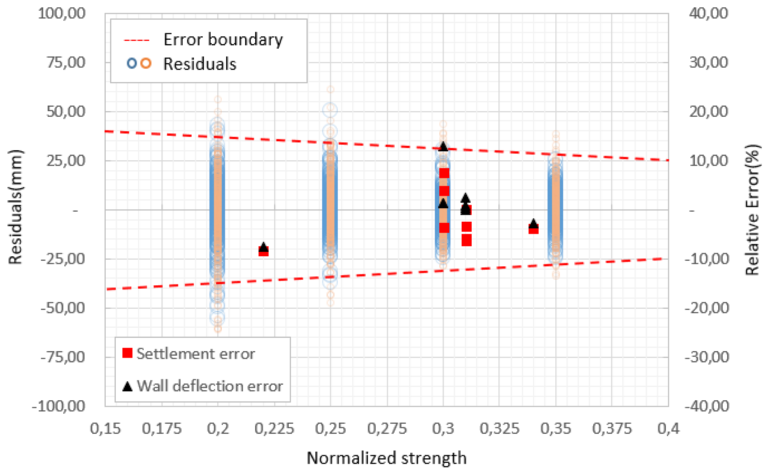
Error boundary
Residuals
Settlement error
Wall deflection error
Residuals(mm)
Relative Error(%)
Normalized strength
0,15 0,175 0,2 0,225 0,25 0,275 0,3 0,325 0,35 0,375 0,4

(b)

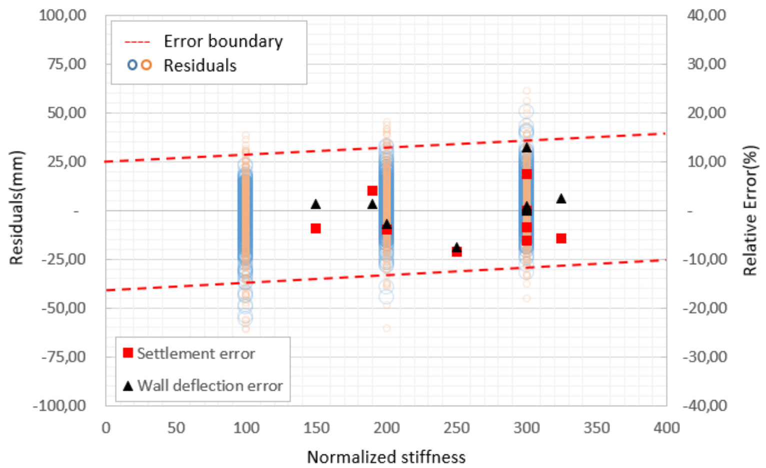
Error boundary
Residuals
Settlement error
Wall deflection error
Residuals(mm)
Relative Error(%)
Normalized stiffness
0 50 100 150 200 250 300 350 400

(c)

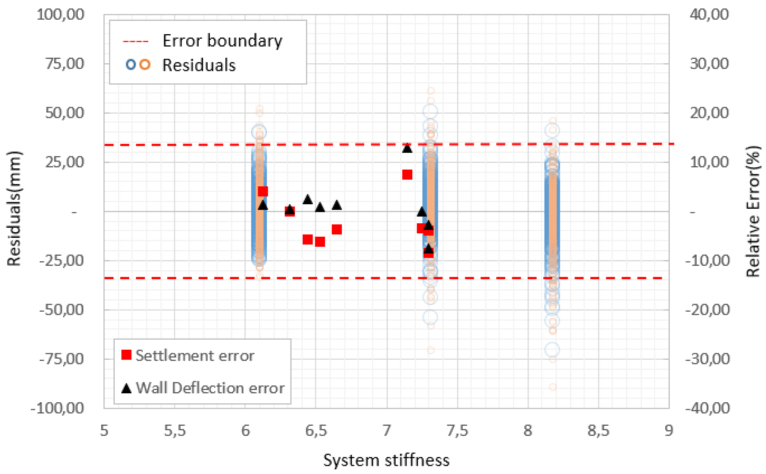
Error boundary
Residuals
Settlement error
Wall Deflection error
Residuals(mm)
Relative Error(%)
System stiffness
100,00
75,00
50,00
25,00
-25,00
-50,00
-75,00
-100,00
40,00
30,00
20,00
10,00
-10,00
-20,00
-30,00
-40,00
5
5,5
6
6,5
7
7,5
8
8,5
9

(d)

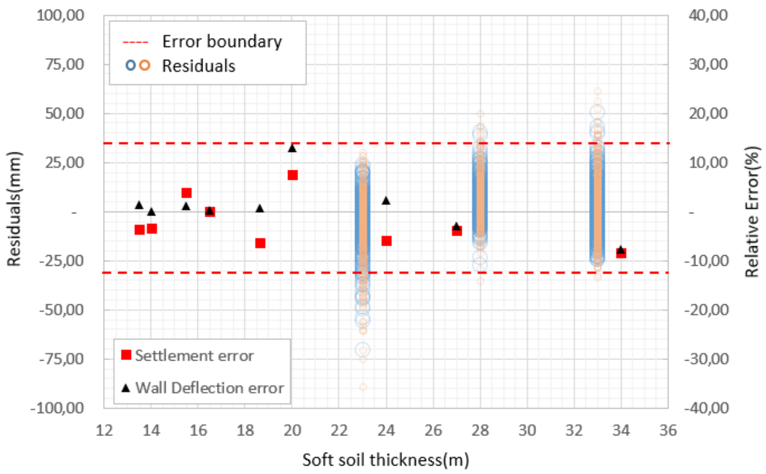
Error boundary
Residuals
Settlement error
Wall Deflection error
Residuals(mm)
Relative Error(%)
Soft soil thickness(m)
100,00
75,00
50,00
25,00
-25,00
-50,00
-75,00
-100,00
40,00
30,00
20,00
10,00
-10,00
-20,00
-30,00
-40,00
12
14
16
18
20
22
24
26
28
30
32
34
36

(e)

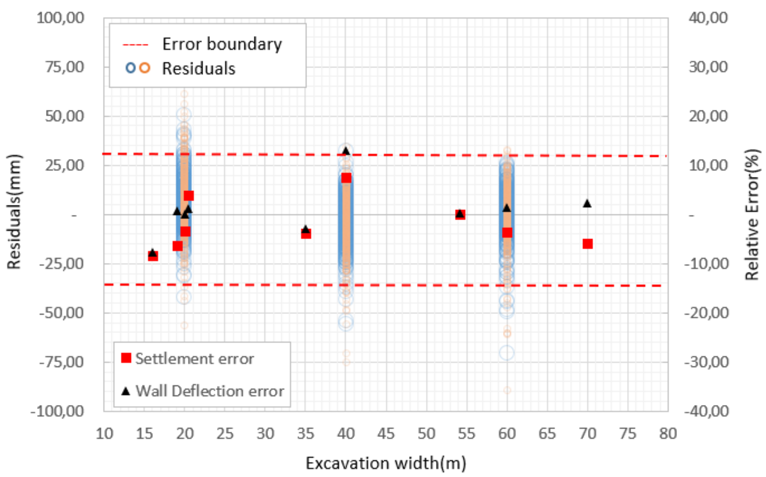
Error boundary
Residuals
Settlement error
Wall Deflection error
Residuals(mm)
Relative Error(%)
Excavation width(m)
100,00
75,00
50,00
25,00
-25,00
-50,00
-75,00
-100,00
40,00
30,00
20,00
10,00
-10,00
-20,00
-30,00
-40,00
10
15
20
25
30
35
40
45
50
55
60
65
70
75
80

(f)

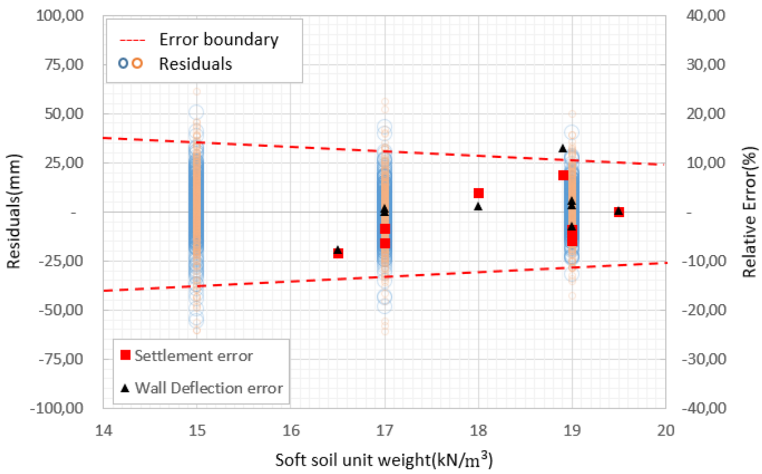

(g)

Figure 6. 8. Residual plots.

6.8. Validation of The Proposed MR Model

To illustrate the regression model's accuracy, 9 well-documented case histories built on soft soils were analyzed. The cases and parameter ranges are shown in the Table 6.3 below. The relation between the measured settlement and wall deformation values in the case studies and the estimated values is shown in Figure 6.9.

Table 6. 3. Summary of case studies.

Case No	Case Name	$H_e(m)$	s_u/σ_v'	E_s/s_u	$ln(K_s)$	$S(m)$	W(m)	γ_s(kN/m³)	References
1	Taiwan Formasa (1993)	18.5	0.34	200	7.30	27	35	19	Zapata-Medina (2007)
2	Pudian Road	17	0.30	190	6.12	15.5	20.4	18	Zhang et al. (2015)
3	Taiwan Power	16.2	0.30	150	6.65	13.5	60	19	Ou et al. (1993)
4	TNEC Taipei	19.7	0.30	300	7.15	20	40	18	Wang et al. (2005)
5	MUNI Metro Project	13	0.22	250	7.30	34	16	16.5	Zapata-Medina (2007)

6	Far East	20	0.31	325	6.44	24	70	19	Bryson and Zapata-Medina (2012)
7	Tai Kai	12.6	0.31	300	6.31	16.5	54.1	19.5	Kung et al. (2007)
8	MRT-2	16.8	0.31	300	6.53	18.6	19	17	Likitlersuang et al. (2013a)
9	MRT-4	16.2	0.31	300	7.25	14	20	17	Likitlersuang et al. (2013a)

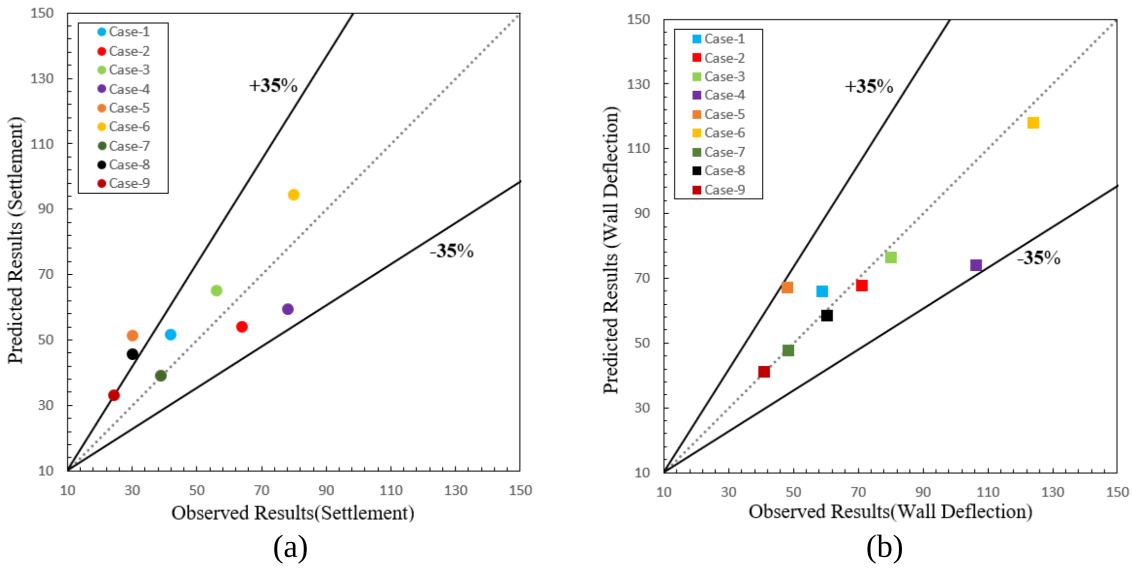

Figure 6. 9. Performance of proposed model for case histories.

As can be seen from these figures, with the given limited data, the closed form solutions proposed in this study estimates the settlements in the range of ±35%. The results are more accurate for wall deflection values.

7. CONCLUSION

In this study, the response of soft soils after excavations is investigated in terms of ground settlements and deformations observed at the supporting walls. For this purpose, 972 generic cases including 3888 pairs of ground settlements and wall deformations were created using software based on the finite element method(FEM).

The results have considered in terms of ground settlements and wall deformations. The retaining structures capacity or factor of safety against overturning/sliding and so on were not investigated although they are important factors in retaining wall design. Closed form solutions (Equations 6.1 and 6.2) have been proposed for calculating these values.

$$log\delta_{vm} = \alpha_0 + \alpha_1 logH_e + \alpha_2 log\, s_u/\sigma_v' + \alpha_3 log\, E_s/s_u + \alpha_4\, log(ln(K_s)) + \alpha_5 logS + \alpha_6 logW + \alpha_7 log\gamma_s \quad (6.1)$$

$$log\delta_{hm} = \beta_0 + \beta_1 logH_e + \beta_2 log\, s_u/\sigma_v' + \beta_3 log\, E_s/s_u + \beta_4\, log(ln(K_s)) + \beta_5 logS + \beta_6 logW + \beta_7 log\gamma_s \quad (6.2)$$

In these equations, the parameters are selected to represent the properties of the soil, excavation and support system. To validate these equations, real case histories obtained from literature has been used.

The following results were obtained in this study:

- Since all parameters and deformations of the cases in Table 6.3 are known, the accuracy of the model is limited to these cases. If more cases are used, more precise results can be obtained.

- In the literature, researchers generally study in the 50% range of deformation estimations, and values in this range are considered successful. In this study, all case results were estimated with an error range of 35%. In this case, it can be said that the study is more successful (Figure 6.9).

- Selected seven parameters (H_e, s_u/σ'_v, E_s/s_u, $ln(K_s)$, S, W, γ_s) and ranges are approximately sufficient to estimate deformations.

- The wall deformations can be estimated better than settlement predictions with the equations proposed (Figure 6.9 shows R^2=53% for surface settlement deformations and R^2=76% for wall deflections).

- According to statistical results, the most effective parameters on wall deflections and ground settlements are H_e, s_u/σ'_v, $ln(K_s)$, W,γ_s, E_s/s_u and S respectively.

- When the parameter-based residual graphs are examined, the error levels are approximately 25mm and the relative error is around 10% in all of them.

- The error level increases with increasing excavation depth (Figure 6.8a) whereas it decreases with increasing normalized strength (Figure 6.8b) and soil unit weight (Figure 6.8g). The overestimation of the model increases (Figure 6.8c) as the normalized stiffness increases. For the other parameters, the errors tend to be approximately horizontal.

- In geotechnical earthquake engineering, it is essential to obtain the shear modulus parameters of the soil by field and/or laboratory tests with the methods specified in chapter 3. However, in static applications, it is not common to detect this module by the tests mentioned above. For this reason, small strain parameters G_0^{ref} and $\gamma_{0.7}$ are often used as constant values in literature studies. In this study, instead of using a fixed value, these parameters were obtained from empirical formulas approximately. For this reason, it can be thought that the estimations obtained give better results than the estimations obtained with the fixed values.

- This study can be used for the deformation predictions of support systems penetrating in the stiff layer. If the all soil deposit is located in the soft soil, using the results of this study can result in misleading answers due to basal heave.

- It is thought that the proposed model can give the preliminary designer an idea about the degree of deformations for the studied soil conditions, model limits and support systems. However, for the final design of the retaining walls, a detailed site-specific analysis should be conducted.

- In deep excavations constructed in city centers, there are usually buildings or roads (surcharge loads) around the excavation. The effect of such structures was not considered in the study. Especially when working on soft soils, these effects must be considered in the analysis phase and deformations must be monitored.

Recommendations for Future Research

- This study was mainly carried out by considering excavations in soils with normally consolidated (OCR=1) or slightly overconsolidated (OCR=1-2) clays. Future studies can be developed considering environments with overconsolidated soils or sandy soils.

- In this thesis, support systems with diaphragm walls and struts are considered. The literature study was carried out in this direction, so the study was limited to such support systems. The scope of the study can be improved by examining cases with different support systems.

- Analyzes are limited to the cases presented in the study, the precision of the estimations can be improved by increasing the number of cases.

- The analyzes were carried out undrained, considering the short-term behavior of the soil. This study can also be performed with drained considering the long-term(consolidation) behavior.

8. REFERENCES

AASHTO, "Standard Specifications for Highway Bridges", 16th Edition, Interim Revisions, American Association of State Highway and Transportation Officials, Washington, DC, USA (**1999**) .

Alpan, I., The geotechnical properties of soils. Earth-Science Reviews, 6(1) (**1970**) 5-49.

Atkinson, J.H., An introduction to the mechanics of soils and foundations: through critical state soil mechanics. McGraw-Hill, London, UK. pp. 158-167, **1993.**

Benz, T., Small-Strain Stiffness of Soils and its Numerical Consequences. Ph.D. dissertation. University Stuttgart, Germany. **2007**

Benz, T., Schwab, R. and Vermeer, P., Small-strain stiffness in geotechnical analyses. Bautechnik, 86 (**2009**) 16-27.

Bryson, L. S. and Zapata-Medina, D. G., Method for estimating system stiffness for excavation support walls. Journal of Geotechnical and Geoenvironmental Engineering, 138(9) (**2012**) 1104-1115.

Bhatkar, T., Barman, D., Mandal, A., & Usmani, A., Prediction of behavior of a deep excavation in soft soil: a case study. International Journal of Geotechnical Engineering, 11(1) (**2017**) 10-19.

Burd, H. J). Beyond 2000 in computational geotechnics: 10 years of PLAXIS International, proceedings of the International Symposium beyond 2000 in Computational Geotechnics. Amsterdam, The Netherlands, (**1999**) 35-44.

Burland, J. B., Ninth Laurits Bjerrum Memorial Lecture:" Small is beautiful"—the stiffness of soils at small strains. Canadian geotechnical journal, 26(4) (**1989**). 499-516.

Brinkgreve RBJ, Broere W, Waterman D., PLAXIS version 8.5 Manual, Rotterdam: A A Balkema. **2006**

Brinkgreve , R. B. J., Kappert, M. H., & Bonnier, P. G., Hysteretic damping in a small-strain stiffness model. Proc. of Num. Mod. in Geomech., NUMOG X, Rhodes, **2007**, 737-742.

Bjerrum, L., Embankments on soft ground, performance of earth and earth-supported structures. In Proc. ASCE Specialty Conf. (Vol. 2, pp. 1-54), **1972.**

Bjerrum, L., Problems of soil mechanics and construction on soft clays and structurally unstable soils. In Proc. 8th ICSMFE (Vol. 3, pp. 111-159), **1973**.

Bowles, J. E., Foundation analysis and design, 5th Ed., McGraw Hill International Editions, Singapore, **1988**.

Casey, B., Germaine, J. T., Abdulhadi, N. O., Kontopoulos, N. S., & Jones, C. A., Undrained Young's modulus of fine-grained soils. Journal of Geotechnical and Geoenvironmental Engineering, 142(2) (**2016**) 04015070.

Clough, G. W., Construction induced movements of in situ walls. Design and performance of earth retaining structures, (**1990**) 439-470.

Clough, G.W. and O'Rourke, T.D. "Wall Deflection and Ground Surface Settlement Induced by Excavation", In Proceedings of the 4th National Geotechnical Conference, Hawlin, Taiwan. (**1990**).

Coduto, D. P., "Geoteknik Mühendisliği İlkeler ve Uygulamalar", Gazi Kitap Evi, Ankara (**2006**).

Çalışan, O., "Design and Measurements of 30 m Deep Excavation", Proc. Prof. İsmet Ordemir'i Anma Toplantısı ve 3. ODTÜ Geoteknik Mühendisliği Sempozyumu, 74-81 (**2005**).

Darendeli, M.B., "Development of a New Family of Normalized Modulus Reduction and Material Damping Curves." PhD Dissertation Department of Civil Engineering. The University of Texas at Austin. (**2001**).

Demirkoç A., "Derin Kazılarda Zemin Çivisi ile Ankrajlı Destek Sistemlerinin Karşılaştırmalı Analizi" , Yıldız Teknik Üniversitesi, Yüksek Lisans Tezi, Fen Bilimleri Enstitüsü, İstanbul, Türkiye (**2007**).

Dong, Yi., Lu, N., McCartney, J. S. and P.E., "Unified Model for Small-Strain Shear Modulus of Variably Saturated Soil", Journal of Geotechnical and Geoenvironmental Engineering, ASCE, ISSN 1090-0241 (**2016**).

Duncan, J. M., & Chang, C. Y., Nonlinear analysis of stress and strain in soils. Journal of the soil mechanics and foundations division, 96(5) (**1970**) 1629-1653.

Duncan, J. M., & Buchignani, A. L., An engineering manual for slope stability analysis. Department of Civil Engineering, University of California, **1976**.

Ding, Z., Jin, J., & Han, T. C., Analysis of the zoning excavation monitoring data of a narrow and deep foundation pit in a soft soil area. Journal of Geophysics and Engineering, 15(4) (**2018**) 1231-1241.

El-Kasaby, E. A., Estimation of guide values for the modulus of elasticity of soil. Bulletin of Faculty of Engineering, Assiut University, 19(1) (**1991**) 1-7.

Finno, R. J., Atmatzidis, D. K., & Perkins, S. B., Observed performance of a deep excavation in clay. Journal of Geotechnical Engineering, 115(8) (**1989**) 1045-1064.

Finno, R. J., & Nerby, S. M., Saturated clay response during braced cut construction. Journal of geotechnical engineering, 115(8) (**1989**) 1065-1084.

Finno, R. J., Bryson, S., & Calvello, M., Performance of a stiff support system in soft clay. Journal of Geotechnical and Geoenvironmental Engineering, 128(8) (**2002**) 660-671.

Goldberg, D.T., Jaworski, W.E., and Gordon, M.D., "Lateral Support Systems and Underpinning", Design and Construction, Federal Highway Administration Report FHWA RD 75-128 (**1976**).

Hardin, B. O., & Drnevich, V. P., Shear modulus and damping in soils: design equations and curves. Journal of the Soil mechanics and Foundations Division, 98(7) (**1972**) 667-692.

Hashash, Y. M., & Whittle, A. J., Ground movement prediction for deep excavations in soft clay. Journal of geotechnical engineering, 122(6) (**1996**) 474-486.

Holtz, R. D., Kovacs, W. D., & Sheahan, T. C. An introduction to geotechnical engineering (Vol. 733). Englewood Cliffs: Prentice-Hall (1981).

Hsieh, P. G., & Ou, C. Y., Shape of ground surface settlement profiles caused by excavation. Canadian geotechnical journal, 35(6) (**1998**) 1004-1017.

Hsieh, Y. M., Dang, P. H., & Lin, H. D., How small strain stiffness and yield surface affect undrained excavation predictions. International Journal of Geomechanics, 17(3) (**2017**) 04016071.

Hsiung B.B. and Sakai, T., "Failure Analysis of Underground Construction-Lessons Learned from Taiwan", Forensic Geotechnical Engineering, 197-208 (**2016**).

Jaky, J., The coefficient of earth pressure at rest. J. of the Society of Hungarian Architects and Engineers, (**1944**) 355-358.

Janbu, N., Soil models in offshore engineering. Géotechnique, 35(3) (**1985**) 241-281.

Jamiolkowski, M. New development in field and laboratory testing of soils. In Proc. 11th ICSMFE (Vol. 1, pp. 57-153) (**1985**).

Jardine, R. J., Potts, D. M., Fourie, A. B., & Burland, J. B., Studies of the influence of non-linear stress–strain characteristics in soil–structure interaction. Géotechnique, 36(3) (**1986**) 377-396.

Karstunen, M., & Yin, Z. Y. Modelling time-dependent behavior of Murro test embankment. Géotechnique, 60(10) (**2010**) 735-749.

Kempfert, H. G., & Gebreselassie, B., Constitutive soil models and soil parameters. Excavations and Foundations in Soft Soils, 57-116, **2006**.

Koiter, W. T. General theorems for elasto-plastic solids. In Prog. Solid Mech, (eds I. N. Sneddon and R. Hill), North-Holland Publ. Company, (**1960**) pp. 165-211.

Kondner, R.L., "Hyperbolic stress-strain response: cohesive soils", J of the Soil Mech. And Found. Eng. ASCE ,Balkema, Rotterdam (**1963**).

Kumbasar, V., and Kip, F., "Zemin Mekaniği Problemleri", Çağlayan Kitapevi, İstanbul (**1999**).

Kung, T. C., Surface settlement induced by excavation with consideration of small strain behavior of Taipei silty clay. PhD thesis, **2003**.

Kung, T. C., & Ou, C. Y., Prediction of surface settlement caused by excavation. In Geotechnical aspects of underground construction in soft ground. Proceedings of the 5th international conference of TC 28 of the ISSMGE, the Netherlands, **2006**, (pp. 853-858).

Kung, G. T., Juang, C. H., Hsiao, E. C., & Hashash, Y. M., Simplified model for wall deflection and ground-surface settlement caused by braced excavation in clays. Journal of Geotechnical and Geoenvironmental Engineering, 133(6) (**2007**) 731-747.

Kung, G. T. C., Ou, C. Y., & Juang, C. H., Modeling small-strain behavior of Taipei clays for finite element analysis of braced excavations. Computers and Geotechnics, 36(1-2) (**2009**) 304-319.

Larsson, R., & Mulabdic, M. Shear moduli in Scandinavian clays. Measurement of initial shear modulus with seismic cones. Empirical correlations for the initial shear modulus in clay (**1991**).

Lambe, T. W., & Whitman, R. V. Soil mechanics, 553 pp(**1969**) .

Lemos, S. G. F. P., & Pires, P. J. M., The Undrained Strength of Soft Clays Determined from Unconventional and Conventional Tests. Soils and Rocks, São Paulo, 40(3) (**2017**) 291-301.

Ladd, C.C., Moh, Z-C., and Gifford, D.G. "Undrained shear strength of soft Bangkok clay." Proc. 4th Asian Regional Conf. on Soil Mech. and Foundation Eng., Bangkok, Vol. (1) (**1971**) 135-140.

Ladd, C. C., & Foott, R. New design procedure for stability of soft clays. Journal of the geotechnical engineering division, 100(7) (**1974**) 763-786.

Ladd, C. C., & Foott, R. Foundation design of embankments constructed on varved clays (No. FHWA-TS-77-214 Final Rpt.) (**1977**).

Leoni, M., Karstunen, M., & Vermeer, P. A. Anisotropic creep model for soft soils. Géotechnique, 58(3) (**2008**) 215-226.

Likitlersuang, S., Surarak, C., Wanatowski, D., Oh, E., & Balasubramaniam, A., Finite element analysis of a deep excavation: A case study from the Bangkok MRT. Soils and foundations, 53(5) (**2013a**) 756-773.

Likitlersuang, S., Surarak, C., Wanatowski, D., Oh, E. and Balasubramaniam, A.S., "Geotechnical Parameters from Pressuremeter Tests for MRT Blue Line Extension in Bangkok" Geomechanics and Engineering, An International Journal, 5(2): 99–118 (**2013b**).

Likitlersuang, S., Teachavorasinskun, S., Surarak, C., Oh, E., & Balasubramaniam, A. Small strain stiffness and stiffness degradation curve of Bangkok Clays. Soils and Foundations, 53(4) (**2013c**) 498-509.

Lim, A., Ou, C. Y., and Hsieh, P. G., "Evaluation of Clay Constitutive Models for Analysis of Deep Excavation under Undrained Conditions", Journal of GeoEngineering, TGS, 5 (1) (**2010**) 9-20.

Lim, A., & Ou, C. Y., Stress paths in deep excavations under undrained conditions and its influence on deformation analysis. Tunnelling and underground space technology, 63 (**2017**) 118-132.

Long, M., Database for retaining wall and ground movements due to deep excavations. Journal of Geotechnical and Geoenvironmental Engineering, 127(3) (**2001**) 203-224.

Mana, A. I., & Clough, G. W., Prediction of movements for braced cuts in clay. Journal of the Geotechnical Engineering Division, 107(6) (**1981**) 759-777.

Marchetti, S. In situ tests by flat dilatometer. Journal of the geotechnical engineering division, 106(3) (**1980**) 299-321.

Mayne, P. W., Christopher, B. R., & DeJong, J. Manual on subsurface investigations. Nat. Highway Inst. Sp. Pub. FHWA NHI-01–031. Fed. Highway Administ, Washington, DC (**2001**). .

Mesri, G., & Wang, C., Discussion of “Correlations for undrained shear strength of Finnish soft clays”. Canadian Geotechnical Journal, 54(5) (**2017**) 745-748.

Mestat, PH, Bourgeois, E and Riou, Y., “Numerical modelling of embankments and underground works”, Computers and Geotechnics, 31 (**2004**) 227-236

Montgomery, D. C., Peck, E. A., & Vining, G. G., Introduction to linear regression analysis. John Wiley & Sons, (**2012)**.

Moormann, C., Analysis of wall and ground movements due to deep excavations in soft soil based on a new worldwide database. Soils and foundations, 44(1) (**2004**) 87-98.

O'Rourke, T. D., Ground movements caused by braced excavations. Journal of the Geotechnical Engineering Division, 107(9) (**1981**) 1159-1178.

Obrzud, R., "On the use of the Hardening Soil model Z_SOİL" GeoMod Ing. SA, Lausanne (**2010**).

Ou, C. Y., Hsieh, P. G., & Chiou, D. C., Characteristics of ground surface settlement during excavation. Canadian geotechnical journal, 30(5) (**1993**) 758-767.

Ou, C. Y., Liao, J. T., & Cheng, W. L., Building response and ground movements induced by a deep excavation. Géotechnique, 50(3) (**2000**) 209-220.

Önalp, A., and Arel, E., Geoteknik Bilgisi I, Zeminler ve Mekaniği, Birsen Yayınevi, İstanbul, **2013**

Peck, R. B., Deep excavations and tunneling in soft ground. Proc. 7th ICSMFE, **1969**, 225-290.

PLAXIS CONNECT Edition V.21, PLAXIS 2D-Reference Manual, 2020 https://communities.bentley.com/products/geotech-analysis/w/plaxissoilvision wiki/46137/manuals---Plaxis (Accessed **January 2022**)

PLAXIS CONNECT Edition V.21, General Information Manual, 2020 https://communities.bentley.com/products/geotech-analysis/w/plaxissoilvision wiki/46137/manuals---Plaxis (Accessed **April 2022**)

PLAXIS 2D. "Reference Manual", Retrieved from http://www.plaxis.nl/files/files/2D-2-Reference.pdf, (Accessed **26 March 2022**)

Roscoe K. H., Schofield A., Thurairajah A. Yielding of clays in states wetter than critical. Géotechnique, Vol. XIII (3) (**1963**) 211-240.

Roscoe, K.H. and Burland, JB., "On the generalized stress-strain behavior of wet clay." In: J. Heyman and FA Leckie, editors. Engineering Plasticity. Cambridge University Press (**1968**) 535-609

Rowe, P. W., "The relation between the shear strength of sands in triaxial compression, plane strain and direct shear", Géotechnique 19(1) (**1969**) 75-86.

Roy, D., & Singh, R. Undrained shear strength gain with consolidation at soft and sensitive soil sites. In Proceedings of the 17th International Conference on Soil

Mechanics and Geotechnical Engineering (Volumes 1, 2, 3 and 4) (**2009**) (pp. 1534-1537). IOS Press.

Schanz, T., Vermeer, P. A., & Bonnier, P. G., The hardening soil model: formulation and verification. In Beyond 2000 in computational geotechnics **1999**, (pp. 281-296). Routledge.

Simpson, B. Development and application of a new soil model for prediction of ground movements. In Predictive soil mechanics: Proceedings of the Wroth Memorial Symposium held at St Catherine's College, Oxford, 27-29 July **1992** (pp. 628-643). Thomas Telford Publishing.

Strahler, A. W., & Stuedlein, A. W. Characterization of model uncertainty in immediate settlement calculations for spread footings on clays. In Proc. 18th Int. Conf. Soil Mechanics and Geotechnical Engineering, **2013**, (pp. 3471-3474).

Stallebrass, S. E., & Taylor, R. N., The development and evaluation of a constitutive model for the prediction of ground movements in overconsolidated clay. Géotechnique, 47(2) (**1997**) 235-253.

Stroud, M. A. The standard penetration test in insensitive clays and soft rocks. In Proceedings of the 1st European Symposium on Penetration Testing, Stockholm, Sweden, **1974**, (Vol. 2, No. 2, pp. 367-375).

Solowski, L.W., "Numerical Methods in Geotechnics", Aalto School of Engineering, Espoo- Finland (**2017**).

Terzaghi, K. and Peck, P.B., "Soil Mechanics in Engineering Practice 2nd Edition", John Wiley & Sons., New York (**1967**).

Ti, K. S., Huat, B. B., Noorzaei, J., Jaafar, M. D. S., & Sew, G. S., A review of basic soil constitutive models for geotechnical application. Electronic Journal of Geotechnical Engineering, 14 (**2009**) 1-18.

Uzielli, M., Statistical analysis of geotechnical data. Geotechnical and Geophysical Site Characterization, 3 (2008) 173-193.

Varathungarajan, D. A., Garfield, S. M., & Wright, S. G., Characterization of undrained shear strength profiles for soft clays at six sites in Texas (No. FHWA/TX-09/0-5824-2). University of Texas at Austin. Center for Transportation Research, **2009**.

Vardanega, P. J., Lau, B. H., Lam, S. Y., Haigh, S. K., Madabhushi, S. P. G., & Bolton, M. D., Laboratory measurement of strength mobilisation in kaolin: link to stress history. Géotechnique Letters, 2(1) (**2012**) 9-15.

Vardanega, P. J., & Bolton, M. D., Stiffness of clays and silts: Normalizing shear modulus and shear strain. Journal of Geotechnical and Geoenvironmental Engineering, 139(9) (**2013**) 1575-1589.

Wang, Z.W., Ng, C.W., Liu, G.B., Characteristics of wall deflections and ground surface settlements in Shanghai. Can Geotech 42(5) (**2005**) 1243–1254

Wang, J. H., Xu, Z. H., & Wang, W. D., Wall and ground movements due to deep excavations in Shanghai soft soils. Journal of Geotechnical and Geoenvironmental Engineering, 136(7) (**2010**) 985-994.

Whittle, A. J., Hashash, Y. M., & Whitman, R. V., Analysis of deep excavation in Boston. Journal of geotechnical engineering, 119(1) (**1993**) 69-90.

Wichtmann, T., & Triantafyllidis, T., Influence of the grain-size distribution curve of quartz sand on the small strain shear modulus G max. Journal of geotechnical and geoenvironmental engineering, 135(10) (**2009**) 1404-1418.

Wroth, C. P., & Houlsby, G. T., Soil mechanics-property characterization and analysis procedures, (**1985**).

Wood, D. M. Soil behavior and critical state soil mechanics. Cambridge university press (**1990**).

Yamashita, S., Kawaguchi, T., Nakata, Y., Mikami, T., Fujiwara, T., and Shibuya, S., "Interpretation of International Parallel Test on The Measurement of Gmax Using Bender Elements", Soils and Foundations, 49(4) (**2009**) 631-650.

Yıldız, A., Karstunen, M., Rezanıa, M. ve Yin., Z.Y. "Killerin Zamana Bağlı Davranışı ve Yeni Gelişmeler", 6. Geoteknik Sempozyomu Çukurova Üniversitesi, Adana, 202-213 (**2015**).

Ying, H. W., Cheng, K., Zhang, L. S., Ou, C. Y., & Yang, Y. W., Evaluation of excavation-induced movements through case histories in Hangzhou. Engineering Computations, (**2020)**.

Zapata-Medina, D. G. Semi-empirical method for designing excavation support systems based on deformation control (**2007**).

Zhang, D. M., Xie, X. C., Li, Z. L., & Zhang, J., Simplified analysis method for predicting the influence of deep excavation on existing tunnels. Computers and Geotechnics, 121 (**2020**) 103477.

Zhang, W., Goh, A. T., & Xuan, F., A simple prediction model for wall deflection caused by braced excavation in clays. Computers and Geotechnics, 63 (**2015**) 67-72.

APPENDICES

APPENDIX-A Generic Cases and FEM Results

Model Group:1

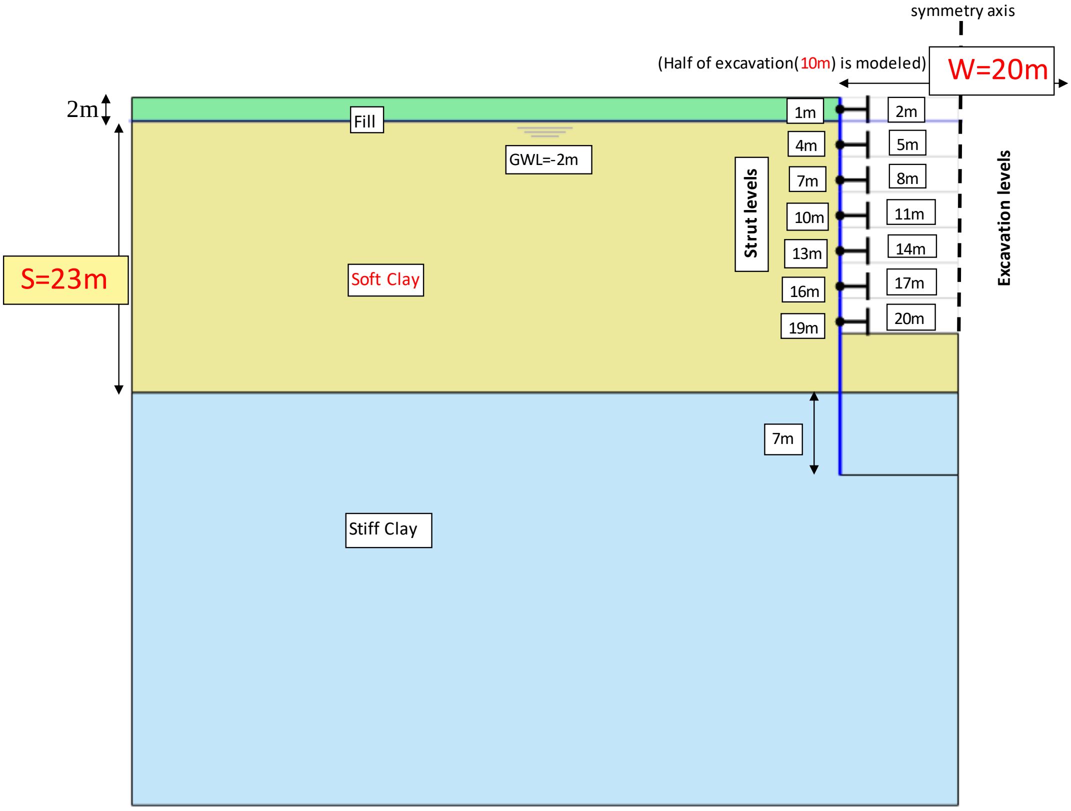

Figure A.1. Model Geometry-1.

Table B. Soil and structure parameters.

Default Soil Parameters		
	Stiff Clay	Fill
	HS	HS
	Undrained(A)	Drained
E_{50}^{ref}	1.00E+05	1.50E+04
E_{oed}^{ref}	1.00E+05	1.50E+04
E_{ur}^{ref}	3.00E+05	4.50E+04
ϕ'	26	30
K_0	0.562	0.5
c'_{ref}	25	1
ν'_{ur}	0.2	0.2
p_{ref}	100	100
R_f	0.9	0.9
$\gamma_{unsat/sat}$	20/20	16/20
R_{inter}	0.65	0.65
m	1	1

Range of parameters	
c_u/σ'_v	0.20-0.25-0.30-0.35
E_{50}/c_u	100-200-300
γ	15-17-19
S	23-28-33
W	20-40-60
H_e	11-14-17-20
$\ln(EI/\gamma_w h_{avg}^4)$	6.097-7.313-8.176

Diaphragm Wall (E=2.0E+7)		
d	EA	EI
0.6	1.2E+07	3.60E+05
0.9	1.8E+07	1.215E+06
1.2	2.4E+07	2.88E+06

Strut	
EA	3.80E+06
$L_{spacing}$	5m
h_{avg}	3m

Generic Cases: 1 to 36

Table.A1. Model parameters and deformation results (Case No: 1 to 36).

Excavation	Soil(γ=15kN/m^3)		Diaphragm Wall(E=2.0E+7)		
H_e(m)	c_u/σ_v'	E_{50}/c_u	d	EA	EI
11-14-17-20	0.2	100-200-300	0.6	1.2E+07	3.60E+05
			0.9	1.8E+07	1.215E+06
			1.2	2.4E+07	2.88E+06

Soft Soil	E_s/s_u		
HSS	100	200	300
E_{50}^{ref}	2895	5789	8685
E_{oed}^{ref}	2895	5789	8685
E_{ur}^{ref}	8685	17367	26055
G_0^{ref}	30759	43418	54281
$\gamma_{0,7}$	3.59E-04	2.54E-04	2.03E-04
ϕ	18	18	18
K_0	0.691	0.691	0.691
E_{dyn}/E_{stat}	8.5	6	5

H=11m	d=0.6	d=0.9	d=1.2	E_{50}/c_u	H=11m	d=0.6	d=0.9	d=1.2
δ_{vm}(mm)	115	66	48	100	δ_{hm}(mm)	147	80	57
	107	58	41	200		127	72	50
	96	54	37	300		120	68	47

H=14m	d=0.6	d=0.9	d=1.2	E_{50}/c_u	H=14m	d=0.6	d=0.9	d=1.2
δ_{vm}(mm)	157	90	62	100	δ_{hm}(mm)	201	108	74
	145	79	56	200		179	99	68
	136	75	52	300		170	95	65

H=17m	d=0.6	d=0.9	d=1.2	E_{50}/c_u	H=17m	d=0.6	d=0.9	d=1.2
δ_{vm}(mm)	201	112	76	100	δ_{hm}(mm)	250	132	89
	185	100	69	200		221	124	83
	174	96	65	300		212	119	79

H=20m	d=0.6	d=0.9	d=1.2	E_{50}/c_u	H=20m	d=0.6	d=0.9	d=1.2
δ_{vm}(mm)	235	126	85	100	δ_{hm}(mm)	285	149	99
	218	114	78	200		252	140	93
	206	112	75	300		242	134	90

Generic Cases: 37 to 72

Table.A2. Model parameters and deformation results (Case No: 37 to 72).

Excavation	Soil(γ=15kN/m^3)		Diaphragm Wall(E=2,0E+7)		
H_e(m)	c_u/σ_v'	E_{50}/c_u	d	EA	EI
11-14-17-20	0.25	100-200-300	0.6	1.2E+07	3.60E+05
			0.9	1.8E+07	1.215E+06
			1.2	2.4E+07	2.88E+06

Soil	E_{50}/c_u		
HSS	100	200	300
E_{50}^{ref}	4000	8000	12000
E_{oed}^{ref}	4000	8000	12000
E_{ur}^{ref}	12000	24000	36000
G_0^{ref}	35000	50000	67500
$\gamma_{0.7}$	3.58E-04	2.51E-04	1.86E-04
ϕ	22	22	22
K_0	0.625	0.625	0.625
E_{dyn}/E_{stat}	7	5	4.5

H=11m	d=0.6	d=0.9	d=1.2	E_{50}/c_u	H=11m	d=0.6	d=0.9	d=1.2
δ_{vm}(mm)	83	49	37	100	δ_{hm}(mm)	105	62	46
	70	43	32	200		91	55	40
	63	38	28	300		80	49	36

H=14m	d=0.6	d=0.9	d=1.2	E_{50}/c_u	H=14m	d=0.6	d=0.9	d=1.2
δ_{vm}(mm)	114	67	51	100	δ_{hm}(mm)	150	85	62
	100	62	44	200		131	77	56
	90	55	40	300		118	70	51

H=17m	d=0.6	d=0.9	d=1.2	E_{50}/c_u	H=17m	d=0.6	d=0.9	d=1.2
δ_{vm}(mm)	146	85	63	100	δ_{hm}(mm)	188	106	76
	129	79	56	200		165	98	69
	117	71	51	300		150	90	64

H=20m	d=0.6	d=0.9	d=1.2	E_{50}/c_u	H=20m	d=0.6	d=0.9	d=1.2
δ_{vm}(mm)	173	99	72	100	δ_{hm}(mm)	220	122	86
	156	92	65	200		192	113	79
	143	84	60	300		175	104	75

Generic Cases: 73 to 108

Table.A3. Model parameters and deformation results (Case No: 73 to 108)

Excavation	Soil(γ=15kN/m^3)		Diaphragm Wall(E=2.0E+7)		
H_e(m)	c_u/σ_v'	E_{50}/c_u	d	EA	EI
11-14-17-20	0.3	100-200-300	0.6	1.2E+07	3.60E+05
			0.9	1.8E+07	1.215E+06
			1.2	2.4E+07	2.88E+06

Soil	E_{50}/c_u		
HSS	100	200	300
E_{50}^{ref}	5400	10800	16200
E_{oed}^{ref}	5400	10800	16200
E_{ur}^{ref}	16200	32400	48600
G_0^{ref}	40500	60750	75938
$\gamma_{0,7}$	3.40E-04	2.27E-04	1.81E-04
ϕ	26.4	26.4	26.4
K_0	0.555	0.555	0.555
E_{dyn}/E_{stat}	6	4.5	3.75

H=11m	d=0.6	d=0.9	d=1.2	E_{50}/c_u	H=11m	d=0.6	d=0.9	d=1.2
δ_{vm}(mm)	61	40	30	100	δ_{hm}(mm)	76	51	37
	50	34	25	200		64	42	32
	43	29	22	300		56	37	29

H=14m	d=0.6	d=0.9	d=1.2	E_{50}/c_u	H=14m	d=0.6	d=0.9	d=1.2
δ_{vm}(mm)	83	55	40	100	δ_{hm}(mm)	110	69	50
	71	47	35	200		96	60	45
	65	42	32	300		84	54	41

H=17m	d=0.6	d=0.9	d=1.2	E_{50}/c_u	H=17m	d=0.6	d=0.9	d=1.2
δ_{vm}(mm)	106	70	50	100	δ_{hm}(mm)	143	87	62
	92	61	45	200		123	78	56
	85	55	41	300		110	71	53

H=20m	d=0.6	d=0.9	d=1.2	E_{50}/c_u	H=20m	d=0.6	d=0.9	d=1.2
δ_{vm}(mm)	127	81	59	100	δ_{hm}(mm)	170	101	72
	113	72	54	200		146	92	67
	104	66	49	300		132	85	63

Generic Cases: 109 to 144

Table A.4. Model parameters and deformation results (Case No: 109 to 144).

Excavation	Soil(γ=15kN/m^3)		Diaphragm Wall(E=2,0E+7)		
H_e(m)	c_u/σ'_v	E_{50}/c_u	d	EA	EI
11-14-17-20	0.35	100-200-300	0.6	1.2E+07	3.60E+05
			0.9	1.8E+07	1.215E+06
			1.2	2.4E+07	2.88E+06

Soil	E_{50}/c_u		
HSS	100	200	300
E_{50}^{ref}	7000	14000	21000
E_{oed}^{ref}	7000	14000	21000
E_{ur}^{ref}	21000	42000	63000
G_0^{ref}	52500	73500	99750
$\gamma_{0.7}$	2.75E-04	1.96E-04	1.45E-04
ϕ	30	30	30
K_0	0.500	0.500	0.500
E_{dyn}/E_{stat}	6	4.2	3.8

H=11m	d=0.6	d=0.9	d=1.2	E_{50}/c_u	H=11m	d=0.6	d=0.9	d=1.2
δ_{vm}(mm)	50	36	30	100	δ_{hm}(mm)	62	44	36
	39	27	21	200		50	35	27
	32	23	18	300		42	30	23

H=14m	d=0.6	d=0.9	d=1.2	E_{50}/c_u	H=14m	d=0.6	d=0.9	d=1.2
δ_{vm}(mm)	69	50	39	100	δ_{hm}(mm)	90	60	47
	57	39	29	200		75	50	37
	49	33	26	300		65	44	34

H=17m	d=0.6	d=0.9	d=1.2	E_{50}/c_u	H=17m	d=0.6	d=0.9	d=1.2
δ_{vm}(mm)	88	64	49	100	δ_{hm}(mm)	116	76	58
	75	51	38	200		99	66	49
	65	44	35	300		86	58	45

H=20m	d=0.6	d=0.9	d=1.2	E_{50}/c_u	H=20m	d=0.6	d=0.9	d=1.2
δ_{vm}(mm)	107	74	57	100	δ_{hm}(mm)	140	90	68
	92	61	46	200		119	79	58
	82	55	42	300		105	72	54

Model Group:2

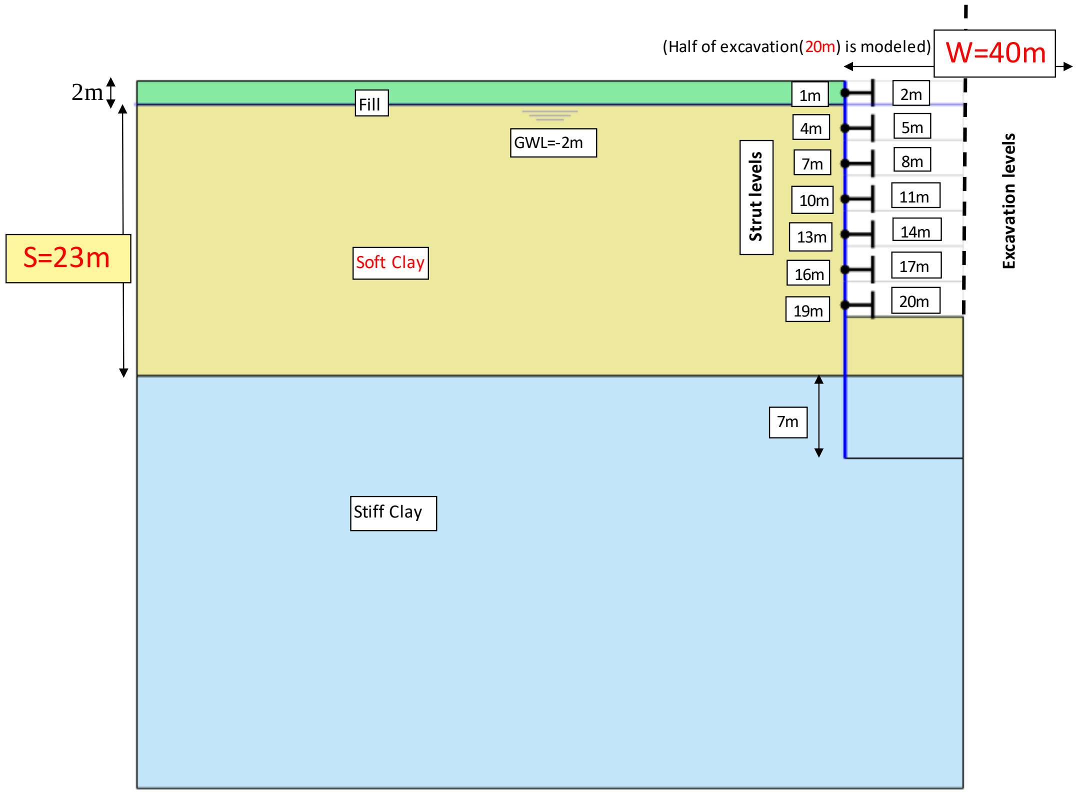

Figure A.2. Model Geometry-2.

Table B. Soil and structure parameters.

Default Soil Parameters		
	Stiff Clay	Fill
	HS	HS
	Undrained(A)	Drained
E_{50}^{ref}	1.00E+05	1.50E+04
E_{oed}^{ref}	1.00E+05	1.50E+04
E_{ur}^{ref}	3.00E+05	4.50E+04
ϕ'	26	30
K_0	0.562	0.5
c'_{ref}	25	1
v'_{ur}	0.2	0.2
p_{ref}	100	100
R_f	0.9	0.9
$\gamma_{unsat/sat}$	20/20	16/20
R_{inter}	0.65	0.65
m	1	1

Range of parameters	
c_u/σ'_v	0.20-0.25-0.30-0.35
E_{50}/c_u	100-200-300
γ	15-17-19
S	23-28-33
W	20-40-60
H_e	11-14-17-20
$\ln(EI/\gamma_w h_{avg}^4)$	6.097-7.313-8.176

Diaphragm Wall (E=2.0E+7)		
d	EA	EI
0.6	1.2E+07	3.60E+05
0.9	1.8E+07	1.215E+06
1.2	2.4E+07	2.88E+06

Strut	
EA	3.80E+06
$L_{spacing}$	5m
h_{avg}	3m

Generic Cases: 145 to 180

Table A.5. Model parameters and deformation results (Case No: 145 to 180).

Excavation	Soil(γ=15kN/m^3)		Diaphragm Wall(E=2,0E+7)		
H_e(m)	c_u/σ_v'	E_{50}/c_u	d	EA	EI
11-14-17-20	0.2	100-200-300	0.6	1.2E+07	3.60E+05
			0.9	1.8E+07	1.215E+06
			1.2	2.4E+07	2.88E+06

Soft Soil	E_{50}/c_u		
HSS	100	200	300
E_{50}^{ref}	2895	5789	8685
E_{oed}^{ref}	2895	5789	8685
E_{ur}^{ref}	8685	17367	26055
G_0^{ref}	30759	43418	54281
$\gamma_{0,7}$	3.59E-04	2.54E-04	2.03E-04
ϕ	18	18	18
K_0	0.691	0.691	0.691
E_{dyn}/E_{stat}	8.5	6	5

H=11m	d=0.6	d=0.9	d=1.2	E_{50}/c_u	H=11m	d=0.6	d=0.9	d=1.2
δ_{vm}(mm)	141	83	62	100	δ_{hm}(mm)	173	99	73
	131	76	55	200		159	90	66
	121	71	51	300		146	86	61

H=14m	d=0.6	d=0.9	d=1.2	E_{50}/c_u	H=14m	d=0.6	d=0.9	d=1.2
δ_{vm}(mm)	192	115	84	100	δ_{hm}(mm)	238	135	97
	181	106	76	200		221	125	90
	170	99	71	300		205	120	84

H=17m	d=0.6	d=0.9	d=1.2	E_{50}/c_u	H=17m	d=0.6	d=0.9	d=1.2
δ_{vm}(mm)	248	141	102	100	δ_{hm}(mm)	300	165	116
	235	133	90	200		276	154	108
	223	126	88	300		259	149	104

H=20m	d=0.6	d=0.9	d=1.2	E_{50}/c_u	H=20m	d=0.6	d=0.9	d=1.2
δ_{vm}(mm)	290	161	119	100	δ_{hm}(mm)	342	187	132
	277	151	105	200		316	176	125
	264	146	101	300		300	169	119

Generic Cases: 181 to 216

Table A.6. Model parameters and deformation results (Case No: 181 to 216).

Excavation	Soil (γ=15kN/m^3)		Diaphragm Wall(E=2,0E+7)		
H_e(m)	c_u/σ_v'	E_{50}/c_u	d	EA	EI
11-14-17-20	0.25	100-200-300	0.6	1.2E+07	3.60E+05
			0.9	1.8E+07	1.215E+06
			1.2	2.4E+07	2.88E+06

Soil	E_{50}/c_u		
HSS	100	200	300
E_{50}^{ref}	4000	8000	12000
E_{oed}^{ref}	4000	8000	12000
E_{ur}^{ref}	12000	24000	36000
G_0^{ref}	35000	50000	67500
$\gamma_{0,7}$	3.58E-04	2.51E-04	1.86E-04
ϕ	22	22	22
K_0	0.625	0.625	0.625
E_{dyn}/E_{stat}	7	5	4.5

H=11m	d=0.6	d=0.9	d=1.2	E_{50}/c_u	H=11m	d=0.6	d=0.9	d=1.2
δ_{vm}(mm)	105	64	49	100	δ_{hm}(mm)	130	78	60
	91	58	44	200		111	72	55
	79	51	39	300		100	64	48

H=14m	d=0.6	d=0.9	d=1.2	E_{50}/c_u	H=14m	d=0.6	d=0.9	d=1.2
δ_{vm}(mm)	144	88	67	100	δ_{hm}(mm)	182	107	82
	126	81	62	200		158	100	75
	114	74	55	300		144	91	68

H=17m	d=0.6	d=0.9	d=1.2	E_{50}/c_u	H=17m	d=0.6	d=0.9	d=1.2
δ_{vm}(mm)	188	113	83	100	δ_{hm}(mm)	232	134	98
	164	104	77	200		202	127	93
	152	97	70	300		186	117	85

H=20m	d=0.6	d=0.9	d=1.2	E_{50}/c_u	H=20m	d=0.6	d=0.9	d=1.2
δ_{vm}(mm)	222	130	98	100	δ_{hm}(mm)	269	156	114
	198	121	90	200		236	147	108
	183	114	83	300		218	137	100

Generic Cases: 217 to 252

Table A.7. Model parameters and deformation results (Case No: 217 to 252).

Excavation	Soil(γ=15kN/m^3)		Diaphragm Wall(E=2,0E+7)		
H_e(m)	c_u/σ'_v	E_{50}/c_u	d	EA	EI
11-14-17-20	0.3	100-200-300	0.6	1.2E+07	3.60E+05
			0.9	1.8E+07	1.215E+06
			1.2	2.4E+07	2.88E+06

Soil	E_{50}/c_u		
HSS	100	200	300
E_{50}^{ref}	5400	10800	16200
E_{oed}^{ref}	5400	10800	16200
E_{ur}^{ref}	16200	32400	48600
G_0^{ref}	40500	60750	75938
$\gamma_{0,7}$	3.40E-04	2.27E-04	1.81E-04
ϕ	26.4	26.4	26.4
K_0	0.555	0.555	0.555
E_{dyn}/E_{stat}	6	4.5	3.75

H=11m	d=0.6	d=0.9	d=1.2	E_{50}/c_u	H=11m	d=0.6	d=0.9	d=1.2
δ_{vm}(mm)	76	58	47	100	δ_{hm}(mm)	95	71	57
	65	47	37	200		81	58	46
	56	40	31	300		71	51	40

H=14m	d=0.6	d=0.9	d=1.2	E_{50}/c_u	H=14m	d=0.6	d=0.9	d=1.2
δ_{vm}(mm)	108	78	63	100	δ_{hm}(mm)	137	95	75
	92	65	51	200		117	81	63
	82	57	45	300		106	73	56

H=17m	d=0.6	d=0.9	d=1.2	E_{50}/c_u	H=17m	d=0.6	d=0.9	d=1.2
δ_{vm}(mm)	137	100	77	100	δ_{hm}(mm)	176	119	91
	121	84	64	200		153	103	79
	109	76	58	300		137	94	72

H=20m	d=0.6	d=0.9	d=1.2	E_{50}/c_u	H=20m	d=0.6	d=0.9	d=1.2
δ_{vm}(mm)	165	117	91	100	δ_{hm}(mm)	209	138	105
	148	100	76	200		183	122	93
	136	93	70	300		164	113	85

Generic Cases: 253 to 288

Table A.8. Model parameters and deformation results (Case No: 253 to 288).

Excavation	Soil(γ=15kN/m^3)		Diaphragm Wall(E=2,0E+7)		
H_e(m)	c_u/σ_v'	E_{50}/c_u	d	EA	EI
11-14-17-20	0.35	100-200-300	0.6	1.2E+07	3.60E+05
			0.9	1.8E+07	1.215E+06
			1.2	2.4E+07	2.88E+06

Soil	E_{50}/c_u		
HSS	100	200	300
E_{50}^{ref}	7000	14000	21000
E_{oed}^{ref}	7000	14000	21000
E_{ur}^{ref}	21000	42000	63000
G_0^{ref}	52500	73500	99750
$\gamma_{0,7}$	2.75E-04	1.96E-04	1.45E-04
ϕ	30	30	30
K_0	0.500	0.500	0.500
E_{dyn}/E_{stat}	6	4.2	3.8

H=11m	d=0.6	d=0.9	d=1.2	E_{50}/c_u	H=11m	d=0.6	d=0.9	d=1.2
δ_{vm}(mm)	64	52	43	100	δ_{hm}(mm)	82	64	52
	51	40	34	200		65	50	42
	42	33	27	300		55	42	34

H=14m	d=0.6	d=0.9	d=1.2	E_{50}/c_u	H=14m	d=0.6	d=0.9	d=1.2
δ_{vm}(mm)	89	69	56	100	δ_{hm}(mm)	117	84	67
	73	55	45	200		96	69	56
	63	47	38	300		82	60	48

H=17m	d=0.6	d=0.9	d=1.2	E_{50}/c_u	H=17m	d=0.6	d=0.9	d=1.2
δ_{vm}(mm)	114	88	70	100	δ_{hm}(mm)	150	105	82
	96	72	58	200		124	90	71
	85	63	51	300		109	79	63

H=20m	d=0.6	d=0.9	d=1.2	E_{50}/c_u	H=20m	d=0.6	d=0.9	d=1.2
δ_{vm}(mm)	139	103	82	100	δ_{hm}(mm)	181	123	95
	120	87	69	200		152	107	84
	108	79	62	300		133	97	76

Model Group:3

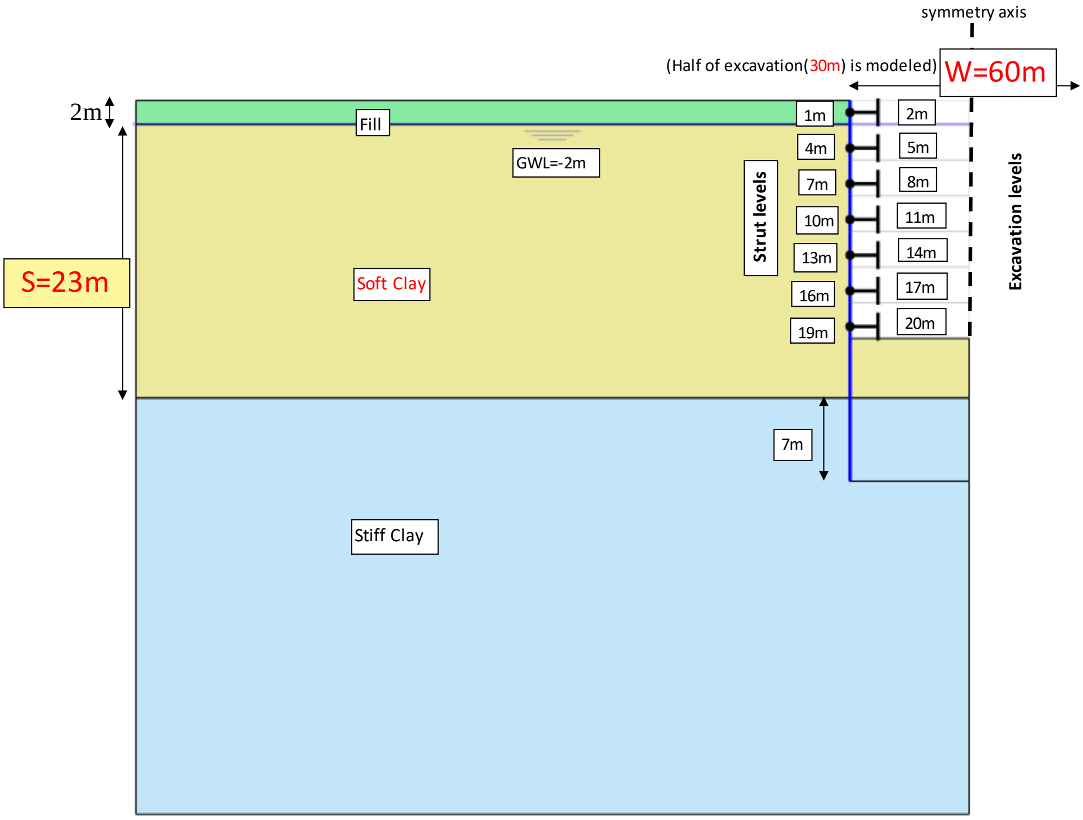

Figure A.3. Model Geometry-3.

Table B. Soil and structure parameters.

Default Soil Parameters		
	Stiff Clay	Fill
	HS	HS
	Undrained(A)	Drained
E_{50}^{ref}	1.00E+05	1.50E+04
E_{oed}^{ref}	1.00E+05	1.50E+04
E_{ur}^{ref}	3.00E+05	4.50E+04
ϕ'	26	30
K_0	0.562	0.5
c'_{ref}	25	1
v'_{ur}	0.2	0.2
p_{ref}	100	100
R_f	0.9	0.9
$\gamma_{unsat/sat}$	20/20	16/20
R_{inter}	0.65	0.65
m	1	1

Range of parameters	
c_u/σ'_v	0.20-0.25-0.30-0.35
E_{50}/c_u	100-200-300
γ	15-17-19
S	23-28-33
W	20-40-60
H_e	11-14-17-20
$\ln(EI/\gamma_w h_{avg}^4)$	6.097-7.313-8.176

Diaphragm Wall (E=2.0E+7)		
d	EA	EI
0.6	1.2E+07	3.60E+05
0.9	1.8E+07	1.215E+06
1.2	2.4E+07	2.88E+06

Strut	
EA	3.80E+06
$L_{spacing}$	5m
h_{avg}	3m

Generic Cases: 289 to 324

Table A.9. Model parameters and deformation results (Case No: 289 to 324).

Excavation	Soil(γ=15kN/m^3)		Diaphragm Wall(E=2,0E+7)		
H_e(m)	c_u/σ_v'	E_{50}/c_u	d	EA	EI
11-14-17-20	0.2	100-200-300	0.6	1.2E+07	3.60E+05
			0.9	1.8E+07	1.215E+06
			1.2	2.4E+07	2.88E+06

Soft Soil	E_{50}/c_u		
HSS	100	200	300
E_{50}^{ref}	2895	5789	8685
E_{oed}^{ref}	2895	5789	8685
E_{ur}^{ref}	8685	17367	26055
G_0^{ref}	30759	43418	54281
$\gamma_{0,7}$	3.59E-04	2.54E-04	2.03E-04
ϕ	18	18	18
K_0	0.691	0.691	0.691
E_{dyn}/E_{stat}	8.5	6	5

H=11m	d=0.6	d=0.9	d=1.2	E_{50}/c_u	H=11m	d=0.6	d=0.9	d=1.2
δ_{vm}(mm)	158	97	73	100	δ_{hm}(mm)	192	114	87
	145	90	65	200		177	105	76
	135	82	61	300		165	98	72

H=14m	d=0.6	d=0.9	d=1.2	E_{50}/c_u	H=14m	d=0.6	d=0.9	d=1.2
δ_{vm}(mm)	214	135	98	100	δ_{hm}(mm)	263	156	114
	201	124	90	200		240	145	104
	190	116	85	300		230	138	99

H=17m	d=0.6	d=0.9	d=1.2	E_{50}/c_u	H=17m	d=0.6	d=0.9	d=1.2
δ_{vm}(mm)	280	166	118	100	δ_{hm}(mm)	331	190	135
	264	156	110	200		305	179	126
	253	149	105	300		292	171	122

H=20m	d=0.6	d=0.9	d=1.2	E_{50}/c_u	H=20m	d=0.6	d=0.9	d=1.2
δ_{vm}(mm)	328	188	140	100	δ_{hm}(mm)	381	215	156
	314	179	129	200		357	203	145
	300	173	123	300		340	197	140

Generic Cases: 325 to 360

Table A.10. Model parameters and deformation results (Case No: 325 to 360).

Excavation	Soil (γ=15kN/m^3)		Diaphragm Wall(E=2,0E+7)		
H_e(m)	c_u/σ_v'	E_{50}/c_u	d	EA	EI
11-14-17-20	0.25	100-200-300	0.6	1.2E+07	3.60E+05
			0.9	1.8E+07	1.215E+06
			1.2	2.4E+07	2.88E+06

Soil	E_{50}/c_u		
HSS	100	200	300
E_{50}^{ref}	4000	8000	12000
E_{oed}^{ref}	4000	8000	12000
E_{ur}^{ref}	12000	24000	36000
G_0^{ref}	35000	50000	67500
$\gamma_{0,7}$	3.58E-04	2.51E-04	1.86E-04
ϕ	22	22	22
K_0	0.625	0.625	0.625
E_{dyn}/E_{stat}	7	5	4.5

H=11m	d=0.6	d=0.9	d=1.2	E_{50}/c_u	H=11m	d=0.6	d=0.9	d=1.2
δ_{vm}(mm)	120	80	65	100	δ_{hm}(mm)	150	97	77
	104	71	54	200		129	86	65
	95	62	47	300		116	76	57

H=14m	d=0.6	d=0.9	d=1.2	E_{50}/c_u	H=14m	d=0.6	d=0.9	d=1.2
δ_{vm}(mm)	166	111	85	100	δ_{hm}(mm)	207	134	101
	145	98	76	200		181	119	90
	134	87	66	300		167	108	81

H=17m	d=0.6	d=0.9	d=1.2	E_{50}/c_u	H=17m	d=0.6	d=0.9	d=1.2
δ_{vm}(mm)	215	139	102	100	δ_{hm}(mm)	263	164	121
	191	126	94	200		231	150	110
	177	115	85	300		214	138	102

H=20m	d=0.6	d=0.9	d=1.2	E_{50}/c_u	H=20m	d=0.6	d=0.9	d=1.2
δ_{vm}(mm)	255	161	121	100	δ_{hm}(mm)	305	188	139
	233	148	110	200		271	174	128
	217	137	100	300		253	161	119

Generic Cases: 361 to 396

Table A.11. Model parameters and deformation results (Case No: 361 to 396).

Excavation	Soil(γ=15kN/m^3)		Diaphragm Wall(E=2,0E+7)		
H_e(m)	c_u/σ_v'	E_{50}/c_u	d	EA	EI
11-14-17-20	0.3	100-200-300	0.6	1.2E+07	3.60E+05
			0.9	1.8E+07	1.215E+06
			1.2	2.4E+07	2.88E+06

Soil	E_{50}/c_u		
HSS	100	200	300
E_{50}^{ref}	5400	10800	16200
E_{oed}^{ref}	5400	10800	16200
E_{ur}^{ref}	16200	32400	48600
G_0^{ref}	40500	60750	75938
$\gamma_{0,7}$	3.40E-04	2.27E-04	1.81E-04
ϕ	26.4	26.4	26.4
K_0	0.555	0.555	0.555
E_{dyn}/E_{stat}	6	4.5	3.75

H=11m	d=0.6	d=0.9	d=1.2	E_{50}/c_u	H=11m	d=0.6	d=0.9	d=1.2
δ_{vm}(mm)	91	71	58	100	δ_{hm}(mm)	113	86	69
	78	58	46	200		98	71	56
	68	49	40	300		85	61	48

H=14m	d=0.6	d=0.9	d=1.2	E_{50}/c_u	H=14m	d=0.6	d=0.9	d=1.2
δ_{vm}(mm)	126	94	76	100	δ_{hm}(mm)	160	114	90
	109	80	63	200		137	97	77
	98	70	56	300		124	87	69

H=17m	d=0.6	d=0.9	d=1.2	E_{50}/c_u	H=17m	d=0.6	d=0.9	d=1.2
δ_{vm}(mm)	161	119	93	100	δ_{hm}(mm)	205	142	109
	145	103	79	200		178	123	95
	131	93	72	300		160	113	87

H=20m	d=0.6	d=0.9	d=1.2	E_{50}/c_u	H=20m	d=0.6	d=0.9	d=1.2
δ_{vm}(mm)	193	139	110	100	δ_{hm}(mm)	243	164	125
	179	123	93	200		211	147	112
	164	113	86	300		193	134	104

Generic Cases: 397 to 432

Table A.12. Model parameters and deformation results (Case No: 397 to 432).

Excavation	Soil(γ=15kN/m^3)		Diaphragm Wall(E=2,0E+7)		
H_e(m)	c_u/σ'_v	E_{50}/c_u	d	EA	EI
11-14-17-20	0.35	100-200-300	0.6	1.2E+07	3.60E+05
			0.9	1.8E+07	1.215E+06
			1.2	2.4E+07	2.88E+06

Soil	E_{50}/c_u		
HSS	100	200	300
E_{50}^{ref}	7000	14000	21000
E_{oed}^{ref}	7000	14000	21000
E_{ur}^{ref}	21000	42000	63000
G_0^{ref}	52500	73500	99750
$\gamma_{0.7}$	2.75E-04	1.96E-04	1.45E-04
ϕ	30	30	30
K_0	0.500	0.500	0.500
E_{dyn}/E_{stat}	6	4.2	3.8

H=11m	d=0.6	d=0.9	d=1.2	E_{50}/c_u	H=11m	d=0.6	d=0.9	d=1.2
δ_{vm}(mm)	80	65	53	100	δ_{hm}(mm)	100	78	63
	67	50	42	200		82	62	51
	53	40	34	300		66	50	42

H=14m	d=0.6	d=0.9	d=1.2	E_{50}/c_u	H=14m	d=0.6	d=0.9	d=1.2
δ_{vm}(mm)	108	84	69	100	δ_{hm}(mm)	138	101	81
	93	68	56	200		116	84	69
	77	57	48	300		98	71	58

H=17m	d=0.6	d=0.9	d=1.2	E_{50}/c_u	H=17m	d=0.6	d=0.9	d=1.2
δ_{vm}(mm)	138	106	85	100	δ_{hm}(mm)	176	127	98
	120	88	71	200		150	108	86
	104	77	63	300		129	94	76

H=20m	d=0.6	d=0.9	d=1.2	E_{50}/c_u	H=20m	d=0.6	d=0.9	d=1.2
δ_{vm}(mm)	169	125	99	100	δ_{hm}(mm)	211	147	113
	150	108	84	200		180	129	102
	133	96	76	300		158	115	92

Model Group:4

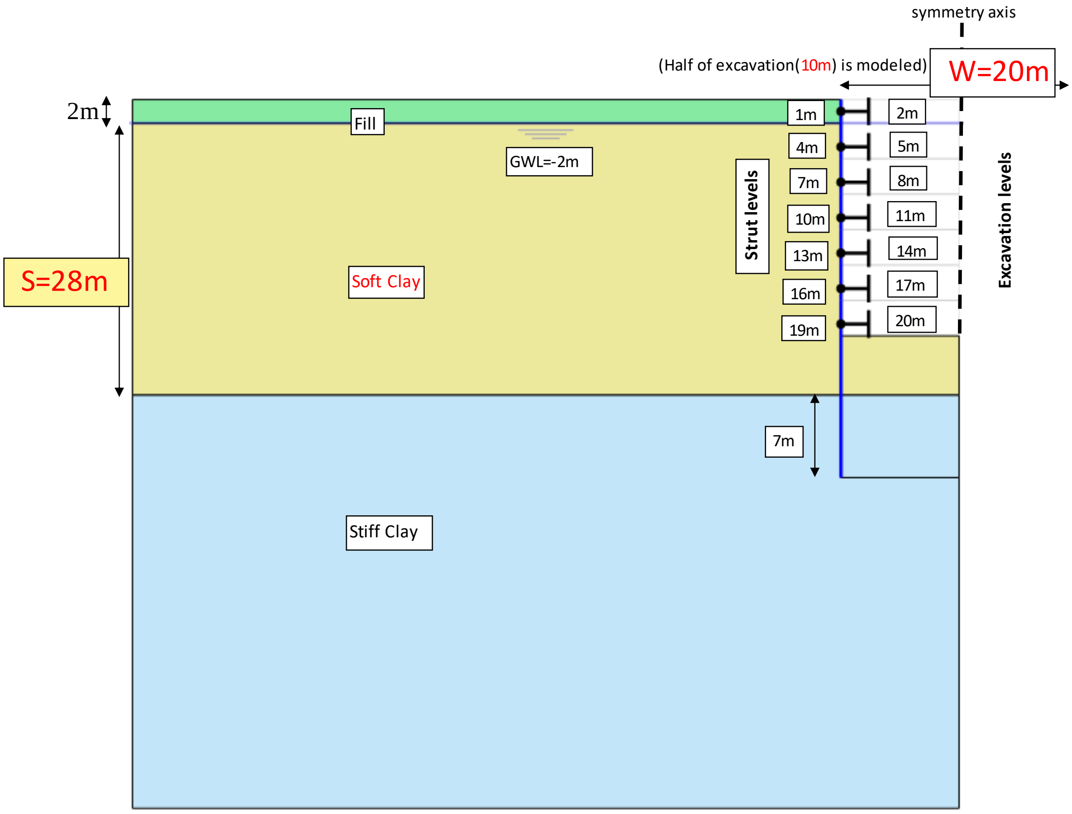

Figure A.4. Model Geometry-4.

Table B. Soil and structure parameters.

Default Soil Parameters		
	Stiff Clay	Fill
	HS	HS
	Undrained(A)	Drained
E_{50}^{ref}	1.00E+05	1.50E+04
E_{oed}^{ref}	1.00E+05	1.50E+04
E_{ur}^{ref}	3.00E+05	4.50E+04
ϕ'	26	30
K_0	0.562	0.5
c'_{ref}	25	1
v'_{ur}	0.2	0.2
p_{ref}	100	100
R_f	0.9	0.9
$\gamma_{unsat/sat}$	20/20	16/20
R_{inter}	0.65	0.65
m	1	1

Range of parameters	
c_u/σ'_v	0.20-0.25-0.30-0.35
E_{50}/c_u	100-200-300
γ	17
S	23-28-33
W	20-40-60
H_e	11-14-17-20
$\ln(EI/\gamma_w h_{avg}^4)$	6.097-7.313-8.176

Diaphragm Wall (E=2,0E+7)		
d	EA	EI
0.6	1.2E+07	3.60E+05
0.9	1.8E+07	1.215E+06
1.2	2.4E+07	2.88E+06

Strut	
EA	3.80E+06
$L_{spacing}$	5m
h_{avg}	3m

Generic Cases: 433 to 468

Table A.13. Model parameters and deformation results (Case No: 433 to 468).

Excavation	Soil(γ=15kN/m^3)		Diaphragm Wall(E=2,0E+7)		
H_e(m)	c_u/σ_v'	E_{50}/c_u	d	EA	EI
11-14-17-20	0.2	100-200-300	0.6	1.2E+07	3.60E+05
			0.9	1.8E+07	1.215E+06
			1.2	2.4E+07	2.88E+06

Soft Soil	E_{50}/c_u		
HSS	100	200	300
E_{50}^{ref}	2895	5789	8685
E_{oed}^{ref}	2895	5789	8685
E_{ur}^{ref}	8685	17367	26055
G_0^{ref}	30759	43418	54281
$\gamma_{0,7}$	3.59E-04	2.54E-04	2.03E-04
ϕ	18	18	18
K_0	0.691	0.691	0.691
E_{dyn}/E_{stat}	8.5	6	5

H=11m	d=0.6	d=0.9	d=1.2	E_{50}/c_u	H=11m	d=0.6	d=0.9	d=1.2
δ_{vm}(mm)	143	78	56	100	δ_{hm}(mm)	180	100	69
	128	71	49	200		159	90	62
	120	66	45	300		140	84	56

H=14m	d=0.6	d=0.9	d=1.2	E_{50}/c_u	H=14m	d=0.6	d=0.9	d=1.2
δ_{vm}(mm)	213	113	80	100	δ_{hm}(mm)	275	148	99
	193	106	72	200		246	135	91
	182	99	68	300		229	124	85

H=17m	d=0.6	d=0.9	d=1.2	E_{50}/c_u	H=17m	d=0.6	d=0.9	d=1.2
δ_{vm}(mm)	288	150	101	100	δ_{hm}(mm)	367	194	126
	262	143	94	200		330	181	118
	249	137	90	300		314	169	112

H=20m	d=0.6	d=0.9	d=1.2	E_{50}/c_u	H=20m	d=0.6	d=0.9	d=1.2
δ_{vm}(mm)	372	183	120	100	δ_{hm}(mm)	457	235	150
	342	176	113	200		416	219	141
	327	169	108	300		395	207	135

Generic Cases: 469 to 504

Table A.14. Model parameters and deformation results (Case No: 469 to 504).

Excavation	Soil (γ=15kN/m^3)		Diaphragm Wall(E=2,0E+7)		
H_e(m)	c_u/σ_v'	E_{50}/c_u	d	EA	EI
11-14-17-20	0.25	100-200-300	0.6	1.2E+07	3.60E+05
			0.9	1.8E+07	1.215E+06
			1.2	2.4E+07	2.88E+06

Soil	E_{50}/c_u		
HSS	100	200	300
E_{50}^{ref}	4000	8000	12000
E_{oed}^{ref}	4000	8000	12000
E_{ur}^{ref}	12000	24000	36000
G_0^{ref}	35000	50000	67500
$\gamma_{0,7}$	3.58E-04	2.51E-04	1.86E-04
ϕ	22	22	22
K_0	0.625	0.625	0.625
E_{dyn}/E_{stat}	7	5	4.5

H=11m	d=0.6	d=0.9	d=1.2	E_{50}/c_u	H=11m	d=0.6	d=0.9	d=1.2
δ_{vm}(mm)	95	60	44	100	δ_{hm}(mm)	120	75	53
	80	50	37	200		102	64	47
	69	44	32	300		89	55	41

H=14m	d=0.6	d=0.9	d=1.2	E_{50}/c_u	H=14m	d=0.6	d=0.9	d=1.2
δ_{vm}(mm)	146	87	63	100	δ_{hm}(mm)	193	111	78
	127	76	54	200		166	97	69
	113	67	49	300		148	87	62

H=17m	d=0.6	d=0.9	d=1.2	E_{50}/c_u	H=17m	d=0.6	d=0.9	d=1.2
δ_{vm}(mm)	196	115	82	100	δ_{hm}(mm)	262	149	103
	173	103	74	200		228	133	93
	156	93	66	300		205	120	85

H=20m	d=0.6	d=0.9	d=1.2	E_{50}/c_u	H=20m	d=0.6	d=0.9	d=1.2
δ_{vm}(mm)	252	144	97	100	δ_{hm}(mm)	331	185	124
	221	129	89	200		285	167	114
	201	119	82	300		259	150	105

Generic Cases: 505 to 540

Table A.15. Model parameters and deformation results (Case No: 505 to 540).

Excavation	Soil(γ=15kN/m^3)		Diaphragm Wall(E=2,0E+7)		
H_e(m)	c_u/σ_v'	E_{50}/c_u	d	EA	EI
11-14-17-20	0.3	100-200-300	0.6	1.2E+07	3.60E+05
			0.9	1.8E+07	1.215E+06
			1.2	2.4E+07	2.88E+06

Soil	E_{50}/c_u		
HSS	100	200	300
E_{50}^{ref}	5400	10800	16200
E_{oed}^{ref}	5400	10800	16200
E_{ur}^{ref}	16200	32400	48600
G_0^{ref}	40500	60750	75938
$\gamma_{0,7}$	3.40E-04	2.27E-04	1.81E-04
ϕ	26.4	26.4	26.4
K_0	0.555	0.555	0.555
E_{dyn}/E_{stat}	6	4.5	3.75

H=11m	d=0.6	d=0.9	d=1.2	E_{50}/c_u	H=11m	d=0.6	d=0.9	d=1.2
δ_{vm}(mm)	63	45	34	100	δ_{hm}(mm)	79	55	43
	52	36	27	200		66	46	35
	45	31	24	300		58	40	31

H=14m	d=0.6	d=0.9	d=1.2	E_{50}/c_u	H=14m	d=0.6	d=0.9	d=1.2
δ_{vm}(mm)	98	65	49	100	δ_{hm}(mm)	129	83	61
	82	54	40	200		109	71	52
	73	47	36	300		95	62	47

H=17m	d=0.6	d=0.9	d=1.2	E_{50}/c_u	H=17m	d=0.6	d=0.9	d=1.2
δ_{vm}(mm)	131	84	64	100	δ_{hm}(mm)	178	113	82
	114	74	54	200		154	99	71
	103	65	50	300		136	87	65

H=20m	d=0.6	d=0.9	d=1.2	E_{50}/c_u	H=20m	d=0.6	d=0.9	d=1.2
δ_{vm}(mm)	168	105	77	100	δ_{hm}(mm)	226	141	100
	146	95	69	200		195	126	88
	133	86	63	300		176	112	83

Generic Cases: 541 to 576

Table A.16. Model parameters and deformation results (Case No: 541 to 576).

Excavation	Soil(γ=15kN/m^3)		Diaphragm Wall(E=2,0E+7)		
H_e(m)	c_u/σ_v'	E_{50}/c_u	d	EA	EI
11-14-17-20	0.35	100-200-300	0.6	1.2E+07	3.60E+05
			0.9	1.8E+07	1.215E+06
			1.2	2.4E+07	2.88E+06

Soil	E_{50}/c_u		
HSS	100	200	300
E_{50}^{ref}	7000	14000	21000
E_{oed}^{ref}	7000	14000	21000
E_{ur}^{ref}	21000	42000	63000
G_0^{ref}	52500	73500	99750
$\gamma_{0,7}$	2.75E-04	1.96E-04	1.45E-04
ϕ	30	30	30
K_0	0.500	0.500	0.500
E_{dyn}/E_{stat}	6	4.2	3.8

H=11m	d=0.6	d=0.9	d=1.2	E_{50}/c_u	H=11m	d=0.6	d=0.9	d=1.2
δ_{vm}(mm)	50	35	28	100	δ_{hm}(mm)	62	43	34
	40	29	23	200		50	37	29
	33	24	19	300		43	31	25

H=14m	d=0.6	d=0.9	d=1.2	E_{50}/c_u	H=14m	d=0.6	d=0.9	d=1.2
δ_{vm}(mm)	76	50	38	100	δ_{hm}(mm)	101	65	48
	63	43	33	200		83	55	43
	53	37	28	300		70	48	37

H=17m	d=0.6	d=0.9	d=1.2	E_{50}/c_u	H=17m	d=0.6	d=0.9	d=1.2
δ_{vm}(mm)	104	66	50	100	δ_{hm}(mm)	144	88	64
	86	58	45	200		118	77	58
	75	52	39	300		101	69	52

H=20m	d=0.6	d=0.6	d=0.6	E_{50}/c_u d=0.9	d=1.2	d=0.6	d=0.9	d=1.2
δ_{vm}(mm)	132	84	62	100	δ_{hm}(mm)	186	113	81
	111	74	57	200		151	99	75
	99	67	51	300		132	89	67

Model Group:5

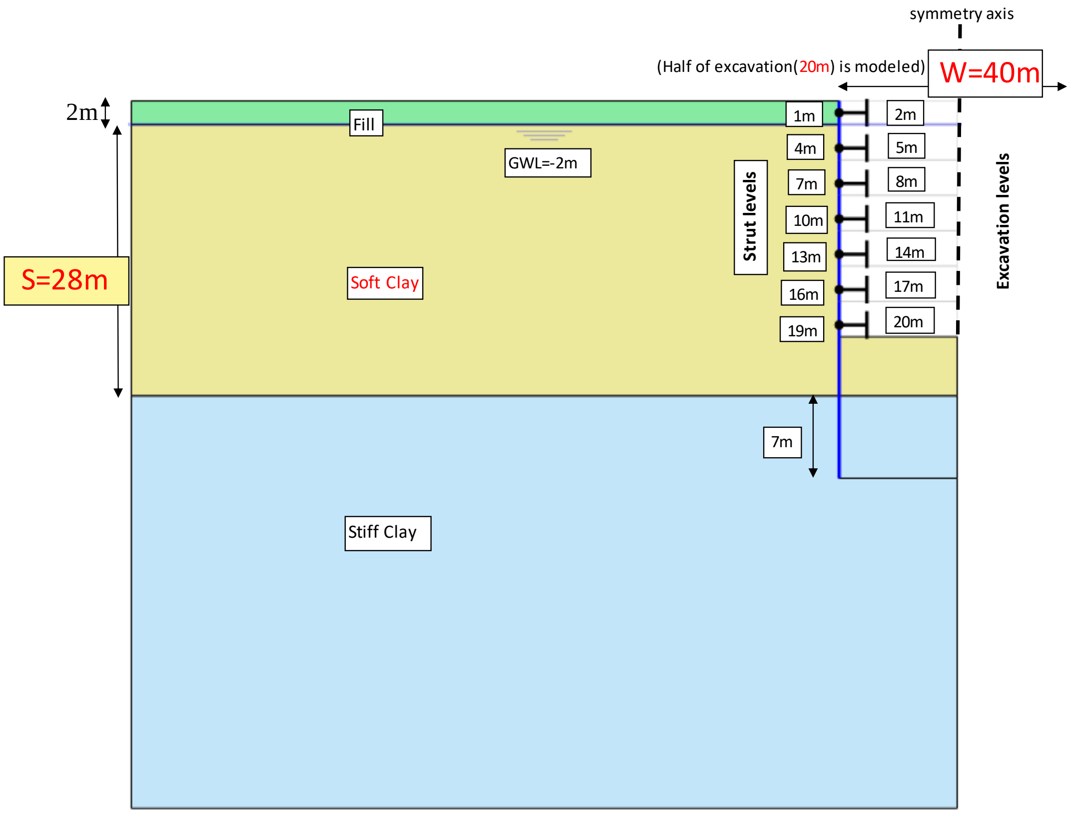

Figure A.5. Model Geometry-5.

Table B. Soil and structure parameters.

Default Soil Parameters		
	Stiff Clay	Fill
	HS	HS
	Undrained(A)	Drained
E_{50}^{ref}	1.00E+05	1.50E+04
E_{oed}^{ref}	1.00E+05	1.50E+04
E_{ur}^{ref}	3.00E+05	4.50E+04
ϕ'	26	30
K_0	0.562	0.5
c'_{ref}	25	1
v'_{ur}	0.2	0.2
p_{ref}	100	100
R_f	0.9	0.9
$\gamma_{unsat/sat}$	20/20	16/20
R_{inter}	0.65	0.65
m	1	1

Range of parameters	
c_u/σ'_v	0.20-0.25-0.30-0.35
E_{50}/c_u	100-200-300
γ	17
S	23-28-33
W	20-40-60
H_e	11-14-17-20
$\ln(EI/\gamma_w h_{avg}^4)$	6.097-7.313-8.176

Diaphragm Wall (E=2,0E+7)		
d	EA	EI
0.6	1.2E+07	3.60E+05
0.9	1.8E+07	1.215E+06
1.2	2.4E+07	2.88E+06

Strut	
EA	3.80E+06
$L_{spacing}$	5m
h_{avg}	3m

Generic Cases: 577 to 612

Table A.17. Model parameters and deformation results (Case No: 577 to 612).

Excavation	Soil(γ=15kN/m^3)		Diaphragm Wall(E=2,0E+7)		
H_e(m)	c_u/σ_v'	E_{50}/c_u	d	EA	EI
11-14-17-20	0.2	100-200-300	0.6	1.2E+07	3.60E+05
			0.9	1.8E+07	1.215E+06
			1.2	2.4E+07	2.88E+06

Soft Soil	E_{50}/c_u		
HSS	100	200	300
E_{50}^{ref}	2895	5789	8685
E_{oed}^{ref}	2895	5789	8685
E_{ur}^{ref}	8685	17367	26055
G_0^{ref}	30759	43418	54281
$\gamma_{0,7}$	3.59E-04	2.54E-04	2.03E-04
ϕ	18	18	18
K_0	0.691	0.691	0.691
E_{dyn}/E_{stat}	8.5	6	5

H=11m	d=0.6	d=0.9	d=1.2	E_{50}/c_u	H=11m	d=0.6	d=0.9	d=1.2
δ_{vm}(mm)	172	103	72	100	δ_{hm}(mm)	214	122	87
	158	92	66	200		194	113	80
	148	89	62	300		176	107	75

H=14m	d=0.6	d=0.9	d=1.2	E_{50}/c_u	H=14m	d=0.6	d=0.9	d=1.2
δ_{vm}(mm)	252	148	105	100	δ_{hm}(mm)	326	180	126
	240	136	98	200		300	167	118
	226	128	91	300		278	160	111

H=17m	d=0.6	d=0.9	d=1.2	E_{50}/c_u	H=17m	d=0.6	d=0.9	d=1.2
δ_{vm}(mm)	351	198	136	100	δ_{hm}(mm)	443	239	162
	330	183	127	200		405	223	154
	310	177	121	300		382	215	146

H=20m	d=0.6	d=0.9	d=1.2	E_{50}/c_u	H=20m	d=0.6	d=0.9	d=1.2
δ_{vm}(mm)	448	241	160	100	δ_{hm}(mm)	549	288	190
	429	227	152	200		514	271	182
	409	218	146	300		488	262	175

Generic Cases: 613 to 648

Table A.18. Model parameters and deformation results (Case No: 613 to 648).

Excavation	Soil (γ=15kN/m^3)		Diaphragm Wall(E=2,0E+7)		
H_e(m)	c_u/σ_v'	E_{50}/c_u	d	EA	EI
11-14-17-20	0.25	100-200-300	0.6	1.2E+07	3.60E+05
			0.9	1.8E+07	1.215E+06
			1.2	2.4E+07	2.88E+06

Soil	E_{50}/c_u		
HSS	100	200	300
E_{50}^{ref}	4000	8000	12000
E_{oed}^{ref}	4000	8000	12000
E_{ur}^{ref}	12000	24000	36000
G_0^{ref}	35000	50000	67500
$\gamma_{0,7}$	3.58E-04	2.51E-04	1.86E-04
ϕ	22	22	22
K_0	0.625	0.625	0.625
E_{dyn}/E_{stat}	7	5	4.5

H=11m	d=0.6	d=0.9	d=1.2	E_{50}/c_u	H=11m	d=0.6	d=0.9	d=1.2
δ_{vm}(mm)	123	76	54	100	δ_{hm}(mm)	150	93	66
	103	68	50	200		127	85	63
	92	60	44	300		112	75	55
H=14m	d=0.6	d=0.9	d=1.2	E_{50}/c_u	H=14m	d=0.6	d=0.9	d=1.2
δ_{vm}(mm)	184	111	79	100	δ_{hm}(mm)	235	139	96
	160	101	75	200		202	126	93
	144	90	67	300		183	114	83
H=17m	d=0.6	d=0.9	d=1.2	E_{50}/c_u	H=17m	d=0.6	d=0.9	d=1.2
δ_{vm}(mm)	249	149	104	100	δ_{hm}(mm)	320	187	129
	218	137	100	200		277	170	124
	197	126	91	300		251	156	113
H=20m	d=0.6	d=0.9	d=1.2	E_{50}/c_u	H=20m	d=0.6	d=0.9	d=1.2
δ_{vm}(mm)	322	184	125	100	δ_{hm}(mm)	406	232	155
	284	172	122	200		351	211	150
	258	160	114	300		322	195	138

Generic Cases: 649 to 684

Table A.19. Model parameters and deformation results (Case No: 649 to 684).

Excavation	Soil(γ=15kN/m^3)		Diaphragm Wall(E=2,0E+7)		
H_e(m)	c_u/σ_v'	E_{50}/c_u	d	EA	EI
11-14-17-20	0.3	100-200-300	0.6	1.2E+07	3.60E+05
			0.9	1.8E+07	1.215E+06
			1.2	2.4E+07	2.88E+06

Soil	E_{50}/c_u		
HSS	100	200	300
E_{50}^{ref}	5400	10800	16200
E_{oed}^{ref}	5400	10800	16200
E_{ur}^{ref}	16200	32400	48600
G_0^{ref}	40500	60750	75938
$\gamma_{0,7}$	3.40E-04	2.27E-04	1.81E-04
ϕ	26.4	26.4	26.4
K_0	0.555	0.555	0.555
E_{dyn}/E_{stat}	6	4.5	3.75

H=11m	d=0.6	d=0.9	d=1.2	E_{50}/c_u	H=11m	d=0.6	d=0.9	d=1.2
δ_{vm}(mm)	82	60	51	100	δ_{hm}(mm)	101	76	62
	71	51	41	200		87	63	50
	61	43	34	300		76	54	43

H=14m	d=0.6	d=0.9	d=1.2	E_{50}/c_u	H=14m	d=0.6	d=0.9	d=1.2
δ_{vm}(mm)	124	86	70	100	δ_{hm}(mm)	161	110	86
	109	75	59	200		138	94	74
	97	66	51	300		124	83	64

H=17m	d=0.6	d=0.9	d=1.2	E_{50}/c_u	H=17m	d=0.6	d=0.9	d=1.2
δ_{vm}(mm)	167	116	94	100	δ_{hm}(mm)	223	147	113
	150	101	78	200		193	129	98
	134	91	70	300		172	116	88

H=20m	d=0.6	d=0.9	d=1.2	E_{50}/c_u	H=20m	d=0.6	d=0.9	d=1.2
δ_{vm}(mm)	215	144	113	100	δ_{hm}(mm)	288	184	135
	192	129	97	200		247	163	122
	175	118	89	300		222	147	112

Generic Cases: 685 to 720

Table A.20. Model parameters and deformation results (Case No: 685 to 720).

Excavation	Soil(γ=15kN/m^3)		Diaphragm Wall(E=2,0E+7)		
H_e(m)	c_u/σ_v'	E_{50}/c_u	d	EA	EI
11-14-17-20	0.35	100-200-300	0.6	1.2E+07	3.60E+05
			0.9	1.8E+07	1.215E+06
			1.2	2.4E+07	2.88E+06

Soil	E_{50}/c_u		
HSS	100	200	300
E_{50}^{ref}	7000	14000	21000
E_{oed}^{ref}	7000	14000	21000
E_{ur}^{ref}	21000	42000	63000
G_0^{ref}	52500	73500	99750
$\gamma_{0,7}$	2.75E-04	1.96E-04	1.45E-04
ϕ	30	30	30
K_0	0.500	0.500	0.500
E_{dyn}/E_{stat}	6	4.2	3.8

H=11m	d=0.6	d=0.9	d=1.2	E_{50}/c_u	H=11m	d=0.6	d=0.9	d=1.2
δ_{vm}(mm)	66	49	45	100	δ_{hm}(mm)	84	62	55
	55	43	36	200		70	54	45
	44	34	28	300		55	42	36

H=14m	d=0.6	d=0.9	d=1.2	E_{50}/c_u	H=14m	d=0.6	d=0.9	d=1.2
δ_{vm}(mm)	97	70	61	100	δ_{hm}(mm)	130	89	75
	84	61	50	200		107	78	63
	70	52	41	300		89	65	53

H=17m	d=0.6	d=0.9	d=1.2	E_{50}/c_u	H=17m	d=0.6	d=0.9	d=1.2
δ_{vm}(mm)	132	94	79	100	δ_{hm}(mm)	181	120	96
	115	83	67	200		150	106	84
	100	72	58	300		127	91	73

H=20m	d=0.6	d=0.9	d=1.2	E_{50}/c_u	H=20m	d=0.6	d=0.9	d=1.2
δ_{vm}(mm)	171	119	97	100	δ_{hm}(mm)	233	153	118
	150	107	84	200		191	136	105
	130	95	74	300		166	119	93

Model Group:6

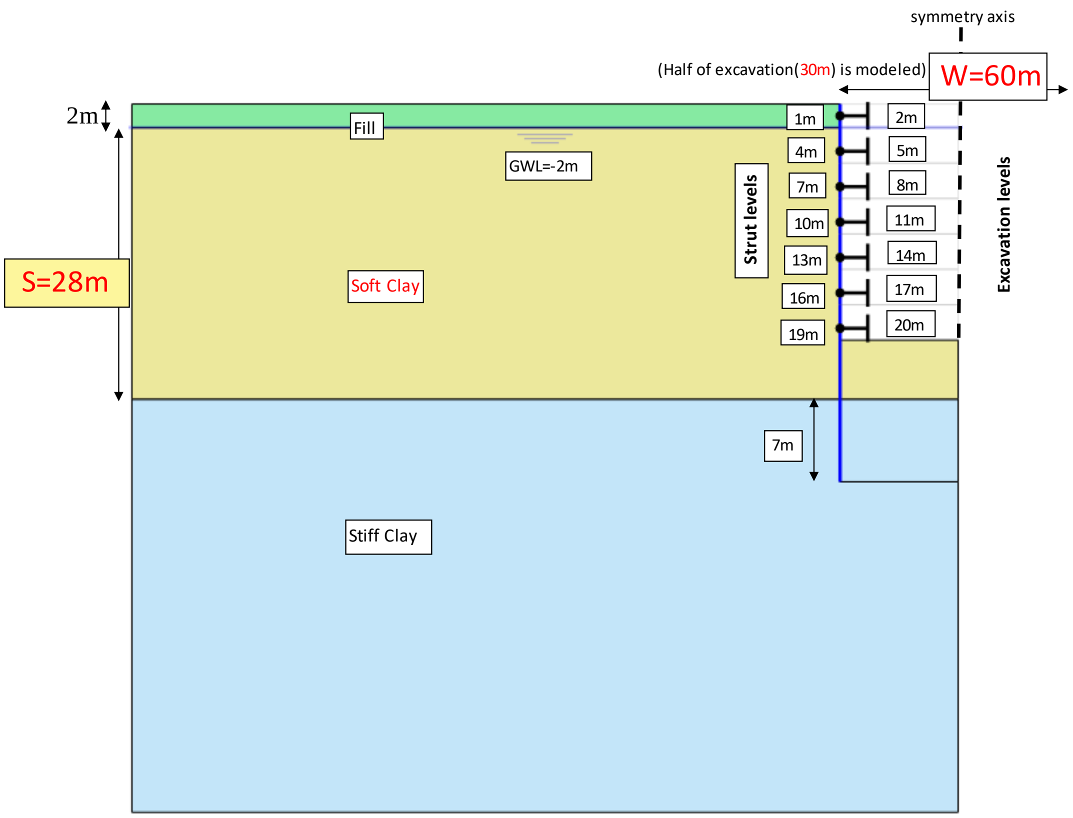

Figure A.6. Model Geometry-6.

Table B. Soil and structure parameters.

Default Soil Parameters		
	Stiff Clay	Fill
	HS	HS
	Undrained(A)	Drained
E_{50}^{ref}	1.00E+05	1.50E+04
E_{oed}^{ref}	1.00E+05	1.50E+04
E_{ur}^{ref}	3.00E+05	4.50E+04
ϕ'	26	30
K_0	0.562	0.5
c'_{ref}	25	1
v'_{ur}	0.2	0.2
p_{ref}	100	100
R_f	0.9	0.9
$\gamma_{unsat/sat}$	20/20	16/20
R_{inter}	0.65	0.65
m	1	1

Range of parameters	
c_u/σ'_v	0.20-0.25-0.30-0.35
E_{50}/c_u	100-200-300
γ	17
S	23-28-33
W	20-40-60
H_e	11-14-17-20
$\ln(EI/\gamma_w h_{avg}^4)$	6.097-7.313-8.176

Diaphragm Wall (E=2,0E+7)		
d	EA	EI
0.6	1.2E+07	3.60E+05
0.9	1.8E+07	1.215E+06
1.2	2.4E+07	2.88E+06

Strut	
EA	3.80E+06
$L_{spacing}$	5m
h_{avg}	3m

Generic Cases: 721 to 756

Table A.21. Model parameters and deformation results (Case No: 721 to 756).

Excavation	Soil(γ=15kN/m^3)		Diaphragm Wall(E=2,0E+7)		
H_e(m)	c_u/σ_v'	E_{50}/c_u	d	EA	EI
11-14-17-20	0.2	100-200-300	0.6	1.2E+07	3.60E+05
			0.9	1.8E+07	1.215E+06
			1.2	2.4E+07	2.88E+06

Soft Soil	E_{50}/c_u		
HSS	100	200	300
E_{50}^{ref}	2895	5789	8685
E_{oed}^{ref}	2895	5789	8685
E_{ur}^{ref}	8685	17367	26055
G_0^{ref}	30759	43418	54281
$\gamma_{0.7}$	3.59E-04	2.54E-04	2.03E-04
ϕ	18	18	18
K_0	0.691	0.691	0.691
E_{dyn}/E_{stat}	8.5	6	5

H=11m	d=0.6	d=0.9	d=1.2	E_{50}/c_u	H=11m	d=0.6	d=0.9	d=1.2
δ_{vm}(mm)	197	119	88	100	δ_{hm}(mm)	239	143	104
	182	110	82	200		220	129	96
	170	103	74	300		203	122	88

H=14m	d=0.6	d=0.9	d=1.2	E_{50}/c_u	H=14m	d=0.6	d=0.9	d=1.2
δ_{vm}(mm)	286	173	128	100	δ_{hm}(mm)	361	208	151
	271	161	119	200		330	194	140
	258	153	110	300		314	184	131

H=17m	d=0.6	d=0.9	d=1.2	E_{50}/c_u	H=17m	d=0.6	d=0.9	d=1.2
δ_{vm}(mm)	393	223	162	100	δ_{hm}(mm)	490	274	191
	375	217	154	200		454	256	180
	356	208	145	300		426	247	171

H=20m	d=0.6	d=0.9	d=1.2	E_{50}/c_u	H=20m	d=0.6	d=0.9	d=1.2
δ_{vm}(mm)	508	270	193	100	δ_{hm}(mm)	610	327	222
	488	265	182	200		571	310	211
	467	256	175	300		546	299	202

Generic Cases: 757 to 792

Table A.22. Model parameters and deformation results (Case No: 757 to 792).

Excavation	Soil (γ=15kN/m^3)		Diaphragm Wall(E=2,0E+7)		
H_e(m)	c_u/σ_v'	E_{50}/c_u	d	EA	EI
11-14-17-20	0.25	100-200-300	0.6	1.2E+07	3.60E+05
			0.9	1.8E+07	1.215E+06
			1.2	2.4E+07	2.88E+06

Soil	E_{50}/c_u		
HSS	100	200	300
E_{50}^{ref}	4000	8000	12000
E_{oed}^{ref}	4000	8000	12000
E_{ur}^{ref}	12000	24000	36000
G_0^{ref}	35000	50000	67500
$\gamma_{0,7}$	3.58E-04	2.51E-04	1.86E-04
ϕ	22	22	22
K_0	0.625	0.625	0.625
E_{dyn}/E_{stat}	7	5	4.5

H=11m	d=0.6	d=0.9	d=1.2	E_{50}/c_u	H=11m	d=0.6	d=0.9	d=1.2
δ_{vm}(mm)	142	89	74	100	δ_{hm}(mm)	178	108	90
	122	80	61	200		150	98	74
	106	72	53	300		130	87	64

H=14m	d=0.6	d=0.9	d=1.2	E_{50}/c_u	H=14m	d=0.6	d=0.9	d=1.2
δ_{vm}(mm)	213	131	105	100	δ_{hm}(mm)	268	158	127
	185	118	90	200		231	147	109
	168	107	80	300		205	133	99

H=17m	d=0.6	d=0.9	d=1.2	E_{50}/c_u	H=17m	d=0.6	d=0.9	d=1.2
δ_{vm}(mm)	288	174	136	100	δ_{hm}(mm)	362	213	164
	253	161	119	200		314	198	145
	228	149	109	300		284	181	133

H=20m	d=0.6	d=0.9	d=1.2	E_{50}/c_u	H=20m	d=0.6	d=0.9	d=1.2
δ_{vm}(mm)	368	212	162	100	δ_{hm}(mm)	458	262	193
	331	202	145	200		398	244	175
	300	189	134	300		364	226	162

Generic Cases: 793 to 828

Table A.23. Model parameters and deformation results (Case No: 793 to 828).

Soil	E_{50}/c_u		
HSS	100	200	300
E_{50}^{ref}	5400	10800	16200
E_{oed}^{ref}	5400	10800	16200
E_{ur}^{ref}	16200	32400	48600
G_0^{ref}	40500	60750	75938
$\gamma_{0,7}$	3.40E-04	2.27E-04	1.81E-04
ϕ	26.4	26.4	26.4
K_0	0.555	0.555	0.555
E_{dyn}/E_{stat}	6	4.5	3.75

Excavation	Soil (γ=15kN/m^3)		Diaphragm Wall(E=2,0E+7)		
H_e(m)	c_u/σ_v'	E_{50}/c_u	d	EA	EI
11-14-17-20	0.3	100-200-300	0.6	1.2E+07	3.60E+05
			0.9	1.8E+07	1.215E+06
			1.2	2.4E+07	2.88E+06

H=11m	d=0.6	d=0.9	d=1.2	E_{50}/c_u	H=11m	d=0.6	d=0.9	d=1.2
δ_{vm}(mm)	100	80	64	100	δ_{hm}(mm)	123	100	79
	84	63	50	200		103	78	63
	73	53	42	300		90	66	53

H=14m	d=0.6	d=0.9	d=1.2	E_{50}/c_u	H=14m	d=0.6	d=0.9	d=1.2
δ_{vm}(mm)	149	110	87	100	δ_{hm}(mm)	190	138	107
	128	91	73	200		160	115	90
	113	79	63	300		142	98	78

H=17m	d=0.6	d=0.9	d=1.2	E_{50}/c_u	H=17m	d=0.6	d=0.9	d=1.2
δ_{vm}(mm)	197	145	113	100	δ_{hm}(mm)	258	182	137
	175	124	96	200		220	152	118
	158	110	86	300		199	136	105

H=20m	d=0.6	d=0.9	d=1.2	E_{50}/c_u	H=20m	d=0.6	d=0.9	d=1.2
δ_{vm}(mm)	254	179	137	100	δ_{hm}(mm)	329	224	164
	225	157	119	200		280	192	145
	208	143	109	300		255	173	132

Generic Cases: 829 to 864

Table A.24. Model parameters and deformation results (Case No: 829 to 864).

Excavation	Soil(γ=15kN/m^3)		Diaphragm Wall(E=2,0E+7)		
H_e(m)	c_u/σ_v'	E_{50}/c_u	d	EA	EI
11-14-17-20	0.35	100-200-300	0.6	1.2E+07	3.60E+05
			0.9	1.8E+07	1.215E+06
			1.2	2.4E+07	2.88E+06

Soil	E_{50}/c_u		
HSS	100	200	300
E_{50}^{ref}	7000	14000	21000
E_{oed}^{ref}	7000	14000	21000
E_{ur}^{ref}	21000	42000	63000
G_0^{ref}	52500	73500	99750
$\gamma_{0,7}$	2.75E-04	1.96E-04	1.45E-04
ϕ	30	30	30
K_0	0.500	0.500	0.500
E_{dyn}/E_{stat}	6	4.2	3.8

H=11m	d=0.6	d=0.9	d=1.2	E_{50}/c_u	H=11m	d=0.6	d=0.9	d=1.2
δ_{vm}(mm)	87	67	60	100	δ_{hm}(mm)	106	84	72
	67	53	45	200		84	66	57
	54	42	37	300		68	53	45

H=14m	d=0.6	d=0.9	d=1.2	E_{50}/c_u	H=14m	d=0.6	d=0.9	d=1.2
δ_{vm}(mm)	124	92	79	100	δ_{hm}(mm)	156	115	97
	101	75	63	200		128	94	77
	85	64	53	300		105	80	65

H=17m	d=0.6	d=0.9	d=1.2	E_{50}/c_u	H=17m	d=0.6	d=0.9	d=1.2
δ_{vm}(mm)	164	121	101	100	δ_{hm}(mm)	213	151	122
	138	100	83	200		175	125	103
	120	88	72	300		149	109	89

H=20m	d=0.6	d=0.9	d=1.2	E_{50}/c_u	H=20m	d=0.6	d=0.9	d=1.2
δ_{vm}(mm)	209	151	119	100	δ_{hm}(mm)	269	187	145
	179	129	103	200		224	160	127
	158	116	93	300		194	142	114

Model Group:7

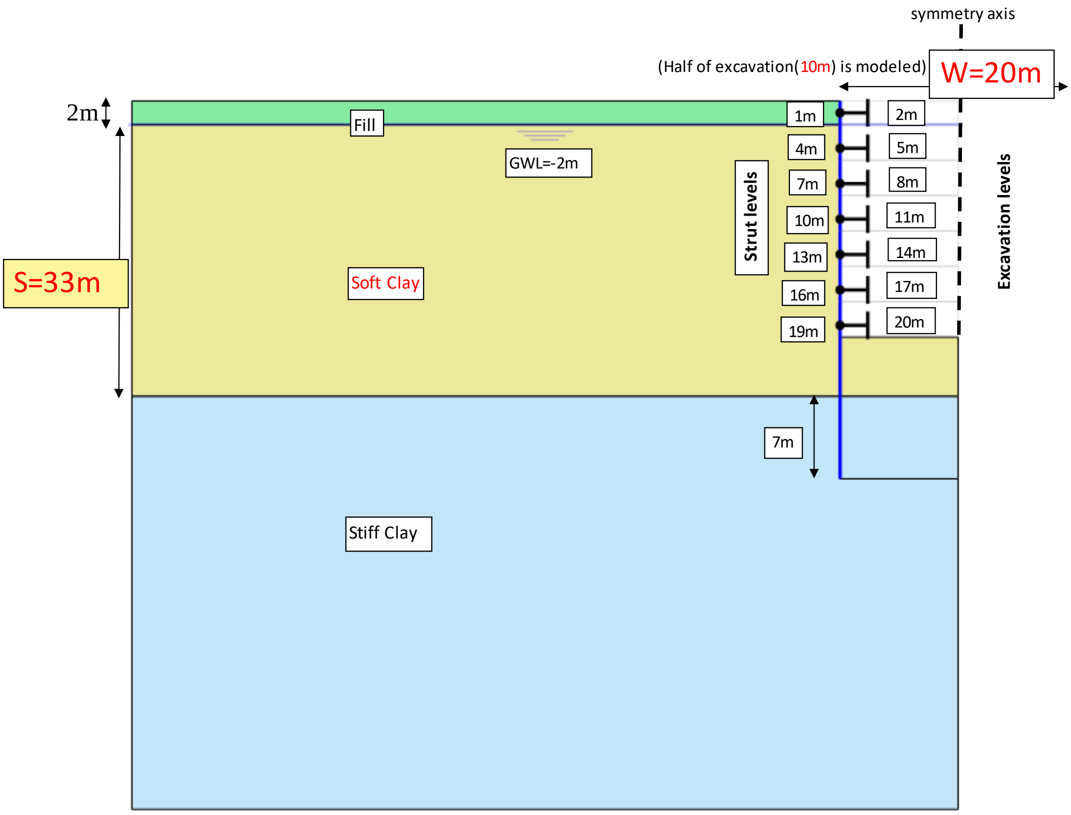

Figure A.7. Model Geometry-7.

Table B. Soil and structure parameters.

Default Soil Parameters		
	Stiff Clay	Fill
	HS	HS
	Undrained(A)	Drained
E_{50}^{ref}	1.00E+05	1.50E+04
E_{oed}^{ref}	1.00E+05	1.50E+04
E_{ur}^{ref}	3.00E+05	4.50E+04
ϕ'	26	30
K_0	0.562	0.5
c'_{ref}	25	1
v'_{ur}	0.2	0.2
p_{ref}	100	100
R_f	0.9	0.9
$\gamma_{unsat/sat}$	20/20	16/20
R_{inter}	0.65	0.65
m	1	1

Range of parameters	
c_u/σ'_v	0,20-0,25-0,30-0,35
E_{50}/c_u	100-200-300
γ	17
S	23-28-33
W	20-40-60
H_e	11-14-17-20
$\ln(EI/\gamma_w h_{avg}^4)$	6,097-7,313-8,176

Diaphragm Wall (E=2,0E+7)		
d	EA	EI
0.6	1.2E+07	3.60E+05
0.9	1.8E+07	1.215E+06
1.2	2.4E+07	2.88E+06

Strut	
EA	3.80E+06
$L_{spacing}$	5m
h_{avg}	3m

Generic Cases: 865 to 900

Table A.25. Model parameters and deformation results (Case No: 865 to 900).

Excavation	Soil(γ=15kN/m^3)		Diaphragm Wall(E=2.0E+7)		
H_e(m)	c_u/σ'_v	E_{50}/c_u	d	EA	EI
11-14-17-20	0.2	100-200-300	0.6	1.2E+07	3.60E+05
			0.9	1.8E+07	1.215E+06
			1.2	2.4E+07	2.88E+06

Soft Soil	E_{50}/c_u		
HSS	100	200	300
E_{50}^{ref}	2895	5789	8685
E_{oed}^{ref}	2895	5789	8685
E_{ur}^{ref}	8685	17367	26055
G_0^{ref}	30759	43418	54281
$\gamma_{0,7}$	3.59E-04	2.54E-04	2.03E-04
ϕ	18	18	18
K_0	0.691	0.691	0.691
E_{dyn}/E_{stat}	8.5	6	5

H=11m	d=0.6	d=0.9	d=1.2	E_{50}/c_u	H=11m	d=0.6	d=0.9	d=1.2
δ_{vm}(mm)	156	87	63	100	δ_{hm}(mm)	197	112	77
	137	80	54	200		167	100	68
	125	73	50	300		154	92	64

H=14m	d=0.6	d=0.9	d=1.2	E_{50}/c_u	H=14m	d=0.6	d=0.9	d=1.2
δ_{vm}(mm)	257	135	93	100	δ_{hm}(mm)	335	174	119
	235	127	83	200		298	161	105
	220	116	79	300		283	150	99

H=17m	d=0.6	d=0.9	d=1.2	E_{50}/c_u	H=17m	d=0.6	d=0.9	d=1.2
δ_{vm}(mm)	367	195	128	100	δ_{hm}(mm)	479	256	163
	337	184	118	200		438	231	151
	324	170	114	300		420	214	142

H=20m	d=0.6	d=0.9	d=1.2	E_{50}/c_u	H=20m	d=0.6	d=0.9	d=1.2
δ_{vm}(mm)	507	255	162	100	δ_{hm}(mm)	653	329	207
	466	245	152	200		596	305	193
	454	232	147	300		576	287	183

Generic Cases: 901 to 936

Table A.26. Model parameters and deformation results (Case No: 901 to 936).

Excavation	Soil(γ=15kN/m^3)		Diaphragm Wall(E=2.0E+7)		
H_e(m)	c_u/σ_v'	E_{50}/c_u	d	EA	EI
11-14-17-20	0.25	100-200-300	0.6	1.2E+07	3.60E+05
			0.9	1.8E+07	1.215E+06
			1.2	2.4E+07	2.88E+06

Soil	E_{50}/c_u		
HSS	100	200	300
E_{50}^{ref}	4000	8000	12000
E_{oed}^{ref}	4000	8000	12000
E_{ur}^{ref}	12000	24000	36000
G_0^{ref}	35000	50000	67500
$\gamma_{0,7}$	3.58E-04	2.51E-04	1.86E-04
ϕ	22	22	22
K_0	0.625	0.625	0.625
E_{dyn}/E_{stat}	7	5	4.5

H=11m	d=0.6	d=0.9	d=1.2	E_{50}/c_u	H=11m	d=0.6	d=0.9	d=1.2
δ_{vm}(mm)	97	64	46	100	δ_{hm}(mm)	125	80	57
	82	52	39	200		105	65	49
	70	46	34	300		91	59	44

H=14m	d=0.6	d=0.9	d=1.2	E_{50}/c_u	H=14m	d=0.6	d=0.9	d=1.2
δ_{vm}(mm)	165	99	71	100	δ_{hm}(mm)	224	129	88
	143	85	61	200		184	109	78
	125	77	54	300		162	98	70

H=17m	d=0.6	d=0.9	d=1.2	E_{50}/c_u	H=17m	d=0.6	d=0.9	d=1.2
δ_{vm}(mm)	241	138	96	100	δ_{hm}(mm)	327	182	123
	210	120	86	200		278	159	112
	190	109	78	300		249	142	101

H=20m	d=0.6	d=0.9	d=1.2	E_{50}/c_u	H=20m	d=0.6	d=0.9	d=1.2
δ_{vm}(mm)	317	181	122	100	δ_{hm}(mm)	433	243	161
	280	162	113	200		368	211	149
	254	149	103	300		339	190	133

Generic Cases: 937 to 972

Table A.27. Model parameters and deformation results (Case No: 937 to 972).

Excavation	Soil(γ=15kN/m^3)		Diaphragm Wall(E=2.0E+7)		
H_e(m)	c_u/σ_v'	E_{50}/c_u	d	EA	EI
11-14-17-20	0.3	100-200-300	0.6	1.2E+07	3.60E+05
			0.9	1.8E+07	1.215E+06
			1.2	2.4E+07	2.88E+06

Soil	E_{50}/c_u		
HSS	100	200	300
E_{50}^{ref}	5400	10800	16200
E_{oed}^{ref}	5400	10800	16200
E_{ur}^{ref}	16200	32400	48600
G_0^{ref}	40500	60750	75938
$\gamma_{0,7}$	3.40E-04	2.27E-04	1.81E-04
ϕ	26.4	26.4	26.4
K_0	0.555	0.555	0.555
E_{dyn}/E_{stat}	6	4.5	3.75

H=11m	d=0.6	d=0.9	d=1.2	E_{50}/c_u	H=11m	d=0.6	d=0.9	d=1.2
δ_{vm}(mm)	66	46	37	100	δ_{hm}(mm)	84	57	46
	52	37	29	200		66	47	36
	45	31	25	300		59	40	32

H=14m	d=0.6	d=0.9	d=1.2	E_{50}/c_u	H=14m	d=0.6	d=0.9	d=1.2
δ_{vm}(mm)	107	71	53	100	δ_{hm}(mm)	141	91	68
	87	59	44	200		113	77	57
	76	50	39	300		100	66	50

H=17m	d=0.6	d=0.9	d=1.2	E_{50}/c_u	H=17m	d=0.6	d=0.9	d=1.2
δ_{vm}(mm)	158	97	73	100	δ_{hm}(mm)	213	131	95
	129	83	62	200		171	111	80
	115	73	55	300		153	97	72

H=20m	d=0.6	d=0.9	d=1.2	E_{50}/c_u	H=20m	d=0.6	d=0.9	d=1.2
δ_{vm}(mm)	205	129	93	100	δ_{hm}(mm)	284	175	123
	174	111	81	200		234	149	106
	158	99	75	300		209	130	97

Generic Cases: 973 to 1008

Table A.28. Model parameters and deformation results (Case No: 973 to 1008).

Excavation	Soil(γ=15kN/m^3)		Diaphragm Wall(E=2.0E+7)		
H_e(m)	c_u/σ_v'	E_{50}/c_u	d	EA	EI
11-14-17-20	0.35	100-200-300	0.6	1.2E+07	3.60E+05
			0.9	1.8E+07	1.215E+06
			1.2	2.4E+07	2.88E+06

Soil	E_{50}/c_u		
HSS	100	200	300
E_{50}^{ref}	7000	14000	21000
E_{oed}^{ref}	7000	14000	21000
E_{ur}^{ref}	21000	42000	63000
G_0^{ref}	52500	73500	99750
$\gamma_{0.7}$	2.75E-04	1.96E-04	1.45E-04
ϕ	30	30	30
K_0	0.500	0.500	0.500
E_{dyn}/E_{stat}	6	4.2	3.8

H=11m	d=0.6	d=0.9	d=1.2	E_{50}/c_u	H=11m	d=0.6	d=0.9	d=1.2
δ_{vm}(mm)	51	36	27	100	δ_{hm}(mm)	63	45	33
	41	29	23	200		52	38	29
	33	24	19	300		43	32	25

H=14m	d=0.6	d=0.9	d=1.2	E_{50}/c_u	H=14m	d=0.6	d=0.9	d=1.2
δ_{vm}(mm)	78	56	40	100	δ_{hm}(mm)	105	70	50
	63	46	35	200		85	58	45
	53	38	30	300		71	50	38

H=17m	d=0.6	d=0.9	d=1.2	E_{50}/c_u	H=17m	d=0.6	d=0.9	d=1.2
δ_{vm}(mm)	113	75	54	100	δ_{hm}(mm)	157	100	71
	94	65	48	200		128	85	63
	80	56	42	300		108	74	55

H=20m	d=0.6	d=0.9	d=1.2	E_{50}/c_u	H=20m	d=0.6	d=0.9	d=1.2
δ_{vm}(mm)	149	95	70	100	δ_{hm}(mm)	211	134	95
	126	85	64	200		173	115	85
	109	75	57	300		148	102	76

Model Group:8

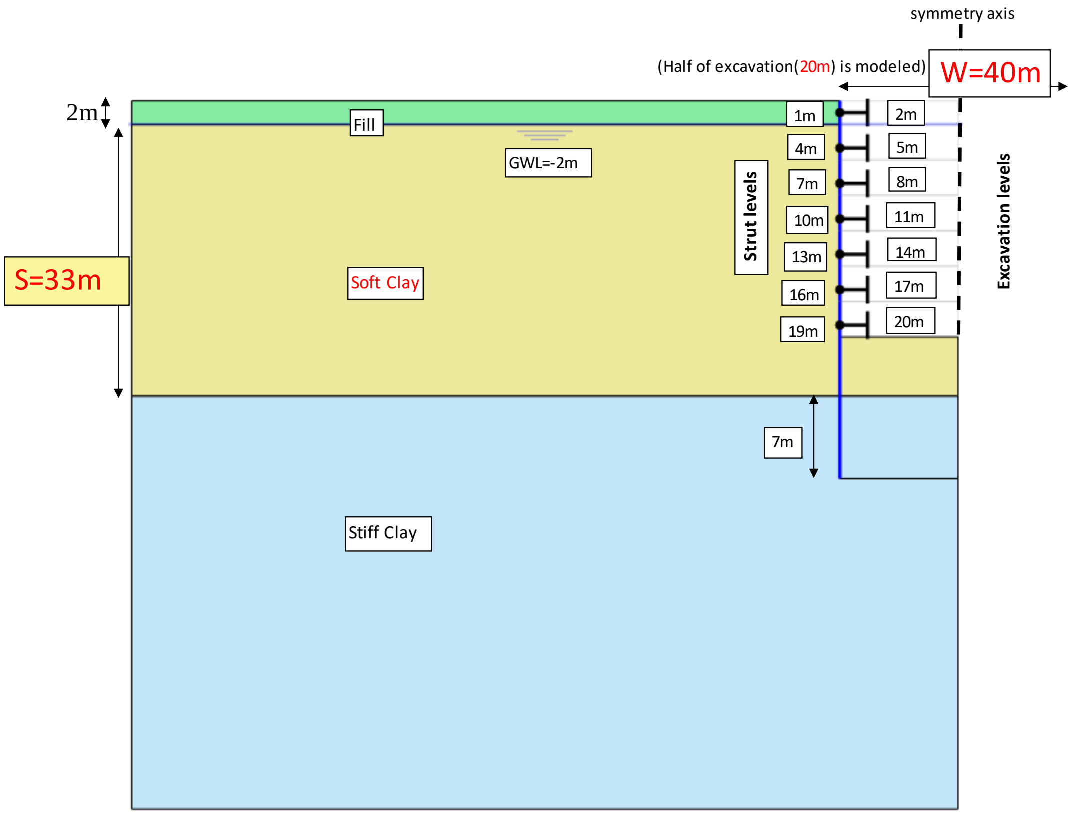

Figure A.8. Model Geometry-8.

Table B. Soil and structure parameters.

Default Soil Parameters		
	Stiff Clay	Fill
	HS	HS
	Undrained(A)	Drained
E_{50}^{ref}	1.00E+05	1.50E+04
E_{oed}^{ref}	1.00E+05	1.50E+04
E_{ur}^{ref}	3.00E+05	4.50E+04
ϕ'	26	30
K_0	0.562	0.5
c'_{ref}	25	1
v'_{ur}	0.2	0.2
p_{ref}	100	100
R_f	0.9	0.9
$\gamma_{unsat/sat}$	20/20	16/20
R_{inter}	0.65	0.65
m	1	1

Range of parameters	
c_u/σ'_v	0,20-0,25-0,30-0,35
E_{50}/c_u	100-200-300
γ	17
S	23-28-33
W	20-40-60
H_e	11-14-17-20
$\ln(EI/\gamma_w h_{avg}^4)$	6,097-7,313-8,176

Diaphragm Wall (E=2,0E+7)		
d	EA	EI
0.6	1.2E+07	3.60E+05
0.9	1.8E+07	1.215E+06
1.2	2.4E+07	2.88E+06

Strut	
EA	3.80E+06
$L_{spacing}$	5m
h_{avg}	3m

Generic Cases: 1009 to 1044

Table A.29. Model parameters and deformation results (Case No: 1009 to 1044).

Excavation	Soil(γ=15kN/m^3)		Diaphragm Wall(E=2.0E+7)		
H_e(m)	c_u/σ_v'	E_{50}/c_u	d	EA	EI
11-14-17-20	0.2	100-200-300	0.6	1.2E+07	3.60E+05
			0.9	1.8E+07	1.215E+06
			1.2	2.4E+07	2.88E+06

Soft Soil	E_{50}/c_u		
HSS	100	200	300
E_{50}^{ref}	2895	5789	8685
E_{oed}^{ref}	2895	5789	8685
E_{ur}^{ref}	8685	17367	26055
G_0^{ref}	30759	43418	54281
$\gamma_{0.7}$	3.59E-04	2.54E-04	2.03E-04
ϕ	18	18	18
K_0	0.691	0.691	0.691
E_{dyn}/E_{stat}	8.5	6	5

H=11m	d=0.6	d=0.9	d=1.2	E_{50}/c_u	H=11m	d=0.6	d=0.9	d=1.2
δ_{vm}(mm)	200	120	78	100	δ_{hm}(mm)	248	143	96
	158	88	64	200		194	106	79
	141	85	58	300		176	103	73

H=14m	d=0.6	d=0.9	d=1.2	E_{50}/c_u	H=14m	d=0.6	d=0.9	d=1.2
δ_{vm}(mm)	320	183	122	100	δ_{hm}(mm)	415	225	150
	264	138	97	200		333	172	122
	244	134	90	300		312	164	113

H=17m	d=0.6	d=0.9	d=1.2	E_{50}/c_u	H=17m	d=0.6	d=0.9	d=1.2
δ_{vm}(mm)	455	255	168	100	δ_{hm}(mm)	593	324	205
	376	198	134	200		478	248	168
	348	191	127	300		452	237	157

H=20m	d=0.6	d=0.9	d=1.2	E_{50}/c_u	H=20m	d=0.6	d=0.9	d=1.2
δ_{vm}(mm)	630	326	208	100	δ_{hm}(mm)	800	417	255
	514	256	167	200		645	321	210
	483	250	159	300		610	309	197

Generic Cases: 1045 to 1080

Table A.30. Model parameters and deformation results (Case No: 1045 to 1080).

Excavation	Soil(γ=15kN/m^3)		Diaphragm Wall(E=2.0E+7)		
H_e(m)	c_u/σ_v'	E_{50}/c_u	d	EA	EI
11-14-17-20	0.25	100-200-300	0.6	1.2E+07	3.60E+05
			0.9	1.8E+07	1.215E+06
			1.2	2.4E+07	2.88E+06

Soil	E_{50}/c_u		
HSS	100	200	300
E_{50}^{ref}	4000	8000	12000
E_{oed}^{ref}	4000	8000	12000
E_{ur}^{ref}	12000	24000	36000
G_0^{ref}	35000	50000	67500
$\gamma_{0,7}$	3.58E-04	2.51E-04	1.86E-04
ϕ	22	22	22
K_0	0.625	0.625	0.625
E_{dyn}/E_{stat}	7	5	4.5

H=11m	d=0.6	d=0.9	d=1.2	E_{50}/c_u	H=11m	d=0.6	d=0.9	d=1.2
δ_{vm}(mm)	109	72	53	100	δ_{hm}(mm)	143	89	65
	93	63	47	200		117	78	59
	80	54	41	300		102	68	51

H=14m	d=0.6	d=0.9	d=1.2	E_{50}/c_u	H=14m	d=0.6	d=0.9	d=1.2
δ_{vm}(mm)	185	110	79	100	δ_{hm}(mm)	247	140	98
	159	97	73	200		205	125	91
	140	87	63	300		181	112	81

H=17m	d=0.6	d=0.9	d=1.2	E_{50}/c_u	H=17m	d=0.6	d=0.9	d=1.2
δ_{vm}(mm)	260	150	107	100	δ_{hm}(mm)	354	199	136
	230	137	100	200		303	177	126
	206	123	89	300		269	157	114

H=20m	d=0.6	d=0.9	d=1.2	E_{50}/c_u	H=20m	d=0.6	d=0.9	d=1.2
δ_{vm}(mm)	345	196	135	100	δ_{hm}(mm)	466	262	174
	304	179	127	200		398	232	162
	274	163	115	300		361	209	146

Generic Cases: 1081 to 1116

Table A.31. Model parameters and deformation results (Case No: 1081 to 1116).

Excavation	Soil(γ=15kN/m^3)		Diaphragm Wall(E=2.0E+7)		
H_e(m)	c_u/σ_v'	E_{50}/c_u	d	EA	EI
11-14-17-20	0.3	100-200-300	0.6	1.2E+07	3.60E+05
			0.9	1.8E+07	1.215E+06
			1.2	2.4E+07	2.88E+06

Soil	E_{50}/c_u		
HSS	100	200	300
E_{50}^{ref}	5400	10800	16200
E_{oed}^{ref}	5400	10800	16200
E_{ur}^{ref}	16200	32400	48600
G_0^{ref}	40500	60750	75938
$\gamma_{0,7}$	3.40E-04	2.27E-04	1.81E-04
ϕ	26.4	26.4	26.4
K_0	0.555	0.555	0.555
E_{dyn}/E_{stat}	6	4.5	3.75

H=11m	d=0.6	d=0.9	d=1.2	E_{50}/c_u	H=11m	d=0.6	d=0.9	d=1.2
δ_{vm}(mm)	72	53	42	100	δ_{hm}(mm)	92	66	53
	60	45	35	200		76	57	45
	52	38	30	300		67	48	39

H=14m	d=0.6	d=0.9	d=1.2	E_{50}/c_u	H=14m	d=0.6	d=0.9	d=1.2
δ_{vm}(mm)	118	80	61	100	δ_{hm}(mm)	155	102	76
	99	69	53	200		128	88	68
	87	59	47	300		113	77	60

H=17m	d=0.6	d=0.9	d=1.2	E_{50}/c_u	H=17m	d=0.6	d=0.9	d=1.2
δ_{vm}(mm)	169	108	83	100	δ_{hm}(mm)	233	144	105
	143	96	72	200		190	126	93
	128	85	65	300		168	111	83

H=20m	d=0.6	d=0.9	d=1.2	E_{50}/c_u	H=20m	d=0.6	d=0.9	d=1.2
δ_{vm}(mm)	223	141	104	100	δ_{hm}(mm)	309	192	135
	191	127	94	200		254	165	122
	172	113	85	300		227	147	111

Generic Cases: 1117 to 1152

Table A.32. Model parameters and deformation results (Case No: 1117 to 1152).

Excavation	Soil(γ=15kN/m^3)		Diaphragm Wall(E=2.0E+7)		
H_e(m)	c_u/σ_v'	E_{50}/c_u	d	EA	EI
11-14-17-20	0.35	100-200-300	0.6	1.2E+07	3.60E+05
			0.9	1.8E+07	1.215E+06
			1.2	2.4E+07	2.88E+06

Soil	E_{50}/c_u		
HSS	100	200	300
E_{50}^{ref}	7000	14000	21000
E_{oed}^{ref}	7000	14000	21000
E_{ur}^{ref}	21000	42000	63000
G_0^{ref}	52500	73500	99750
$\gamma_{0,7}$	2.75E-04	1.96E-04	1.45E-04
ϕ	30	30	30
K_0	0.500	0.500	0.500
E_{dyn}/E_{stat}	6	4.2	3.8

H=11m	d=0.6	d=0.9	d=1.2	E_{50}/c_u	H=11m	d=0.6	d=0.9	d=1.2
δ_{vm}(mm)	55	46	43	100	δ_{hm}(mm)	70	57	53
	48	37	32	200		60	49	42
	39	30	25	300		50	38	32

H=14m	d=0.6	d=0.9	d=1.2	E_{50}/c_u	H=14m	d=0.6	d=0.9	d=1.2
δ_{vm}(mm)	85	64	57	100	δ_{hm}(mm)	115	82	70
	76	55	45	200		96	71	58
	62	46	37	300		80	59	47

H=17m	d=0.6	d=0.9	d=1.2	E_{50}/c_u	H=17m	d=0.6	d=0.9	d=1.2
δ_{vm}(mm)	123	88	74	100	δ_{hm}(mm)	170	116	92
	106	76	61	200		140	100	78
	90	64	51	300		118	84	66

H=20m	d=0.6	d=0.9	d=1.2	E_{50}/c_u	H=20m	d=0.6	d=0.9	d=1.2
δ_{vm}(mm)	162	114	94	100	δ_{hm}(mm)	229	153	118
	141	99	79	200		188	132	101
	122	86	67	300		160	112	88

Model Group:9

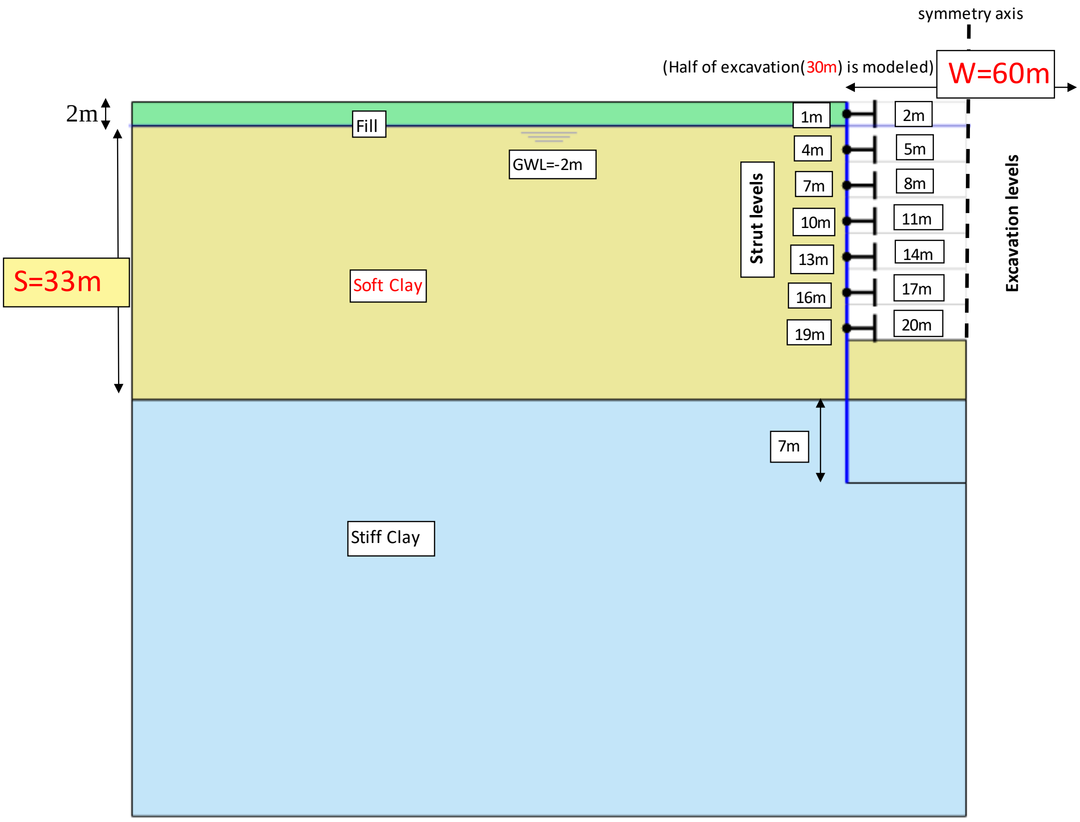

Figure A.9. Model Geometry-9.

Table B. Soil and structure parameters.

Default Soil Parameters		
	Stiff Clay	Fill
	HS	HS
	Undrained(A)	Drained
E_{50}^{ref}	1.00E+05	1.50E+04
E_{oed}^{ref}	1.00E+05	1.50E+04
E_{ur}^{ref}	3.00E+05	4.50E+04
ϕ'	26	30
K_0	0.562	0.5
c'_{ref}	25	1
v'_{ur}	0.2	0.2
p_{ref}	100	100
R_f	0.9	0.9
$\gamma_{unsat/sat}$	20/20	16/20
R_{inter}	0.65	0.65
m	1	1

Range of parameters	
c_u/σ_v'	0,20-0,25-0,30-0,35
E_{50}/c_u	100-200-300
γ	17
S	23-28-33
W	20-40-60
H_e	11-14-17-20
$\ln(EI/\gamma_w h_{avg}^4)$	6,097-7,313-8,176

Diaphragm Wall (E=2,0E+7)		
d	EA	EI
0.6	1.2E+07	3.60E+05
0.9	1.8E+07	1.215E+06
1.2	2.4E+07	2.88E+06

Strut	
EA	3.80E+06
$L_{spacing}$	5m
h_{avg}	3m

Generic Cases: 1153 to 1188

Table A.33. Model parameters and deformation results (Case No: 1153 to 1188).

Excavation	Soil(γ=15kN/m^3)		Diaphragm Wall(E=2.0E+7)		
H_e(m)	c_u/σ_v'	E_{50}/c_u	d	EA	EI
11-14-17-20	0.2	100-200-300	0.6	1.2E+07	3.60E+05
			0.9	1.8E+07	1.215E+06
			1.2	2.4E+07	2.88E+06

Soft Soil	E_{50}/c_u		
HSS	100	200	300
E_{50}^{ref}	2895	5789	8685
E_{oed}^{ref}	2895	5789	8685
E_{ur}^{ref}	8685	17367	26055
G_0^{ref}	30759	43418	54281
$\gamma_{0,7}$	3.59E-04	2.54E-04	2.03E-04
ϕ	18	18	18
K_0	0.691	0.691	0.691
E_{dyn}/E_{stat}	8.5	6	5

H=11m	d=0.6	d=0.9	d=1.2	E_{50}/c_u	H=11m	d=0.6	d=0.9	d=1.2
δ_{vm}(mm)	224	139	102	100	δ_{hm}(mm)	271	170	123
	202	125	90	200		240	152	107
	183	115	83	300		221	140	103

H=14m	d=0.6	d=0.9	d=1.2	E_{50}/c_u	H=14m	d=0.6	d=0.9	d=1.2
δ_{vm}(mm)	355	213	155	100	δ_{hm}(mm)	455	262	186
	333	193	140	200		411	237	169
	312	182	130	300		379	224	158

H=17m	d=0.6	d=0.9	d=1.2	E_{50}/c_u	H=17m	d=0.6	d=0.9	d=1.2
δ_{vm}(mm)	518	300	206	100	δ_{hm}(mm)	657	369	254
	476	277	193	200		595	336	233
	449	262	184	300		559	316	221

H=20m	d=0.6	d=0.9	d=1.2	E_{50}/c_u	H=20m	d=0.6	d=0.9	d=1.2
δ_{vm}(mm)	716	381	253	100	δ_{hm}(mm)	886	471	308
	672	365	242	200		819	437	293
	638	349	233	300		778	415	275

Generic Cases: 1189 to 1224

Table A.34. Model parameters and deformation results (Case No: 1189 to 1224).

Excavation	Soil(γ=15kN/m^3)		Diaphragm Wall(E=2.0E+7)		
H_e(m)	c_u/σ_v'	E_{50}/c_u	d	EA	EI
11-14-17-20	0.25	100-200-300	0.6	1.2E+07	3.60E+05
			0.9	1.8E+07	1.215E+06
			1.2	2.4E+07	2.88E+06

Soil	E_{50}/c_u		
HSS	100	200	300
E_{50}^{ref}	4000	8000	12000
E_{oed}^{ref}	4000	8000	12000
E_{ur}^{ref}	12000	24000	36000
G_0^{ref}	35000	50000	67500
$\gamma_{0,7}$	3.58E-04	2.51E-04	1.86E-04
ϕ	22	22	22
K_0	0.625	0.625	0.625
E_{dyn}/E_{stat}	7	5	4.5

H=11m	d=0.6	d=0.9	d=1.2	E_{50}/c_u	H=11m	d=0.6	d=0.9	d=1.2
δ_{vm}(mm)	152	96	70	100	δ_{hm}(mm)	188	116	86
	126	87	66	200		159	109	81
	110	77	57	300		134	95	71

H=14m	d=0.6	d=0.9	d=1.2	E_{50}/c_u	H=14m	d=0.6	d=0.9	d=1.2
δ_{vm}(mm)	247	148	108	100	δ_{hm}(mm)	310	185	132
	212	137	103	200		263	167	126
	189	122	91	300		231	151	113

H=17m	d=0.6	d=0.9	d=1.2	E_{50}/c_u	H=17m	d=0.6	d=0.9	d=1.2
δ_{vm}(mm)	351	206	150	100	δ_{hm}(mm)	441	261	183
	304	192	142	200		384	238	176
	275	174	130	300		350	214	160

H=20m	d=0.6	d=0.9	d=1.2	E_{50}/c_u	H=20m	d=0.6	d=0.9	d=1.2
δ_{vm}(mm)	469	266	190	100	δ_{hm}(mm)	592	342	235
	410	254	182	200		511	312	222
	370	235	169	300		473	287	207

Generic Cases: 1225 to 1260

Table A.35. Model parameters and deformation results (Case No: 1225 to 1260).

Excavation	Soil(γ=15kN/m^3)		Diaphragm Wall(E=2.0E+7)		
H_e(m)	c_u/σ_v'	E_{50}/c_u	d	EA	EI
11-14-17-20	0.3	100-200-300	0.6	1.2E+07	3.60E+05
			0.9	1.8E+07	1.215E+06
			1.2	2.4E+07	2.88E+06

Soil	E_{50}/c_u		
HSS	100	200	300
E_{50}^{ref}	5400	10800	16200
E_{oed}^{ref}	5400	10800	16200
E_{ur}^{ref}	16200	32400	48600
G_0^{ref}	40500	60750	75938
$\gamma_{0,7}$	3.40E-04	2.27E-04	1.81E-04
ϕ	26.4	26.4	26.4
K_0	0.555	0.555	0.555
E_{dyn}/E_{stat}	6	4.5	3.75

H=11m	d=0.6	d=0.9	d=1.2	E_{50}/c_u	H=11m	d=0.6	d=0.9	d=1.2
δ_{vm}(mm)	102	83	67	100	δ_{hm}(mm)	125	104	84
	81	63	53	200		100	78	66
	73	54	43	300		90	66	53

H=14m	d=0.6	d=0.9	d=1.2	E_{50}/c_u	H=14m	d=0.6	d=0.9	d=1.2
δ_{vm}(mm)	161	120	93	100	δ_{hm}(mm)	204	155	116
	133	98	78	200		166	121	97
	122	86	67	300		151	107	83

H=17m	d=0.6	d=0.9	d=1.2	E_{50}/c_u	H=17m	d=0.6	d=0.9	d=1.2
δ_{vm}(mm)	228	163	127	100	δ_{hm}(mm)	297	210	157
	196	136	107	200		247	170	133
	180	121	95	300		224	153	118

H=20m	d=0.6	d=0.9	d=1.2	E_{50}/c_u	H=20m	d=0.6	d=0.9	d=1.2
δ_{vm}(mm)	299	215	162	100	δ_{hm}(mm)	396	274	200
	262	181	139	200		333	226	174
	239	164	127	300		304	203	156

Generic Cases: 1261 to 1296

Table A.36. Model parameters and deformation results (Case No: 1261 to 1296).

Excavation	Soil(γ=15kN/m^3)		Diaphragm Wall(E=2.0E+7)		
H_e(m)	c_u/σ'_v	E_{50}/c_u	d	EA	EI
11-14-17-20	0.35	100-200-300	0.6	1.2E+07	3.60E+05
			0.9	1.8E+07	1.215E+06
			1.2	2.4E+07	2.88E+06

Soil	E_{50}/c_u		
HSS	100	200	300
E_{50}^{ref}	7000	14000	21000
E_{oed}^{ref}	7000	14000	21000
E_{ur}^{ref}	21000	42000	63000
G_0^{ref}	52500	73500	99750
$\gamma_{0.7}$	2.75E-04	1.96E-04	1.45E-04
ϕ	30	30	30
K_0	0.500	0.500	0.500
E_{dyn}/E_{stat}	6	4.2	3.8

H=11m	d=0.6	d=0.9	d=1.2	E_{50}/c_u	H=11m	d=0.6	d=0.9	d=1.2
δ_{vm}(mm)	88	64	62	100	δ_{hm}(mm)	108	80	76
	67	53	47	200		85	67	58
	54	43	37	300		69	54	46

H=14m	d=0.6	d=0.9	d=1.2	E_{50}/c_u	H=14m	d=0.6	d=0.9	d=1.2
δ_{vm}(mm)	132	94	84	100	δ_{hm}(mm)	164	118	104
	105	79	66	200		132	99	82
	87	67	55	300		109	84	68

H=17m	d=0.6	d=0.9	d=1.2	E_{50}/c_u	H=17m	d=0.6	d=0.9	d=1.2
δ_{vm}(mm)	184	126	110	100	δ_{hm}(mm)	236	161	137
	150	109	89	200		190	138	111
	130	95	77	300		161	119	96

H=20m	d=0.6	d=0.9	d=1.2	E_{50}/c_u	H=20m	d=0.6	d=0.9	d=1.2
δ_{vm}(mm)	238	164	139	100	δ_{hm}(mm)	313	213	174
	199	144	116	200		252	182	145
	178	128	103	300		220	159	128

Model Group:10

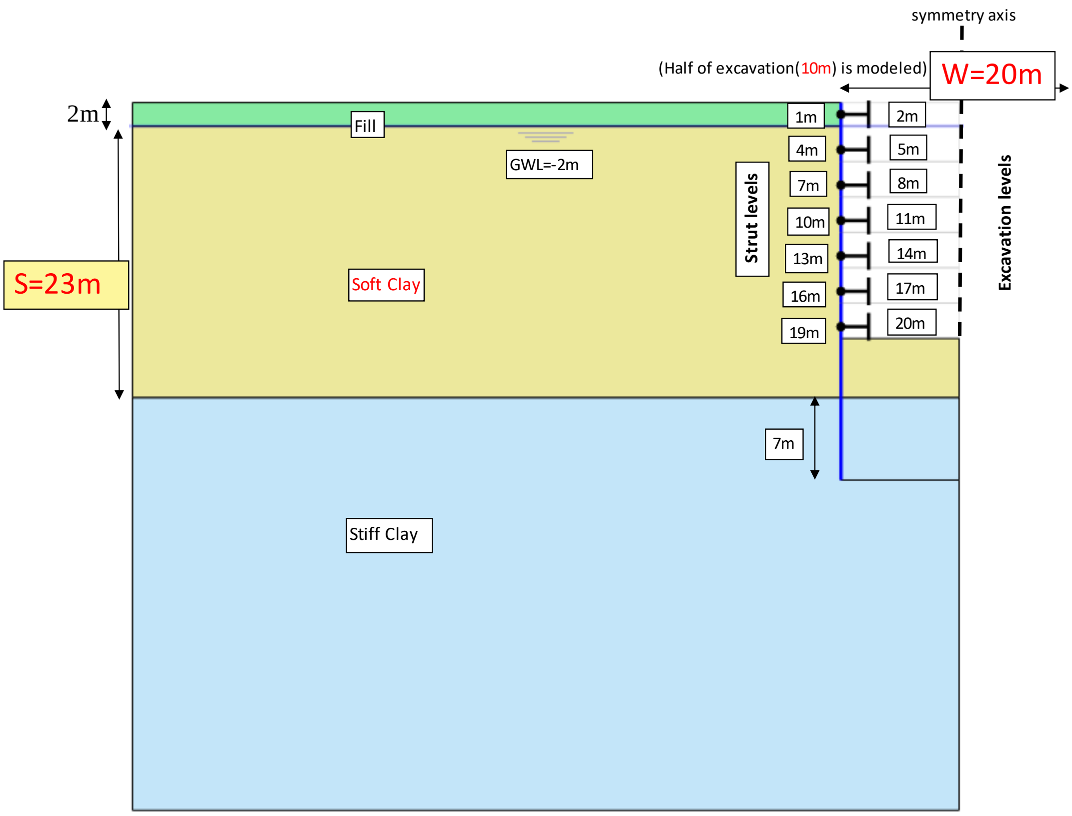

Figure A.10. Model Geometry-10.

Table B. Soil and structure parameters.

Default Soil Parameters		
	Stiff Clay	Fill
	HS	HS
	Undrained(A)	Drained
E_{50}^{ref}	1.00E+05	1.50E+04
E_{oed}^{ref}	1.00E+05	1.50E+04
E_{ur}^{ref}	3.00E+05	3.00E+04
ϕ'	26	30
K_0	0.562	0.5
c'_{ref}	25	1
v'_{ur}	0.2	0.2
p_{ref}	100	100
R_f	0.9	0.9
$\gamma_{unsat/sat}$	20/20	16/20
R_{inter}	0.65	0.65
m	1	1

Range of parameters	
c_u/σ'_v	0.20-0.25-0.30-0.35
E_{50}/c_u	100-200-300
γ	15-17-19
S	23-28-33
W	20-40-60
H_e	11-14-17-20
$\ln(EI/\gamma_w h_{avg}^4)$	6.097-7.313-8.176

Diaphragm Wall (E=2.0E+7)		
d	EA	EI
0.6	1.2E+07	3.60E+05
0.9	1.8E+07	1.215E+06
1.2	2.4E+07	2.88E+06

Strut	
EA	3.80E+06
$L_{spacing}$	5m
h_{avg}	3m

Generic Cases: 1297 to 1332

Table A.37. Model parameters and deformation results (Case No: 1297 to 1332).

Excavation	Soil(γ=17kN/m^3)		Diaphragm Wall(E=2.0E+7)		
H_e(m)	c_u/σ_v'	E_{50}/c_u	d	EA	EI
11-14-17-20	0.2	100-200-300	0.6	1.2E+07	3.60E+05
			0.9	1.8E+07	1.215E+06
			1.2	2.4E+07	2.88E+06

Soft Soil	E_{50}/c_u		
HSS	100	200	300
E_{50}^{ref}	2895	5789	8685
E_{oed}^{ref}	2895	5789	8685
E_{ur}^{ref}	8685	17367	26055
G_0^{ref}	30759	43418	54281
$\gamma_{0,7}$	3.59E-04	2.54E-04	2.03E-04
ϕ	18	18	18
K_0	0.691	0.691	0.691
E_{dyn}/E_{stat}	8.5	6	5

H=11m	d=0.6	d=0.9	d=1.2	E_{50}/c_u	H=11m	d=0.6	d=0.9	d=1.2
δ_{vm}(mm)	86	54	38	100	δ_{hm}(mm)	113	65	46
	77	46	32	200		98	56	40
	70	41	30	300		90	52	38

H=14m	d=0.6	d=0.9	d=1.2	E_{50}/c_u	H=14m	d=0.6	d=0.9	d=1.2
δ_{vm}(mm)	116	72	51	100	δ_{hm}(mm)	154	89	60
	106	62	45	200		140	78	56
	98	58	42	300		128	73	53

H=17m	d=0.6	d=0.9	d=1.2	E_{50}/c_u	H=17m	d=0.6	d=0.9	d=1.2
δ_{vm}(mm)	144	89	61	100	δ_{hm}(mm)	190	110	73
	133	78	57	200		169	97	69
	126	74	54	300		161	92	66

H=20m	d=0.6	d=0.9	d=1.2	E_{50}/c_u	H=20m	d=0.6	d=0.9	d=1.2
δ_{vm}(mm)	172	103	69	100	δ_{hm}(mm)	215	124	82
	158	91	66	200		194	113	79
	151	86	63	300		183	107	76

Generic Cases: 1333 to 1368

Table A.38. Model parameters and deformation results (Case No: 1333 to 1368).

Excavation	Soil (γ=17kN/m^3)		Diaphragm Wall(E=2.0E+7)		
H_e(m)	c_u/σ_v'	E_{50}/c_u	d	EA	EI
11-14-17-20	0.25	100-200-300	0.6	1.2E+07	3.60E+05
			0.9	1.8E+07	1.215E+06
			1.2	2.4E+07	2.88E+06

Soil	E_{50}/c_u		
HSS	100	200	300
E_{50}^{ref}	4000	8000	12000
E_{oed}^{ref}	4000	8000	12000
E_{ur}^{ref}	12000	24000	36000
G_0^{ref}	35000	50000	67500
$\gamma_{0,7}$	3.58E-04	2.51E-04	1.86E-04
ϕ	22	22	22
K_0	0.625	0.625	0.625
E_{dyn}/E_{stat}	7	5	4.5

H=11m	d=0.6	d=0.9	d=1.2	E_{50}/c_u	H=11m	d=0.6	d=0.9	d=1.2
δ_{vm}(mm)	63	40	30	100	δ_{hm}(mm)	79	50	37
	52	34	24	200		66	44	31
	45	30	22	300		57	38	29

H=14m	d=0.6	d=0.9	d=1.2	E_{50}/c_u	H=14m	d=0.6	d=0.9	d=1.2
δ_{vm}(mm)	87	56	39	100	δ_{hm}(mm)	115	69	49
	75	48	34	200		97	61	44
	65	42	32	300		85	54	41

H=17m	d=0.6	d=0.9	d=1.2	E_{50}/c_u	H=17m	d=0.6	d=0.9	d=1.2
δ_{vm}(mm)	106	70	48	100	δ_{hm}(mm)	144	87	61
	92	60	44	200		123	77	56
	84	54	41	300		109	69	52

H=20m	d=0.6	d=0.9	d=1.2	E_{50}/c_u	H=20m	d=0.6	d=0.9	d=1.2
δ_{vm}(mm)	125	80	56	100	δ_{hm}(mm)	169	101	70
	110	72	51	200		142	90	65
	100	65	48	300		128	81	61

Generic Cases: 1369 to 1404

Table A.39. Model parameters and deformation results (Case No: 1369 to 1404).

Excavation	Soil (γ=17kN/m^3)		Diaphragm Wall(E=2.0E+7)		
H_e(m)	c_u/σ_v'	E_{50}/c_u	d	EA	EI
11-14-17-20	0.3	100-200-300	0.6	1.2E+07	3.60E+05
			0.9	1.8E+07	1.215E+06
			1.2	2.4E+07	2.88E+06

Soil	E_{50}/c_u		
HSS	100	200	300
E_{50}^{ref}	5400	10800	16200
E_{oed}^{ref}	5400	10800	16200
E_{ur}^{ref}	16200	32400	48600
G_0^{ref}	40500	60750	75938
$\gamma_{0.7}$	3.40E-04	2.27E-04	1.81E-04
ϕ	26.4	26.4	26.4
K_0	0.555	0.555	0.555
E_{dyn}/E_{stat}	6	4.5	3.75

H=11m	d=0.6	d=0.9	d=1.2	E_{50}/c_u	H=11m	d=0.6	d=0.9	d=1.2
δ_{vm}(mm)	46	34	28	100	δ_{hm}(mm)	59	42	33
	37	25	20	200		47	33	25
	31	22	17	300		40	28	22

H=14m	d=0.6	d=0.9	d=1.2	E_{50}/c_u	H=14m	d=0.6	d=0.9	d=1.2
δ_{vm}(mm)	64	45	37	100	δ_{hm}(mm)	83	56	44
	52	35	28	200		69	46	35
	46	32	25	300		62	42	32

H=17m	d=0.6	d=0.9	d=1.2	E_{50}/c_u	H=17m	d=0.6	d=0.9	d=1.2
δ_{vm}(mm)	80	57	45	100	δ_{hm}(mm)	107	70	54
	66	45	35	200		88	59	45
	59	41	33	300		80	54	42

H=20m	d=0.6	d=0.9	d=1.2	E_{50}/c_u	H=20m	d=0.6	d=0.9	d=1.2
δ_{vm}(mm)	96	67	52	100	δ_{hm}(mm)	125	83	63
	80	55	42	200		104	72	54
	72	51	39	300		95	66	50

Generic Cases: 1405 to 1440

Table A.40. Model parameters and deformation results (Case No: 1405 to 1440).

Excavation	Soil (γ=17kN/m^3)		Diaphragm Wall(E=2.0E+7)		
H_e(m)	c_u/σ'_v	E_{50}/c_u	d	EA	EI
11-14-17-20	0.35	100-200-300	0.6	1.2E+07	3.60E+05
			0.9	1.8E+07	1.215E+06
			1.2	2.4E+07	2.88E+06

Soil	E_{50}/c_u		
HSS	100	200	300
E_{50}^{ref}	7000	14000	21000
E_{oed}^{ref}	7000	14000	21000
E_{ur}^{ref}	21000	42000	63000
G_0^{ref}	52500	73500	99750
$\gamma_{0,7}$	2.75E-04	1.96E-04	1.45E-04
ϕ	30	30	30
K_0	0.500	0.500	0.500
E_{dyn}/E_{stat}	6	4.2	3.8

H=11m	d=0.6	d=0.9	d=1.2	E_{50}/c_u	H=11m	d=0.6	d=0.9	d=1.2
δ_{vm}(mm)	38	30	25	100	δ_{hm}(mm)	48	37	30
	29	21	18	200		37	28	23
	24	18	14	300		31	23	19

H=14m	d=0.6	d=0.9	d=1.2	E_{50}/c_u	H=14m	d=0.6	d=0.9	d=1.2
δ_{vm}(mm)	54	39	32	100	δ_{hm}(mm)	68	48	39
	41	30	24	200		55	38	31
	35	26	20	300		46	33	26

H=17m	d=0.6	d=0.9	d=1.2	E_{50}/c_u	H=17m	d=0.6	d=0.9	d=1.2
δ_{vm}(mm)	66	48	39	100	δ_{hm}(mm)	86	60	47
	53	38	31	200		72	50	39
	46	33	27	300		62	44	35

H=20m	d=0.6	d=0.9	d=1.2	E_{50}/c_u	H=20m	d=0.6	d=0.9	d=1.2
δ_{vm}(mm)	79	57	46	100	δ_{hm}(mm)	103	71	56
	64	47	38	200		86	61	48
	57	41	33	300		74	54	43

Model Group:11

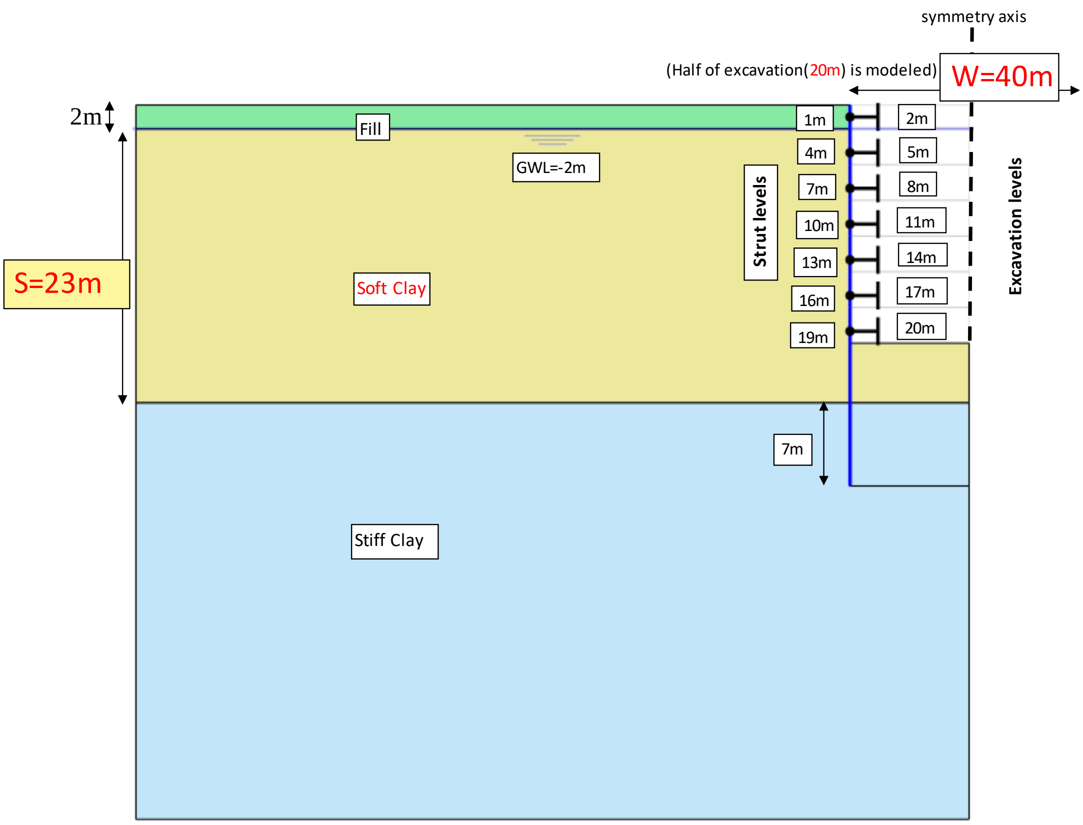

Figure A.11. Model Geometry-11.

Table B. Soil and structure parameters.

Default Soil Parameters		
	Stiff Clay	Fill
	HS	HS
	Undrained(A)	Drained
E_{50}^{ref}	1.00E+05	1.50E+04
E_{oed}^{ref}	1.00E+05	1.50E+04
E_{ur}^{ref}	3.00E+05	3.00E+04
ϕ'	26	30
K_0	0.562	0.5
c'_{ref}	25	1
v'_{ur}	0.2	0.2
p_{ref}	100	100
R_f	0.9	0.9
$\gamma_{unsat/sat}$	20/20	16/20
R_{inter}	0.65	0.65
m	1	1

Range of parameters	
c_u/σ'_v	0.20-0.25-0.30-0.35
E_{50}/c_u	100-200-300
γ	15-17-19
S	23-28-33
W	20-40-60
H_e	11-14-17-20
$\ln(EI/\gamma_w h_{avg}^4)$	6.097-7.313-8.176

Diaphragm Wall (E=2.0E+7)		
d	EA	EI
0.6	1.2E+07	3.60E+05
0.9	1.8E+07	1.215E+06
1.2	2.4E+07	2.88E+06

Strut	
EA	3.80E+06
$L_{spacing}$	5m
h_{avg}	3m

Generic Cases: 1441 to 1476

Table A.41. Model parameters and deformation results (Case No: 1441 to 1476).

Excavation	Soil(γ=17kN/m^3)		Diaphragm Wall(E=2.0E+7)		
H_e(m)	c_u/σ_v'	E_{50}/c_u	d	EA	EI
11-14-17-20	0.2	100-200-300	0.6	1.2E+07	3.60E+05
			0.9	1.8E+07	1.215E+06
			1.2	2.4E+07	2.88E+06

Soft Soil	E_{50}/c_u		
HSS	100	200	300
E_{50}^{ref}	2895	5789	8685
E_{oed}^{ref}	2895	5789	8685
E_{ur}^{ref}	8685	17367	26055
G_0^{ref}	30759	43418	54281
$\gamma_{0,7}$	3.59E-04	2.54E-04	2.03E-04
ϕ	18	18	18
K_0	0.691	0.691	0.691
E_{dyn}/E_{stat}	8.5	6	5

H=11m	d=0.6	d=0.9	d=1.2	E_{50}/c_u	H=11m	d=0.6	d=0.9	d=1.2
δ_{vm}(mm)	105	68	48	100	δ_{hm}(mm)	130	83	59
	96	60	43	200		119	73	53
	88	55	41	300		110	68	49

H=14m	d=0.6	d=0.9	d=1.2	E_{50}/c_u	H=14m	d=0.6	d=0.9	d=1.2
δ_{vm}(mm)	144	94	67	100	δ_{hm}(mm)	182	111	79
	134	82	60	200		167	101	73
	127	77	58	300		156	95	69

H=17m	d=0.6	d=0.9	d=1.2	E_{50}/c_u	H=17m	d=0.6	d=0.9	d=1.2
δ_{vm}(mm)	182	118	83	100	δ_{hm}(mm)	224	138	96
	169	104	76	200		207	126	91
	160	99	72	300		194	119	88

H=20m	d=0.6	d=0.9	d=1.2	E_{50}/c_u	H=20m	d=0.6	d=0.9	d=1.2
δ_{vm}(mm)	212	135	95	100	δ_{hm}(mm)	259	159	109
	205	123	88	200		238	145	105
	193	118	84	300		222	139	101

Generic Cases: 1477 to 1512

Table A.42. Model parameters and deformation results (Case No: 1477 to 1512).

Excavation	Soil (γ=17kN/m^3)		Diaphragm Wall(E=2.0E+7)		
H_e(m)	c_u/σ'_v	E_{50}/c_u	d	EA	EI
11-14-17-20	0.25	100-200-300	0.6	1.2E+07	3.60E+05
			0.9	1.8E+07	1.215E+06
			1.2	2.4E+07	2.88E+06

Soil	E_{50}/c_u		
HSS	100	200	300
E_{50}^{ref}	4000	8000	12000
E_{oed}^{ref}	4000	8000	12000
E_{ur}^{ref}	12000	24000	36000
G_0^{ref}	35000	50000	67500
$\gamma_{0,7}$	3.58E-04	2.51E-04	1.86E-04
ϕ	22	22	22
K_0	0.625	0.625	0.625
E_{dyn}/E_{stat}	7	5	4.5

H=11m	d=0.6	d=0.9	d=1.2	E_{50}/c_u	H=11m	d=0.6	d=0.9	d=1.2
δ_{vm}(mm)	76	53	43	100	δ_{hm}(mm)	95	66	52
	68	45	33	200		85	56	43
	60	40	30	300		74	51	38

H=14m	d=0.6	d=0.9	d=1.2	E_{50}/c_u	H=14m	d=0.6	d=0.9	d=1.2
δ_{vm}(mm)	108	73	59	100	δ_{hm}(mm)	136	90	69
	97	63	47	200		124	79	59
	87	58	43	300		109	72	54

H=17m	d=0.6	d=0.9	d=1.2	E_{50}/c_u	H=17m	d=0.6	d=0.9	d=1.2
δ_{vm}(mm)	136	94	74	100	δ_{hm}(mm)	173	112	86
	121	80	61	200		154	99	75
	110	74	57	300		139	92	71

H=20m	d=0.6	d=0.9	d=1.2	E_{50}/c_u	H=20m	d=0.6	d=0.9	d=1.2
δ_{vm}(mm)	160	112	86	100	δ_{hm}(mm)	201	131	98
	147	95	72	200		179	118	88
	134	90	68	300		161	109	83

Generic Cases: 1513 to 1548

Table A.43. Model parameters and deformation results (Case No: 1513 to 1548).

Excavation	Soil (γ=17kN/m^3)		Diaphragm Wall(E=2.0E+7)		
H_e(m)	c_u/σ_v'	E_{50}/c_u	d	EA	EI
11-14-17-20	0.3	100-200-300	0.6	1.2E+07	3.60E+05
			0.9	1.8E+07	1.215E+06
			1.2	2.4E+07	2.88E+06

Soil	E_{50}/c_u		
HSS	100	200	300
E_{50}^{ref}	5400	10800	16200
E_{oed}^{ref}	5400	10800	16200
E_{ur}^{ref}	16200	32400	48600
G_0^{ref}	40500	60750	75938
$\gamma_{0,7}$	3.40E-04	2.27E-04	1.81E-04
ϕ	26.4	26.4	26.4
K_0	0.555	0.555	0.555
E_{dyn}/E_{stat}	6	4.5	3.75

H=11m	d=0.6	d=0.9	d=1.2	E_{50}/c_u	H=11m	d=0.6	d=0.9	d=1.2
δ_{vm}(mm)	59	47	40	100	δ_{hm}(mm)	77	59	48
	50	38	30	200		64	47	38
	43	31	26	300		54	40	33

H=14m	d=0.6	d=0.9	d=1.2	E_{50}/c_u	H=14m	d=0.6	d=0.9	d=1.2
δ_{vm}(mm)	83	63	52	100	δ_{hm}(mm)	106	77	62
	71	51	40	200		91	64	51
	63	44	36	300		79	56	45

H=17m	d=0.6	d=0.9	d=1.2	E_{50}/c_u	H=17m	d=0.6	d=0.9	d=1.2
δ_{vm}(mm)	104	79	65	100	δ_{hm}(mm)	137	95	77
	90	65	52	200		115	82	64
	81	58	47	300		102	73	59

H=20m	d=0.6	d=0.9	d=1.2	E_{50}/c_u	H=20m	d=0.6	d=0.9	d=1.2
δ_{vm}(mm)	125	93	75	100	δ_{hm}(mm)	162	112	87
	109	80	62	200		137	99	76
	99	72	57	300		121	89	71

Generic Cases: 1549 to 1584

Table A.44. Model parameters and deformation results (Case No: 1549 to 1584).

Excavation	Soil (γ=17kN/m^3)		Diaphragm Wall(E=2.0E+7)		
H_e(m)	c_u/σ_v'	E_{50}/c_u	d	EA	EI
11-14-17-20	0.35	100-200-300	0.6	1.2E+07	3.60E+05
			0.9	1.8E+07	1.215E+06
			1.2	2.4E+07	2.88E+06

Soil	E_{50}/c_u		
HSS	100	200	300
E_{50}^{ref}	7000	14000	21000
E_{oed}^{ref}	7000	14000	21000
E_{ur}^{ref}	21000	42000	63000
G_0^{ref}	52500	73500	99750
$\gamma_{0,7}$	2.75E-04	1.96E-04	1.45E-04
ϕ	30	30	30
K_0	0.500	0.500	0.500
E_{dyn}/E_{stat}	6	4.2	3.8

H=11m	d=0.6	d=0.9	d=1.2	E_{50}/c_u	H=11m	d=0.6	d=0.9	d=1.2
δ_{vm}(mm)	50	42	36	100	δ_{hm}(mm)	63	51	43
	42	33	27	200		52	41	34
	33	26	22	300		42	34	28

H=14m	d=0.6	d=0.9	d=1.2	E_{50}/c_u	H=14m	d=0.6	d=0.9	d=1.2
δ_{vm}(mm)	69	55	46	100	δ_{hm}(mm)	88	66	55
	58	43	36	200		74	55	45
	48	36	30	300		62	47	39

H=17m	d=0.6	d=0.9	d=1.2	E_{50}/c_u	H=17m	d=0.6	d=0.9	d=1.2
δ_{vm}(mm)	87	69	57	100	δ_{hm}(mm)	111	82	68
	74	57	47	200		94	71	57
	63	48	41	300		80	61	50

H=20m	d=0.6	d=0.9	d=1.2	E_{50}/c_u	H=20m	d=0.6	d=0.9	d=1.2
δ_{vm}(mm)	104	82	67	100	δ_{hm}(mm)	132	97	79
	89	70	56	200		113	85	68
	78	61	51	300		97	75	62

Model Group:12

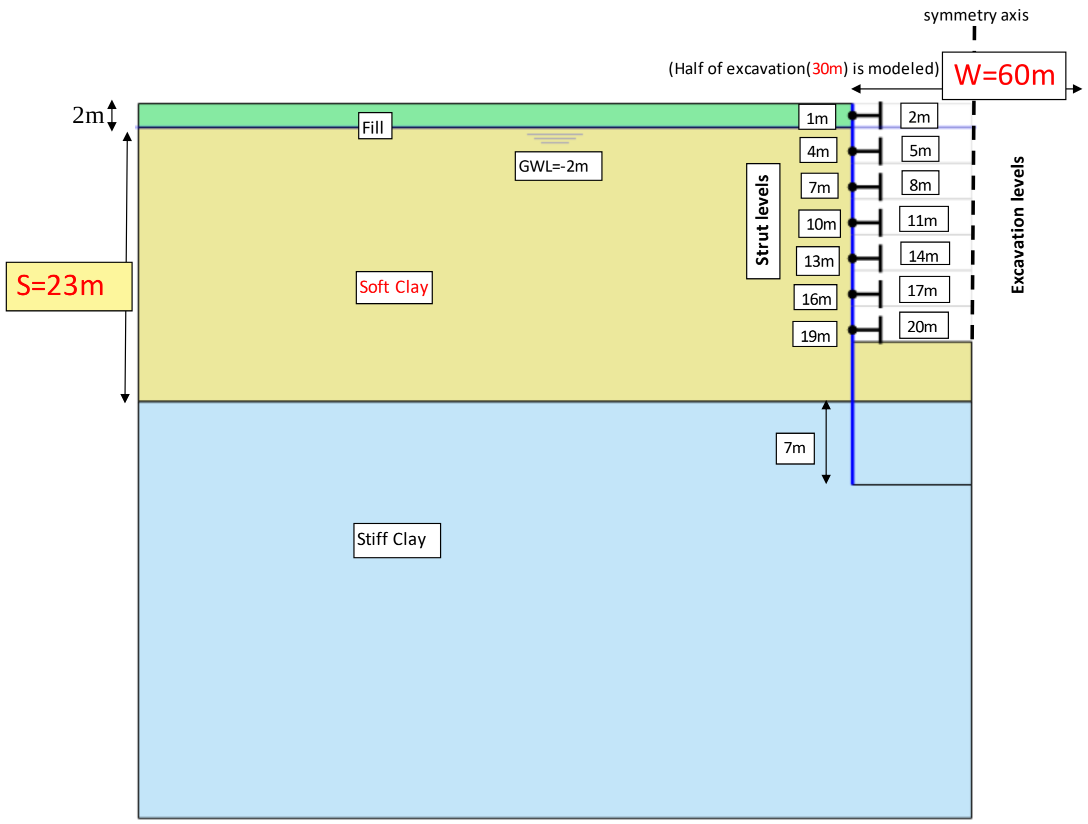

Figure A.12. Model Geometry-12.

Table B. Soil and structure parameters.

Default Soil Parameters		
	Stiff Clay	Fill
	HS	HS
	Undrained(A)	Drained
E_{50}^{ref}	1.00E+05	1.50E+04
E_{oed}^{ref}	1.00E+05	1.50E+04
E_{ur}^{ref}	3.00E+05	3.00E+04
ϕ'	26	30
K_0	0.562	0.5
c'_{ref}	25	1
v'_{ur}	0.2	0.2
p_{ref}	100	100
R_f	0.9	0.9
$\gamma_{unsat/sat}$	20/20	16/20
R_{inter}	0.65	0.65
m	1	1

Range of parameters	
c_u/σ_v'	0.20-0.25-0.30-0.35
E_{50}/c_u	100-200-300
γ	15-17-19
S	23-28-33
W	20-40-60
H_e	11-14-17-20
$\ln(EI/\gamma_w h_{avg}^4)$	6.097-7.313-8.176

Diaphragm Wall (E=2.0E+7)		
d	EA	EI
0.6	1.2E+07	3.60E+05
0.9	1.8E+07	1.215E+06
1.2	2.4E+07	2.88E+06

Strut	
EA	3.80E+06
$L_{spacing}$	5m
h_{avg}	3m

Generic Cases: 1585 to 1620

Table A.45. Model parameters and deformation results (Case No: 1585 to 1620).

Excavation	Soil(γ=17kN/m^3)		Diaphragm Wall(E=2.0E+7)		
H_e(m)	c_u/σ_v'	E_{50}/c_u	d	EA	EI
11-14-17-20	0.2	100-200-300	0.6	1.2E+07	3.60E+05
			0.9	1.8E+07	1.215E+06
			1.2	2.4E+07	2.88E+06

Soft Soil	E_{50}/c_u		
HSS	100	200	300
E_{50}^{ref}	2895	5789	8685
E_{oed}^{ref}	2895	5789	8685
E_{ur}^{ref}	8685	17367	26055
G_0^{ref}	30759	43418	54281
$\gamma_{0,7}$	3.59E-04	2.54E-04	2.03E-04
ϕ	18	18	18
K_0	0.691	0.691	0.691
E_{dyn}/E_{stat}	8.5	6	5

H=11m	d=0.6	d=0.9	d=1.2	E_{50}/c_u	H=11m	d=0.6	d=0.9	d=1.2
δ_{vm}(mm)	120	81	61	100	δ_{hm}(mm)	147	96	73
	110	71	54	200		134	86	63
	103	65	49	300		123	79	58

H=14m	d=0.6	d=0.9	d=1.2	E_{50}/c_u	H=14m	d=0.6	d=0.9	d=1.2
δ_{vm}(mm)	165	110	82	100	δ_{hm}(mm)	204	130	97
	152	98	75	200		187	119	88
	145	92	69	300		174	111	82

H=17m	d=0.6	d=0.9	d=1.2	E_{50}/c_u	H=17m	d=0.6	d=0.9	d=1.2
δ_{vm}(mm)	206	139	103	100	δ_{hm}(mm)	255	160	119
	193	126	94	200		234	148	109
	185	119	89	300		218	140	103

H=20m	d=0.6	d=0.9	d=1.2	E_{50}/c_u	H=20m	d=0.6	d=0.9	d=1.2
δ_{vm}(mm)	248	161	118	100	δ_{hm}(mm)	293	184	134
	234	147	109	200		271	172	125
	223	142	104	300		256	164	121

Generic Cases: 1621 to 1656

Table A.46. Model parameters and deformation results (Case No: 1621 to 1656).

Excavation	Soil (γ=17kN/m^3)		Diaphragm Wall(E=2.0E+7)		
H_e(m)	c_u/σ_v'	E_{50}/c_u	d	EA	EI
11-14-17-20	0.25	100-200-300	0.6	1.2E+07	3.60E+05
			0.9	1.8E+07	1.215E+06
			1.2	2.4E+07	2.88E+06

Soil	E_{50}/c_u		
HSS	100	200	300
E_{50}^{ref}	4000	8000	12000
E_{oed}^{ref}	4000	8000	12000
E_{ur}^{ref}	12000	24000	36000
G_0^{ref}	35000	50000	67500
$\gamma_{0,7}$	3.58E-04	2.51E-04	1.86E-04
ϕ	22	22	22
K_0	0.625	0.625	0.625
E_{dyn}/E_{stat}	7	5	4.5

H=11m	d=0.6	d=0.9	d=1.2	E_{50}/c_u	H=11m	d=0.6	d=0.9	d=1.2
δ_{vm}(mm)	91	65	52	100	δ_{hm}(mm)	113	81	63
	80	56	42	200		98	69	53
	70	47	36	300		86	59	45

H=14m	d=0.6	d=0.9	d=1.2	E_{50}/c_u	H=14m	d=0.6	d=0.9	d=1.2
δ_{vm}(mm)	126	88	68	100	δ_{hm}(mm)	159	108	83
	112	78	59	200		140	96	72
	100	68	52	300		125	83	65

H=17m	d=0.6	d=0.9	d=1.2	E_{50}/c_u	H=17m	d=0.6	d=0.9	d=1.2
δ_{vm}(mm)	159	112	86	100	δ_{hm}(mm)	200	134	101
	143	99	75	200		175	120	92
	129	88	68	300		160	108	83

H=20m	d=0.6	d=0.9	d=1.2	E_{50}/c_u	H=20m	d=0.6	d=0.9	d=1.2
δ_{vm}(mm)	191	132	101	100	δ_{hm}(mm)	234	156	116
	174	119	89	200		206	142	108
	158	108	82	300		189	129	99

Generic Cases: 1657 to 1692

Table A.47. Model parameters and deformation results (Case No: 1657 to 1692).

Excavation	Soil (γ=17kN/m^3)		Diaphragm Wall(E=2.0E+7)		
H_e(m)	c_u/σ_v'	E_{50}/c_u	d	EA	EI
11-14-17-20	0.3	100-200-300	0.6	1.2E+07	3.60E+05
			0.9	1.8E+07	1.215E+06
			1.2	2.4E+07	2.88E+06

Soil	E_{50}/c_u		
HSS	100	200	300
E_{50}^{ref}	5400	10800	16200
E_{oed}^{ref}	5400	10800	16200
E_{ur}^{ref}	16200	32400	48600
G_0^{ref}	40500	60750	75938
$\gamma_{0,7}$	3.40E-04	2.27E-04	1.81E-04
ϕ	26.4	26.4	26.4
K_0	0.555	0.555	0.555
E_{dyn}/E_{stat}	6	4.5	3.75

H=11m	d=0.6	d=0.9	d=1.2	E_{50}/c_u	H=11m	d=0.6	d=0.9	d=1.2
δ_{vm}(mm)	78	57	49	100	δ_{hm}(mm)	98	71	57
	62	46	38	200		77	57	47
	51	40	32	300		64	50	40

H=14m	d=0.6	d=0.9	d=1.2	E_{50}/c_u	H=14m	d=0.6	d=0.9	d=1.2
δ_{vm}(mm)	105	75	62	100	δ_{hm}(mm)	131	93	74
	85	63	51	200		107	77	63
	73	55	45	300		93	69	55

H=17m	d=0.6	d=0.9	d=1.2	E_{50}/c_u	H=17m	d=0.6	d=0.9	d=1.2
δ_{vm}(mm)	129	94	77	100	δ_{hm}(mm)	163	113	91
	108	80	65	200		136	98	79
	95	72	59	300		120	89	72

H=20m	d=0.6	d=0.9	d=1.2	E_{50}/c_u	H=20m	d=0.6	d=0.9	d=1.2
δ_{vm}(mm)	155	113	92	100	δ_{hm}(mm)	190	134	106
	131	99	78	200		160	117	95
	119	90	72	300		142	108	88

Generic Cases: 1693 to 1728

Table A.48. Model parameters and deformation results (Case No: 1693 to 1728).

Excavation	Soil (γ=17kN/m^3)		Diaphragm Wall(E=2.0E+7)		
H_e(m)	c_u/σ_v'	E_{50}/c_u	d	EA	EI
11-14-17-20	0.35	100-200-300	0.6	1.2E+07	3.60E+05
			0.9	1.8E+07	1.215E+06
			1.2	2.4E+07	2.88E+06

Soil	E_{50}/c_u		
HSS	100	200	300
E_{50}^{ref}	7000	14000	21000
E_{oed}^{ref}	7000	14000	21000
E_{ur}^{ref}	21000	42000	63000
G_0^{ref}	52500	73500	99750
$\gamma_{0,7}$	2.75E-04	1.96E-04	1.45E-04
ϕ	30	30	30
K_0	0.500	0.500	0.500
E_{dyn}/E_{stat}	6	4.2	3.8

H=11m	d=0.6	d=0.9	d=1.2	E_{50}/c_u	H=11m	d=0.6	d=0.9	d=1.2
δ_{vm}(mm)	58	51	45	100	δ_{hm}(mm)	72	62	54
	50	41	35	200		62	51	43
	41	33	28	300		53	41	35

H=14m	d=0.6	d=0.9	d=1.2	E_{50}/c_u	H=14m	d=0.6	d=0.9	d=1.2
δ_{vm}(mm)	79	67	59	100	δ_{hm}(mm)	101	81	69
	69	54	46	200		87	67	57
	60	46	38	300		75	57	48

H=17m	d=0.6	d=0.9	d=1.2	E_{50}/c_u	H=17m	d=0.6	d=0.9	d=1.2
δ_{vm}(mm)	101	85	72	100	δ_{hm}(mm)	129	99	85
	88	69	59	200		110	86	71
	79	60	50	300		98	74	62

H=20m	d=0.6	d=0.9	d=1.2	E_{50}/c_u	H=20m	d=0.6	d=0.9	d=1.2
δ_{vm}(mm)	123	101	85	100	δ_{hm}(mm)	154	117	99
	108	85	72	200		133	103	86
	97	76	62	300		117	92	76

Model Group:13

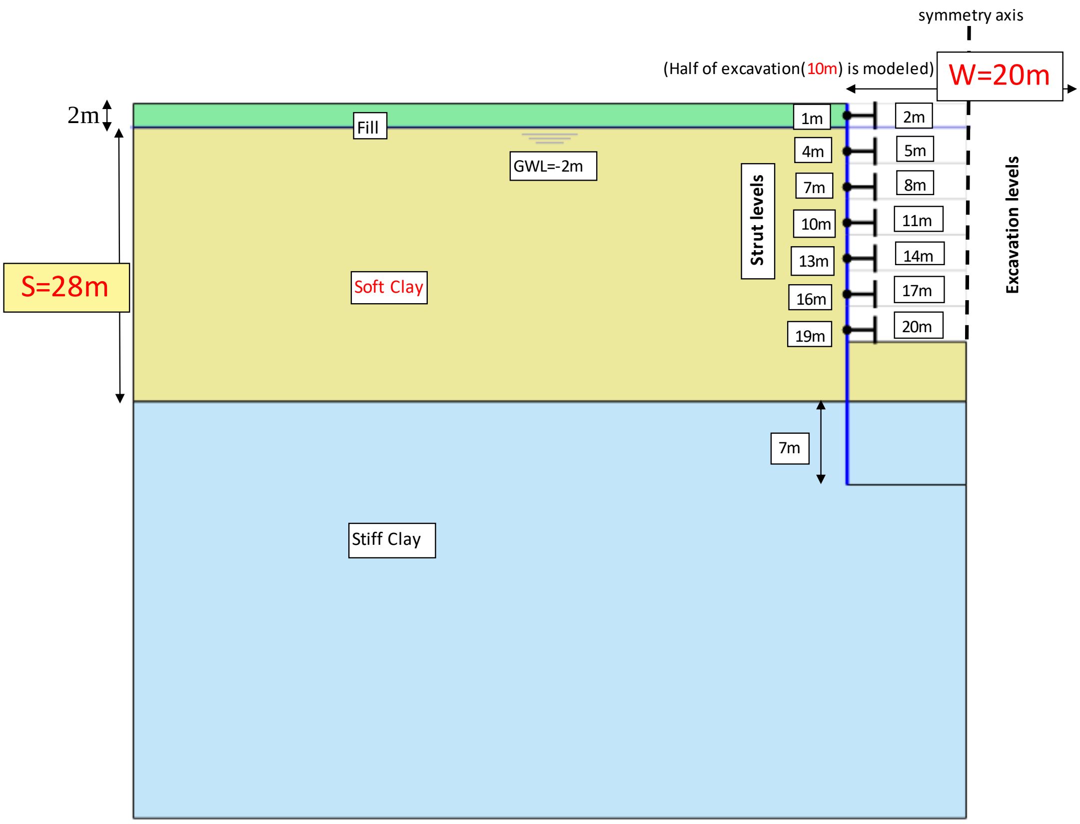

Figure A.13. Model Geometry-13.

Table B. Soil and structure parameters.

Default Soil Parameters	Stiff Clay	Fill
	HS	HS
	Undrained(A)	Drained
E_{50}^{ref}	1.00E+05	1.50E+04
E_{oed}^{ref}	1.00E+05	1.50E+04
E_{ur}^{ref}	3.00E+05	3.00E+04
ϕ'	26	30
K_0	0.562	0.5
c'_{ref}	25	1
v'_{ur}	0.2	0.2
p_{ref}	100	100
R_f	0.9	0.9
$\gamma_{unsat/sat}$	20/20	16/20
R_{inter}	0.65	0.65
m	1	1

Range of parameters	
c_u/σ'_v	0.20-0.25-0.30-0.35
E_{50}/c_u	100-200-300
γ	15-17-19
S	25-30-35
W	20-40-60
H_e	11-14-17-20
$\ln(EI/\gamma_w h_{avg}^4)$	6.097-7.313-8.176

Diaphragm Wall (E=2.0E+7)		
d	EA	EI
0.6	1.2E+07	3.60E+05
0.9	1.8E+07	1.215E+06
1.2	2.4E+07	2.88E+06

Strut	
EA	3.80E+06
$L_{spacing}$	5m
h_{avg}	3m

Generic Cases: 1729 to 1764

Table A.49. Model parameters and deformation results (Case No: 1729 to 1764).

Excavation	Soil(γ=17kN/m^3)		Diaphragm Wall(E=2.0E+7)		
H_e(m)	c_u/σ_v'	E_{50}/c_u	d	EA	EI
11-14-17-20	0.2	100-200-300	0.6	1.2E+07	3.60E+05
			0.9	1.8E+07	1.215E+06
			1.2	2.4E+07	2.88E+06

Soft Soil	E_{50}/c_u		
HSS	100	200	300
E_{50}^{ref}	2895	5789	8685
E_{oed}^{ref}	2895	5789	8685
E_{ur}^{ref}	8685	17367	26055
G_0^{ref}	30759	43418	54281
$\gamma_{0,7}$	3.59E-04	2.54E-04	2.03E-04
ϕ	18	18	18
K_0	0.691	0.691	0.691
E_{dyn}/E_{stat}	8.5	6	5

H=11m	d=0.6	d=0.9	d=1.2	E_{50}/c_u	H=11m	d=0.6	d=0.9	d=1.2
δ_{vm}(mm)	95	61	43	100	δ_{hm}(mm)	124	76	53
	85	52	37	200		108	66	47
	78	48	34	300		98	60	43

H=14m	d=0.6	d=0.9	d=1.2	E_{50}/c_u	H=14m	d=0.6	d=0.9	d=1.2
δ_{vm}(mm)	150	88	60	100	δ_{hm}(mm)	196	111	75
	137	76	55	200		175	98	69
	125	72	50	300		161	91	64

H=17m	d=0.6	d=0.9	d=1.2	E_{50}/c_u	H=17m	d=0.6	d=0.9	d=1.2
δ_{vm}(mm)	198	114	79	100	δ_{hm}(mm)	262	145	99
	183	102	73	200		232	132	93
	170	96	67	300		217	124	85

H=20m	d=0.6	d=0.9	d=1.2	E_{50}/c_u	H=20m	d=0.6	d=0.9	d=1.2
δ_{vm}(mm)	242	139	96	100	δ_{hm}(mm)	318	178	120
	223	127	89	200		281	163	112
	209	121	83	300		256	152	105

Generic Cases: 1765 to 1800

Table A.50. Model parameters and deformation results (Case No: 1765 to 1800).

Excavation	Soil (γ=17kN/m^3)		Diaphragm Wall(E=2.0E+7)		
H_e(m)	c_u/σ_v'	E_{50}/c_u	d	EA	EI
11-14-17-20	0.25	100-200-300	0.6	1.2E+07	3.60E+05
			0.9	1.8E+07	1.215E+06
			1.2	2.4E+07	2.88E+06

Soil	E_{50}/c_u		
HSS	100	200	300
E_{50}^{ref}	4000	8000	12000
E_{oed}^{ref}	4000	8000	12000
E_{ur}^{ref}	12000	24000	36000
G_0^{ref}	35000	50000	67500
$\gamma_{0,7}$	3.58E-04	2.51E-04	1.86E-04
ϕ	22	22	22
K_0	0.625	0.625	0.625
E_{dyn}/E_{stat}	7	5	4.5

H=11m	d=0.6	d=0.9	d=1.2	E_{50}/c_u	H=11m	d=0.6	d=0.9	d=1.2
δ_{vm}(mm)	66	42	31	100	δ_{hm}(mm)	85	54	39
	55	37	28	200		70	47	36
	47	32	24	300		60	41	31

H=14m	d=0.6	d=0.9	d=1.2	E_{50}/c_u	H=14m	d=0.6	d=0.9	d=1.2
δ_{vm}(mm)	99	61	44	100	δ_{hm}(mm)	135	81	57
	86	55	41	200		113	71	53
	76	49	36	300		97	63	47

H=17m	d=0.6	d=0.9	d=1.2	E_{50}/c_u	H=17m	d=0.6	d=0.9	d=1.2
δ_{vm}(mm)	134	78	57	100	δ_{hm}(mm)	183	107	76
	114	73	54	200		155	95	71
	103	66	48	300		135	87	63

H=20m	d=0.6	d=0.9	d=1.2	E_{50}/c_u	H=20m	d=0.6	d=0.9	d=1.2
δ_{vm}(mm)	164	100	72	100	δ_{hm}(mm)	225	133	94
	142	91	67	200		191	119	88
	128	83	61	300		169	107	79

Generic Cases: 1801 to 1836

Table A.51. Model parameters and deformation results (Case No: 1801 to 1836).

Excavation	Soil (γ=17kN/m^3)		Diaphragm Wall(E=2.0E+7)		
H_e(m)	c_u/σ_v'	E_{50}/c_u	d	EA	EI
11-14-17-20	0.3	100-200-300	0.6	1.2E+07	3.60E+05
			0.9	1.8E+07	1.215E+06
			1.2	2.4E+07	2.88E+06

Soil	E_{50}/c_u		
HSS	100	200	300
E_{50}^{ref}	5400	10800	16200
E_{oed}^{ref}	5400	10800	16200
E_{ur}^{ref}	16200	32400	48600
G_0^{ref}	40500	60750	75938
$\gamma_{0,7}$	3.40E-04	2.27E-04	1.81E-04
ϕ	26.4	26.4	26.4
K_0	0.555	0.555	0.555
E_{dyn}/E_{stat}	6	4.5	3.75

H=11m	d=0.6	d=0.9	d=1.2	E_{50}/c_u	H=11m	d=0.6	d=0.9	d=1.2
δ_{vm}(mm)	47	33	29	100	δ_{hm}(mm)	59	42	35
	37	26	20	200		47	34	27
	31	23	18	300		41	30	24

H=14m	d=0.6	d=0.9	d=1.2	E_{50}/c_u	H=14m	d=0.6	d=0.9	d=1.2
δ_{vm}(mm)	71	48	39	100	δ_{hm}(mm)	91	61	49
	56	39	29	200		74	51	38
	49	35	27	300		65	46	35

H=17m	d=0.6	d=0.9	d=1.2	E_{50}/c_u	H=17m	d=0.6	d=0.9	d=1.2
δ_{vm}(mm)	94	62	50	100	δ_{hm}(mm)	127	82	64
	75	52	38	200		104	70	52
	67	47	36	300		91	63	47

H=20m	d=0.6	d=0.9	d=1.2	E_{50}/c_u	H=20m	d=0.6	d=0.9	d=1.2
δ_{vm}(mm)	116	78	62	100	δ_{hm}(mm)	160	103	78
	94	66	48	200		130	88	65
	85	59	46	300		115	79	61

Generic Cases: 1837 to 1872

Table A.52. Model parameters and deformation results (Case No: 1837 to 1872).

Excavation	Soil (γ=17kN/m^3)		Diaphragm Wall(E=2.0E+7)		
H_e(m)	c_u/σ_v'	E_{50}/c_u	d	EA	EI
11-14-17-20	0.35	100-200-300	0.6	1.2E+07	3.60E+05
			0.9	1.8E+07	1.215E+06
			1.2	2.4E+07	2.88E+06

Soil	E_{50}/c_u		
HSS	100	200	300
E_{50}^{ref}	7000	14000	21000
E_{oed}^{ref}	7000	14000	21000
E_{ur}^{ref}	21000	42000	63000
G_0^{ref}	52500	73500	99750
$\gamma_{0,7}$	2.75E-04	1.96E-04	1.45E-04
ϕ	30	30	30
K_0	0.500	0.500	0.500
E_{dyn}/E_{stat}	6	4.2	3.8

H=11m	d=0.6	d=0.9	d=1.2	E_{50}/c_u	H=11m	d=0.6	d=0.9	d=1.2
δ_{vm}(mm)	38	31	26	100	δ_{hm}(mm)	48	38	32
	29	23	18	200		37	29	23
	24	18	14	300		32	23	19

H=14m	d=0.6	d=0.9	d=1.2	E_{50}/c_u	H=14m	d=0.6	d=0.9	d=1.2
δ_{vm}(mm)	55	42	33	100	δ_{hm}(mm)	70	52	41
	43	33	24	200		56	42	32
	36	27	21	300		47	35	28

H=17m	d=0.6	d=0.9	d=1.2	E_{50}/c_u	H=17m	d=0.6	d=0.9	d=1.2
δ_{vm}(mm)	73	54	42	100	δ_{hm}(mm)	98	68	53
	58	43	33	200		79	56	42
	49	36	28	300		66	48	37

H=20m	d=0.6	d=0.9	d=1.2	E_{50}/c_u	H=20m	d=0.6	d=0.9	d=1.2
δ_{vm}(mm)	89	65	51	100	δ_{hm}(mm)	122	83	64
	73	53	41	200		99	72	54
	62	47	36	300		85	62	48

Model Group:14

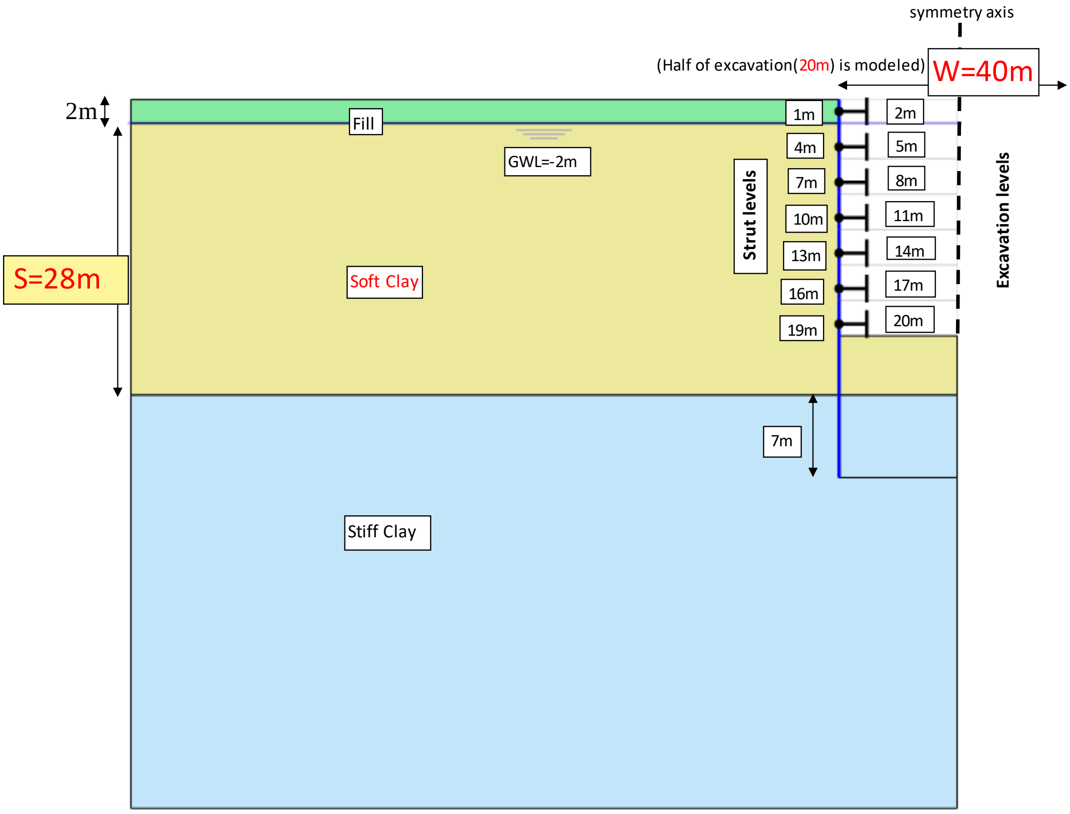

Figure A.14. Model Geometry-14.

Table B. Soil and structure parameters.

Default Soil Parameters		
	Stiff Clay	Fill
	HS	HS
	Undrained(A)	Drained
E_{50}^{ref}	1.00E+05	1.50E+04
E_{oed}^{ref}	1.00E+05	1.50E+04
E_{ur}^{ref}	3.00E+05	3.00E+04
ϕ'	26	30
K_0	0.562	0.5
c'_{ref}	25	1
v'_{ur}	0.2	0.2
p_{ref}	100	100
R_f	0.9	0.9
$\gamma_{unsat/sat}$	20/20	16/20
R_{inter}	0.65	0.65
m	1	1

Range of parameters	
c_u/σ'_v	0.20-0.25-0.30-0.35
E_{50}/c_u	100-200-300
γ	15-17-19
S	25-30-35
W	20-40-60
H_e	11-14-17-20
$\ln(EI/\gamma_w h_{avg}^4)$	6.097-7.313-8.176

Diaphragm Wall (E=2.0E+7)		
d	EA	EI
0.6	1.2E+07	3.60E+05
0.9	1.8E+07	1.215E+06
1.2	2.4E+07	2.88E+06

Strut	
EA	3.80E+06
$L_{spacing}$	5m
h_{avg}	3m

Generic Cases: 1873 to 1908

Table A.53. Model parameters and deformation results (Case No: 1873 to 1908).

Excavation	Soil(γ=17kN/m^3)		Diaphragm Wall(E=2.0E+7)		
H_e(m)	c_u/σ_v'	E_{50}/c_u	d	EA	EI
11-14-17-20	0.2	100-200-300	0.6	1.2E+07	3.60E+05
			0.9	1.8E+07	1.215E+06
			1.2	2.4E+07	2.88E+06

Soft Soil	E_{50}/c_u		
HSS	100	200	300
E_{50}^{ref}	2895	5789	8685
E_{oed}^{ref}	2895	5789	8685
E_{ur}^{ref}	8685	17367	26055
G_0^{ref}	30759	43418	54281
$\gamma_{0,7}$	3.59E-04	2.54E-04	2.03E-04
ϕ	18	18	18
K_0	0.691	0.691	0.691
E_{dyn}/E_{stat}	8.5	6	5

H=11m	d=0.6	d=0.9	d=1.2	E_{50}/c_u	H=11m	d=0.6	d=0.9	d=1.2
δ_{vm}(mm)	121	80	60	100	δ_{hm}(mm)	152	98	72
	110	70	49	200		137	85	60
	100	63	48	300		122	80	58

H=14m	d=0.6	d=0.9	d=1.2	E_{50}/c_u	H=14m	d=0.6	d=0.9	d=1.2
δ_{vm}(mm)	189	113	87	100	δ_{hm}(mm)	238	141	101
	170	101	72	200		211	124	89
	159	95	71	300		198	119	87

H=17m	d=0.6	d=0.9	d=1.2	E_{50}/c_u	H=17m	d=0.6	d=0.9	d=1.2
δ_{vm}(mm)	243	148	111	100	δ_{hm}(mm)	315	189	132
	225	137	95	200		284	166	117
	213	128	94	300		267	159	116

H=20m	d=0.6	d=0.9	d=1.2	E_{50}/c_u	H=20m	d=0.6	d=0.9	d=1.2
δ_{vm}(mm)	302	182	134	100	δ_{hm}(mm)	384	230	158
	279	170	118	200		350	205	143
	265	161	117	300		325	197	141

Generic Cases: 1909 to 1944

Table A.54. Model parameters and deformation results (Case No: 1909 to 1944).

Excavation	Soil (γ=17kN/m^3)		Diaphragm Wall(E=2.0E+7)		
H_e(m)	c_u/σ_v'	E_{50}/c_u	d	EA	EI
11-14-17-20	0.25	100-200-300	0.6	1.2E+07	3.60E+05
			0.9	1.8E+07	1.215E+06
			1.2	2.4E+07	2.88E+06

Soil	E_{50}/c_u		
HSS	100	200	300
E_{50}^{ref}	4000	8000	12000
E_{oed}^{ref}	4000	8000	12000
E_{ur}^{ref}	12000	24000	36000
G_0^{ref}	35000	50000	67500
$\gamma_{0,7}$	3.58E-04	2.51E-04	1.86E-04
ϕ	22	22	22
K_0	0.625	0.625	0.625
E_{dyn}/E_{stat}	7	5	4.5

H=11m	d=1.2	d=1.2	d=1.2	E_{50}/c_u	H=11m	d=1.2	d=1.2	d=1.2
δ_{vm}(mm)	84	60	47	100	δ_{hm}(mm)	101	75	58
	71	50	36	200		89	63	44
	62	43	33	300		77	54	43

H=14m	d=1.2	d=1.2	d=1.2	E_{50}/c_u	H=14m	d=1.2	d=1.2	d=1.2
δ_{vm}(mm)	128	87	66	100	δ_{hm}(mm)	160	108	82
	111	76	53	200		142	93	67
	98	67	51	300		124	84	63

H=17m	d=1.2	d=1.2	d=1.2	E_{50}/c_u	H=17m	d=1.2	d=1.2	d=1.2
δ_{vm}(mm)	168	114	88	100	δ_{hm}(mm)	218	141	106
	150	98	71	200		192	125	90
	134	88	68	300		171	114	86

H=20m	d=1.2	d=1.2	d=1.2	E_{50}/c_u	H=20m	d=1.2	d=1.2	d=1.2
δ_{vm}(mm)	206	143	108	100	δ_{hm}(mm)	273	175	129
	185	126	89	200		238	156	113
	168	112	86	300		212	142	107

Generic Cases: 1945 to 1980

Table A.55. Model parameters and deformation results (Case No: 1945 to 1980).

Excavation	Soil (γ=17kN/m^3)		Diaphragm Wall(E=2.0E+7)		
H_e(m)	c_u/σ_v'	E_{50}/c_u	d	EA	EI
11-14-17-20	0.3	100-200-300	0.6	1.2E+07	3.60E+05
			0.9	1.8E+07	1.215E+06
			1.2	2.4E+07	2.88E+06

Soil	E_{50}/c_u		
HSS	100	200	300
E_{50}^{ref}	5400	10800	16200
E_{oed}^{ref}	5400	10800	16200
E_{ur}^{ref}	16200	32400	48600
G_0^{ref}	40500	60750	75938
$\gamma_{0,7}$	3.40E-04	2.27E-04	1.81E-04
ϕ	26.4	26.4	26.4
K_0	0.555	0.555	0.555
E_{dyn}/E_{stat}	6	4.5	3.75

H=11m	d=0.6	d=0.9	d=1.2	E_{50}/c_u	H=11m	d=0.6	d=0.9	d=1.2
δ_{vm}(mm)	63	50	43	100	δ_{hm}(mm)	80	62	53
	50	37	32	200		63	47	41
	42	32	26	300		54	41	34

H=14m	d=0.6	d=0.9	d=1.2	E_{50}/c_u	H=14m	d=0.6	d=0.9	d=1.2
δ_{vm}(mm)	94	70	58	100	δ_{hm}(mm)	121	87	72
	76	54	44	200		96	69	57
	66	48	38	300		83	62	49

H=17m	d=0.6	d=0.9	d=1.2	E_{50}/c_u	H=17m	d=0.6	d=0.9	d=1.2
δ_{vm}(mm)	125	90	73	100	δ_{hm}(mm)	163	113	90
	102	73	60	200		130	93	75
	90	65	52	300		114	84	67

H=20m	d=0.6	d=0.9	d=1.2	E_{50}/c_u	H=20m	d=0.6	d=0.9	d=1.2
δ_{vm}(mm)	152	112	90	100	δ_{hm}(mm)	203	140	109
	127	91	75	200		165	117	94
	113	83	66	300		144	106	84

Generic Cases: 1981 to 2016

Table A.56. Model parameters and deformation results (Case No: 1981 to 2016).

Excavation	Soil (γ=17kN/m^3)		Diaphragm Wall(E=2.0E+7)		
H_e(m)	c_u/σ_v'	E_{50}/c_u	d	EA	EI
11-14-17-20	0.35	100-200-300	0.6	1.2E+07	3.60E+05
			0.9	1.8E+07	1.215E+06
			1.2	2.4E+07	2.88E+06

Soil	E_{50}/c_u		
HSS	100	200	300
E_{50}^{ref}	7000	14000	21000
E_{oed}^{ref}	7000	14000	21000
E_{ur}^{ref}	21000	42000	63000
G_0^{ref}	52500	73500	99750
$\gamma_{0,7}$	2.75E-04	1.96E-04	1.45E-04
ϕ	30	30	30
K_0	0.500	0.500	0.500
E_{dyn}/E_{stat}	6	4.2	3.8

H=11m	d=0.6	d=0.9	d=1.2	E_{50}/c_u	H=11m	d=0.6	d=0.9	d=1.2
δ_{vm}(mm)	50	44	37	100	δ_{hm}(mm)	65	54	46
	41	34	29	200		53	42	36
	32	26	23	300		42	34	29

H=14m	d=0.6	d=0.9	d=1.2	E_{50}/c_u	H=14m	d=0.6	d=0.9	d=1.2
δ_{vm}(mm)	72	59	49	100	δ_{hm}(mm)	93	73	60
	60	47	39	200		76	60	49
	49	39	32	300		62	50	41

H=17m	d=0.6	d=0.9	d=1.2	E_{50}/c_u	H=17m	d=0.6	d=0.9	d=1.2
δ_{vm}(mm)	95	76	63	100	δ_{hm}(mm)	127	94	77
	80	62	51	200		104	78	63
	67	53	44	300		85	67	55

H=20m	d=0.6	d=0.9	d=1.2	E_{50}/c_u	H=20m	d=0.6	d=0.9	d=1.2
δ_{vm}(mm)	117	93	76	100	δ_{hm}(mm)	156	116	93
	100	78	64	200		130	98	79
	85	67	56	300		108	85	70

Model Group:15

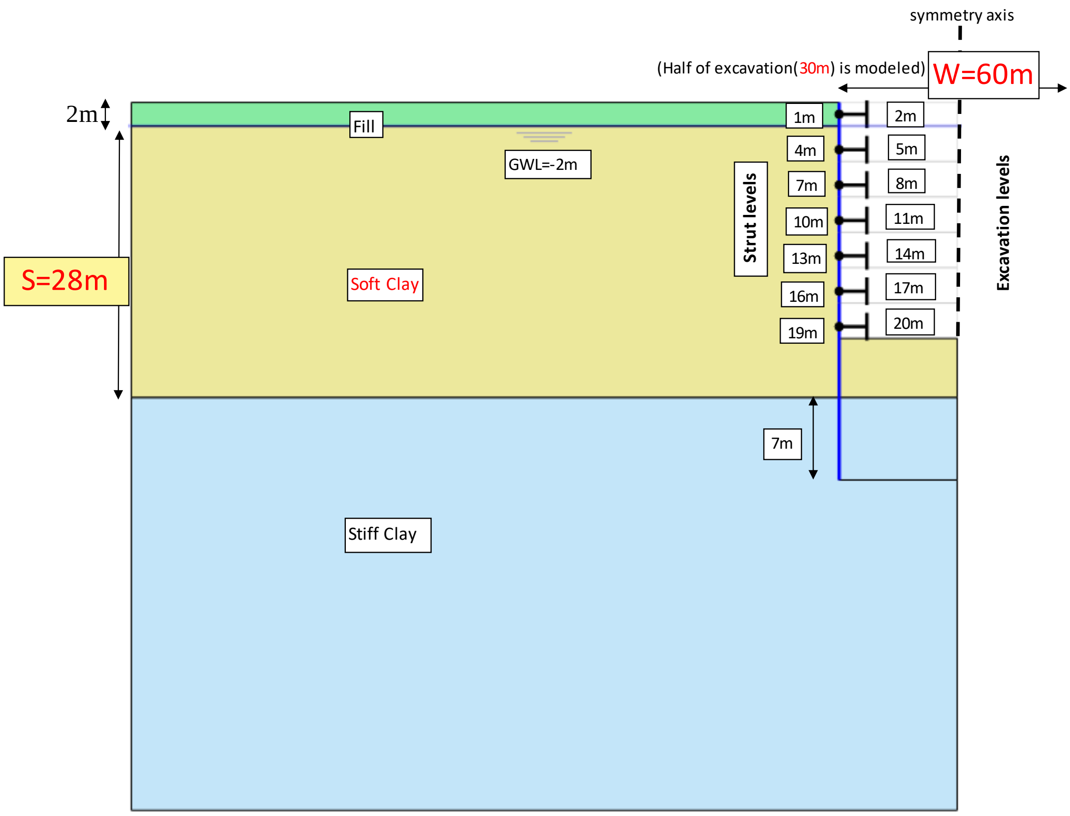

Figure A.15. Model Geometry-15.

Table B. Soil and structure parameters.

Default Soil Parameters		
Stiff Clay		Fill
HS		HS
Undrained(A)		Drained
E_{50}^{ref}	1.00E+05	1.50E+04
E_{oed}^{ref}	1.00E+05	1.50E+04
E_{ur}^{ref}	3.00E+05	3.00E+04
ϕ'	26	30
K_0	0.562	0.5
c'_{ref}	25	1
v'_{ur}	0.2	0.2
p_{ref}	100	100
R_f	0.9	0.9
$\gamma_{unsat/sat}$	20/20	16/20
R_{inter}	0.65	0.65
m	1	1

Range of parameters	
c_u/σ'_v	0.20-0.25-0.30-0.35
E_{50}/c_u	100-200-300
γ	15-17-19
S	25-30-35
W	20-40-60
H_e	11-14-17-20
$\ln(EI/\gamma_w h_{avg}^4)$	6.097-7.313-8.176

Diaphragm Wall (E=2.0E+7)		
d	EA	EI
0.6	1.2E+07	3.60E+05
0.9	1.8E+07	1.215E+06
1.2	2.4E+07	2.88E+06

Strut	
EA	3.80E+06
$L_{spacing}$	5m
h_{avg}	3m

Generic Cases: 2017 to 2052

Table A.57. Model parameters and deformation results (Case No: 2017 to 2052).

Excavation	Soil(γ=17kN/m^3)		Diaphragm Wall(E=2.0E+7)		
H_e(m)	c_u/σ_v'	E_{50}/c_u	d	EA	EI
11-14-17-20	0.2	100-200-300	0.6	1.2E+07	3.60E+05
			0.9	1.8E+07	1.215E+06
			1.2	2.4E+07	2.88E+06

Soft Soil	E_{50}/c_u		
HSS	100	200	300
E_{50}^{ref}	2895	5789	8685
E_{oed}^{ref}	2895	5789	8685
E_{ur}^{ref}	8685	17367	26055
G_0^{ref}	30759	43418	54281
$\gamma_{0,7}$	3.59E-04	2.54E-04	2.03E-04
ϕ	18	18	18
K_0	0.691	0.691	0.691
E_{dyn}/E_{stat}	8.5	6	5

H=11m	d=0.6	d=0.9	d=1.2	E_{50}/c_u	H=11m	d=0.6	d=0.9	d=1.2
δ_{vm}(mm)	140	96	69	100	δ_{hm}(mm)	172	115	86
	125	84	59	200		150	102	74
	114	78	57	300		138	92	68

H=14m	d=0.6	d=0.9	d=1.2	E_{50}/c_u	H=14m	d=0.6	d=0.9	d=1.2
δ_{vm}(mm)	214	135	99	100	δ_{hm}(mm)	264	161	121
	195	124	89	200		239	150	107
	182	113	85	300		218	140	102

H=17m	d=0.6	d=0.9	d=1.2	E_{50}/c_u	H=17m	d=0.6	d=0.9	d=1.2
δ_{vm}(mm)	279	176	130	100	δ_{hm}(mm)	347	213	154
	256	163	118	200		319	198	140
	244	150	112	300		298	185	134

H=20m	d=0.6	d=0.9	d=1.2	E_{50}/c_u	H=20m	d=0.6	d=0.9	d=1.2
δ_{vm}(mm)	354	217	155	100	δ_{hm}(mm)	430	259	183
	327	204	144	200		391	242	173
	303	192	138	300		369	227	164

Generic Cases: 2053 to 2088

Table A.58. Model parameters and deformation results (Case No: 2053 to 2088).

Excavation	Soil (γ=17kN/m^3)		Diaphragm Wall(E=2.0E+7)		
H_e(m)	c_u/σ_v'	E_{50}/c_u	d	EA	EI
11-14-17-20	0.25	100-200-300	0.6	1.2E+07	3.60E+05
			0.9	1.8E+07	1.215E+06
			1.2	2.4E+07	2.88E+06

Soil	E_{50}/c_u		
HSS	100	200	300
E_{50}^{ref}	4000	8000	12000
E_{oed}^{ref}	4000	8000	12000
E_{ur}^{ref}	12000	24000	36000
G_0^{ref}	35000	50000	67500
$\gamma_{0,7}$	3.58E-04	2.51E-04	1.86E-04
ϕ	22	22	22
K_0	0.625	0.625	0.625
E_{dyn}/E_{stat}	7	5	4.5

H=11m	d=0.6	d=0.9	d=1.2	E_{50}/c_u	H=11m	d=0.6	d=0.9	d=1.2
δ_{vm}(mm)	100	73	58	100	δ_{hm}(mm)	122	91	70
	85	61	44	200		105	75	54
	73	51	41	300		90	65	51

H=14m	d=0.6	d=0.9	d=1.2	E_{50}/c_u	H=14m	d=0.6	d=0.9	d=1.2
δ_{vm}(mm)	150	104	79	100	δ_{hm}(mm)	188	128	95
	130	91	65	200		163	112	80
	114	79	61	300		143	98	76

H=17m	d=0.6	d=0.9	d=1.2	E_{50}/c_u	H=17m	d=0.6	d=0.9	d=1.2
δ_{vm}(mm)	197	136	105	100	δ_{hm}(mm)	252	166	126
	176	118	88	200		220	149	108
	157	106	83	300		197	131	102

H=20m	d=0.6	d=0.9	d=1.2	E_{50}/c_u	H=20m	d=0.6	d=0.9	d=1.2
δ_{vm}(mm)	243	168	127	100	δ_{hm}(mm)	308	207	152
	216	148	110	200		270	185	135
	195	135	105	300		244	166	128

Generic Cases: 2089 to 2124

Table A.59. Model parameters and deformation results (Case No: 2089 to 2124).

Excavation	Soil (γ=17kN/m^3)		Diaphragm Wall(E=2.0E+7)		
H_e(m)	c_u/σ_v'	E_{50}/c_u	d	EA	EI
11-14-17-20	0.3	100-200-300	0.6	1.2E+07	3.60E+05
			0.9	1.8E+07	1.215E+06
			1.2	2.4E+07	2.88E+06

Soil	E_{50}/c_u		
HSS	100	200	300
E_{50}^{ref}	5400	10800	16200
E_{oed}^{ref}	5400	10800	16200
E_{ur}^{ref}	16200	32400	48600
G_0^{ref}	40500	60750	75938
$\gamma_{0,7}$	3.40E-04	2.27E-04	1.81E-04
ϕ	26.4	26.4	26.4
K_0	0.555	0.555	0.555
E_{dyn}/E_{stat}	6	4.5	3.75

H=11m	d=0.6	d=0.9	d=1.2	E_{50}/c_u	H=11m	d=0.6	d=0.9	d=1.2
δ_{vm}(mm)	79	62	53	100	δ_{hm}(mm)	97	76	63
	62	49	41	200		78	61	50
	52	41	35	300		64	52	44

H=14m	d=0.6	d=0.9	d=1.2	E_{50}/c_u	H=14m	d=0.6	d=0.9	d=1.2
δ_{vm}(mm)	114	85	70	100	δ_{hm}(mm)	144	105	84
	92	69	56	200		115	87	71
	79	60	49	300		99	75	62

H=17m	d=0.6	d=0.9	d=1.2	E_{50}/c_u	H=17m	d=0.6	d=0.9	d=1.2
δ_{vm}(mm)	147	110	91	100	δ_{hm}(mm)	189	135	107
	123	90	74	200		156	114	92
	109	81	66	300		137	100	82

H=20m	d=0.6	d=0.9	d=1.2	E_{50}/c_u	H=20m	d=0.6	d=0.9	d=1.2
δ_{vm}(mm)	179	135	110	100	δ_{hm}(mm)	232	166	131
	153	113	92	200		194	142	115
	137	103	83	300		171	127	103

Generic Cases: 2125 to 2160

Table A.59. Model parameters and deformation results (Case No: 2125 to 2160).

Excavation	Soil (γ=17kN/m^3)		Diaphragm Wall(E=2.0E+7)		
H_e(m)	c_u/σ_v'	E_{50}/c_u	d	EA	EI
11-14-17-20	0.35	100-200-300	0.6	1.2E+07	3.60E+05
			0.9	1.8E+07	1.215E+06
			1.2	2.4E+07	2.88E+06

Soil	E_{50}/c_u		
HSS	100	200	300
E_{50}^{ref}	7000	14000	21000
E_{oed}^{ref}	7000	14000	21000
E_{ur}^{ref}	21000	42000	63000
G_0^{ref}	52500	73500	99750
$\gamma_{0,7}$	2.75E-04	1.96E-04	1.45E-04
ϕ	30	30	30
K_0	0.500	0.500	0.500
E_{dyn}/E_{stat}	6	4.2	3.8

H=11m	d=0.6	d=0.9	d=1.2	E_{50}/c_u	H=11m	d=0.6	d=0.9	d=1.2
δ_{vm}(mm)	58	55	47	100	δ_{hm}(mm)	75	69	58
	51	43	36	200		65	54	45
	40	33	29	300		52	43	37

H=14m	d=0.6	d=0.9	d=1.2	E_{50}/c_u	H=14m	d=0.6	d=0.9	d=1.2
δ_{vm}(mm)	84	75	62	100	δ_{hm}(mm)	107	92	76
	72	58	50	200		92	74	62
	61	48	41	300		76	61	52

H=17m	d=0.6	d=0.9	d=1.2	E_{50}/c_u	H=17m	d=0.6	d=0.9	d=1.2
δ_{vm}(mm)	110	95	80	100	δ_{hm}(mm)	143	116	95
	96	76	64	200		122	95	80
	83	63	54	300		104	81	68

H=20m	d=0.6	d=0.9	d=1.2	E_{50}/c_u	H=20m	d=0.6	d=0.9	d=1.2
δ_{vm}(mm)	138	116	96	100	δ_{hm}(mm)	178	142	114
	122	95	80	200		153	119	99
	106	83	69	300		131	103	87

Model Group:16

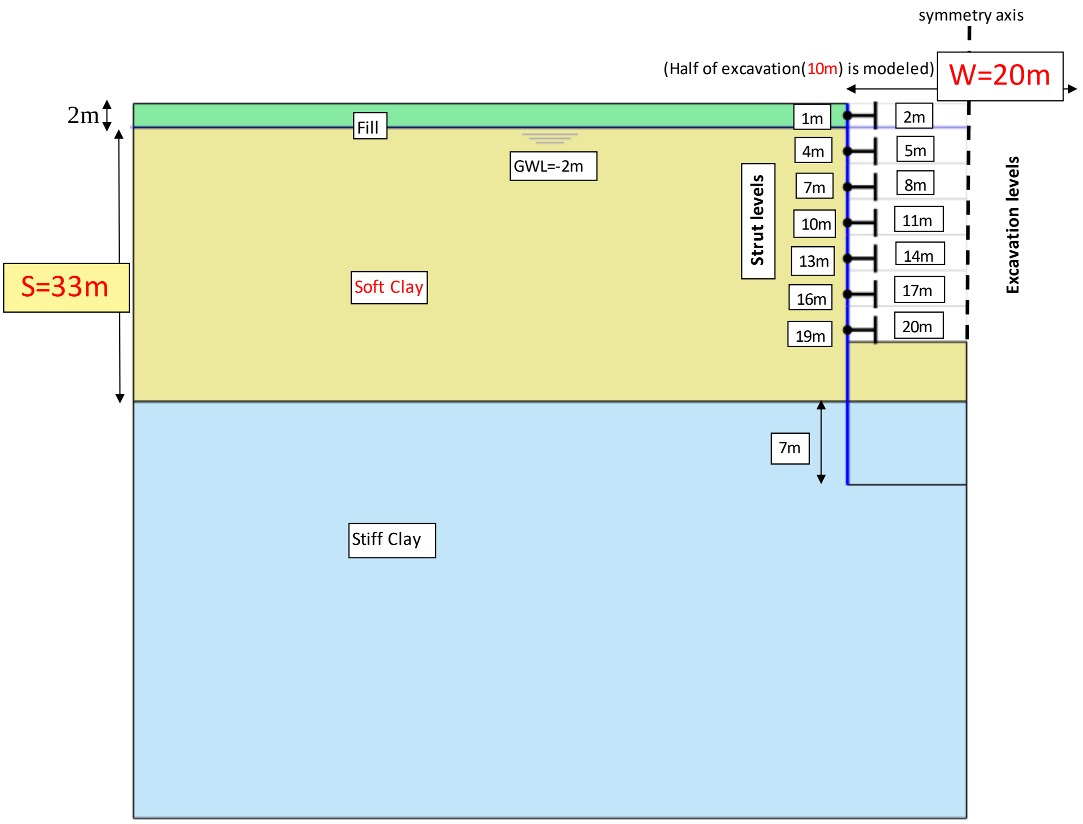

Figure A.16. Model Geometry-16.

Table B. Soil and structure parameters.

Default Soil Parameters		
	Stiff Clay	Fill
	HS	HS
	Undrained(A)	Drained
E_{50}^{ref}	1.00E+05	1.50E+04
E_{oed}^{ref}	1.00E+05	1.50E+04
E_{ur}^{ref}	3.00E+05	4.50E+04
ϕ'	26	30
K_0	0.562	0.5
c'_{ref}	25	1
v'_{ur}	0.2	0.2
p_{ref}	100	100
R_f	0.9	0.9
$\gamma_{unsat/sat}$	20/20	16/20
R_{inter}	0.65	0.65
m	1	1

Range of parameters	
c_u/σ'_v	0.20-0.25-0.30-0.35
E_{50}/c_u	100-200-300
γ	15-17-19
S	25-30-35
W	20-40-60
H_e	11-14-17-20
$\ln(EI/\gamma_w h_{avg}^4)$	6.097-7.313-8.176

Diaphragm Wall (E=2.0E+7)		
d	EA	EI
0.6	1.2E+07	3.60E+05
0.9	1.8E+07	1.215E+06
1.2	2.4E+07	2.88E+06

Strut	
EA	3.80E+06
$L_{spacing}$	5m
h_{avg}	3m

Generic Cases: 2161 to 2196

Table A.60. Model parameters and deformation results (Case No: 2161 to 2196).

Excavation	Soil(γ=17kN/m^3)		Diaphragm Wall(E=2.0E+7)		
H_e(m)	c_u/σ_v'	E_{50}/c_u	d	EA	EI
11-14-17-20	0.2	100-200-300	0.6	1.2E+07	3.60E+05
			0.9	1.8E+07	1.215E+06
			1.2	2.4E+07	2.88E+06

Soft Soil	E_{50}/c_u		
HSS	100	200	300
E_{50}^{ref}	2895	5789	8685
E_{oed}^{ref}	2895	5789	8685
E_{ur}^{ref}	8685	17367	26055
G_0^{ref}	30759	43418	54281
$\gamma_{0,7}$	3.59E-04	2.54E-04	2.03E-04
ϕ	18	18	18
K_0	0.691	0.691	0.691
E_{dyn}/E_{stat}	8.5	6	5

H=11m	d=0.6	d=0.9	d=1.2	E_{50}/c_u	H=11m	d=0.6	d=0.9	d=1.2
δ_{vm}(mm)	98	64	46	100	δ_{hm}(mm)	126	80	57
	86	55	40	200		110	67	51
	78	49	36	300		98	62	46

H=14m	d=0.6	d=0.9	d=1.2	E_{50}/c_u	H=14m	d=0.6	d=0.9	d=1.2
δ_{vm}(mm)	168	99	69	100	δ_{hm}(mm)	217	127	86
	151	88	63	200		191	112	80
	138	81	57	300		175	103	73

H=17m	d=0.6	d=0.9	d=1.2	E_{50}/c_u	H=17m	d=0.6	d=0.9	d=1.2
δ_{vm}(mm)	240	134	93	100	δ_{hm}(mm)	317	178	117
	218	122	86	200		282	161	111
	204	113	79	300		265	147	104

H=20m	d=0.6	d=0.9	d=1.2	E_{50}/c_u	H=20m	d=0.6	d=0.9	d=1.2
δ_{vm}(mm)	311	173	119	100	δ_{hm}(mm)	409	229	153
	286	159	110	200		367	208	143
	266	147	104	300		349	191	134

Generic Cases: 2197 to 2232

Table A.61. Model parameters and deformation results (Case No: 2197 to 2232).

Excavation	Soil (γ=17kN/m^3)		Diaphragm Wall(E=2.0E+7)		
H_e(m)	c_u/σ_v'	E_{50}/c_u	d	EA	EI
11-14-17-20	0.25	100-200-300	0.6	1.2E+07	3.60E+05
			0.9	1.8E+07	1.215E+06
			1.2	2.4E+07	2.88E+06

Soil	E_{50}/c_u		
HSS	100	200	300
E_{50}^{ref}	4000	8000	12000
E_{oed}^{ref}	4000	8000	12000
E_{ur}^{ref}	12000	24000	36000
G_0^{ref}	35000	50000	67500
$\gamma_{0,7}$	3.58E-04	2.51E-04	1.86E-04
ϕ	22	22	22
K_0	0.625	0.625	0.625
E_{dyn}/E_{stat}	7	5	4.5

H=11m	d=0.6	d=0.9	d=1.2	E_{50}/c_u	H=11m	d=0.6	d=0.9	d=1.2
δ_{vm}(mm)	65	44	31	100	δ_{hm}(mm)	82	56	41
	55	37	29	200		70	46	36
	47	32	25	300		60	41	32

H=14m	d=0.6	d=0.9	d=1.2	E_{50}/c_u	H=14m	d=0.6	d=0.9	d=1.2
δ_{vm}(mm)	106	67	48	100	δ_{hm}(mm)	140	89	63
	89	58	44	200		116	73	57
	77	52	39	300		100	66	50

H=17m	d=0.6	d=0.9	d=1.2	E_{50}/c_u	H=17m	d=0.6	d=0.9	d=1.2
δ_{vm}(mm)	152	94	65	100	δ_{hm}(mm)	208	127	89
	129	82	60	200		174	107	80
	113	73	54	300		149	96	71

H=20m	d=0.6	d=0.9	d=1.2	E_{50}/c_u	H=20m	d=0.6	d=0.9	d=1.2
δ_{vm}(mm)	194	119	85	100	δ_{hm}(mm)	273	163	114
	168	105	78	200		228	140	104
	149	96	70	300		198	127	94

Generic Cases: 2233 to 2268

Table A.62. Model parameters and deformation results (Case No: 2233 to 2268).

Excavation	Soil(γ=17kN/m^3)		Diaphragm Wall(E=2.0E+7)		
H_e(m)	c_u/σ_v'	E_{50}/c_u	d	EA	EI
11-14-17-20	0.3	100-200-300	0.6	1.2E+07	3.60E+05
			0.9	1.8E+07	1.215E+06
			1.2	2.4E+07	2.88E+06

Soil	E_{50}/c_u		
HSS	100	200	300
E_{50}^{ref}	5400	10800	16200
E_{oed}^{ref}	5400	10800	16200
E_{ur}^{ref}	16200	32400	48600
G_0^{ref}	40500	60750	75938
$\gamma_{0,7}$	3.40E-04	2.27E-04	1.81E-04
ϕ	26.4	26.4	26.4
K_0	0.555	0.555	0.555
E_{dyn}/E_{stat}	6	4.5	3.75

H=11m	d=0.6	d=0.9	d=1.2	E_{50}/c_u	H=11m	d=0.6	d=0.9	d=1.2
δ_{vm}(mm)	47	33	29	100	δ_{hm}(mm)	60	43	36
	37	26	20	200		48	33	26
	31	23	19	300		41	30	24

H=14m	d=0.6	d=0.9	d=1.2	E_{50}/c_u	H=14m	d=0.6	d=0.9	d=1.2
δ_{vm}(mm)	73	50	41	100	δ_{hm}(mm)	95	64	51
	57	39	30	200		76	52	39
	49	36	28	300		66	46	37

H=17m	d=0.6	d=0.9	d=1.2	E_{50}/c_u	H=17m	d=0.6	d=0.9	d=1.2
δ_{vm}(mm)	103	68	54	100	δ_{hm}(mm)	139	90	70
	81	55	41	200		110	74	55
	69	50	39	300		94	67	51

H=20m	d=0.6	d=0.9	d=1.2	E_{50}/c_u	H=20m	d=0.6	d=0.9	d=1.2
δ_{vm}(mm)	132	85	68	100	δ_{hm}(mm)	186	117	89
	105	71	53	200		147	98	73
	91	65	50	300		123	88	68

Generic Cases: 2269 to 2304

Table A.63. Model parameters and deformation results (Case No: 2269 to 2304).

Excavation	Soil(γ=17kN/m^3)		Diaphragm Wall(E=2.0E+7)		
H_e(m)	c_u/σ_v'	E_{50}/c_u	d	EA	EI
11-14-17-20	0.35	100-200-300	0.6	1.2E+07	3.60E+05
			0.9	1.8E+07	1.215E+06
			1.2	2.4E+07	2.88E+06

Soil	E_{50}/c_u		
HSS	100	200	300
E_{50}^{ref}	7000	14000	21000
E_{oed}^{ref}	7000	14000	21000
E_{ur}^{ref}	21000	42000	63000
G_0^{ref}	52500	73500	99750
$\gamma_{0,7}$	2.75E-04	1.96E-04	1.45E-04
ϕ	30	30	30
K_0	0.500	0.500	0.500
E_{dyn}/E_{stat}	6	4.2	3.8

H=11m	d=0.6	d=0.9	d=1.2	E_{50}/c_u	H=11m	d=0.6	d=0.9	d=1.2
δ_{vm}(mm)	39	30	23	100	δ_{hm}(mm)	49	37	29
	29	23	17	200		37	29	22
	24	18	15	300		31	23	19

H=14m	d=0.6	d=0.9	d=1.2	E_{50}/c_u	H=14m	d=0.6	d=0.9	d=1.2
δ_{vm}(mm)	56	42	31	100	δ_{hm}(mm)	73	52	38
	43	33	24	200		56	42	32
	36	27	22	300		47	35	28

H=17m	d=0.6	d=0.9	d=1.2	E_{50}/c_u	H=17m	d=0.6	d=0.9	d=1.2
δ_{vm}(mm)	77	56	40	100	δ_{hm}(mm)	102	70	51
	59	45	33	200		80	59	44
	50	37	29	300		66	49	39

H=20m	d=0.6	d=0.9	d=1.2	E_{50}/c_u	H=20m	d=0.6	d=0.9	d=1.2
δ_{vm}(mm)	97	69	49	100	δ_{hm}(mm)	134	91	66
	77	57	43	200		105	77	58
	65	48	39	300		88	65	51

Model Group:17

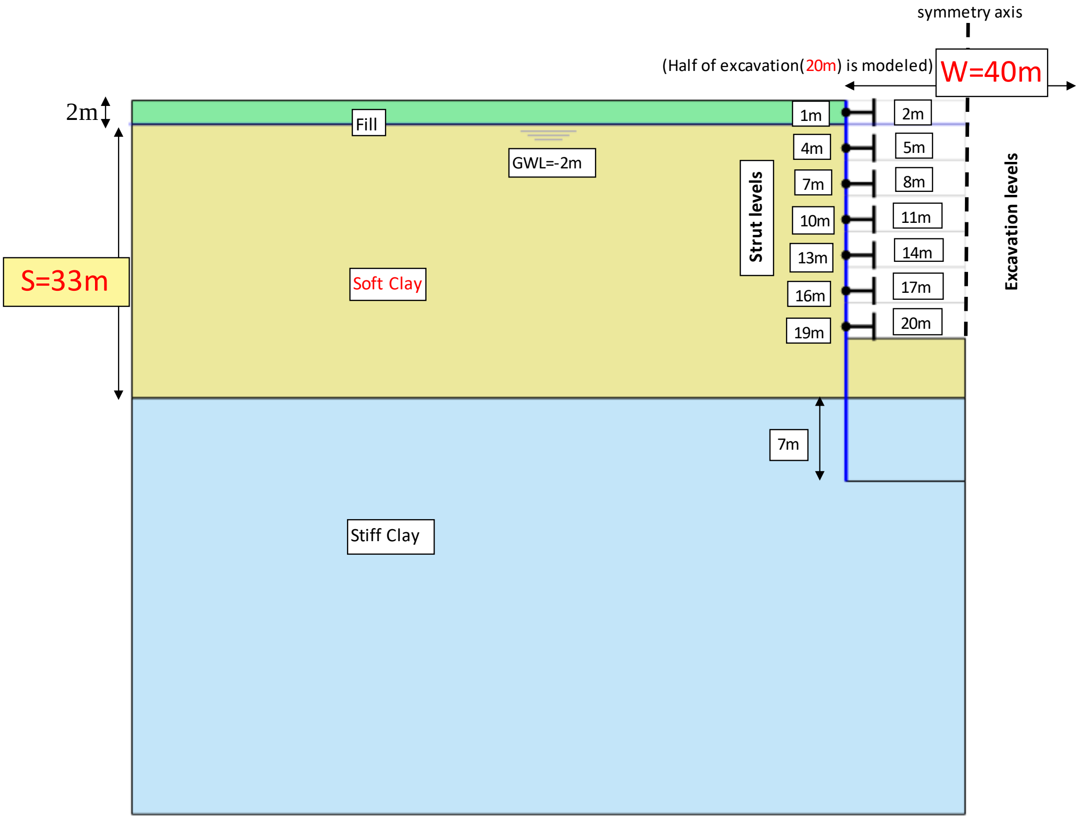

Figure A.17. Model Geometry-17.

Table B. Soil and structure parameters

Default Soil Parameters		
	Stiff Clay	Fill
	HS	HS
	Undrained(A)	Drained
E_{50}^{ref}	1.00E+05	1.50E+04
E_{oed}^{ref}	1.00E+05	1.50E+04
E_{ur}^{ref}	3.00E+05	4.50E+04
ϕ'	26	30
K_0	0.562	0.5
c'_{ref}	25	1
v'_{ur}	0.2	0.2
p_{ref}	100	100
R_f	0.9	0.9
$\gamma_{unsat/sat}$	20/20	16/20
R_{inter}	0.65	0.65
m	1	1

Range of parameters	
c_u/σ'_v	0.20-0.25-0.30-0.35
E_{50}/c_u	100-200-300
γ	15-17-19
S	25-30-35
W	20-40-60
H_e	11-14-17-20
$\ln(EI/\gamma_w h_{avg}^4)$	6.097-7.313-8.176

Diaphragm Wall (E=2.0E+7)		
d	EA	EI
0.6	1.2E+07	3.60E+05
0.9	1.8E+07	1.215E+06
1.2	2.4E+07	2.88E+06

Strut	
EA	3.80E+06
$L_{spacing}$	5m
h_{avg}	3m

Generic Cases: 2305 to 2340

Table A.64. Model parameters and deformation results (Case No: 2305 to 2340).

Excavation	Soil(γ=17kN/m^3)		Diaphragm Wall(E=2.0E+7)		
H_e(m)	c_u/σ_v'	E_{50}/c_u	d	EA	EI
11-14-17-20	0.2	100-200-300	0.6	1.2E+07	3.60E+05
			0.9	1.8E+07	1.215E+06
			1.2	2.4E+07	2.88E+06

Soft Soil	E_{50}/c_u		
HSS	100	200	300
E_{50}^{ref}	2895	5789	8685
E_{oed}^{ref}	2895	5789	8685
E_{ur}^{ref}	8685	17367	26055
G_0^{ref}	30759	43418	54281
$\gamma_{0,7}$	3.59E-04	2.54E-04	2.03E-04
ϕ	18	18	18
K_0	0.691	0.691	0.691
E_{dyn}/E_{stat}	8.5	6	5

H=11m	d=0.6	d=0.9	d=1.2	E_{50}/c_u	H=11m	d=0.6	d=0.9	d=1.2
δ_{vm}(mm)	110	75	57	100	δ_{hm}(mm)	139	92	68
	98	62	45	200		120	76	55
	88	56	43	300		111	70	53

H=14m	d=0.6	d=0.9	d=1.2	E_{50}/c_u	H=14m	d=0.6	d=0.9	d=1.2
δ_{vm}(mm)	187	116	84	100	δ_{hm}(mm)	242	144	101
	164	99	67	200		207	124	85
	151	90	66	300		191	115	83

H=17m	d=0.6	d=0.9	d=1.2	E_{50}/c_u	H=17m	d=0.6	d=0.9	d=1.2
δ_{vm}(mm)	260	155	109	100	δ_{hm}(mm)	346	198	136
	235	135	91	200		303	175	119
	220	126	90	300		284	161	115

H=20m	d=0.6	d=0.9	d=1.2	E_{50}/c_u	H=20m	d=0.6	d=0.9	d=1.2
δ_{vm}(mm)	328	194	134	100	δ_{hm}(mm)	442	254	170
	298	173	115	200		393	224	153
	281	163	114	300		367	206	147

Generic Cases: 2341 to 2376

Table A.65. Model parameters and deformation results (Case No: 2341 to 2376).

Excavation	Soil (γ=17kN/m^3)		Diaphragm Wall(E=2.0E+7)		
H_e(m)	c_u/σ_v'	E_{50}/c_u	d	EA	EI
11-14-17-20	0.25	100-200-300	0.6	1.2E+07	3.60E+05
			0.9	1.8E+07	1.215E+06
			1.2	2.4E+07	2.88E+06

Soil	E_{50}/c_u		
HSS	100	200	300
E_{50}^{ref}	4000	8000	12000
E_{oed}^{ref}	4000	8000	12000
E_{ur}^{ref}	12000	24000	36000
G_0^{ref}	35000	50000	67500
$\gamma_{0,7}$	3.58E-04	2.51E-04	1.86E-04
ϕ	22	22	22
K_0	0.625	0.625	0.625
E_{dyn}/E_{stat}	7	5	4.5

H=11m	d=0.6	d=0.9	d=1.2	E_{50}/c_u	H=11m	d=0.6	d=0.9	d=1.2
δ_{vm}(mm)	69	47	41	100	δ_{hm}(mm)	88	59	52
	62	45	33	200		78	56	42
	52	37	30	300		67	47	38

H=14m	d=0.6	d=0.9	d=1.2	E_{50}/c_u	H=14m	d=0.6	d=0.9	d=1.2
δ_{vm}(mm)	113	73	60	100	δ_{hm}(mm)	151	94	74
	99	69	50	200		129	88	64
	86	59	46	300		110	75	58

H=17m	d=0.6	d=0.9	d=1.2	E_{50}/c_u	H=17m	d=0.6	d=0.9	d=1.2
δ_{vm}(mm)	162	100	79	100	δ_{hm}(mm)	221	133	99
	142	95	68	200		188	123	88
	125	82	63	300		163	107	81

H=20m	d=0.6	d=0.9	d=1.2	E_{50}/c_u	H=20m	d=0.6	d=0.9	d=1.2
δ_{vm}(mm)	207	128	98	100	δ_{hm}(mm)	291	175	128
	183	119	87	200		244	158	114
	163	106	80	300		214	139	104

Generic Cases: 2377 to 2412

Table A.66. Model parameters and deformation results (Case No: 2377 to 2412).

Excavation	Soil(γ=17kN/m^3)		Diaphragm Wall(E=2.0E+7)		
H_e(m)	c_u/σ_v'	E_{50}/c_u	d	EA	EI
11-14-17-20	0.3	100-200-300	0.6	1.2E+07	3.60E+05
			0.9	1.8E+07	1.215E+06
			1.2	2.4E+07	2.88E+06

Soil	E_{50}/c_u		
HSS	100	200	300
E_{50}^{ref}	5400	10800	16200
E_{oed}^{ref}	5400	10800	16200
E_{ur}^{ref}	16200	32400	48600
G_0^{ref}	40500	60750	75938
$\gamma_{0,7}$	3.40E-04	2.27E-04	1.81E-04
ϕ	26.4	26.4	26.4
K_0	0.555	0.555	0.555
E_{dyn}/E_{stat}	6	4.5	3.75

H=11m	d=0.6	d=0.9	d=1.2	E_{50}/c_u	H=11m	d=0.6	d=0.9	d=1.2
δ_{vm}(mm)	53	45	40	100	δ_{hm}(mm)	65	57	49
	44	33	25	200		55	42	33
	37	28	23	300		48	36	31

H=14m	d=0.6	d=0.9	d=1.2	E_{50}/c_u	H=14m	d=0.6	d=0.9	d=1.2
δ_{vm}(mm)	78	64	53	100	δ_{hm}(mm)	99	81	66
	66	48	37	200		85	61	47
	56	42	34	300		73	54	44

H=17m	d=0.6	d=0.9	d=1.2	E_{50}/c_u	H=17m	d=0.6	d=0.9	d=1.2
δ_{vm}(mm)	106	84	68	100	δ_{hm}(mm)	145	107	85
	91	65	50	200		120	84	64
	79	58	46	300		103	75	59

H=20m	d=0.6	d=0.9	d=1.2	E_{50}/c_u	H=20m	d=0.6	d=0.9	d=1.2
δ_{vm}(mm)	137	104	84	100	δ_{hm}(mm)	192	135	105
	116	82	63	200		158	108	82
	102	74	58	300		133	97	77

Generic Cases: 2413 to 2448

Table A.67. Model parameters and deformation results (Case No: 2413 to 2448).

Excavation	Soil(γ=17kN/m^3)		Diaphragm Wall(E=2.0E+7)		
H_e(m)	c_u/σ_v'	E_{50}/c_u	d	EA	EI
11-14-17-20	0.35	100-200-300	0.6	1.2E+07	3.60E+05
			0.9	1.8E+07	1.215E+06
			1.2	2.4E+07	2.88E+06

Soil	E_{50}/c_u		
HSS	100	200	300
E_{50}^{ref}	7000	14000	21000
E_{oed}^{ref}	7000	14000	21000
E_{ur}^{ref}	21000	42000	63000
G_0^{ref}	52500	73500	99750
$\gamma_{0,7}$	2.75E-04	1.96E-04	1.45E-04
ϕ	30	30	30
K_0	0.500	0.500	0.500
E_{dyn}/E_{stat}	6	4.2	3.8

H=11m	d=0.6	d=0.9	d=1.2	E_{50}/c_u	H=11m	d=0.6	d=0.9	d=1.2
δ_{vm}(mm)	48	41	34	100	δ_{hm}(mm)	60	50	42
	37	30	26	200		47	38	34
	29	24	21	300		37	31	27

H=14m	d=0.6	d=0.9	d=1.2	E_{50}/c_u	H=14m	d=0.6	d=0.9	d=1.2
δ_{vm}(mm)	67	53	44	100	δ_{hm}(mm)	84	66	54
	52	40	34	200		67	51	44
	41	33	28	300		54	43	36

H=17m	d=0.6	d=0.9	d=1.2	E_{50}/c_u	H=17m	d=0.6	d=0.9	d=1.2
δ_{vm}(mm)	89	67	56	100	δ_{hm}(mm)	116	87	69
	70	54	44	200		92	69	57
	57	45	37	300		74	58	48

H=20m	d=0.6	d=0.9	d=1.2	E_{50}/c_u	H=20m	d=0.6	d=0.9	d=1.2
δ_{vm}(mm)	112	82	67	100	δ_{hm}(mm)	151	108	84
	88	67	55	200		117	88	71
	73	57	47	300		95	74	61

Model Group:18

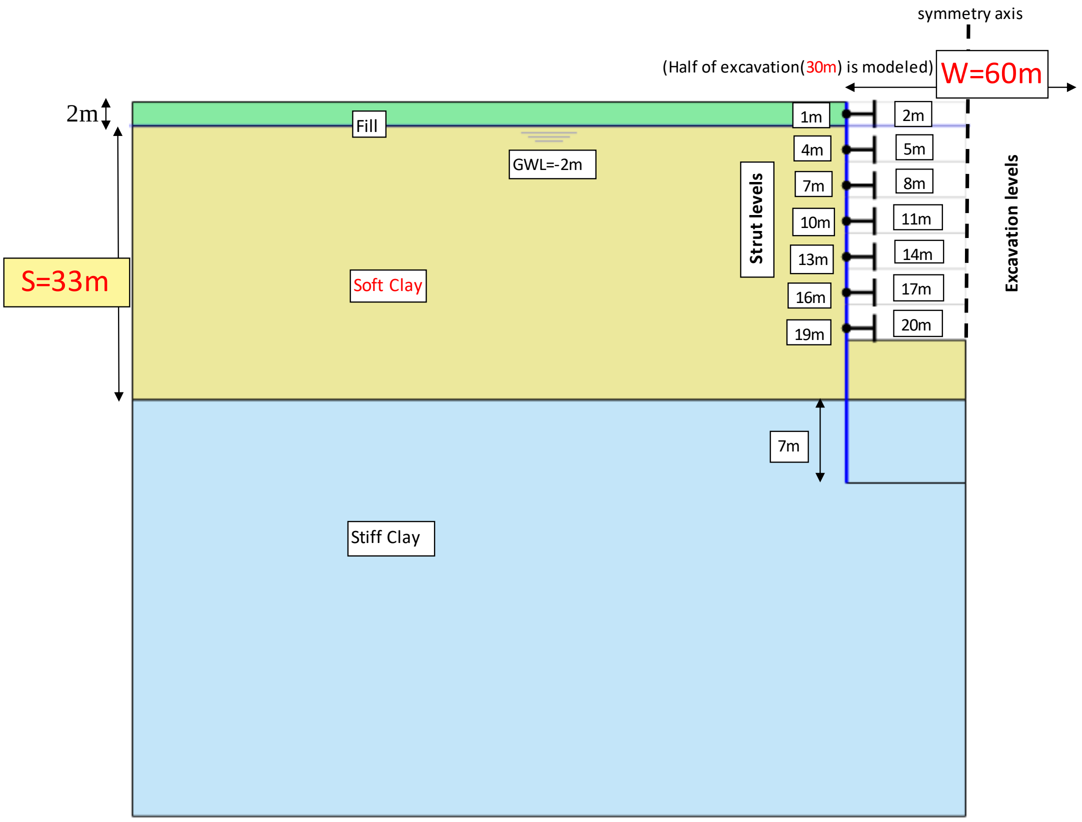

Figure A.18. Model Geometry-18.

Table B. Soil and structure parameters

Default Soil Parameters		
	Stiff Clay	Fill
	HS	HS
	Undrained(A)	Drained
E_{50}^{ref}	1.00E+05	1.50E+04
E_{oed}^{ref}	1.00E+05	1.50E+04
E_{ur}^{ref}	3.00E+05	4.50E+04
ϕ'	26	30
K_0	0.562	0.5
c'_{ref}	25	1
v'_{ur}	0.2	0.2
p_{ref}	100	100
R_f	0.9	0.9
$\gamma_{unsat/sat}$	20/20	16/20
R_{inter}	0.65	0.65
m	1	1

Range of parameters	
c_u/σ'_v	0.20-0.25-0.30-0.35
E_{50}/c_u	100-200-300
γ	15-17-19
S	25-30-35
W	20-40-60
H_e	11-14-17-20
$\ln(EI/\gamma_w h_{avg}^4)$	6.097-7.313-8.176

Diaphragm Wall (E=2.0E+7)		
d	EA	EI
0.6	1.2E+07	3.60E+05
0.9	1.8E+07	1.215E+06
1.2	2.4E+07	2.88E+06

Strut	
EA	3.80E+06
$L_{spacing}$	5m
h_{avg}	3m

Generic Cases: 2449 to 2484

Table A.68. Model parameters and deformation results (Case No: 2449 to 2484).

Excavation	Soil(γ=17kN/m^3)		Diaphragm Wall(E=2.0E+7)		
H_e(m)	c_u/σ_v'	E_{50}/c_u	d	EA	EI
11-14-17-20	0.2	100-200-300	0.6	1.2E+07	3.60E+05
			0.9	1.8E+07	1.215E+06
			1.2	2.4E+07	2.88E+06

Soft Soil	E_{50}/c_u		
HSS	100	200	300
E_{50}^{ref}	2895	5789	8685
E_{oed}^{ref}	2895	5789	8685
E_{ur}^{ref}	8685	17367	26055
G_0^{ref}	30759	43418	54281
$\gamma_{0,7}$	3.59E-04	2.54E-04	2.03E-04
ϕ	18	18	18
K_0	0.691	0.691	0.691
E_{dyn}/E_{stat}	8.5	6	5

H=11m	d=0.6	d=0.9	d=1.2	E_{50}/c_u	H=11m	d=0.6	d=0.9	d=1.2
δ_{vm}(mm)	147	103	71	100	δ_{hm}(mm)	177	126	87
	132	91	64	200		155	111	76
	119	81	61	300		143	99	73

H=14m	d=0.6	d=0.9	d=1.2	E_{50}/c_u	H=14m	d=0.6	d=0.9	d=1.2
δ_{vm}(mm)	242	157	109	100	δ_{hm}(mm)	303	193	133
	220	141	99	200		269	171	118
	203	129	95	300		250	156	115

H=17m	d=0.6	d=0.9	d=1.2	E_{50}/c_u	H=17m	d=0.6	d=0.9	d=1.2
δ_{vm}(mm)	341	212	152	100	δ_{hm}(mm)	429	266	182
	313	194	139	200		390	237	166
	292	180	133	300		362	221	161

H=20m	d=0.6	d=0.9	d=1.2	E_{50}/c_u	H=20m	d=0.6	d=0.9	d=1.2
δ_{vm}(mm)	424	275	192	100	δ_{hm}(mm)	550	339	229
	397	252	176	200		501	311	213
	379	236	172	300		478	285	207

Generic Cases: 2485 to 2520

Table A.69. Model parameters and deformation results (Case No: 2485 to 2520).

Excavation	Soil (γ=17kN/m^3)		Diaphragm Wall(E=2.0E+7)		
H_e(m)	c_u/σ_v'	E_{50}/c_u	d	EA	EI
11-14-17-20	0.25	100-200-300	0.6	1.2E+07	3.60E+05
			0.9	1.8E+07	1.215E+06
			1.2	2.4E+07	2.88E+06

Soil	E_{50}/c_u		
HSS	100	200	300
E_{50}^{ref}	4000	8000	12000
E_{oed}^{ref}	4000	8000	12000
E_{ur}^{ref}	12000	24000	36000
G_0^{ref}	35000	50000	67500
$\gamma_{0,7}$	3.58E-04	2.51E-04	1.86E-04
ϕ	22	22	22
K_0	0.625	0.625	0.625
E_{dyn}/E_{stat}	7	5	4.5

H=11m	d=0.6	d=0.9	d=1.2	E_{50}/c_u	H=11m	d=0.6	d=0.9	d=1.2
δ_{vm}(mm)	102	75	60	100	δ_{hm}(mm)	123	95	75
	86	64	47	200		105	78	58
	73	54	42	300		91	67	52

H=14m	d=0.6	d=0.9	d=1.2	E_{50}/c_u	H=14m	d=0.6	d=0.9	d=1.2
δ_{vm}(mm)	163	115	89	100	δ_{hm}(mm)	200	144	111
	139	100	74	200		169	123	89
	121	85	67	300		150	106	83

H=17m	d=0.6	d=0.9	d=1.2	E_{50}/c_u	H=17m	d=0.6	d=0.9	d=1.2
δ_{vm}(mm)	224	156	121	100	δ_{hm}(mm)	291	196	147
	197	136	100	200		247	171	126
	176	120	93	300		218	149	115

H=20m	d=0.6	d=0.9	d=1.2	E_{50}/c_u	H=20m	d=0.6	d=0.9	d=1.2
δ_{vm}(mm)	285	200	154	100	δ_{hm}(mm)	374	251	186
	255	174	130	200		320	219	162
	229	155	122	300		288	194	149

Generic Cases: 2521 to 2556

Table A.70. Model parameters and deformation results (Case No: 2521 to 2556).

Excavation	Soil(γ=17kN/m^3)		Diaphragm Wall(E=2.0E+7)		
H_e(m)	c_u/σ_v'	E_{50}/c_u	d	EA	EI
11-14-17-20	0.3	100-200-300	0.6	1.2E+07	3.60E+05
			0.9	1.8E+07	1.215E+06
			1.2	2.4E+07	2.88E+06

Soil	E_{50}/c_u		
HSS	100	200	300
E_{50}^{ref}	5400	10800	16200
E_{oed}^{ref}	5400	10800	16200
E_{ur}^{ref}	16200	32400	48600
G_0^{ref}	40500	60750	75938
$\gamma_{0.7}$	3.40E-04	2.27E-04	1.81E-04
ϕ	26.4	26.4	26.4
K_0	0.555	0.555	0.555
E_{dyn}/E_{stat}	6	4.5	3.75

H=11m	d=0.6	d=0.9	d=1.2	E_{50}/c_u	H=11m	d=0.6	d=0.9	d=1.2
δ_{vm}(mm)	80	59	54	100	δ_{hm}(mm)	100	75	68
	63	49	41	200		77	61	52
	52	41	35	300		65	52	45

H=14m	d=0.6	d=0.9	d=1.2	E_{50}/c_u	H=14m	d=0.6	d=0.9	d=1.2
δ_{vm}(mm)	118	85	75	100	δ_{hm}(mm)	147	106	92
	93	73	59	200		118	90	74
	81	62	51	300		101	77	65

H=17m	d=0.6	d=0.9	d=1.2	E_{50}/c_u	H=17m	d=0.6	d=0.9	d=1.2
δ_{vm}(mm)	162	117	98	100	δ_{hm}(mm)	206	143	120
	130	97	78	200		166	122	98
	114	86	70	300		141	108	88

H=20m	d=0.6	d=0.9	d=1.2	E_{50}/c_u	H=20m	d=0.6	d=0.9	d=1.2
δ_{vm}(mm)	205	146	124	100	δ_{hm}(mm)	266	183	150
	168	123	101	200		215	157	125
	150	111	91	300		186	140	113

Generic Cases: 2557 to 2592

Table A.71. Model parameters and deformation results (Case No: 2557 to 2592).

Excavation	Soil(γ=17kN/m^3)		Diaphragm Wall(E=2.0E+7)		
H_e(m)	c_u/σ_v'	E_{50}/c_u	d	EA	EI
11-14-17-20	0.35	100-200-300	0.6	1.2E+07	3.60E+05
			0.9	1.8E+07	1.215E+06
			1.2	2.4E+07	2.88E+06

Soil	E_{50}/c_u		
HSS	100	200	300
E_{50}^{ref}	7000	14000	21000
E_{oed}^{ref}	7000	14000	21000
E_{ur}^{ref}	21000	42000	63000
G_0^{ref}	52500	73500	99750
$\gamma_{0,7}$	2.75E-04	1.96E-04	1.45E-04
ϕ	30	30	30
K_0	0.500	0.500	0.500
E_{dyn}/E_{stat}	6	4.2	3.8

H=11m	d=0.6	d=0.9	d=1.2	E_{50}/c_u	H=11m	d=0.6	d=0.9	d=1.2
δ_{vm}(mm)	63	50	48	100	δ_{hm}(mm)	80	62	59
	52	43	38	200		66	54	47
	40	34	29	300		51	43	37

H=14m	d=0.6	d=0.9	d=1.2	E_{50}/c_u	H=14m	d=0.6	d=0.9	d=1.2
δ_{vm}(mm)	91	67	64	100	δ_{hm}(mm)	112	84	78
	73	60	51	200		94	75	64
	60	49	42	300		75	62	53

H=17m	d=0.6	d=0.9	d=1.2	E_{50}/c_u	H=17m	d=0.6	d=0.9	d=1.2
δ_{vm}(mm)	123	91	81	100	δ_{hm}(mm)	156	111	99
	100	80	67	200		127	100	85
	83	67	57	300		103	84	71

H=20m	d=0.6	d=0.9	d=1.2	E_{50}/c_u	H=20m	d=0.6	d=0.9	d=1.2
δ_{vm}(mm)	154	115	101	100	δ_{hm}(mm)	198	142	124
	128	101	85	200		164	127	106
	109	87	73	300		135	108	91

Model Group:19

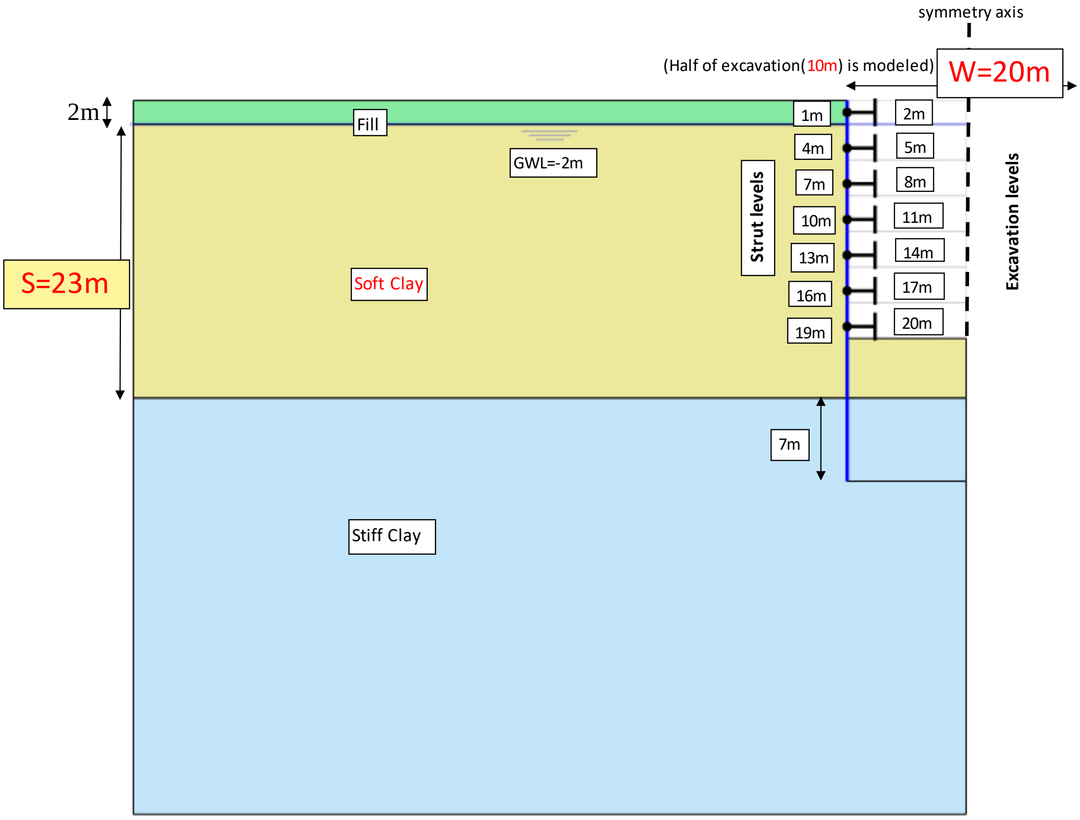

Figure A.19. Model Geometry-19.

Table B. Soil and structure parameters

Default Soil Parameters		
	Stiff Clay	Fill
	HS	HS
	Undrained(A)	Drained
E_{50}^{ref}	1.00E+05	1.50E+04
E_{oed}^{ref}	1.00E+05	1.50E+04
E_{ur}^{ref}	3.00E+05	4.50E+04
ϕ'	26	30
K_0	0.562	0.5
c'_{ref}	25	1
v'_{ur}	0.2	0.2
p_{ref}	100	100
R_f	0.9	0.9
$\gamma_{unsat/sat}$	20/20	16/20
R_{inter}	0.65	0.65
m	1	1

Range of parameters	
c_u/σ_v'	0.20-0.25-0.30-0.35
E_{50}/c_u	100-200-300
γ	15-17-19
S	23-28-33
W	20-40-60
H_e	11-14-17-20
$\ln(EI/\gamma_w h_{avg}^4)$	6.097-7.313-8.176

Diaphragm Wall (E=2.0E+7)		
d	EA	EI
0.6	1.2E+07	3.60E+05
0.9	1.8E+07	1.215E+06
1.2	2.4E+07	2.88E+06

Strut	
EA	3.80E+06
$L_{spacing}$	5m
h_{avg}	3m

Generic Cases: 2593 to 2628

Table A.72. Model parameters and deformation results (Case No: 2593 to 2628).

Excavation	Soil(γ=19kN/m^3)		Diaphragm Wall(E=2.0E+7)		
H_e(m)	c_u/σ_v'	E_{50}/c_u	d	EA	EI
11-14-17-20	0.2	100-200-300	0.6	1.2E+07	3.60E+05
			0.9	1.8E+07	1.215E+06
			1.2	2.4E+07	2.88E+06

Soft Soil	E_{50}/c_u		
HSS	100	200	300
E_{50}^{ref}	2895	5789	8685
E_{oed}^{ref}	2895	5789	8685
E_{ur}^{ref}	8685	17367	26055
G_0^{ref}	30759	43418	54281
$\gamma_{0,7}$	3.59E-04	2.54E-04	2.03E-04
ϕ	18	18	18
K_0	0.691	0.691	0.691
E_{dyn}/E_{stat}	8.5	6	5

H=11m	d=0.6	d=0.9	d=1.2	E_{50}/c_u	H=11m	d=0.6	d=0.9	d=1.2
δ_{vm}(mm)	72	46	34	100	δ_{hm}(mm)	90	56	40
	62	39	28	200		79	49	35
	57	36	25	300		71	44	33

H=14m	d=0.6	d=0.9	d=1.2	E_{50}/c_u	H=14m	d=0.6	d=0.9	d=1.2
δ_{vm}(mm)	98	62	46	100	δ_{hm}(mm)	130	76	53
	88	53	38	200		114	68	48
	82	50	35	300		105	64	45

H=17m	d=0.6	d=0.9	d=1.2	E_{50}/c_u	H=17m	d=0.6	d=0.9	d=1.2
δ_{vm}(mm)	119	75	56	100	δ_{hm}(mm)	160	93	66
	108	67	47	200		142	84	60
	102	62	45	300		130	79	57

H=20m	d=0.6	d=0.9	d=1.2	E_{50}/c_u	H=20m	d=0.6	d=0.9	d=1.2
δ_{vm}(mm)	139	87	64	100	δ_{hm}(mm)	180	105	75
	126	78	54	200		159	98	70
	119	74	54	300		147	92	66

Generic Cases: 2629 to 2664

Table A.73. Model parameters and deformation results (Case No: 2629 to 2664).

Excavation	Soil(γ=19kN/m^3)		Diaphragm Wall(E=2.0E+7)		
H_e(m)	c_u/σ_v'	E_{50}/c_u	d	EA	EI
11-14-17-20	0.25	100-200-300	0.6	1.2E+07	3.60E+05
			0.9	1.8E+07	1.215E+06
			1.2	2.4E+07	2.88E+06

Soil	E_{50}/c_u		
HSS	100	200	300
E_{50}^{ref}	4000	8000	12000
E_{oed}^{ref}	4000	8000	12000
E_{ur}^{ref}	12000	24000	36000
G_0^{ref}	35000	50000	67500
$\gamma_{0,7}$	3.58E-04	2.51E-04	1.86E-04
ϕ	22	22	22
K_0	0.625	0.625	0.625
E_{dyn}/E_{stat}	7	5	4.5

H=11m	d=0.6	d=0.9	d=1.2	E_{50}/c_u	H=11m	d=0.6	d=0.9	d=1.2
δ_{vm}(mm)	52	35	27	100	δ_{hm}(mm)	65	43	34
	43	28	21	200		54	36	27
	36	25	19	300		46	32	24

H=14m	d=0.6	d=0.9	d=1.2	E_{50}/c_u	H=14m	d=0.6	d=0.9	d=1.2
δ_{vm}(mm)	71	47	37	100	δ_{hm}(mm)	95	58	45
	60	39	29	200		80	52	38
	52	35	26	300		69	46	34

H=17m	d=0.6	d=0.9	d=1.2	E_{50}/c_u	H=17m	d=0.6	d=0.9	d=1.2
δ_{vm}(mm)	87	59	46	100	δ_{hm}(mm)	119	72	55
	75	49	38	200		102	64	48
	66	45	34	300		89	59	44

H=20m	d=0.6	d=0.9	d=1.2	E_{50}/c_u	H=20m	d=0.6	d=0.9	d=1.2
δ_{vm}(mm)	102	69	54	100	δ_{hm}(mm)	138	85	64
	88	58	44	200		117	77	57
	79	54	40	300		103	70	53

Generic Cases: 2665 to 2700

Table A.74. Model parameters and deformation results (Case No: 2665 to 2700).

Excavation	Soil(γ=19kN/m^3)		Diaphragm Wall(E=2.0E+7)		
H_e(m)	c_u/σ_v'	E_{50}/c_u	d	EA	EI
11-14-17-20	0.3	100-200-300	0.6	1.2E+07	3.60E+05
			0.9	1.8E+07	1.215E+06
			1.2	2.4E+07	2.88E+06

Soil	E_{50}/c_u		
HSS	100	200	300
E_{50}^{ref}	5400	10800	16200
E_{oed}^{ref}	5400	10800	16200
E_{ur}^{ref}	16200	32400	48600
G_0^{ref}	40500	60750	75938
$\gamma_{0,7}$	3.40E-04	2.27E-04	1.81E-04
ϕ	26.4	26.4	26.4
K_0	0.555	0.555	0.555
E_{dyn}/E_{stat}	6	4.5	3.75

H=11m	d=0.6	d=0.9	d=1.2	E_{50}/c_u	H=11m	d=0.6	d=0.9	d=1.2
δ_{vm}(mm)	38	30	25	100	δ_{hm}(mm)	48	38	30
	30	22	18	200		38	28	23
	26	19	15	300		33	24	20

H=14m	d=0.6	d=0.9	d=1.2	E_{50}/c_u	H=14m	d=0.6	d=0.9	d=1.2
δ_{vm}(mm)	54	40	32	100	δ_{hm}(mm)	68	49	39
	43	31	24	200		56	40	31
	37	27	21	300		49	35	28

H=17m	d=0.6	d=0.9	d=1.2	E_{50}/c_u	H=17m	d=0.6	d=0.9	d=1.2
δ_{vm}(mm)	66	49	40	100	δ_{hm}(mm)	86	61	48
	55	39	31	200		73	51	39
	48	34	28	300		64	45	36

H=20m	d=0.6	d=0.9	d=1.2	E_{50}/c_u	H=20m	d=0.6	d=0.9	d=1.2
δ_{vm}(mm)	77	58	46	100	δ_{hm}(mm)	100	70	55
	65	47	37	200		86	61	47
	57	42	34	300		75	55	44

Generic Cases: 2701 to 2736

Table A.75. Model parameters and deformation results (Case No: 2701 to 2736).

Excavation	Soil(γ=19kN/m^3)		Diaphragm Wall(E=2.0E+7)		
H_e(m)	c_u/σ_v'	E_{50}/c_u	d	EA	EI
11-14-17-20	0.35	100-200-300	0.6	1.2E+07	3.60E+05
			0.9	1.8E+07	1.215E+06
			1.2	2.4E+07	2.88E+06

Soil	E_{50}/c_u		
HSS	100	200	300
E_{50}^{ref}	7000	14000	21000
E_{oed}^{ref}	7000	14000	21000
E_{ur}^{ref}	21000	42000	63000
G_0^{ref}	52500	73500	99750
$\gamma_{0,7}$	2.75E-04	1.96E-04	1.45E-04
ϕ	30	30	30
K_0	0.500	0.500	0.500
E_{dyn}/E_{stat}	6	4.2	3.8

H=11m	d=0.6	d=0.9	d=1.2	E_{50}/c_u	H=11m	d=0.6	d=0.9	d=1.2
δ_{vm}(mm)	34	28	23	100	δ_{hm}(mm)	42	33	28
	25	19	16	200		31	25	21
	20	15	12	300		26	20	17

H=14m	d=0.6	d=0.9	d=1.2	E_{50}/c_u	H=14m	d=0.6	d=0.9	d=1.2
δ_{vm}(mm)	43	35	29	100	δ_{hm}(mm)	55	42	35
	34	26	21	200		44	33	27
	28	21	17	300		37	28	23

H=17m	d=0.6	d=0.9	d=1.2	E_{50}/c_u	H=17m	d=0.6	d=0.9	d=1.2
δ_{vm}(mm)	54	42	35	100	δ_{hm}(mm)	69	51	42
	43	33	27	200		57	42	34
	37	27	22	300		49	36	29

H=20m	d=0.6	d=0.9	d=1.2	E_{50}/c_u	H=20m	d=0.6	d=0.9	d=1.2
δ_{vm}(mm)	62	50	41	100	δ_{hm}(mm)	79	59	49
	51	40	33	200		67	51	41
	45	34	28	300		59	45	36

Model Group:20

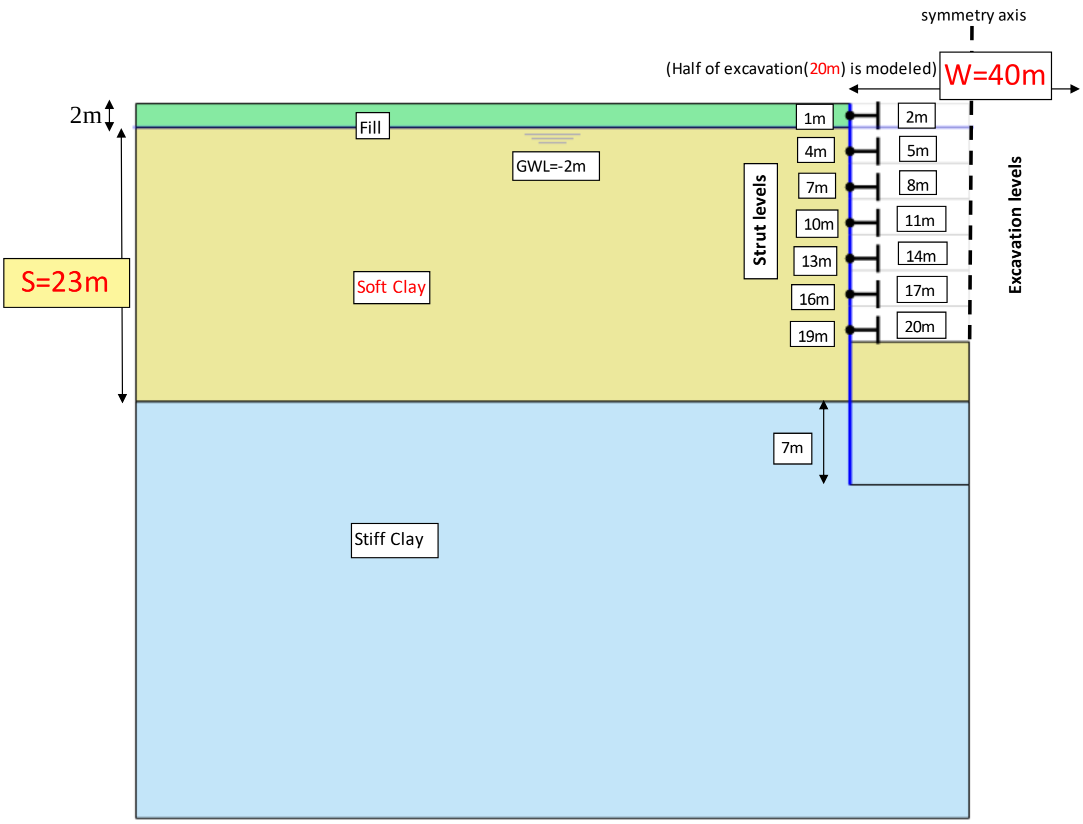

Figure A.20. Model Geometry-20.

Table B. Soil and structure parameters

Default Soil Parameters		
	Stiff Clay	Fill
	HS	HS
	Undrained(A)	Drained
E_{50}^{ref}	1.00E+05	1.50E+04
E_{oed}^{ref}	1.00E+05	1.50E+04
E_{ur}^{ref}	3.00E+05	4.50E+04
ϕ'	26	30
K_0	0.562	0.5
c'_{ref}	25	1
v'_{ur}	0.2	0.2
p_{ref}	100	100
R_f	0.9	0.9
$\gamma_{unsat/sat}$	20/20	16/20
R_{inter}	0.65	0.65
m	1	1

Range of parameters	
c_u/σ'_v	0.20-0.25-0.30-0.35
E_{50}/c_u	100-200-300
γ	15-17-19
S	23-28-33
W	20-40-60
H_e	11-14-17-20
$\ln(EI/\gamma_w h_{avg}^4)$	6.097-7.313-8.176

Diaphragm Wall (E=2.0E+7)		
d	EA	EI
0.6	1.2E+07	3.60E+05
0.9	1.8E+07	1.215E+06
1.2	2.4E+07	2.88E+06

Strut	
EA	3.80E+06
$L_{spacing}$	5m
h_{avg}	3m

Generic Cases: 2737 to 2772

Table A.76. Model parameters and deformation results (Case No: 2737 to 2772).

Excavation	Soil(γ=19kN/m^3)		Diaphragm Wall(E=2.0E+7)		
H_e(m)	c_u/σ_v'	E_{50}/c_u	d	EA	EI
11-14-17-20	0.2	100-200-300	0.6	1.2E+07	3.60E+05
			0.9	1.8E+07	1.215E+06
			1.2	2.4E+07	2.88E+06

Soft Soil	E_{50}/c_u		
HSS	100	200	300
E_{50}^{ref}	2895	5789	8685
E_{oed}^{ref}	2895	5789	8685
E_{ur}^{ref}	8685	17367	26055
G_0^{ref}	30759	43418	54281
$\gamma_{0,7}$	3.59E-04	2.54E-04	2.03E-04
ϕ	18	18	18
K_0	0.691	0.691	0.691
E_{dyn}/E_{stat}	8.5	6	5

H=11m	d=0.6	d=0.9	d=1.2	E_{50}/c_u	H=11m	d=0.6	d=0.9	d=1.2
δ_{vm}(mm)	91	61	44	100	δ_{hm}(mm)	109	73	52
	79	51	39	200		98	63	47
	72	47	34	300		89	58	43

H=14m	d=0.6	d=0.9	d=1.2	E_{50}/c_u	H=14m	d=0.6	d=0.9	d=1.2
δ_{vm}(mm)	124	83	61	100	δ_{hm}(mm)	155	98	70
	111	70	53	200		139	86	65
	104	66	49	300		128	82	60

H=17m	d=0.6	d=0.9	d=1.2	E_{50}/c_u	H=17m	d=0.6	d=0.9	d=1.2
δ_{vm}(mm)	153	103	76	100	δ_{hm}(mm)	192	121	87
	140	89	67	200		173	108	81
	131	83	63	300		162	103	77

H=20m	d=0.6	d=0.9	d=1.2	E_{50}/c_u	H=20m	d=0.6	d=0.9	d=1.2
δ_{vm}(mm)	179	120	89	100	δ_{hm}(mm)	218	138	99
	164	106	80	200		197	126	94
	156	100	75	300		184	121	90

Generic Cases: 2773 to 2808

Table A.77. Model parameters and deformation results (Case No: 2773 to 2808).

Excavation	Soil (γ=19kN/m^3)		Diaphragm Wall(E=2.0E+7)		
H_e(m)	c_u/σ_v'	E_{50}/c_u	d	EA	EI
11-14-17-20	0.25	100-200-300	0.6	1.2E+07	3.60E+05
			0.9	1.8E+07	1.215E+06
			1.2	2.4E+07	2.88E+06

Soil	E_{50}/c_u		
HSS	100	200	300
E_{50}^{ref}	4000	8000	12000
E_{oed}^{ref}	4000	8000	12000
E_{ur}^{ref}	12000	24000	36000
G_0^{ref}	35000	50000	67500
$\gamma_{0,7}$	3.58E-04	2.51E-04	1.86E-04
ϕ	22	22	22
K_0	0.625	0.625	0.625
E_{dyn}/E_{stat}	7	5	4.5

H=11m	d=0.6	d=0.9	d=1.2	E_{50}/c_u	H=11m	d=0.6	d=0.9	d=1.2
δ_{vm}(mm)	68	47	38	100	δ_{hm}(mm)	84	58	46
	57	40	31	200		70	51	39
	48	34	25	300		60	43	32

H=14m	d=0.6	d=0.9	d=1.2	E_{50}/c_u	H=14m	d=0.6	d=0.9	d=1.2
δ_{vm}(mm)	95	64	51	100	δ_{hm}(mm)	120	77	61
	80	55	42	200		101	70	53
	69	49	37	300		89	61	46

H=17m	d=0.6	d=0.9	d=1.2	E_{50}/c_u	H=17m	d=0.6	d=0.9	d=1.2
δ_{vm}(mm)	117	81	63	100	δ_{hm}(mm)	149	96	76
	100	69	55	200		128	88	68
	89	63	48	300		113	79	60

H=20m	d=0.6	d=0.9	d=1.2	E_{50}/c_u	H=20m	d=0.6	d=0.9	d=1.2
δ_{vm}(mm)	137	97	75	100	δ_{hm}(mm)	172	111	88
	119	83	66	200		148	104	79
	106	76	59	300		131	94	72

Generic Cases: 2809 to 2844

Table A.78. Model parameters and deformation results (Case No: 2809 to 2844).

Excavation	Soil(γ=19kN/m^3)		Diaphragm Wall(E=2.0E+7)		
H_e(m)	c_u/σ_v'	E_{50}/c_u	d	EA	EI
11-14-17-20	0.3	100-200-300	0.6	1.2E+07	3.60E+05
			0.9	1.8E+07	1.215E+06
			1.2	2.4E+07	2.88E+06

Soil	E_{50}/c_u		
HSS	100	200	300
E_{50}^{ref}	5400	10800	16200
E_{oed}^{ref}	5400	10800	16200
E_{ur}^{ref}	16200	32400	48600
G_0^{ref}	40500	60750	75938
$\gamma_{0.7}$	3.40E-04	2.27E-04	1.81E-04
ϕ	26.4	26.4	26.4
K_0	0.555	0.555	0.555
E_{dyn}/E_{stat}	6	4.5	3.75

H=11m	d=0.6	d=0.9	d=1.2	E_{50}/c_u	H=11m	d=0.6	d=0.9	d=1.2
δ_{vm}(mm)	54	43	37	100	δ_{hm}(mm)	68	53	45
	41	32	27	200		52	40	34
	35	27	22	300		45	35	29

H=14m	d=0.6	d=0.9	d=1.2	E_{50}/c_u	H=14m	d=0.6	d=0.9	d=1.2
δ_{vm}(mm)	75	56	47	100	δ_{hm}(mm)	94	68	57
	58	44	35	200		74	55	45
	51	38	30	300		65	49	40

H=17m	d=0.6	d=0.9	d=1.2	E_{50}/c_u	H=17m	d=0.6	d=0.9	d=1.2
δ_{vm}(mm)	91	69	58	100	δ_{hm}(mm)	117	83	69
	73	55	45	200		93	69	56
	66	49	40	300		83	63	51

H=20m	d=0.6	d=0.9	d=1.2	E_{50}/c_u	H=20m	d=0.6	d=0.9	d=1.2
δ_{vm}(mm)	108	81	67	100	δ_{hm}(mm)	136	98	80
	87	68	55	200		109	82	67
	79	60	50	300		98	76	62

Generic Cases: 2845 to 2880

Table A.79. Model parameters and deformation results (Case No: 2845 to 2880).

Excavation	Soil(γ=19kN/m^3)		Diaphragm Wall(E=2.0E+7)		
H_e(m)	c_u/σ_v'	E_{50}/c_u	d	EA	EI
11-14-17-20	0.35	100-200-300	0.6	1.2E+07	3.60E+05
			0.9	1.8E+07	1.215E+06
			1.2	2.4E+07	2.88E+06

Soil	E_{50}/c_u		
HSS	100	200	300
E_{50}^{ref}	7000	14000	21000
E_{oed}^{ref}	7000	14000	21000
E_{ur}^{ref}	21000	42000	63000
G_0^{ref}	52500	73500	99750
$\gamma_{0,7}$	2.75E-04	1.96E-04	1.45E-04
ϕ	30	30	30
K_0	0.500	0.500	0.500
E_{dyn}/E_{stat}	6	4.2	3.8

H=11m	d=0.6	d=0.9	d=1.2	E_{50}/c_u	H=11m	d=0.6	d=0.9	d=1.2
δ_{vm}(mm)	47	40	34	100	δ_{hm}(mm)	59	48	41
	35	28	24	200		45	36	31
	28	23	19	300		37	29	25

H=14m	d=0.6	d=0.9	d=1.2	E_{50}/c_u	H=14m	d=0.6	d=0.9	d=1.2
δ_{vm}(mm)	64	51	42	100	δ_{hm}(mm)	78	62	52
	48	38	32	200		61	48	40
	40	31	26	300		52	40	33

H=17m	d=0.6	d=0.9	d=1.2	E_{50}/c_u	H=17m	d=0.6	d=0.9	d=1.2
δ_{vm}(mm)	78	62	52	100	δ_{hm}(mm)	96	76	62
	61	48	41	200		78	60	50
	52	41	34	300		66	52	43

H=20m	d=0.6	d=0.9	d=1.2	E_{50}/c_u	H=20m	d=0.6	d=0.9	d=1.2
δ_{vm}(mm)	92	73	60	100	δ_{hm}(mm)	111	88	71
	74	59	50	200		92	71	60
	64	51	43	300		79	63	53

Model Group:21

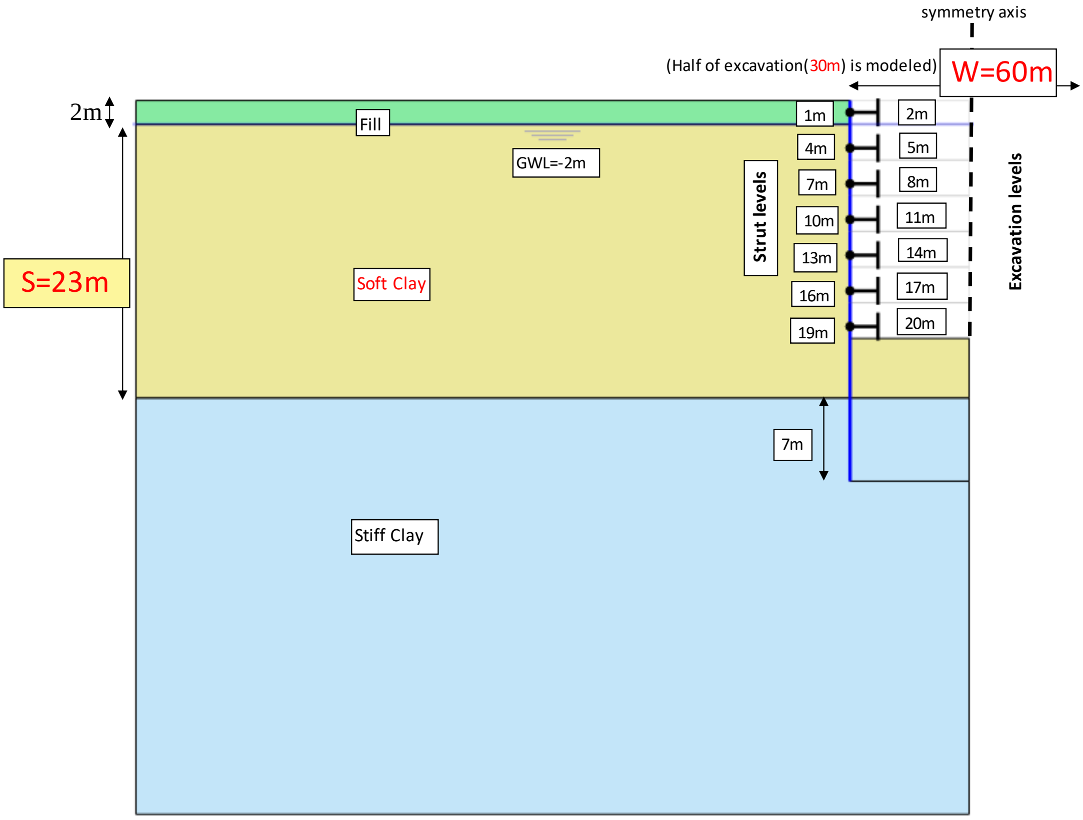

Figure A.21. Model Geometry-21.

Table B. Soil and structure parameters

Default Soil Parameters		
	Stiff Clay	Fill
	HS	HS
	Undrained(A)	Drained
E_{50}^{ref}	1.00E+05	1.50E+04
E_{oed}^{ref}	1.00E+05	1.50E+04
E_{ur}^{ref}	3.00E+05	4.50E+04
ϕ'	26	30
K_0	0.562	0.5
c'_{ref}	25	1
v'_{ur}	0.2	0.2
p_{ref}	100	100
R_f	0.9	0.9
$\gamma_{unsat/sat}$	20/20	16/20
R_{inter}	0.65	0.65
m	1	1

Range of parameters	
c_u/σ_v'	0.20-0.25-0.30-0.35
E_{50}/c_u	100-200-300
γ	15-17-19
S	23-28-33
W	20-40-60
H_e	11-14-17-20
$\ln(EI/\gamma_w h_{avg}^4)$	6.097-7.313-8.176

Diaphragm Wall (E=2.0E+7)		
d	EA	EI
0.6	1.2E+07	3.60E+05
0.9	1.8E+07	1.215E+06
1.2	2.4E+07	2.88E+06

Strut	
EA	3.80E+06
$L_{spacing}$	5m
h_{avg}	3m

Generic Cases: 2881 to 2916

Table A.80. Model parameters and deformation results (Case No: 2881 to 2916).

Excavation	Soil(γ=19kN/m^3)		Diaphragm Wall(E=2.0E+7)		
H_e(m)	c_u/σ_v'	E_{50}/c_u	d	EA	EI
11-14-17-20	0.2	100-200-300	0.6	1.2E+07	3.60E+05
			0.9	1.8E+07	1.215E+06
			1.2	2.4E+07	2.88E+06

Soft Soil	E_{50}/c_u		
HSS	100	200	300
E_{50}^{ref}	2895	5789	8685
E_{oed}^{ref}	2895	5789	8685
E_{ur}^{ref}	8685	17367	26055
G_0^{ref}	30759	43418	54281
$\gamma_{0,7}$	3.59E-04	2.54E-04	2.03E-04
ϕ	18	18	18
K_0	0.691	0.691	0.691
E_{dyn}/E_{stat}	8.5	6	5

H=11m	d=0.6	d=0.9	d=1.2	E_{50}/c_u	H=11m	d=0.6	d=0.9	d=1.2
δ_{vm}(mm)	103	70	51	100	δ_{hm}(mm)	129	84	60
	91	63	47	200		112	75	56
	84	57	42	300		103	69	51

H=14m	d=0.6	d=0.9	d=1.2	E_{50}/c_u	H=14m	d=0.6	d=0.9	d=1.2
δ_{vm}(mm)	142	95	70	100	δ_{hm}(mm)	177	113	81
	129	84	64	200		159	103	77
	118	79	59	300		148	97	72

H=17m	d=0.6	d=0.9	d=1.2	E_{50}/c_u	H=17m	d=0.6	d=0.9	d=1.2
δ_{vm}(mm)	176	120	88	100	δ_{hm}(mm)	219	141	101
	163	108	81	200		197	130	97
	153	101	76	300		184	121	91

H=20m	d=0.6	d=0.9	d=1.2	E_{50}/c_u	H=20m	d=0.6	d=0.9	d=1.2
δ_{vm}(mm)	207	143	103	100	δ_{hm}(mm)	251	163	116
	197	128	96	200		229	150	114
	184	122	90	300		213	143	108

Generic Cases: 2917 to 2952

Table A.81. Model parameters and deformation results (Case No: 2917 to 2952).

Excavation	Soil (γ=19kN/m^3)		Diaphragm Wall(E=2.0E+7)		
H_e(m)	c_u/σ_v'	E_{50}/c_u	d	EA	EI
11-14-17-20	0.25	100-200-300	0.6	1.2E+07	3.60E+05
			0.9	1.8E+07	1.215E+06
			1.2	2.4E+07	2.88E+06

Soil	E_{50}/c_u		
HSS	100	200	300
E_{50}^{ref}	4000	8000	12000
E_{oed}^{ref}	4000	8000	12000
E_{ur}^{ref}	12000	24000	36000
G_0^{ref}	35000	50000	67500
$\gamma_{0.7}$	3.58E-04	2.51E-04	1.86E-04
ϕ	22	22	22
K_0	0.625	0.625	0.625
E_{dyn}/E_{stat}	7	5	4.5

H=11m	d=0.6	d=0.9	d=1.2	E_{50}/c_u	H=11m	d=0.6	d=0.9	d=1.2
δ_{vm}(mm)	81	57	47	100	δ_{hm}(mm)	100	70	57
	66	48	37	200		82	60	47
	57	40	30	300		70	50	38

H=14m	d=0.6	d=0.9	d=1.2	E_{50}/c_u	H=14m	d=0.6	d=0.9	d=1.2
δ_{vm}(mm)	111	76	63	100	δ_{hm}(mm)	140	93	75
	94	66	51	200		115	83	64
	81	57	44	300		103	72	55

H=17m	d=0.6	d=0.9	d=1.2	E_{50}/c_u	H=17m	d=0.6	d=0.9	d=1.2
δ_{vm}(mm)	136	96	77	100	δ_{hm}(mm)	174	115	92
	118	84	65	200		147	104	81
	106	74	57	300		131	92	72

H=20m	d=0.6	d=0.9	d=1.2	E_{50}/c_u	H=20m	d=0.6	d=0.9	d=1.2
δ_{vm}(mm)	164	116	91	100	δ_{hm}(mm)	200	135	107
	140	101	79	200		171	124	95
	128	92	71	300		155	111	87

Generic Cases: 2953 to 2988

Table A.82. Model parameters and deformation results (Case No: 2953 to 2988).

Excavation	Soil(γ=19kN/m^3)		Diaphragm Wall(E=2.0E+7)		
H_e(m)	c_u/σ_v'	E_{50}/c_u	d	EA	EI
11-14-17-20	0.3	100-200-300	0.6	1.2E+07	3.60E+05
			0.9	1.8E+07	1.215E+06
			1.2	2.4E+07	2.88E+06

Soil	E_{50}/c_u		
HSS	100	200	300
E_{50}^{ref}	5400	10800	16200
E_{oed}^{ref}	5400	10800	16200
E_{ur}^{ref}	16200	32400	48600
G_0^{ref}	40500	60750	75938
$\gamma_{0,7}$	3.40E-04	2.27E-04	1.81E-04
ϕ	26.4	26.4	26.4
K_0	0.555	0.555	0.555
E_{dyn}/E_{stat}	6	4.5	3.75

H=11m	d=0,6	d=0,9	d=1,2	E_{50}/c_u	H=11m	d=0,6	d=0,9	d=1,2
δ_{vm}(mm)	64	52	44	100	δ_{hm}(mm)	81	63	53
	51	39	33	200		64	49	41
	43	34	28	300		55	43	36
H=14m	d=0,6	d=0,9	d=1,2	E_{50}/c_u	H=14m	d=0,6	d=0,9	d=1,2
δ_{vm}(mm)	87	69	57	100	δ_{hm}(mm)	111	83	69
	71	53	44	200		88	66	55
	62	47	38	300		78	60	49
H=17m	d=0,6	d=0,9	d=1,2	E_{50}/c_u	H=17m	d=0,6	d=0,9	d=1,2
δ_{vm}(mm)	110	84	70	100	δ_{hm}(mm)	136	101	84
	89	67	57	200		113	82	69
	79	60	50	300		98	76	62
H=20m	d=0,6	d=0,9	d=1,2	E_{50}/c_u	H=20m	d=0,6	d=0,9	d=1,2
δ_{vm}(mm)	128	100	83	100	δ_{hm}(mm)	158	118	98
	107	82	69	200		131	99	83
	96	75	63	300		117	93	76

Generic Cases: 2989 to 3024

Table A.83. Model parameters and deformation results (Case No: 2989 to 3024).

Excavation	Soil(γ=19kN/m^3)		Diaphragm Wall(E=2.0E+7)		
H_e(m)	c_u/σ_v'	E_{50}/c_u	d	EA	EI
11-14-17-20	0.35	100-200-300	0.6	1.2E+07	3.60E+05
			0.9	1.8E+07	1.215E+06
			1.2	2.4E+07	2.88E+06

Soil	E_{50}/c_u		
HSS	100	200	300
E_{50}^{ref}	7000	14000	21000
E_{oed}^{ref}	7000	14000	21000
E_{ur}^{ref}	21000	42000	63000
G_0^{ref}	52500	73500	99750
$\gamma_{0,7}$	2.75E-04	1.96E-04	1.45E-04
ϕ	30	30	30
K_0	0.500	0.500	0.500
E_{dyn}/E_{stat}	6	4.2	3.8

H=11m	d=0.6	d=0.9	d=1.2	E_{50}/c_u	H=11m	d=0.6	d=0.9	d=1.2
δ_{vm}(mm)	52	48	41	100	δ_{hm}(mm)	65	58	49
	43	35	29	200		54	45	36
	35	28	23	300		44	36	30

H=14m	d=0.6	d=0.9	d=1.2	E_{50}/c_u	H=14m	d=0.6	d=0.9	d=1.2
δ_{vm}(mm)	71	61	50	100	δ_{hm}(mm)	89	74	60
	58	47	38	200		74	60	48
	49	39	32	300		61	49	41

H=17m	d=0.6	d=0.9	d=1.2	E_{50}/c_u	H=17m	d=0.6	d=0.9	d=1.2
δ_{vm}(mm)	87	76	61	100	δ_{hm}(mm)	110	91	73
	73	59	49	200		93	74	60
	63	50	42	300		79	63	52

H=20m	d=0.6	d=0.9	d=1.2	E_{50}/c_u	H=20m	d=0.6	d=0.9	d=1.2
δ_{vm}(mm)	105	89	73	100	δ_{hm}(mm)	130	105	85
	89	73	61	200		110	89	73
	78	64	53	300		95	78	65

Model Group:22

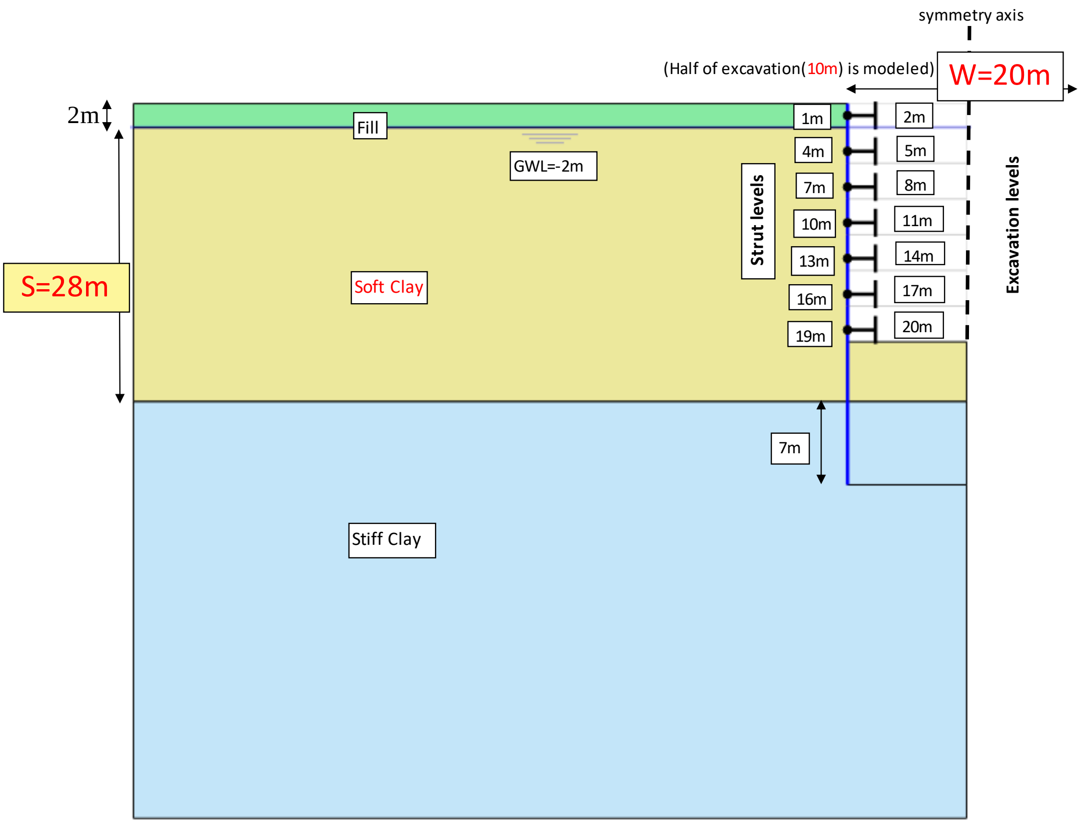

Figure A.22. Model Geometry-22.

Table B. Soil and structure parameters

Default Soil Parameters		
	Stiff Clay	Fill
	HS	HS
	Undrained(A)	Drained
E_{50}^{ref}	1.00E+05	1.50E+04
E_{oed}^{ref}	1.00E+05	1.50E+04
E_{ur}^{ref}	3.00E+05	4.50E+04
ϕ'	26	30
K_0	0.562	0.5
c'_{ref}	25	1
v'_{ur}	0.2	0.2
p_{ref}	100	100
R_f	0.9	0.9
$\gamma_{unsat/sat}$	20/20	16/20
R_{inter}	0.65	0.65
m	1	1

Range of parameters	
c_u/σ'_v	0.20-0.25-0.30-0.35
E_{50}/c_u	100-200-300
γ	15-17-19
S	23-28-33
W	20-40-60
H_e	11-14-17-20
$\ln(EI/\gamma_w h_{avg}^4)$	6.097-7.313-8.176

Diaphragm Wall (E=2.0E+7)		
d	EA	EI
0.6	1.2E+07	3.60E+05
0.9	1.8E+07	1.215E+06
1.2	2.4E+07	2.88E+06

Strut	
EA	3.80E+06
$L_{spacing}$	5m
h_{avg}	3m

Generic Cases: 3025 to 3060

Table A.84. Model parameters and deformation results (Case No: 3025 to 3060).

Excavation	Soil(γ=19kN/m^3)		Diaphragm Wall(E=2.0E+7)		
H_e(m)	c_u/σ_v'	E_{50}/c_u	d	EA	EI
11-14-17-20	0.2	100-200-300	0.6	1.2E+07	3.60E+05
			0.9	1.8E+07	1.215E+06
			1.2	2.4E+07	2.88E+06

Soft Soil	E_{50}/c_u		
HSS	100	200	300
E_{50}^{ref}	2895	5789	8685
E_{oed}^{ref}	2895	5789	8685
E_{ur}^{ref}	8685	17367	26055
G_0^{ref}	30759	43418	54281
$\gamma_{0,7}$	3.59E-04	2.54E-04	2.03E-04
ϕ	18	18	18
K_0	0.691	0.691	0.691
E_{dyn}/E_{stat}	8.5	6	5

H=11m	d=0.6	d=0.9	d=1.2	E_{50}/c_u	H=11m	d=0.6	d=0.9	d=1.2
δ_{vm}(mm)	76	46	36	100	δ_{hm}(mm)	93	56	45
	65	42	31	200		82	52	38
	58	38	29	300		76	48	36

H=14m	d=0.6	d=0.9	d=1.2	E_{50}/c_u	H=14m	d=0.6	d=0.9	d=1.2
δ_{vm}(mm)	112	68	51	100	δ_{hm}(mm)	153	87	64
	104	64	45	200		134	80	57
	95	58	42	300		120	75	54

H=17m	d=0.6	d=0.9	d=1.2	E_{50}/c_u	H=17m	d=0.6	d=0.9	d=1.2
δ_{vm}(mm)	147	86	66	100	δ_{hm}(mm)	206	113	83
	140	82	60	200		182	107	76
	129	76	56	300		166	100	72

H=20m	d=0.6	d=0.9	d=1.2	E_{50}/c_u	H=20m	d=0.6	d=0.9	d=1.2
δ_{vm}(mm)	176	105	80	100	δ_{hm}(mm)	244	139	101
	169	101	72	200		220	129	92
	156	94	69	300		200	123	88

Generic Cases: 3061 to 3096

Table A.85. Model parameters and deformation results (Case No: 3061 to 3096).

Excavation	Soil (γ=19kN/m^3)		Diaphragm Wall(E=2.0E+7)		
H_e(m)	c_u/σ_v'	E_{50}/c_u	d	EA	EI
11-14-17-20	0.25	100-200-300	0.6	1.2E+07	3.60E+05
			0.9	1.8E+07	1.215E+06
			1.2	2.4E+07	2.88E+06

Soil	E_{50}/c_u		
HSS	100	200	300
E_{50}^{ref}	4000	8000	12000
E_{oed}^{ref}	4000	8000	12000
E_{ur}^{ref}	12000	24000	36000
G_0^{ref}	35000	50000	67500
$\gamma_{0,7}$	3.58E-04	2.51E-04	1.86E-04
ϕ	22	22	22
K_0	0.625	0.625	0.625
E_{dyn}/E_{stat}	7	5	4.5

H=11m	d=0.6	d=0.9	d=1.2	E_{50}/c_u	H=11m	d=0.6	d=0.9	d=1.2
δ_{vm}(mm)	52	35	28	100	δ_{hm}(mm)	68	45	35
	42	29	22	200		54	37	29
	36	25	20	300		46	33	26

H=14m	d=0.6	d=0.9	d=1.2	E_{50}/c_u	H=14m	d=0.6	d=0.9	d=1.2
δ_{vm}(mm)	78	52	39	100	δ_{hm}(mm)	106	67	49
	64	44	33	200		85	57	43
	57	39	30	300		73	51	39

H=17m	d=0.6	d=0.9	d=1.2	E_{50}/c_u	H=17m	d=0.6	d=0.9	d=1.2
δ_{vm}(mm)	104	68	49	100	δ_{hm}(mm)	146	89	65
	86	56	43	200		118	77	58
	76	52	39	300		102	69	51

H=20m	d=0.6	d=0.9	d=1.2	E_{50}/c_u	H=20m	d=0.6	d=0.9	d=1.2
δ_{vm}(mm)	128	81	59	100	δ_{hm}(mm)	180	109	79
	105	69	53	200		146	95	71
	94	64	49	300		126	86	65

Generic Cases: 3097 to 3132

Table A.86. Model parameters and deformation results (Case No: 3097 to 3132).

Excavation	Soil(γ=19kN/m^3)		Diaphragm Wall(E=2.0E+7)		
H_e(m)	c_u/σ_v'	E_{50}/c_u	d	EA	EI
11-14-17-20	0.3	100-200-300	0.6	1.2E+07	3.60E+05
			0.9	1.8E+07	1.215E+06
			1.2	2.4E+07	2.88E+06

Soil	E_{50}/c_u		
HSS	100	200	300
E_{50}^{ref}	5400	10800	16200
E_{oed}^{ref}	5400	10800	16200
E_{ur}^{ref}	16200	32400	48600
G_0^{ref}	40500	60750	75938
$\gamma_{0.7}$	3.40E-04	2.27E-04	1.81E-04
ϕ	26.4	26.4	26.4
K_0	0.555	0.555	0.555
E_{dyn}/E_{stat}	6	4.5	3.75

H=11m	d=0.6	d=0.9	d=1.2	E_{50}/c_u	H=11m	d=0.6	d=0.9	d=1.2
δ_{vm}(mm)	39	31	26	100	δ_{hm}(mm)	49	38	32
	30	21	18	200		39	28	23
	25	19	14	300		33	25	19
H=14m	d=0.6	d=0.9	d=1.2	E_{50}/c_u	H=14m	d=0.6	d=0.9	d=1.2
δ_{vm}(mm)	56	42	34	100	δ_{hm}(mm)	72	53	41
	44	31	24	200		58	40	32
	37	28	21	300		50	36	28
H=17m	d=0.6	d=0.9	d=1.2	E_{50}/c_u	H=17m	d=0.6	d=0.9	d=1.2
δ_{vm}(mm)	75	54	43	100	δ_{hm}(mm)	100	69	53
	59	41	32	200		80	55	43
	50	37	28	300		68	49	39
H=20m	d=0.6	d=0.9	d=1.2	E_{50}/c_u	H=20m	d=0.6	d=0.9	d=1.2
δ_{vm}(mm)	89	64	51	100	δ_{hm}(mm)	124	83	64
	73	51	40	200		99	69	53
	63	46	36	300		85	62	49

Generic Cases: 3133 to 3168

Table A.87. Model parameters and deformation results (Case No: 3133 to 3168).

Excavation	Soil(γ=19kN/m^3)		Diaphragm Wall(E=2.0E+7)		
H_e(m)	c_u/σ_v'	E_{50}/c_u	d	EA	EI
11-14-17-20	0.35	100-200-300	0.6	1.2E+07	3.60E+05
			0.9	1.8E+07	1.215E+06
			1.2	2.4E+07	2.88E+06

Soil	E_{50}/c_u		
HSS	100	200	300
E_{50}^{ref}	7000	14000	21000
E_{oed}^{ref}	7000	14000	21000
E_{ur}^{ref}	21000	42000	63000
G_0^{ref}	52500	73500	99750
$\gamma_{0,7}$	2.75E-04	1.96E-04	1.45E-04
ϕ	30	30	30
K_0	0.500	0.500	0.500
E_{dyn}/E_{stat}	6	4.2	3.8

H=11m	d=0.6	d=0.9	d=1.2	E_{50}/c_u	H=11m	d=0.6	d=0.9	d=1.2
δ_{vm}(mm)	34	27	23	100	δ_{hm}(mm)	41	33	28
	24	19	17	200		32	25	21
	20	16	13	300		26	20	17

H=14m	d=0.6	d=0.9	d=1.2	E_{50}/c_u	H=14m	d=0.6	d=0.9	d=1.2
δ_{vm}(mm)	44	34	30	100	δ_{hm}(mm)	56	43	36
	34	26	22	200		46	34	28
	29	22	18	300		37	29	23

H=17m	d=0.6	d=0.9	d=1.2	E_{50}/c_u	H=17m	d=0.6	d=0.9	d=1.2
δ_{vm}(mm)	58	43	36	100	δ_{hm}(mm)	73	54	45
	45	34	28	200		61	44	36
	38	29	23	300		51	39	31

H=20m	d=0.6	d=0.9	d=1.2	E_{50}/c_u	H=20m	d=0.6	d=0.9	d=1.2
δ_{vm}(mm)	70	51	44	100	δ_{hm}(mm)	91	64	53
	56	42	35	200		76	55	45
	48	36	30	300		64	49	39

Model Group:23

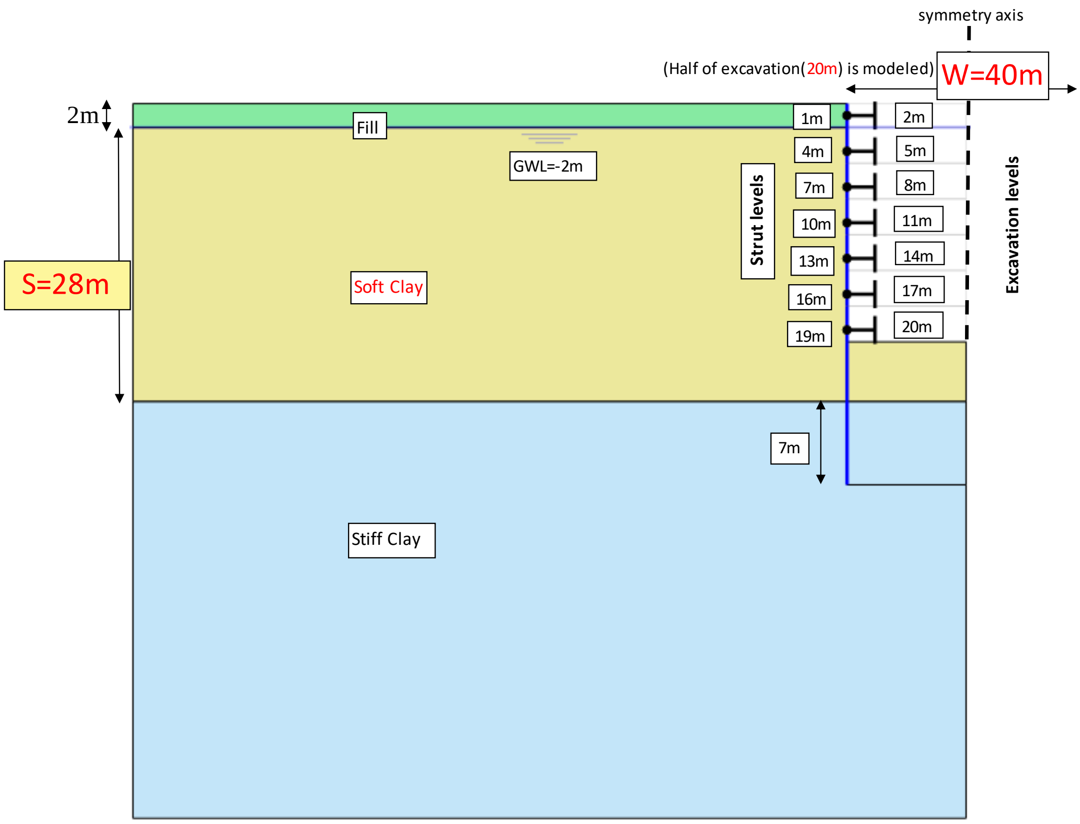

Figure A.23. Model Geometry-23.

Table B. Soil and structure parameters

Default Soil Parameters		
	Stiff Clay	Fill
	HS	HS
	Undrained(A)	Drained
E_{50}^{ref}	1.00E+05	1.50E+04
E_{oed}^{ref}	1.00E+05	1.50E+04
E_{ur}^{ref}	3.00E+05	4.50E+04
ϕ'	26	30
K_0	0.562	0.5
c'_{ref}	25	1
v'_{ur}	0.2	0.2
p_{ref}	100	100
R_f	0.9	0.9
$\gamma_{unsat/sat}$	20/20	16/20
R_{inter}	0.65	0.65
m	1	1

Range of parameters	
c_u/σ_v'	0.20-0.25-0.30-0.35
E_{50}/c_u	100-200-300
γ	15-17-19
S	23-28-33
W	20-40-60
H_e	11-14-17-20
$\ln(EI/\gamma_w h_{avg}^4)$	6.097-7.313-8.176

Diaphragm Wall (E=2.0E+7)		
d	EA	EI
0.6	1.2E+07	3.60E+05
0.9	1.8E+07	1.215E+06
1.2	2.4E+07	2.88E+06

Strut	
EA	3.80E+06
$L_{spacing}$	5m
h_{avg}	3m

Generic Cases: 3169 to 3204

Table A.88. Model parameters and deformation results (Case No: 3169 to 3204).

Excavation	Soil(γ=19kN/m^3)		Diaphragm Wall(E=2.0E+7)		
H_e(m)	c_u/σ_v'	E_{50}/c_u	d	EA	EI
11-14-17-20	0.2	100-200-300	0.6	1.2E+07	3.60E+05
			0.9	1.8E+07	1.215E+06
			1.2	2.4E+07	2.88E+06

Soft Soil	E_{50}/c_u		
HSS	100	200	300
E_{50}^{ref}	2895	5789	8685
E_{oed}^{ref}	2895	5789	8685
E_{ur}^{ref}	8685	17367	26055
G_0^{ref}	30759	43418	54281
$\gamma_{0,7}$	3.59E-04	2.54E-04	2.03E-04
ϕ	18	18	18
K_0	0.691	0.691	0.691
E_{dyn}/E_{stat}	8.5	6	5

H=11m	d=0.6	d=0.9	d=1.2	E_{50}/c_u	H=11m	d=0.6	d=0.9	d=1.2
δ_{vm}(mm)	100	68	49	100	δ_{hm}(mm)	122	81	59
	85	57	44	200		103	69	53
	78	52	38	300		95	64	47

H=14m	d=0.6	d=0.9	d=1.2	E_{50}/c_u	H=14m	d=0.6	d=0.9	d=1.2
δ_{vm}(mm)	153	97	71	100	δ_{hm}(mm)	191	119	83
	134	86	64	200		165	105	77
	123	79	58	300		152	97	71

H=17m	d=0.6	d=0.9	d=1.2	E_{50}/c_u	H=17m	d=0.6	d=0.9	d=1.2
δ_{vm}(mm)	198	124	92	100	δ_{hm}(mm)	254	154	107
	178	112	84	200		224	139	102
	165	104	77	300		208	131	95

H=20m	d=0.6	d=0.9	d=1.2	E_{50}/c_u	H=20m	d=0.6	d=0.9	d=1.2
δ_{vm}(mm)	237	148	108	100	δ_{hm}(mm)	306	186	130
	212	137	103	200		269	171	126
	200	129	96	300		253	161	117

Generic Cases: 3205 to 3240

Table A.89. Model parameters and deformation results (Case No: 3205 to 3240).

Excavation	Soil (γ=19kN/m^3)		Diaphragm Wall(E=2.0E+7)		
H_e(m)	c_u/σ_v'	E_{50}/c_u	d	EA	EI
11-14-17-20	0.25	100-200-300	0.6	1.2E+07	3.60E+05
			0.9	1.8E+07	1.215E+06
			1.2	2.4E+07	2.88E+06

Soil	E_{50}/c_u		
HSS	100	200	300
E_{50}^{ref}	4000	8000	12000
E_{oed}^{ref}	4000	8000	12000
E_{ur}^{ref}	12000	24000	36000
G_0^{ref}	35000	50000	67500
$\gamma_{0,7}$	3.58E-04	2.51E-04	1.86E-04
ϕ	22	22	22
K_0	0.625	0.625	0.625
E_{dyn}/E_{stat}	7	5	4.5

H=11m	d=0.6	d=0.9	d=1.2	E_{50}/c_u	H=11m	d=0.6	d=0.9	d=1.2
δ_{vm}(mm)	69	50	41	100	δ_{hm}(mm)	84	62	50
	57	38	30	200		72	48	39
	48	35	27	300		60	44	35

H=14m	d=0.6	d=0.9	d=1.2	E_{50}/c_u	H=14m	d=0.6	d=0.9	d=1.2
δ_{vm}(mm)	103	73	57	100	δ_{hm}(mm)	129	90	70
	88	58	46	200		110	73	57
	75	54	42	300		95	67	53

H=17m	d=0.6	d=0.9	d=1.2	E_{50}/c_u	H=17m	d=0.6	d=0.9	d=1.2
δ_{vm}(mm)	135	94	72	100	δ_{hm}(mm)	175	118	88
	116	77	61	200		150	99	76
	102	72	56	300		129	91	71

H=20m	d=0.6	d=0.9	d=1.2	E_{50}/c_u	H=20m	d=0.6	d=0.9	d=1.2
δ_{vm}(mm)	162	114	88	100	δ_{hm}(mm)	216	145	108
	143	96	75	200		185	123	95
	126	90	71	300		160	114	89

Generic Cases: 3241 to 3276

Table A.90. Model parameters and deformation results (Case No: 3241 to 3276).

Excavation	Soil(γ=19kN/m^3)		Diaphragm Wall(E=2.0E+7)		
H_e(m)	c_u/σ_v'	E_{50}/c_u	d	EA	EI
11-14-17-20	0.3	100-200-300	0.6	1.2E+07	3.60E+05
			0.9	1.8E+07	1.215E+06
			1.2	2.4E+07	2.88E+06

Soil	E_{50}/c_u		
HSS	100	200	300
E_{50}^{ref}	5400	10800	16200
E_{oed}^{ref}	5400	10800	16200
E_{ur}^{ref}	16200	32400	48600
G_0^{ref}	40500	60750	75938
$\gamma_{0,7}$	3.40E-04	2.27E-04	1.81E-04
ϕ	26.4	26.4	26.4
K_0	0.555	0.555	0.555
E_{dyn}/E_{stat}	6	4.5	3.75

H=11m	d=0.6	d=0.9	d=1.2	E_{50}/c_u	H=11m	d=0.6	d=0.9	d=1.2
δ_{vm}(mm)	52	44	36	100	δ_{hm}(mm)	66	54	45
	41	33	27	200		52	42	35
	36	27	22	300		45	36	29

H=14m	d=0.6	d=0.9	d=1.2	E_{50}/c_u	H=14m	d=0.6	d=0.9	d=1.2
δ_{vm}(mm)	76	60	48	100	δ_{hm}(mm)	94	73	59
	60	47	37	200		77	59	47
	53	40	32	300		67	52	41

H=17m	d=0.6	d=0.9	d=1.2	E_{50}/c_u	H=17m	d=0.6	d=0.9	d=1.2
δ_{vm}(mm)	98	75	61	100	δ_{hm}(mm)	124	93	75
	80	61	49	200		104	78	62
	71	54	42	300		90	69	54

H=20m	d=0.6	d=0.9	d=1.2	E_{50}/c_u	H=20m	d=0.6	d=0.9	d=1.2
δ_{vm}(mm)	118	91	73	100	δ_{hm}(mm)	153	113	90
	99	75	61	200		128	96	76
	88	67	54	300		112	86	69

Generic Cases: 3277 to 3312

Table A.91. Model parameters and deformation results (Case No: 3277 to 3312).

Excavation	Soil(γ=19kN/m^3)		Diaphragm Wall(E=2.0E+7)		
H_e(m)	c_u/σ_v'	E_{50}/c_u	d	EA	EI
11-14-17-20	0.35	100-200-300	0.6	1.2E+07	3.60E+05
			0.9	1.8E+07	1.215E+06
			1.2	2.4E+07	2.88E+06

Soil	E_{50}/c_u		
HSS	100	200	300
E_{50}^{ref}	7000	14000	21000
E_{oed}^{ref}	7000	14000	21000
E_{ur}^{ref}	21000	42000	63000
G_0^{ref}	52500	73500	99750
$\gamma_{0,7}$	2.75E-04	1.96E-04	1.45E-04
ϕ	30	30	30
K_0	0.500	0.500	0.500
E_{dyn}/E_{stat}	6	4.2	3.8

H=11m	d=0.6	d=0.9	d=1.2	E_{50}/c_u	H=11m	d=0.6	d=0.9	d=1.2
δ_{vm}(mm)	47	39	36	100	δ_{hm}(mm)	58	47	43
	35	28	25	200		45	36	32
	29	23	20	300		37	29	26

H=14m	d=0.6	d=0.9	d=1.2	E_{50}/c_u	H=14m	d=0.6	d=0.9	d=1.2
δ_{vm}(mm)	64	51	45	100	δ_{hm}(mm)	80	63	55
	49	39	33	200		63	49	42
	40	32	27	300		53	41	35

H=17m	d=0.6	d=0.9	d=1.2	E_{50}/c_u	H=17m	d=0.6	d=0.9	d=1.2
δ_{vm}(mm)	82	64	56	100	δ_{hm}(mm)	103	79	69
	64	50	43	200		82	63	53
	54	43	36	300		68	55	46

H=20m	d=0.6	d=0.9	d=1.2	E_{50}/c_u	H=20m	d=0.6	d=0.9	d=1.2
δ_{vm}(mm)	98	75	67	100	δ_{hm}(mm)	125	93	81
	79	62	53	200		101	78	66
	67	54	46	300		85	69	58

Model Group:24

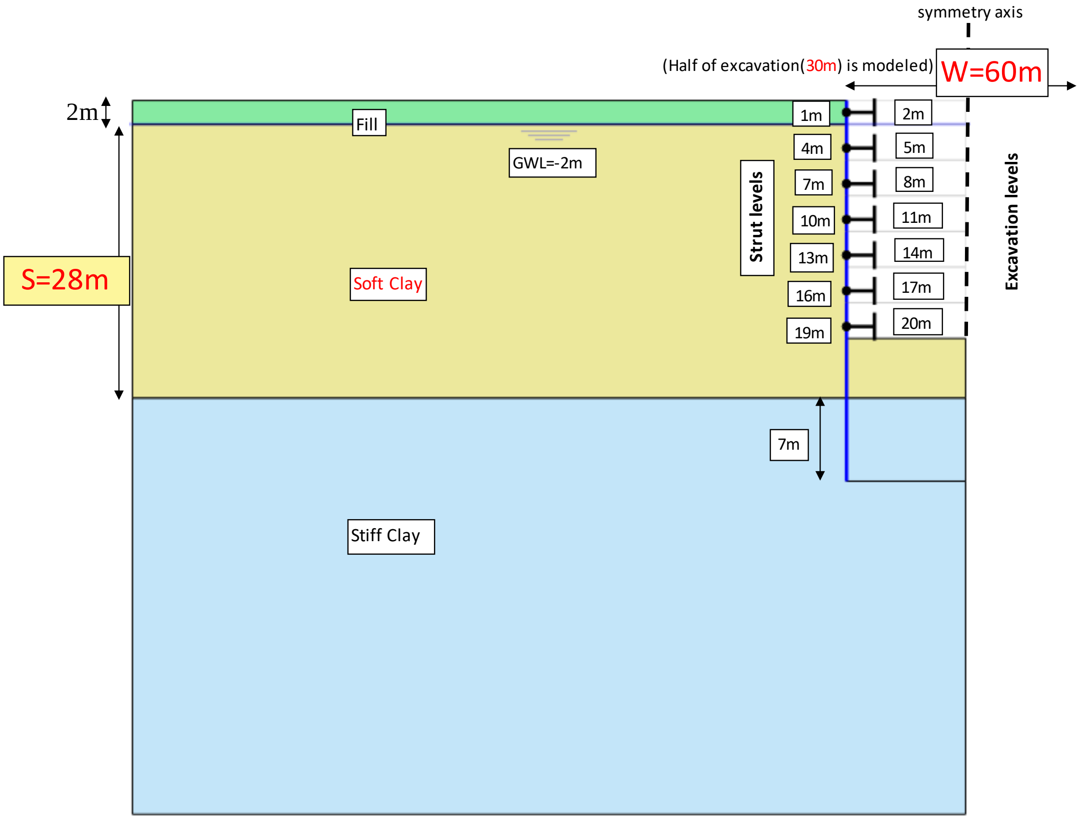

Figure A.24. Model Geometry-24.

Table B. Soil and structure parameters

Default Soil Parameters		
	Stiff Clay	Fill
	HS	HS
	Undrained(A)	Drained
E_{50}^{ref}	1.00E+05	1.50E+04
E_{oed}^{ref}	1.00E+05	1.50E+04
E_{ur}^{ref}	3.00E+05	4.50E+04
ϕ'	26	30
K_0	0.562	0.5
c'_{ref}	25	1
v'_{ur}	0.2	0.2
p_{ref}	100	100
R_f	0.9	0.9
$\gamma_{unsat/sat}$	20/20	16/20
R_{inter}	0.65	0.65
m	1	1

Range of parameters	
c_u/σ'_v	0.20-0.25-0.30-0.35
E_{50}/c_u	100-200-300
γ	15-17-19
S	23-28-33
W	20-40-60
H_e	11-14-17-20
$\ln(EI/\gamma_w h_{avg}^4)$	6.097-7.313-8.176

Diaphragm Wall (E=2.0E+7)		
d	EA	EI
0.6	1.2E+07	3.60E+05
0.9	1.8E+07	1.215E+06
1.2	2.4E+07	2.88E+06

Strut	
EA	3.80E+06
$L_{spacing}$	5m
h_{avg}	3m

Generic Cases: 3313 to 3348

Table A.92. Model parameters and deformation results (Case No: 3313 to 3348).

Excavation	Soil(γ=19kN/m^3)		Diaphragm Wall(E=2.0E+7)		
H_e(m)	c_u/σ_v'	E_{50}/c_u	d	EA	EI
11-14-17-20	0.2	100-200-300	0.6	1.2E+07	3.60E+05
			0.9	1.8E+07	1.215E+06
			1.2	2.4E+07	2.88E+06

Soft Soil	E_{50}/c_u		
HSS	100	200	300
E_{50}^{ref}	2895	5789	8685
E_{oed}^{ref}	2895	5789	8685
E_{ur}^{ref}	8685	17367	26055
G_0^{ref}	30759	43418	54281
$\gamma_{0,7}$	3.59E-04	2.54E-04	2.03E-04
ϕ	18	18	18
K_0	0.691	0.691	0.691
E_{dyn}/E_{stat}	8.5	6	5

H=11m	d=0.6	d=0.9	d=1.2	E_{50}/c_u	H=11m	d=0.6	d=0.9	d=1.2
δ_{vm}(mm)	116	78	58	100	δ_{hm}(mm)	139	95	70
	99	69	52	200		123	84	64
	90	64	47	300		108	76	57

H=14m	d=0.6	d=0.9	d=1.2	E_{50}/c_u	H=14m	d=0.6	d=0.9	d=1.2
δ_{vm}(mm)	176	112	81	100	δ_{hm}(mm)	215	138	98
	155	102	76	200		190	125	92
	142	94	70	300		172	113	85

H=17m	d=0.6	d=0.9	d=1.2	E_{50}/c_u	H=17m	d=0.6	d=0.9	d=1.2
δ_{vm}(mm)	226	144	107	100	δ_{hm}(mm)	283	178	128
	206	134	101	200		256	164	123
	192	124	93	300		236	152	113

H=20m	d=0.6	d=0.9	d=1.2	E_{50}/c_u	H=20m	d=0.6	d=0.9	d=1.2
δ_{vm}(mm)	268	177	131	100	δ_{hm}(mm)	340	215	155
	250	166	125	200		306	199	149
	234	156	116	300		286	186	139

Generic Cases: 3349 to 3384

Table A.93. Model parameters and deformation results (Case No: 3349 to 3384).

Excavation	Soil (γ=19kN/m^3)		Diaphragm Wall(E=2.0E+7)		
H_e(m)	c_u/σ_v'	E_{50}/c_u	d	EA	EI
11-14-17-20	0.25	100-200-300	0.6	1.2E+07	3.60E+05
			0.9	1.8E+07	1.215E+06
			1.2	2.4E+07	2.88E+06

Soil	E_{50}/c_u		
HSS	100	200	300
E_{50}^{ref}	4000	8000	12000
E_{oed}^{ref}	4000	8000	12000
E_{ur}^{ref}	12000	24000	36000
G_0^{ref}	35000	50000	67500
$\gamma_{0,7}$	3.58E-04	2.51E-04	1.86E-04
ϕ	22	22	22
K_0	0.625	0.625	0.625
E_{dyn}/E_{stat}	7	5	4.5

H=11m	d=0.6	d=0.9	d=1.2	E_{50}/c_u	H=11m	d=0.6	d=0.9	d=1.2
δ_{vm}(mm)	86	61	51	100	δ_{hm}(mm)	105	76	63
	68	50	41	200		83	62	51
	58	43	34	300		71	53	43

H=14m	d=0.6	d=0.9	d=1.2	E_{50}/c_u	H=14m	d=0.6	d=0.9	d=1.2
δ_{vm}(mm)	127	88	70	100	δ_{hm}(mm)	158	108	86
	103	73	58	200		128	91	73
	90	65	51	300		110	81	64

H=17m	d=0.6	d=0.9	d=1.2	E_{50}/c_u	H=17m	d=0.6	d=0.9	d=1.2
δ_{vm}(mm)	164	115	88	100	δ_{hm}(mm)	210	139	107
	137	97	77	200		173	121	96
	121	88	69	300		150	109	85

H=20m	d=0.6	d=0.9	d=1.2	E_{50}/c_u	H=20m	d=0.6	d=0.9	d=1.2
δ_{vm}(mm)	197	139	108	100	δ_{hm}(mm)	255	170	128
	168	119	97	200		211	150	118
	152	110	87	300		186	135	108

Generic Cases: 3385 to 3420

Table A.94. Model parameters and deformation results (Case No: 3385 to 3420).

Excavation	Soil (γ=19kN/m^3)		Diaphragm Wall(E=2.0E+7)		
H_e(m)	c_u/σ_v'	E_{50}/c_u	d	EA	EI
11-14-17-20	0.3	100-200-300	0.6	1.2E+07	3.60E+05
			0.9	1.8E+07	1.215E+06
			1.2	2.4E+07	2.88E+06

Soil	E_{50}/c_u		
HSS	100	200	300
E_{50}^{ref}	5400	10800	16200
E_{oed}^{ref}	5400	10800	16200
E_{ur}^{ref}	16200	32400	48600
G_0^{ref}	40500	60750	75938
$\gamma_{0,7}$	3.40E-04	2.27E-04	1.81E-04
ϕ	26.4	26.4	26.4
K_0	0.555	0.555	0.555
E_{dyn}/E_{stat}	6	4.5	3.75

H=11m	d=0.6	d=0.9	d=1.2	E_{50}/c_u	H=11m	d=0.6	d=0.9	d=1.2
δ_{vm}(mm)	65	54	48	100	δ_{hm}(mm)	82	67	58
	51	41	33	200		64	51	42
	44	35	27	300		54	44	34

H=14m	d=0.6	d=0.9	d=1.2	E_{50}/c_u	H=14m	d=0.6	d=0.9	d=1.2
δ_{vm}(mm)	93	74	63	100	δ_{hm}(mm)	116	90	77
	74	57	46	200		93	72	58
	63	50	39	300		80	62	50

H=17m	d=0.6	d=0.9	d=1.2	E_{50}/c_u	H=17m	d=0.6	d=0.9	d=1.2
δ_{vm}(mm)	121	92	78	100	δ_{hm}(mm)	154	113	94
	97	74	61	200		123	93	75
	85	66	52	300		106	84	66

H=20m	d=0.6	d=0.9	d=1.2	E_{50}/c_u	H=20m	d=0.6	d=0.9	d=1.2
δ_{vm}(mm)	146	111	92	100	δ_{hm}(mm)	188	137	113
	119	93	76	200		152	115	93
	107	82	67	300		133	103	83

Generic Cases: 3421 to 3456

Table A.95. Model parameters and deformation results (Case No: 3421 to 3456).

Excavation	Soil(γ=19kN/m^3)		Diaphragm Wall(E=2.0E+7)		
H_e(m)	c_u/σ_v'	E_{50}/c_u	d	EA	EI
11-14-17-20	0.35	100-200-300	0.6	1.2E+07	3.60E+05
			0.9	1.8E+07	1.215E+06
			1.2	2.4E+07	2.88E+06

Soil	E_{50}/c_u		
HSS	100	200	300
E_{50}^{ref}	7000	14000	21000
E_{oed}^{ref}	7000	14000	21000
E_{ur}^{ref}	21000	42000	63000
G_0^{ref}	52500	73500	99750
$\gamma_{0,7}$	2.75E-04	1.96E-04	1.45E-04
ϕ	30	30	30
K_0	0.500	0.500	0.500
E_{dyn}/E_{stat}	6	4.2	3.8

H=11m	d=0.6	d=0.9	d=1.2	E_{50}/c_u	H=11m	d=0.6	d=0.9	d=1.2
δ_{vm}(mm)	56	48	44	100	δ_{hm}(mm)	70	60	53
	43	36	30	200		54	45	39
	35	29	25	300		44	37	32

H=14m	d=0.6	d=0.9	d=1.2	E_{50}/c_u	H=14m	d=0.6	d=0.9	d=1.2
δ_{vm}(mm)	77	64	56	100	δ_{hm}(mm)	95	80	69
	59	49	41	200		75	62	52
	49	40	35	300		63	51	44

H=17m	d=0.6	d=0.9	d=1.2	E_{50}/c_u	H=17m	d=0.6	d=0.9	d=1.2
δ_{vm}(mm)	98	80	71	100	δ_{hm}(mm)	121	99	85
	78	63	53	200		98	79	66
	66	53	45	300		83	67	58

H=20m	d=0.6	d=0.9	d=1.2	E_{50}/c_u	H=20m	d=0.6	d=0.9	d=1.2
δ_{vm}(mm)	116	97	83	100	δ_{hm}(mm)	146	119	101
	96	78	66	200		121	96	82
	83	67	57	300		103	84	71

Model Group:25

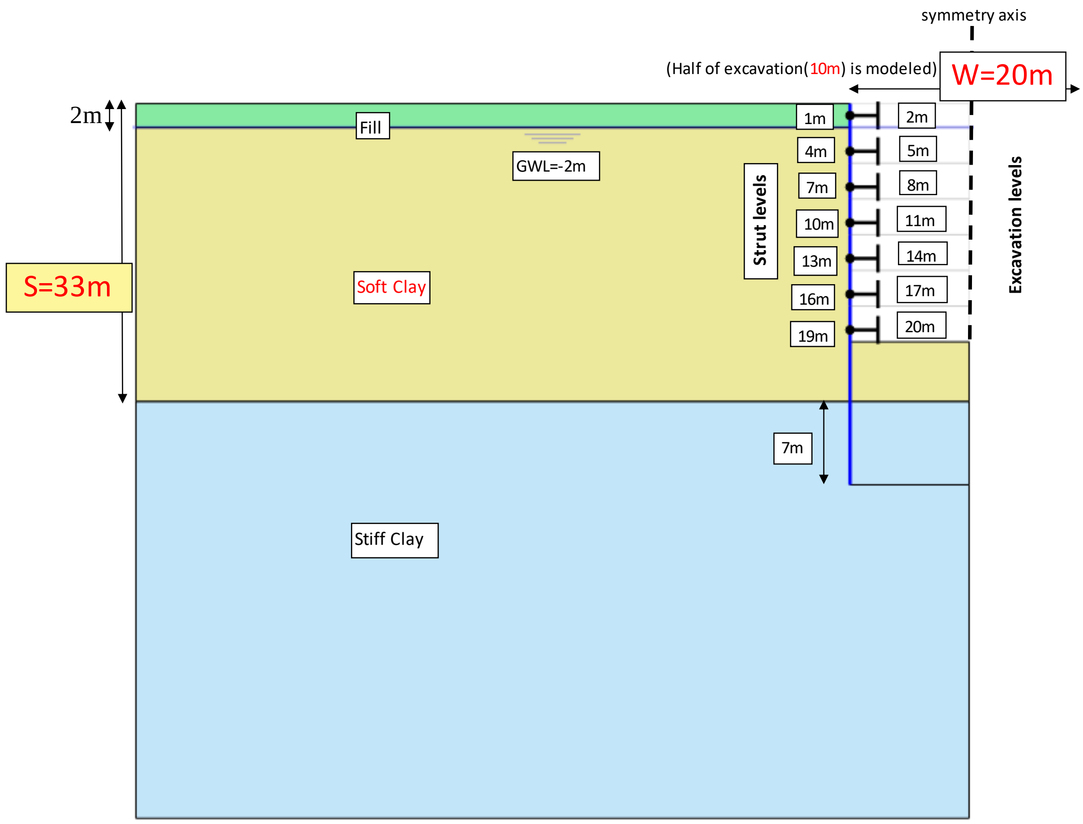

Figure A.25. Model Geometry-25.

Table B. Soil and structure parameters

Default Soil Parameters		
	Stiff Clay	Fill
	HS	HS
	Undrained(A)	Drained
E_{50}^{ref}	1.00E+05	1.50E+04
E_{oed}^{ref}	1.00E+05	1.50E+04
E_{ur}^{ref}	3.00E+05	4.50E+04
ϕ'	26	30
K_0	0.562	0.5
c'_{ref}	25	1
ν'_{ur}	0.2	0.2
p_{ref}	100	100
R_f	0.9	0.9
$\gamma_{unsat/sat}$	20/20	16/20
R_{inter}	0.65	0.65
m	1	1

Range of parameters	
c_u/σ_v'	0.20-0.25-0.30-0.35
E_{50}/c_u	100-200-300
γ	15-17-19
S	23-28-33
W	20-40-60
H_e	11-14-17-20
$\ln(EI/\gamma_w h_{avg}^4)$	6.097-7.313-8.176

Diaphragm Wall (E=2.0E+7)		
d	EA	EI
0.6	1.2E+07	3.60E+05
0.9	1.8E+07	1.215E+06
1.2	2.4E+07	2.88E+06

Strut	
EA	3.80E+06
$L_{spacing}$	5m
h_{avg}	3m

Generic Cases: 3457 to 3492

Table A.96. Model parameters and deformation results (Case No: 3457 to 3492).

Excavation	Soil(γ=19kN/m^3)		Diaphragm Wall(E=2.0E+7)		
H_e(m)	c_u/σ_v'	E_{50}/c_u	d	EA	EI
11-14-17-20	0.2	100-200-300	0.6	1.2E+07	3.60E+05
			0.9	1.8E+07	1.215E+06
			1.2	2.4E+07	2.88E+06

Soft Soil	E_{50}/c_u		
HSS	100	200	300
E_{50}^{ref}	2895	5789	8685
E_{oed}^{ref}	2895	5789	8685
E_{ur}^{ref}	8685	17367	26055
G_0^{ref}	30759	43418	54281
$\gamma_{0,7}$	3.59E-04	2.54E-04	2.03E-04
ϕ	18	18	18
K_0	0.691	0.691	0.691
E_{dyn}/E_{stat}	8.5	6	5

H=11m	d=0.6	d=0.9	d=1.2	E_{50}/c_u	H=11m	d=0.6	d=0.9	d=1.2
δ_{vm}(mm)	77	50	37	100	δ_{hm}(mm)	97	62	46
	64	43	32	200		83	54	40
	59	39	29	300		74	48	37

H=14m	d=0.6	d=0.9	d=1.2	E_{50}/c_u	H=14m	d=0.6	d=0.9	d=1.2
δ_{vm}(mm)	123	78	56	100	δ_{hm}(mm)	163	99	70
	110	69	49	200		141	88	63
	99	62	46	300		126	80	59

H=17m	d=0.6	d=0.9	d=1.2	E_{50}/c_u	H=17m	d=0.6	d=0.9	d=1.2
δ_{vm}(mm)	177	105	76	100	δ_{hm}(mm)	241	138	97
	156	96	67	200		208	126	86
	146	87	64	300		186	116	82

H=20m	d=0.6	d=0.9	d=1.2	E_{50}/c_u	H=20m	d=0.6	d=0.9	d=1.2
δ_{vm}(mm)	224	131	93	100	δ_{hm}(mm)	307	176	122
	204	121	85	200		271	161	111
	187	112	80	300		245	149	106

Generic Cases: 3493 to 3528

Table A.97. Model parameters and deformation results (Case No: 3493 to 3528).

Excavation	Soil(γ=19kN/m^3)		Diaphragm Wall(E=2.0E+7)		
H_e(m)	c_u/σ_v'	E_{50}/c_u	d	EA	EI
11-14-17-20	0.25	100-200-300	0.6	1.2E+07	3.60E+05
			0.9	1.8E+07	1.215E+06
			1.2	2.4E+07	2.88E+06

Soil	E_{50}/c_u		
HSS	100	200	300
E_{50}^{ref}	4000	8000	12000
E_{oed}^{ref}	4000	8000	12000
E_{ur}^{ref}	12000	24000	36000
G_0^{ref}	35000	50000	67500
$\gamma_{0,7}$	3.58E-04	2.51E-04	1.86E-04
ϕ	22	22	22
K_0	0.625	0.625	0.625
E_{dyn}/E_{stat}	7	5	4.5

H=11m	d=0.6	d=0.9	d=1.2	E_{50}/c_u	H=11m	d=0.6	d=0.9	d=1.2
δ_{vm}(mm)	52	33	27	100	δ_{hm}(mm)	68	44	34
	42	29	23	200		53	38	29
	37	25	20	300		46	33	26

H=14m	d=0.6	d=0.9	d=1.2	E_{50}/c_u	H=14m	d=0.6	d=0.9	d=1.2
δ_{vm}(mm)	80	53	40	100	δ_{hm}(mm)	110	69	52
	64	45	34	200		86	60	46
	57	39	31	300		74	51	40

H=17m	d=0.6	d=0.9	d=1.2	E_{50}/c_u	H=17m	d=0.6	d=0.9	d=1.2
δ_{vm}(mm)	113	73	53	100	δ_{hm}(mm)	156	98	72
	92	62	47	200		124	85	63
	80	55	43	300		108	74	56

H=20m	d=0.6	d=0.9	d=1.2	E_{50}/c_u	H=20m	d=0.6	d=0.9	d=1.2
δ_{vm}(mm)	147	92	67	100	δ_{hm}(mm)	205	127	91
	118	80	59	200		164	110	81
	105	71	55	300		141	96	73

Generic Cases: 3529 to 3564

Table A.98. Model parameters and deformation results (Case No: 3529 to 3564).

Excavation	Soil(γ=19kN/m^3)		Diaphragm Wall(E=2.0E+7)		
H_e(m)	c_u/σ_v'	E_{50}/c_u	d	EA	EI
11-14-17-20	0.3	100-200-300	0.6	1.2E+07	3.60E+05
			0.9	1.8E+07	1.215E+06
			1.2	2.4E+07	2.88E+06

Soil	E_{50}/c_u		
HSS	100	200	300
E_{50}^{ref}	5400	10800	16200
E_{oed}^{ref}	5400	10800	16200
E_{ur}^{ref}	16200	32400	48600
G_0^{ref}	40500	60750	75938
$\gamma_{0,7}$	3.40E-04	2.27E-04	1.81E-04
ϕ	26.4	26.4	26.4
K_0	0.555	0.555	0.555
E_{dyn}/E_{stat}	6	4.5	3.75

H=11m	d=0.6	d=0.9	d=1.2	E_{50}/c_u	H=11m	d=0.6	d=0.9	d=1.2
δ_{vm}(mm)	39	30	26	100	δ_{hm}(mm)	50	38	32
	29	22	17	200		38	29	22
	25	19	14	300		33	25	19

H=14m	d=0.6	d=0.9	d=1.2	E_{50}/c_u	H=14m	d=0.6	d=0.9	d=1.2
δ_{vm}(mm)	57	42	34	100	δ_{hm}(mm)	72	53	43
	43	33	25	200		57	43	32
	38	29	22	300		49	37	29

H=17m	d=0.6	d=0.9	d=1.2	E_{50}/c_u	H=17m	d=0.6	d=0.9	d=1.2
δ_{vm}(mm)	77	56	45	100	δ_{hm}(mm)	101	72	56
	59	44	34	200		80	59	45
	51	38	30	300		69	52	40

H=20m	d=0.6	d=0.9	d=1.2	E_{50}/c_u	H=20m	d=0.6	d=0.9	d=1.2
δ_{vm}(mm)	96	70	56	100	δ_{hm}(mm)	132	92	71
	76	57	43	200		105	77	59
	66	49	38	300		89	67	52

Generic Cases: 3565to 3600

Table A.99. Model parameters and deformation results (Case No: 3565to 3600).

Excavation	Soil(γ=19kN/m^3)		Diaphragm Wall(E=2.0E+7)		
H_e(m)	c_u/σ_v'	E_{50}/c_u	d	EA	EI
11-14-17-20	0.35	100-200-300	0.6	1.2E+07	3.60E+05
			0.9	1.8E+07	1.215E+06
			1.2	2.4E+07	2.88E+06

Soil	E_{50}/c_u		
HSS	100	200	300
E_{50}^{ref}	7000	14000	21000
E_{oed}^{ref}	7000	14000	21000
E_{ur}^{ref}	21000	42000	63000
G_0^{ref}	52500	73500	99750
$\gamma_{0,7}$	2.75E-04	1.96E-04	1.45E-04
ϕ	30	30	30
K_0	0.500	0.500	0.500
E_{dyn}/E_{stat}	6	4.2	3.8

H=11m	d=0.6	d=0.9	d=1.2	E_{50}/c_u	H=11m	d=0.6	d=0.9	d=1.2
δ_{vm}(mm)	32	27	23	100	δ_{hm}(mm)	41	33	29
	25	19	17	200		32	25	21
	20	15	13	300		26	20	17

H=14m	d=0.6	d=0.9	d=1.2	E_{50}/c_u	H=14m	d=0.6	d=0.9	d=1.2
δ_{vm}(mm)	44	35	30	100	δ_{hm}(mm)	55	43	37
	34	26	22	200		46	34	28
	28	22	18	300		38	29	24

H=17m	d=0.6	d=0.9	d=1.2	E_{50}/c_u	H=17m	d=0.6	d=0.9	d=1.2
δ_{vm}(mm)	57	45	38	100	δ_{hm}(mm)	73	56	46
	45	35	29	200		61	46	37
	38	30	24	300		51	39	32

H=20m	d=0.6	d=0.9	d=1.2	E_{50}/c_u	H=20m	d=0.6	d=0.9	d=1.2
δ_{vm}(mm)	71	55	45	100	δ_{hm}(mm)	95	70	56
	58	44	36	200		78	58	47
	49	38	30	300		65	51	40

Model Group:26

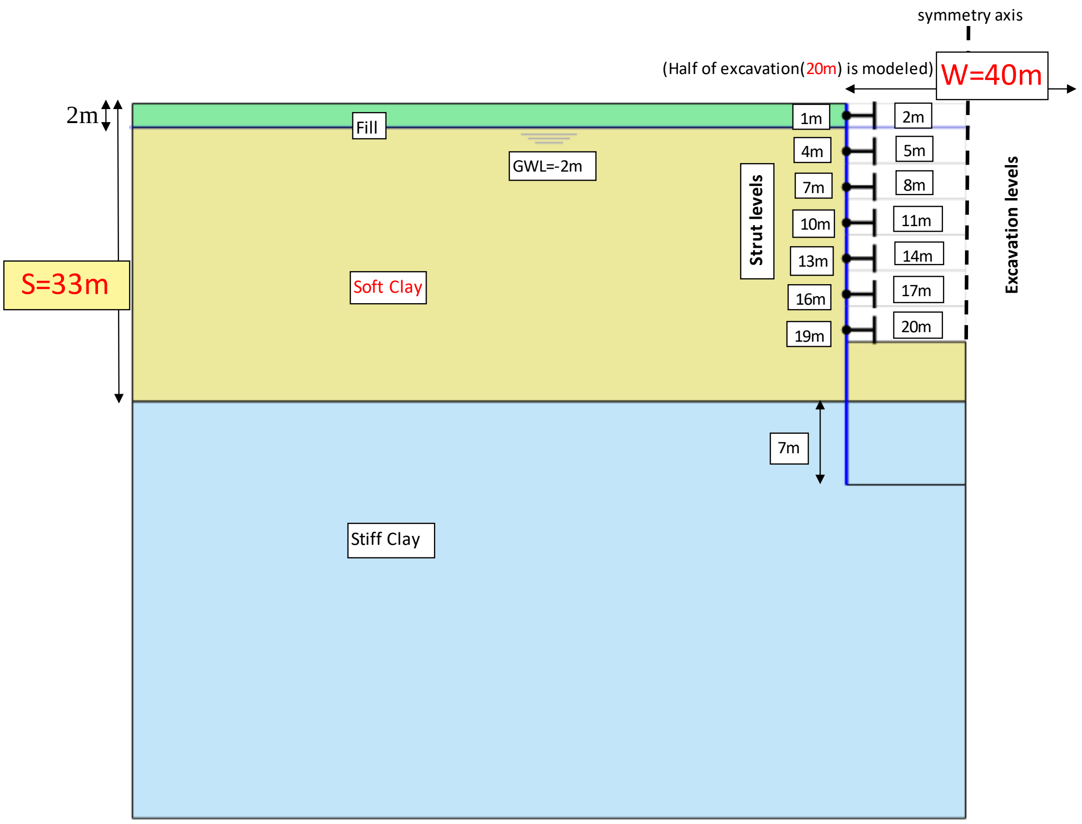

Figure A.26. Model Geometry-26.

Table B. Soil and structure parameters

Default Soil Parameters		
	Stiff Clay	Fill
	HS	HS
	Undrained(A)	Drained
E_{50}^{ref}	1.00E+05	1.50E+04
E_{oed}^{ref}	1.00E+05	1.50E+04
E_{ur}^{ref}	3.00E+05	4.50E+04
ϕ'	26	30
K_0	0.562	0.5
c'_{ref}	25	1
v'_{ur}	0.2	0.2
p_{ref}	100	100
R_f	0.9	0.9
$\gamma_{unsat/sat}$	20/20	16/20
R_{inter}	0.65	0.65
m	1	1

Range of parameters	
c_u/σ'_v	0.20-0.25-0.30-0.35
E_{50}/c_u	100-200-300
γ	15-17-19
S	23-28-33
W	20-40-60
H_e	11-14-17-20
$\ln(EI/\gamma_w h_{avg}^4)$	6.097-7.313-8.176

Diaphragm Wall (E=2.0E+7)		
d	EA	EI
0.6	1.2E+07	3.60E+05
0.9	1.8E+07	1.215E+06
1.2	2.4E+07	2.88E+06

Strut	
EA	3.80E+06
$L_{spacing}$	5m
h_{avg}	3m

Generic Cases: 3601 to 3636

Table A.100. Model parameters and deformation results (Case No: 3601 to 3636).

Excavation	Soil(γ=19kN/m^3)		Diaphragm Wall(E=2.0E+7)		
H_e(m)	c_u/σ_v'	E_{50}/c_u	d	EA	EI
11-14-17-20	0.2	100-200-300	0.6	1.2E+07	3.60E+05
			0.9	1.8E+07	1.215E+06
			1.2	2.4E+07	2.88E+06

Soft Soil	E_{50}/c_u		
HSS	100	200	300
E_{50}^{ref}	2895	5789	8685
E_{oed}^{ref}	2895	5789	8685
E_{ur}^{ref}	8685	17367	26055
G_0^{ref}	30759	43418	54281
$\gamma_{0,7}$	3.59E-04	2.54E-04	2.03E-04
ϕ	18	18	18
K_0	0.691	0.691	0.691
E_{dyn}/E_{stat}	8.5	6	5

H=11m	d=0.6	d=0.9	d=1.2	E_{50}/c_u	H=11m	d=0.6	d=0.9	d=1.2
δ_{vm}(mm)	98	68	51	100	δ_{hm}(mm)	120	83	61
	74	49	38	200		92	59	47
	66	44	34	300		83	54	42

H=14m	d=0.6	d=0.9	d=1.2	E_{50}/c_u	H=14m	d=0.6	d=0.9	d=1.2
δ_{vm}(mm)	161	106	76	100	δ_{hm}(mm)	204	131	92
	120	77	59	200		155	95	72
	108	71	53	300		136	89	66

H=17m	d=0.6	d=0.9	d=1.2	E_{50}/c_u	H=17m	d=0.6	d=0.9	d=1.2
δ_{vm}(mm)	225	143	102	100	δ_{hm}(mm)	295	182	125
	172	105	78	200		226	134	98
	157	98	70	300		201	124	90

H=20m	d=0.6	d=0.9	d=1.2	E_{50}/c_u	H=20m	d=0.6	d=0.9	d=1.2
δ_{vm}(mm)	288	179	128	100	δ_{hm}(mm)	380	229	159
	221	132	98	200		290	171	124
	200	125	88	300		261	159	116

Generic Cases: 3637 to 3672

Table A.101. Model parameters and deformation results (Case No: 3637 to 3672).

Excavation	Soil(γ=19kN/m^3)		Diaphragm Wall(E=2.0E+7)		
H_e(m)	c_u/σ_v'	E_{50}/c_u	d	EA	EI
11-14-17-20	0.25	100-200-300	0.6	1.2E+07	3.60E+05
			0.9	1.8E+07	1.215E+06
			1.2	2.4E+07	2.88E+06

Soil	E_{50}/c_u		
HSS	100	200	300
E_{50}^{ref}	4000	8000	12000
E_{oed}^{ref}	4000	8000	12000
E_{ur}^{ref}	12000	24000	36000
G_0^{ref}	35000	50000	67500
$\gamma_{0,7}$	3.58E-04	2.51E-04	1.86E-04
ϕ	22	22	22
K_0	0.625	0.625	0.625
E_{dyn}/E_{stat}	7	5	4.5

H=11m	d=0.6	d=0.9	d=1.2	E_{50}/c_u	H=11m	d=0.6	d=0.9	d=1.2
δ_{vm}(mm)	59	45	36	100	δ_{hm}(mm)	75	55	45
	49	33	25	200		62	42	33
	41	30	22	300		52	38	29

H=14m	d=0.6	d=0.9	d=1.2	E_{50}/c_u	H=14m	d=0.6	d=0.9	d=1.2
δ_{vm}(mm)	92	67	50	100	δ_{hm}(mm)	118	81	63
	74	50	38	200		97	64	50
	63	46	34	300		81	59	44

H=17m	d=0.6	d=0.9	d=1.2	E_{50}/c_u	H=17m	d=0.6	d=0.9	d=1.2
δ_{vm}(mm)	127	90	66	100	δ_{hm}(mm)	168	113	83
	104	70	52	200		138	91	69
	88	63	47	300		116	82	61

H=20m	d=0.6	d=0.9	d=1.2	E_{50}/c_u	H=20m	d=0.6	d=0.9	d=1.2
δ_{vm}(mm)	159	109	81	100	δ_{hm}(mm)	219	142	104
	132	88	67	200		178	118	89
	114	81	60	300		149	106	80

Generic Cases: 3673 to 3708

Table A.102. Model parameters and deformation results (Case No: 3673 to 3708).

Excavation	Soil(γ=19kN/m^3)		Diaphragm Wall(E=2.0E+7)		
H_e(m)	c_u/σ_v'	E_{50}/c_u	d	EA	EI
11-14-17-20	0.3	100-200-300	0.6	1.2E+07	3.60E+05
			0.9	1.8E+07	1.215E+06
			1.2	2.4E+07	2.88E+06

Soil	E_{50}/c_u		
HSS	100	200	300
E_{50}^{ref}	5400	10800	16200
E_{oed}^{ref}	5400	10800	16200
E_{ur}^{ref}	16200	32400	48600
G_0^{ref}	40500	60750	75938
$\gamma_{0,7}$	3.40E-04	2.27E-04	1.81E-04
ϕ	26.4	26.4	26.4
K_0	0.555	0.555	0.555
E_{dyn}/E_{stat}	6	4.5	3.75

H=11m	d=0.6	d=0.9	d=1.2	E_{50}/c_u	H=11m	d=0.6	d=0.9	d=1.2
δ_{vm}(mm)	48	39	34	100	δ_{hm}(mm)	60	48	42
	35	29	25	200		44	37	32
	30	24	20	300		39	31	25

H=14m	d=0.6	d=0.9	d=1.2	E_{50}/c_u	H=14m	d=0.6	d=0.9	d=1.2
δ_{vm}(mm)	67	50	44	100	δ_{hm}(mm)	85	64	55
	50	40	34	200		64	51	43
	44	34	27	300		57	44	35

H=17m	d=0.6	d=0.9	d=1.2	E_{50}/c_u	H=17m	d=0.6	d=0.9	d=1.2
δ_{vm}(mm)	89	66	54	100	δ_{hm}(mm)	115	83	70
	67	53	44	200		87	69	56
	59	46	37	300		77	60	47

H=20m	d=0.6	d=0.9	d=1.2	E_{50}/c_u	H=20m	d=0.6	d=0.9	d=1.2
δ_{vm}(mm)	111	81	65	100	δ_{hm}(mm)	148	104	84
	85	66	54	200		112	87	69
	74	58	45	300		98	76	59

Generic Cases: 3709 to 3744

Table A.103. Model parameters and deformation results (Case No: 3709 to 3744).

Excavation	Soil(γ=19kN/m^3)		Diaphragm Wall(E=2.0E+7)		
H_e(m)	c_u/σ_v'	E_{50}/c_u	d	EA	EI
11-14-17-20	0.35	100-200-300	0.6	1.2E+07	3.60E+05
			0.9	1.8E+07	1.215E+06
			1.2	2.4E+07	2.88E+06

Soil	E_{50}/c_u		
HSS	100	200	300
E_{50}^{ref}	7000	14000	21000
E_{oed}^{ref}	7000	14000	21000
E_{ur}^{ref}	21000	42000	63000
G_0^{ref}	52500	73500	99750
$\gamma_{0,7}$	2.75E-04	1.96E-04	1.45E-04
ϕ	30	30	30
K_0	0.500	0.500	0.500
E_{dyn}/E_{stat}	6	4.2	3.8

H=11m	d=0.6	d=0.9	d=1.2	E_{50}/c_u	H=11m	d=0.6	d=0.9	d=1.2
δ_{vm}(mm)	42	35	32	100	δ_{hm}(mm)	52	43	40
	31	26	23	200		40	33	29
	25	21	18	300		32	27	23

H=14m	d=0.6	d=0.9	d=1.2	E_{50}/c_u	H=14m	d=0.6	d=0.9	d=1.2
δ_{vm}(mm)	55	45	40	100	δ_{hm}(mm)	69	55	50
	42	34	28	200		54	43	36
	34	28	23	300		44	36	30

H=17m	d=0.6	d=0.9	d=1.2	E_{50}/c_u	H=17m	d=0.6	d=0.9	d=1.2
δ_{vm}(mm)	70	55	49	100	δ_{hm}(mm)	89	70	61
	55	43	34	200		70	56	44
	44	36	30	300		58	47	39

H=20m	d=0.6	d=0.9	d=1.2	E_{50}/c_u	H=20m	d=0.6	d=0.9	d=1.2
δ_{vm}(mm)	84	67	59	100	δ_{hm}(mm)	111	84	73
	67	52	43	200		88	69	54
	55	45	37	300		72	58	48

Model Group:27

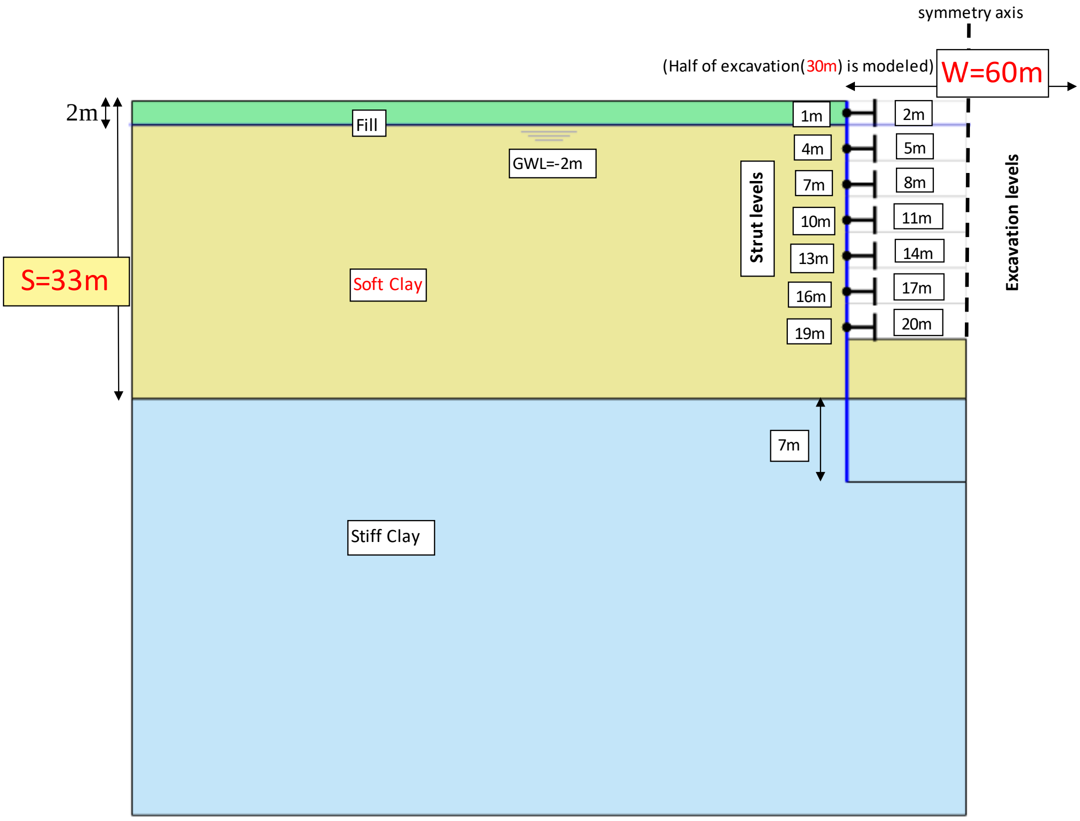

Figure A.27. Model Geometry-27.

Table B. Soil and structure parameters

Default Soil Parameters		
	Stiff Clay	Fill
	HS	HS
	Undrained(A)	Drained
E_{50}^{ref}	1.00E+05	1.50E+04
E_{oed}^{ref}	1.00E+05	1.50E+04
E_{ur}^{ref}	3.00E+05	4.50E+04
ϕ'	26	30
K_0	0.562	0.5
c'_{ref}	25	1
v'_{ur}	0.2	0.2
p_{ref}	100	100
R_f	0.9	0.9
$\gamma_{unsat/sat}$	20/20	16/20
R_{inter}	0.65	0.65
m	1	1

Range of parameters	
c_u/σ'_v	0.20-0.25-0.30-0.35
E_{50}/c_u	100-200-300
γ	15-17-19
S	23-28-33
W	20-40-60
H_e	11-14-17-20
$\ln(EI/\gamma_w h_{avg}^4)$	6.097-7.313-8.176

Diaphragm Wall (E=2.0E+7)		
d	EA	EI
0.6	1.2E+07	3.60E+05
0.9	1.8E+07	1.215E+06
1.2	2.4E+07	2.88E+06

Strut	
EA	3.80E+06
$L_{spacing}$	5m
h_{avg}	3m

Generic Cases: 3745 to 3780

Table A.104. Model parameters and deformation results (Case No: 3745 to 3780).

Excavation	Soil(γ=19kN/m^3)		Diaphragm Wall(E=2.0E+7)		
H_e(m)	c_u/σ_v'	E_{50}/c_u	d	EA	EI
11-14-17-20	0.2	100-200-300	0.6	1.2E+07	3.60E+05
			0.9	1.8E+07	1.215E+06
			1.2	2.4E+07	2.88E+06

Soft Soil	E_{50}/c_u		
HSS	100	200	300
E_{50}^{ref}	2895	5789	8685
E_{oed}^{ref}	2895	5789	8685
E_{ur}^{ref}	8685	17367	26055
G_0^{ref}	30759	43418	54281
$\gamma_{0,7}$	3.59E-04	2.54E-04	2.03E-04
ϕ	18	18	18
K_0	0.691	0.691	0.691
E_{dyn}/E_{stat}	8.5	6	5

H=11m	d=0.6	d=0.9	d=1.2	E_{50}/c_u	H=11m	d=0.6	d=0.9	d=1.2
δ_{vm}(mm)	117	82	63	100	δ_{hm}(mm)	141	101	75
	101	70	55	200		122	85	68
	91	64	48	300		109	78	59

H=14m	d=0.6	d=0.9	d=1.2	E_{50}/c_u	H=14m	d=0.6	d=0.9	d=1.2
δ_{vm}(mm)	189	127	94	100	δ_{hm}(mm)	232	155	110
	164	111	86	200		201	134	104
	149	104	76	300		182	125	92

H=17m	d=0.6	d=0.9	d=1.2	E_{50}/c_u	H=17m	d=0.6	d=0.9	d=1.2
δ_{vm}(mm)	264	168	127	100	δ_{hm}(mm)	331	212	149
	235	153	116	200		291	189	141
	216	144	105	300		269	175	128

H=20m	d=0.6	d=0.9	d=1.2	E_{50}/c_u	H=20m	d=0.6	d=0.9	d=1.2
δ_{vm}(mm)	329	208	162	100	δ_{hm}(mm)	422	265	189
	300	192	147	200		379	240	180
	278	183	136	300		350	224	166

Generic Cases: 3781 to 3816

Table A.104. Model parameters and deformation results (Case No: 3781 to 3816).

Excavation	Soil(γ=19kN/m^3)		Diaphragm Wall(E=2.0E+7)		
H_e(m)	c_u/σ_v'	E_{50}/c_u	d	EA	EI
11-14-17-20	0.25	100-200-300	0.6	1.2E+07	3.60E+05
			0.9	1.8E+07	1.215E+06
			1.2	2.4E+07	2.88E+06

Soil	E_{50}/c_u		
HSS	100	200	300
E_{50}^{ref}	4000	8000	12000
E_{oed}^{ref}	4000	8000	12000
E_{ur}^{ref}	12000	24000	36000
G_0^{ref}	35000	50000	67500
$\gamma_{0,7}$	3.58E-04	2.51E-04	1.86E-04
ϕ	22	22	22
K_0	0.625	0.625	0.625
E_{dyn}/E_{stat}	7	5	4.5

H=11m	d=0.6	d=0.9	d=1.2	E_{50}/c_u	H=11m	d=0.6	d=0.9	d=1.2
δ_{vm}(mm)	85	62	52	100	δ_{hm}(mm)	105	78	65
	68	49	36	200		83	60	45
	57	43	34	300		71	54	42

H=14m	d=0.6	d=0.9	d=1.2	E_{50}/c_u	H=14m	d=0.6	d=0.9	d=1.2
δ_{vm}(mm)	130	94	75	100	δ_{hm}(mm)	162	115	92
	103	77	57	200		129	92	71
	91	68	53	300		111	84	65

H=17m	d=0.6	d=0.9	d=1.2	E_{50}/c_u	H=17m	d=0.6	d=0.9	d=1.2
δ_{vm}(mm)	178	127	101	100	δ_{hm}(mm)	230	157	122
	146	105	79	200		183	130	99
	127	95	74	300		157	117	91

H=20m	d=0.6	d=0.9	d=1.2	E_{50}/c_u	H=20m	d=0.6	d=0.9	d=1.2
δ_{vm}(mm)	224	158	128	100	δ_{hm}(mm)	291	198	153
	188	132	101	200		235	168	127
	166	121	95	300		205	152	118

Generic Cases: 3817 to 3852

Table A.105. Model parameters and deformation results (Case No: 3817 to 3852).

Excavation	Soil(γ=19kN/m^3)		Diaphragm Wall(E=2.0E+7)		
H_e(m)	c_u/σ_v'	E_{50}/c_u	d	EA	EI
11-14-17-20	0.3	100-200-300	0.6	1.2E+07	3.60E+05
			0.9	1.8E+07	1.215E+06
			1.2	2.4E+07	2.88E+06

Soil	E_{50}/c_u		
HSS	100	200	300
E_{50}^{ref}	5400	10800	16200
E_{oed}^{ref}	5400	10800	16200
E_{ur}^{ref}	16200	32400	48600
G_0^{ref}	40500	60750	75938
$\gamma_{0,7}$	3.40E-04	2.27E-04	1.81E-04
ϕ	26.4	26.4	26.4
K_0	0.555	0.555	0.555
E_{dyn}/E_{stat}	6	4.5	3.75

H=11m	d=0.6	d=0.9	d=1.2	E_{50}/c_u	H=11m	d=0.6	d=0.9	d=1.2
δ_{vm}(mm)	65	54	42	100	δ_{hm}(mm)	82	67	53
	51	41	34	200		64	53	43
	43	34	30	300		54	44	38

H=14m	d=0.6	d=0.9	d=1.2	E_{50}/c_u	H=14m	d=0.6	d=0.9	d=1.2
δ_{vm}(mm)	94	75	57	100	δ_{hm}(mm)	116	94	70
	74	59	48	200		93	74	60
	63	51	43	300		79	63	55

H=17m	d=0.6	d=0.9	d=1.2	E_{50}/c_u	H=17m	d=0.6	d=0.9	d=1.2
δ_{vm}(mm)	124	98	74	100	δ_{hm}(mm)	156	123	91
	100	79	64	200		127	99	80
	86	69	58	300		108	87	73

H=20m	d=0.6	d=0.9	d=1.2	E_{50}/c_u	H=20m	d=0.6	d=0.9	d=1.2
δ_{vm}(mm)	155	120	92	100	δ_{hm}(mm)	201	152	114
	127	99	81	200		161	125	101
	111	88	74	300		137	110	92

Generic Cases: 3853 to 3888

Table A.106. Model parameters and deformation results (Case No: 3853 to 3888).

Excavation	Soil(γ=19kN/m^3)		Diaphragm Wall(E=2.0E+7)		
H_e(m)	c_u/σ_v'	E_{50}/c_u	d	EA	EI
11-14-17-20	0.35	100-200-300	0.6	1.2E+07	3.60E+05
			0.9	1.8E+07	1.215E+06
			1.2	2.4E+07	2.88E+06

Soil	E_{50}/c_u		
HSS	100	200	300
E_{50}^{ref}	7000	14000	21000
E_{oed}^{ref}	7000	14000	21000
E_{ur}^{ref}	21000	42000	63000
G_0^{ref}	52500	73500	99750
$\gamma_{0,7}$	2.75E-04	1.96E-04	1.45E-04
ϕ	30	30	30
K_0	0.500	0.500	0.500
E_{dyn}/E_{stat}	6	4.2	3.8

H=11m	d=0.6	d=0.9	d=1.2	E_{50}/c_u	H=11m	d=0.6	d=0.9	d=1.2
δ_{vm}(mm)	57	47	45	100	δ_{hm}(mm)	70	59	55
	43	36	31	200		55	46	40
	35	29	26	300		45	36	33

H=14m	d=0.6	d=0.9	d=1.2	E_{50}/c_u	H=14m	d=0.6	d=0.9	d=1.2
δ_{vm}(mm)	77	63	57	100	δ_{hm}(mm)	96	77	71
	60	50	42	200		75	62	53
	50	41	36	300		63	51	45

H=17m	d=0.6	d=0.9	d=1.2	E_{50}/c_u	H=17m	d=0.6	d=0.9	d=1.2
δ_{vm}(mm)	99	79	71	100	δ_{hm}(mm)	124	99	89
	79	65	55	200		99	81	69
	67	54	47	300		84	68	59

H=20m	d=0.6	d=0.9	d=1.2	E_{50}/c_u	H=20m	d=0.6	d=0.9	d=1.2
δ_{vm}(mm)	123	97	87	100	δ_{hm}(mm)	154	122	107
	98	81	69	200		124	101	86
	85	69	59	300		105	86	74